

**TELECONNECTIONS AND LONG RANGE PREDICTION  
OF SUMMER MONSOON RAINFALL VARIABILITY  
OVER BANGLADESH**

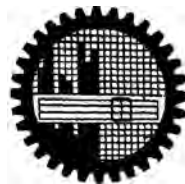
Ph. D Thesis

(Physics)

Md. Mizanur Rahman

Roll No. 10061405P

Session: October 2006



DEPARTMENT OF PHYSICS  
BANGLADESH UNIVERSITY OF ENGINEERING & TECHNOLOGY (BUET)  
DHAKA-1000, BANGLADESH  
August 2013

**Teleconnections and Long Range Prediction of Summer Monsoon  
Rainfall Variability over Bangladesh**

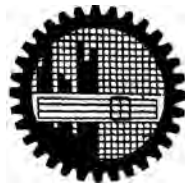
**A Dissertation Submitted to the Department of Physics, Bangladesh University of  
Engineering & Technology, Dhaka, in Partial Fulfillment of the Requirement for  
the Degree of**

**DOCTOR OF PHILOSOPHY IN PHYSICS**

**by  
Md. Mizanur Rahman**

**Examination Roll No. : 10061405P**

**Session : October 2006**



**DEPARTMENT OF PHYSICS  
BANGLADESH UNIVERSITY OF ENGINEERING & TECHNOLOGY (BUET)  
DHAKA-1000, BANGLADESH**

August 2013

## **CANDIDATE'S DECLARATION**

It is hereby declared that this thesis or any part of it has not been submitted elsewhere for the award of any degree or diploma.

---

**Md. Mizanur Rahman**

**BANGLADESH UNIVERSITY OF ENGINEERING & TECHNOLOGY (BUET), DHAKA**  
**DEPARTMENT OF PHYSICS**



*Certification of Thesis Work*

The thesis titled "**Teleconnections and Long Range Prediction of Summer Monsoon Rainfall Variability over Bangladesh**" submitted by Md. Mizanur Rahman, Roll No. 10061405P, Registration No. 0403596 Session: October 2006, has been accepted as satisfactory in partial fulfilment of the requirement for the degree of Doctor of Philosophy (Ph.D) in Physics on 03 August 2013.

**BOARD OF EXAMINERS**

1. \_\_\_\_\_ Chairman  
Dr. Md. Rafi Uddin (Supervisor)  
Associate Professor  
Department of Physics, BUET, Dhaka
2. \_\_\_\_\_ Member  
Prof. Dr. Md. Mahbub Alam (Co-supervisor)  
Head, Theoretical Division,  
SAARC Meteorological Research Centre (SMRC), Dhaka,
3. \_\_\_\_\_ Member  
Head (Ex-officio)  
Department of Physics, BUET, Dhaka
4. \_\_\_\_\_ Member  
Prof. Dr. Md. Abu Hashan Bhuiyan  
Department of Physics, BUET, Dhaka
5. \_\_\_\_\_ Member  
Dr. Nasreen Akter  
Assistant Professor  
Department of Physics, BUET, Dhaka
6. \_\_\_\_\_ Member  
Prof. Dr. Mohammad Rezaur Rahman  
Institute of Water and Flood Management (IWFM), BUET, Dhaka
7. \_\_\_\_\_ Member  
Prof. Hiroshi Uyeda (External)  
Hydrosphere Atmospheric Research Centre  
Nagoya University, Nagoya, Japan

*DEDICATED To  
MY  
BELOVED PARENTS AND  
FAMILY*

## *Acknowledgements*

*All praises is due to Almighty Allah. I am very much grateful to Him for giving me the opportunity to complete this research work,*

*First of all, I sincerely thank my supervisor to Dr. Md. Rafi Uddin, Associate Professor, Department of Physics, Bangladesh University of Engineering & Technology (BUET), for his guidance, valuable suggestions, and kind encouragement throughout the course of study. Without his support this work would have not been completed. I also wish to express my hearty thanks to my co-supervisor Prof. Dr. Md. Mahbub Alam, Head, Theoretical Division, SAARC Meteorological Research Centre (SMRC), Dhaka, for his guidance, inspiring suggestions to carry out this research work, I would like to thank the rest of my doctoral committee members for their encouragement, insightful comments.*

*I am very much grateful to Dr. Md. Nazrul Islam, Ex-Associate Professor, Department of Physics, BUET, for his encouraging to enrollment for Ph.D course in Department of Physics, BUET.*

*I am also very much thankful to Prof. Dr. Md. Mostak Hossain, Head, Department of Physics, BUET for keen interest and useful discussions in various stages of this research work,*

*I would also like to express my gratitude to Prof. Dr. Md. Abu Hashan Bhuiyan, Prof. Dr. Jiban Podder, Prof. Dr. Md. Firoz Alam Khan, Prof. Dr. A. K. M. Akther Hossain, Mrs. Fahima Khanam, Dr. Afia Begum and Dr. Md. Forhad Mina, Associate Professor and all others teachers of the Department of Physics, BUET for their cooperation.*

*I am thankful to the Director, SAARC Meteorological Research Centre (SMRC), Dhaka, for providing Research facilities during the course of this research work,*

*I am happy to mention here, my deep gratitude to Professor F. Giorgi, Head, Earth System Science, International Centre for Theoretical Physics (ICTP), Italy, for giving me an excellent opportunity to stay at ICTP & providing the lab facilities for my Ph.D research work,*

*I am thankful to Sujit Kumar Debsarma, Scientist, Theoretical Division, SMRC, Dr. Samarendra Kurmaakar, Ex-Director, SMRC and Nasreen Akter, Assistant Professor, Department of physics, BUET for their valuable suggestions and help in understanding the specific issues related to Monsoon.*

*I would like to thank to Meteorological Research Institute (MRI), Scientists, Tsukuba, Japan, for their support and provided me high resolution AGCM data for doing my Ph.D research work,*

*Moral support and encouragement given by my friends and colleagues Aziz Ahmed, Abdur Rahman, Md. Shahidulla, Mohamed El Sayed Hassan shaltout (Egypt) Ms. Nazlee Ferdousi, Md. Majajul Alam Sarker, Dr. Md. Nazmul Ahasan, Mr. Mohan Kumar Das, Sk. Md. Abubakar Abdullah, Farhana F. Nessa and many others foreign friends have helped me in many ways in compiling this research work,*

*I shall always remain indebted to my parents, brothers and sisters whose faith, confidence and blessings helped me to accomplish my desire to earn a doctoral degree. I wish to thank my wife for her unfailing support, care, and encouragement during my research work,*

## **Abstract**

In Bangladesh, the agricultural economy with large growing population is closely linked with the performance of its monsoon systems, namely summer monsoon (SM), active during June to September, which receives 70.7% of the annual rainfall of the country. In the view of critical influence of summer monsoon rainfall (SMR) on agricultural activities, industrial production and other water based enterprises in Bangladesh, prediction of the SMR is important for the policy making and planning of the country in mitigating efforts. Therefore, long-range forecasting (LRF) of SMR is a high priority in Bangladesh as there is no dynamical and statistical model to give the LRF for Bangladesh.

In this study, interannual and decadal variability of SMR using long term historical data for 48-year (1961-2008) has been used. An attempt is made to study the rainfall variability over Bangladesh on administrative divisional scale in detail. The teleconnections of SMR with various global parameters have been investigated and an empirical regression model has been developed for prediction of SMR. A high resolution (20 km) climate model named MRI-AGCM (Atmospheric General Circulation Model) output data has been used to predict the seasonal SMR during past 28 years (1979-2006) and results have also been verified with the regression model. The first 25 years (1979-2003) data of AGCM has been used for calibration and remaining three years data (2004-2006) has been used for validation. SMR scenario/projection has also been generated by this model for near future (2015-2034) and future (2075-2099) for Bangladesh.

The interannual variability of SMR shows random fluctuations, the decadal variability shows alternate epochs of above and below normal rainfall. The epochs tend to last for a decade or two. However, no long-term trends have been detected. The long-term average of SMR is 1701 mm, with a standard deviation of 199 mm. Its coefficient of variation is 11.6%. In Bangladesh, the interannual variability of SMR is very high; the interannual variability of SMR occasionally leads to large-scale deficient/droughts and excess/floods over the different parts of Bangladesh.

Teleconnections between SMR and global parameters have been investigated, and it has been found that above normal SMR is associated with warm Sea Surface Temperature (SST) in the month of February over southwest Indian Ocean and it is positively and

significantly correlated with correlation coefficient (CC) 0.44 (significant at 1% level). The correlations are weak over rest of the Indian Ocean and Bay of Bengal. The correlations are insignificant throughout the Indian Ocean and Bay of Bengal for the others month. It is observed that above-normal SMR is associated with warm Surface Air Temperature (SAT) in the month of April over Somalia and is positively and significantly correlated with  $CC=0.59$  (significant at 1% level). The correlations are weak over rest of the part of the globe. Above-normal SMR is associated with high Mean Sea Level Pressure (MSLP) in the month of April over central Pacific Ocean is positively and significantly correlated with  $CC=0.53$  (significant at 1% level).

The statistical model has been developed using three predictors namely SST, SAT and MSLP anomalies and it represents various forcing on SMR. The model showed reasonably good result during the training period 1979-2002 and performed well during the independent verification period 2003-2012 (10-year).

AGCM generated SMR scenario is calibrated with observed (rain-gauge) data during the period 1979-2003. The bias correction method of the World Climate Research Programme (WCRP) is utilized for validation of AGCM generated SMR during the period 2004-2006. Better performance of AGCM through validation encourages utilizing it in SMR forecast for Bangladesh. The change of near future SMR was forecasted for Bangladesh by -27.6 to 24.7% for the period 2015-2034. Similarly, the change of future SMR was forecasted for Bangladesh by -29.4 to 29.4% during the period 2075-2099. On an average near future and future SMR may change by -0.5% and 0.4% during the period 2015-2034 and 2075-2099, respectively.

AGCM calibrated and regression model mean SMR are compared with observed seasonal mean SMR during the period 1979-2006, it is seen that both AGCM and regression model SMR are close to observed rainfall for the period 1979-2006.

## Contents

|  | <b>Page No.</b> |
|--|-----------------|
| <b>Acknowledgements</b>                          | v               |
| <b>Abstract</b>                                  | vii             |
| <b>Contents</b>                                  | ix              |
| <b>List of Figures</b>                           | xiv             |
| <b>List of Tables</b>                            | xx              |
| <b>Abbreviations</b>                             | xxii            |
| <b>CHAPTER 1: INTRODUCTION</b>                   |                 |
| 1.1 Introduction                                 | 1               |
| 1.2 Climatological features of SM season         | 3               |
| 1.2.1 Surface temperature                        | 6               |
| 1.2.2 Mean sea level pressure                    | 7               |
| 1.2.3 Tropospheric winds                         | 10              |
| 1.3 Chief synoptic features during the SM season | 14              |
| 1.3.1 Westerly waves                             | 14              |
| 1.3.2 Inter-tropical convergence zone            | 14              |
| 1.4 Monsoon depression                           | 18              |
| 1.5 Objectives with specific aims                | 22              |
| 1.6 Thesis at a glance                           | 23              |
| <b>CHAPTER 2: LITERATURE REVIEW</b>              |                 |
| 2.1 Reviews on SMR                               | 25              |
| 2.2 Review on teleconnection                     | 31              |
| 2.3 Review on AGCM rainfall                      | 33              |
| <b>CHAPTER 3: DATA AND METHODOLOGY</b>           |                 |
| 3.1 Data used                                    | 37              |
| 3.1.1 Rainfall                                   | 37              |
| 3.1.2 NECP/NCAR reanalysis data                  | 38              |
| 3.1.3 Sea surface temperature                    | 38              |
| 3.1.4 Outgoing long wave radiation (OLR)         | 39              |

|        |                                       |    |
|--------|---------------------------------------|----|
| 3.1.5  | Monsoon depression data               | 39 |
| 3.1.6  | MRI-AGCM simulations data             | 39 |
| 3.2    | Methods                               | 40 |
| 3.2.1  | Rainfall data processing methods      | 40 |
| 3.2.2  | Statistical model development process | 41 |
| 3.2.3  | Linear correlation                    | 41 |
| 3.2.4  | Sliding correlations                  | 42 |
| 3.2.5  | Significance between two means        | 43 |
| 3.2.6  | Regression analysis                   | 43 |
| 3.2.7  | Multiple linear regression            | 46 |
| 3.2.8  | Moving averages                       | 48 |
| 3.2.9  | Coefficient of variance               | 48 |
| 3.2.10 | Cramer's test                         | 48 |
| 3.2.11 | Calibration process of AGCM           | 49 |

## **CHAPTER 4: RAINFALL VARIABILITY OF SUMMER MONSOON**

|       |  |    |
|-------|--|----|
| 4.1   | Introduction   | 50 |
| 4.2   | Interannual variability of SMR   | 51 |
| 4.3   | SMR patterns   | 52 |
| 4.3.1 | Identification of homogeneous administrative divisional monsoon rainfall | 54 |
| 4.4   | Statistical properties of SMR  | 59 |
| 4.4.1 | Mean seasonal rainfall and its annual contribution                       | 59 |
| 4.4.2 | Standard deviation and coefficient of variation                          | 59 |
| 4.4.3 | Range and extreme years  | 59 |
| 4.5   | Excess and deficient rainfall years of SM                                | 61 |
| 4.5.1 | Dhaka administrative divisional rainfall                                 | 63 |
| 4.5.2 | Chittagong administrative divisional rainfall                            | 63 |
| 4.5.3 | Rajshahi administrative divisional rainfall                              | 65 |
| 4.5.4 | Khulna administrative divisional rainfall                                | 65 |
| 4.5.5 | Barisal administrative divisional rainfall                               | 66 |
| 4.5.6 | Sylhet administrative divisional rainfall                                | 67 |
| 4.6   | Decadal variability of SMR   | 68 |

|       |                                |    |
|-------|--------------------------------|----|
| 4.6.1 | SMR over Bangladesh            | 68 |
| 4.6.2 | Dhaka divisional rainfall      | 69 |
| 4.6.3 | Chittagong divisional rainfall | 69 |
| 4.6.4 | Rajshahi divisional rainfall   | 71 |
| 4.6.5 | Khulna divisional rainfall     | 71 |
| 4.6.6 | Barisal divisional rainfall    | 72 |
| 4.6.7 | Sylhet divisional rainfall     | 72 |

## **CHAPTER 5: TELECONNECTION OF SUMMER MONSOON RAINFALL**

|        |   |     |
|--------|---|-----|
| 5.1    | Introduction  | 75  |
| 5.2    | Global correlation patterns                                     | 76  |
| 5.2.1  | Sea surface temperature of June-September (JJAS)                | 76  |
| 5.2.2  | Sea surface temperature of March-May (MAM)                      | 77  |
| 5.2.3  | Sea surface temperature of December-February (DJF)              | 77  |
| 5.2.4  | Monthly sea surface temperature of January through May          | 79  |
| 5.2.5  | Surface air temperature of June-September (JJAS)                | 81  |
| 5.2.6  | Surface air temperature of March-May (MAM)                      | 82  |
| 5.2.7  | Surface air temperature of December-February (DJF)              | 82  |
| 5.2.8  | Monthly surface air temperature of January through May          | 83  |
| 5.2.9  | Mean sea level pressure of June-September (JJAS)                | 86  |
| 5.2.10 | Mean sea level pressure of March-May (MAM)                      | 87  |
| 5.2.11 | Mean sea level pressure of December-February (DJF)              | 87  |
| 5.2.12 | Monthly mean sea level pressure of January through May          | 88  |
| 5.3    | Teleconnection between SMR and ENSO                             | 91  |
| 5.3.1  | ENSO impact on SMR  | 92  |
| 5.3.2  | SST anomalies during the extremes of SM season                  | 96  |
| 5.3.3  | SST anomalies around SM region during El-Niño years             | 98  |
| 5.3.4  | Low-level circulation anomalies in extreme years of SM activity | 100 |
| 5.3.5  | Secular variations in ENSO-associated circulation anomalies     | 103 |
| 5.4    | SMR and Indian Ocean dipole                                     | 104 |

|       |   |     |
|-------|---|-----|
| 5.4.1 | IODM and its variability                                | 105 |
| 5.4.2 | Interannual and decadal variability                     | 105 |
| 5.4.3 | Relationship between SMR and IODM                       | 107 |
| 5.4.4 | Circulation associated with active dipole phases        | 107 |
| 5.4.5 | SST anomalies associated with active dipole events      | 109 |
| 5.4.6 | Circulation features associated with extreme SMR phases | 112 |
| 5.5   | SST anomalies associated with extreme SMR phases        | 112 |

## **CHAPTER 6: PREDICTOR IDENTIFICATION AND DEVELOPMENT OF REGRESSION MODEL**

|       |  |     |
|-------|--|-----|
| 6.1   | Introduction                                       | 113 |
| 6.2   | Approach for predictor identification              | 115 |
| 6.3   | Identification of predictors for SM                | 115 |
| 6.3.1 | Sea Surface Temperature (SST)                      | 116 |
| 6.3.2 | Surface Air Temperature (SAT)                      | 116 |
| 6.3.3 | Mean Sea Level Pressure (SLP)                      | 116 |
| 6.4   | Predictors selection                               | 116 |
| 6.4.1 | Sea Surface Temperature (SST)                      | 117 |
| 6.4.2 | Surface Air Temperature (SAT)                      | 117 |
| 6.4.3 | Mean Sea Level Pressure (SLP)                      | 117 |
| 6.5   | Development of long range forecast for SM          | 120 |
| 6.5.1 | Selection of procedures for LRF                    | 122 |
| 6.5.2 | Development of a multiple regression model for SMR | 123 |

## **CHAPTER 7: DYNAMICAL PREDICTION OF SUMMER MONSOON RAINFALL**

|       |  |     |
|-------|--|-----|
| 7.1   | Introduction                                 | 129 |
| 7.2   | Monsoon rainfall scenario over Bangladesh    | 132 |
| 7.3   | Model description and experimental design    | 134 |
| 7.3.1 | Model description                            | 134 |
| 7.3.2 | Experimental design                          | 136 |
| 7.4   | Results and discussion                       | 138 |
| 7.4.1 | Simulation of SMR over SAARC region          | 138 |
| 7.4.2 | Interannual variation of SMR over Bangladesh | 139 |
| 7.4.3 | Calibration of SMR over Bangladesh           | 141 |

|   |   |     |
|---|---|-----|
| 7.4.4                                     | Validation of SMR over Bangladesh   | 143 |
| 7.5                                       | Projection of SMR over Bangladesh   | 144 |
| 7.5.1                                     | Projections of SMR for the near future (2015-2034)  | 144 |
| 7.5.2                                     | SMR projections for the future (2075-2099)  | 146 |
| 7.6                                       | Comparison of seasonal SMR among observed rainfall, AGCM rainfall and regression model rainfall | 148 |
| <b>CHAPTER 8: SUMMARY AND FUTURE WORK</b> |   |     |
| 8.1                                       | Summary   | 151 |
| 8.2                                       | Future works  | 155 |
| <b>REFERENCES</b>                         |   | 156 |
| <b>List of Publications</b>               |   | 166 |

## List of Figures

- Fig. 1.1: Spatial pattern of seasonal mean precipitation (mm) during (a) premonsoon, (b) monsoon, (c) postmonsoon and (d) winter over Bangladesh for the period 1961-2008.
- Fig. 1.2: Year to year variation of food grain production and SMR during June - September, 1969-2008. The values shown are backward differenced crop production and standardized monsoon rainfall index expressed as change from their respective values in previous years.
- Fig. 1.3: Spatial pattern of seasonal mean sea level pressure during (a) premonsoon, (b) monsoon, (c) postmonsoon and (d) winter over South Asia for the period 1961-2008.
- Fig. 1.4: Spatial pattern of seasonal mean surface temperature (MST) at 2m during (a) premonsoon, (b) monsoon, (c) postmonsoon and (d) winter over South Asia for the period 1961-2008.
- Fig. 1.5: Circulation pattern of seasonal mean wind (m/s) at 1000 hPa during (a) premonsoon, (b) monsoon, (c) postmonsoon and (d) winter for the period 1961-2008.
- Fig. 1.6: Spatial pattern of seasonal and monthly mean surface temperature (MST) at 2m during (a) monsoon, (b) June, (c) July, (d) August and (d) September over South Asia for the period 1961-2008.
- Fig. 1.7: Spatial pattern of seasonal and monthly mean sea level pressure (MSLP) during (a) monsoon, (b) June, (c) July, (d) August and (e) September over South Asia for the period 1961-2008.
- Fig. 1.8: Circulation pattern of seasonal and monthly mean wind (m/s) at 1000 hPa during (a) monsoon, (b) June, (c) July, (d) August and (e) September over South Asia for the period 1961-2008.
- Fig. 1.9: Circulation pattern of seasonal and monthly mean wind (m/s) at 850 hPa during (a) monsoon, (b) June, (c) July, (d) August and (e) September over Asia for the period 1961-2008.
- Fig. 1.10: Circulation pattern of seasonal and monthly mean wind (m/s) at 200 hPa during (a) monsoon, (b) June, (c) July, (d) August and (e) September over Asia for the period 1961-2008.

- Fig. 1.11: Spatial pattern of monthly mean outgoing long-wave radiation (OLR) ( $\text{w/m}^2$ ) during (a) January, (b) February, (c) March, (d) April, (e) May and (f) June over South Asia for the period 1961-2008.
- Fig. 1.12: Same as Figure 1.11, but for (g) July, (h) August, (i) September, (j) October, (k) November and (l) December.
- Fig. 1.13: Tracks of storms during (a) June and (b) July over Bay of Bengal (BOB) (source IMD)
- Fig. 1.14: Same as Fig. 1.13, but for (c) August and (d) September.
- Fig. 1.15: Trends in monsoon depression frequency over Bay of Bengal (BOB).
- Fig. 3.1: Rain gauge network stations considered over Bangladesh.
- Fig. 3.2: Administrative divisions of Bangladesh.
- Fig. 4.1: Interannual variability of SMR of Bangladesh.
- Fig. 4.2: The spatial distribution of SMR of Bangladesh during the period 1961-2008.
- Fig. 4.3: Annual cycle of rainfall (mm) over Bangladesh including six administrative divisions namely (a) All-Bangladesh, (b) Dhaka, (c) Chittagong and (d) Sylhet.
- Fig. 4.4: Same as Fig. 4.3, but for (e) Rajshahi, (f) Khulna and (g) Barisal.
- Fig. 4.5a: Dhaka administrative divisional rainfall variability during the period 1961-2008 and its association with ENSO. Horizontal dash line represents CV (%).
- Fig. 4.5b: Same as Fig. 4.5a, but for Chittagong divisional rainfall.
- Fig. 4.5c: Same as Fig. 4.5a, but for Rajshahi divisional rainfall.
- Fig. 4.5d: Same as Fig. 4.5a, but for Khulna divisional rainfall.
- Fig. 4.5e: Same as Fig. 4.5a, but for Barisal divisional rainfall.
- Fig. 4.5f: Same as Fig. 4.5a, but for Sylhet divisional rainfall.
- Fig. 4.6: The values of Cramer's  $t$ -statistics for the 11-year running means of SMR of Bangladesh depicting decadal variability and the epochs of above and below-normal rainfall. Values are plotted at the centre of the 11-year period.
- Fig. 4.6a: Same as Fig. 4.6, but for Dhaka divisional rainfall.
- Fig. 4.6b: Same as Fig. 4.6, but for Chittagong divisional rainfall.
- Fig. 4.6c: Same as Fig. 4.6, but for Rajshahi divisional rainfall.
- Fig. 4.6d: Same as Fig. 4.6, but for Khulna divisional rainfall.

- Fig. 4.6e: Same as Fig. 4.6, but for Barisal divisional rainfall.
- Fig. 4.6f: Same as Fig. 4.6, but for Sylhet divisional rainfall.
- Fig. 5.1: Spatial pattern of seasonal (June-September) correlation coefficients between SST and SMR of Bangladesh.
- Fig. 5.2: Same as Fig. 5.1, but for pre-monsoon (MAM) season.
- Fig. 5.3: Same as Fig. 5.1, but for winter (DJF) season.
- Fig. 5.4a: Spatial pattern of January correlation coefficients between SST and SMR of Bangladesh.
- Fig. 5.4b: Same as Fig. 5.4a, but for the month of February.
- Fig. 5.4c: Same as Fig. 5.4a, but for the month of March.
- Fig. 5.4d: Same as Fig. 5.4a, but for the month of April.
- Fig. 5.4e: Same as Fig. 5.4a, but for the month of May.
- Fig. 5.5: Spatial pattern of monsoon seasonal (June-September) correlation coefficients between SAT and SMR of Bangladesh.
- Fig. 5.6: Same as Fig. 5.5, but for pre-monsoon (MAM) season.
- Fig. 5.7: Same as Fig. 5.5, but for winter (DJF) season.
- Fig. 5.8a: Spatial pattern of January correlation coefficients between SAT and SMR of Bangladesh.
- Fig. 5.8b: Same as Fig.5.8a, but for the month of February.
- Fig. 5.8c: Same as Fig.5.8a, but for the month of March.
- Fig. 5.8d: Same as Fig.5.8a, but for the month of April.
- Fig. 5.8e: Same as Fig.5.8a, but for the month of May.
- Fig. 5.9: Spatial pattern of monsoon seasonal (June-September) correlation coefficients between MSLP and SMR of Bangladesh.
- Fig. 5.10: Same as Fig. 5.9, but for pre-monsoon (MAM) season.
- Fig. 5.11: Same as Fig. 5.9, but for winter (DJF) season.
- Fig. 5.12a: Spatial pattern of January correlation coefficients between MSLP and SMR of Bangladesh.
- Fig. 5.12b: Same as Fig.5.12a, but for the month of February.
- Fig. 5.12c: Same as Fig.5.12a, but for the month of March.
- Fig. 5.12d: Same as Fig.5.12a, but for the month of April.
- Fig. 5.12e: Same as Fig.5.12a, but for the month of May.
- Fig. 5.13: 21-year sliding correlation of SMR with Nino3 SSTs during the pre-monsoon and monsoon seasons.

- Fig. 5.14: Scatter diagram showing the relationship between Nino3 SST and SMR during the period (a) 1961-1984 and (b) 1985-2008.
- Fig. 5.15: Composite monsoon seasonal (JJAS) SST anomalies ( $^{\circ}\text{C}$ ) during (a) excess rainfall years, (b) deficient rainfall years and (c) excess minus deficient years.
- Fig. 5.16: Composite monsoon seasonal SST anomalies ( $^{\circ}\text{C}$ ) during El-Nino years for the two sub-periods (a) 1985-2008 and (b) 1961-1984 and also the (c) difference between the two sub-periods.
- Fig. 5.17: Composite wind anomalies (m/s) at 850 hPa during the SM season for (a) excess/flood rainfall years and (b) deficient/drought rainfall years during the period 1961-2008
- Fig. 5.18: Composite wind anomalies (m/s) at 850 hPa during the SM season for El Nino years during the two sub- periods (a) 1985-2008 and (b) 1961-1984.
- Fig. 5.19: Map showing the locations of two blocks over the western IO and the southeastern IO.
- Fig. 5.20: Variability of JJAS IODM (a) year to year interannual variability and (b) the values of Cramer's t-statistics of 11 year running mean depicting decadal variability and the epochs of above and below normal rainfall. Values are plotted at the centre of 11 year period.
- Fig. 5.21: Composite wind anomalies (m/s) at 850 hPa during the SM season for (a) Positive IOD and (b) Negative IOD during the period 1961-2008.
- Fig. 5.22: Composite seasonal SST anomalies ( $^{\circ}\text{C}$ ) for SM during the (a) positive IOD, (b) negative IOD phases of IODM and (c) difference between the positive and negative IOD.
- Fig. 6.1: Correlation maps between SMR of Bangladesh and SSTs in the month of February. The solid rectangular box indicates are significant at 5% level.
- Fig. 6.2: Correlation maps between SMR of Bangladesh and SATs in the month of April. The solid rectangular box indicates are significant at 1% level.
- Fig. 6.3: Correlation maps between SMR of Bangladesh and SLPs in the month of April. The solid rectangular box indicates are significant at 1% level.
- Fig. 6.4: Geographical locations of the three predictors.
- Fig. 6.5: Sliding window (21-year) correlations between the predictors SST anomaly (P1), SAT anomaly (P2) and SLP anomaly (P3) and SMR of Bangladesh during the period 1961-2007. Central year of the sliding

window is shown in the figure. 5% significant level is indicated as solid line.

- Fig. 6.6: Comparison between observed and regression model SMR during the period 1979-2002.
- Fig. 6.7: Comparison between observed and regression model (predicted value) SMR during the verification period (test period) 2003-2012 and 2013 represents rainfall forecast for SM over Bangladesh.
- Fig. 7.1: Schematic diagram of time-slice method.
- Fig. 7.2: Schematic diagram of SST setting for the end of 21st century simulation.
- Fig. 7.3: SMR (mm/d) obtained from (a) TRMM V6 during the period 1998-2010 and (b) high resolution AGCM during the period 1979-2003.
- Fig. 7.4: Comparison between observed and model simulated (un-calibrated) SMR (mm) during the period 1979-2003.
- Fig. 7.5: Comparison between observed and model calibrated SMR (mm) during the period 1979-2003.
- Fig. 7.6: Spatial distribution of SMR (mm/d) for (a) model and (b) observed over Bangladesh during the period 1979-2003.
- Fig. 7.7: Comparison between observed and model calibrated SMR (mm) during the period 2004-2006 and averaged SMR at the same period.
- Fig. 7.8: Percentage departure of SMR (near future) over Bangladesh during the period 2015-2034.
- Fig. 7.9: The spatial distribution of SMR anomaly (mm/d) over Bangladesh averaged during the period 2015-2034 and base period (1979-2003).
- Fig. 7.10: Percentage departure of SMR (future) over Bangladesh during the period 2075-2099.
- Fig. 7.11: The spatial distribution of SMR anomaly (mm/d) over Bangladesh averaged during the period 2075-2099 and base period (1979-2003).
- Fig. 7.12a: Comparison between observed rainfall and model simulated (uncalibrated) rainfall and regression model SMR during the period 1979-2006.
- Fig. 7.12b: Comparison between observed rainfall and model calibrated rainfall and regression model SMR for the period 1979-2006.
- Fig. 7.13: Comparison between mean observed rainfall, mean AGCM calibrated rainfall with regression model mean SMR during the period 1979-2006.

## **List of Tables**

- Table 4.1: Seasonal rainfall anomalies observed over Bangladesh during extreme SMR years during the period 1961-2008.
- Table 4.2: Statistical properties of SMR over Bangladesh and six administrative divisions for the period 1961- 2008.
- Table 4.3: Correlations between SMR and different administrative divisions of Bangladesh. Most of the values are significant about above 5% level, for the period 1961-2008.
- Table 4.4: SMR of Bangladesh and its administrative division's highest and lowest rainfall records and range during the period 1961-2008.
- Table 4.5: Excess rainfall year (1961-2008) of SM season  
Excess year  $\geq$  mean + C.V.
- Table 4.6: Deficient rainfall year (1961-2008) of SM season  
Deficit year  $\leq$  mean - C.V.
- Table 5.1: The correlations between SMR and ENSO during the period 1961-2008.
- Table 5.2: SMR anomalies during the El Niño years over the two halves of the period 1961-2008.
- Table 5.3: Standardized difference in SST anomalies between the tropical western Indian Ocean and tropical southeast Indian Ocean for the SM season (JJAS) depicting IODM intensity. Table shows the 11 active positive and 8 negative events.
- Table 6.1: Details of predictors used for the Bangladesh SMR forecast during the period 1961-2007.
- Table 6.2: Inter-correlation square matrix among the predictors that was used in the regression model during the period 1961-2007.
- Table 6.3: Forecast verification statistics of the model output computed for the period 1979-2002.
- Table 7.1: The specifications of the MRI-AGCM (high resolution, 20-km) model.
- Table 7.2: External forcings.
- Table 7.3: Statistical characteristics of observed and model simulated (un-calibrated) SMR (mm) over Bangladesh during the period 1979-2003.
- Table 7.4: Statistical characteristics of observed and model calibrated SMR (mm) over Bangladesh during the period 1979-2003.

## Abbreviations

|       |  |
|-------|--|
| AGCM  | : Atmospheric General Circulation Model              |
| AMIP  | : Atmospheric Model Intercomparison Project          |
| AOGCM | : Atmosphere-Ocean General Circulation Model         |
| BMD   | : Bangladesh Meteorological Department               |
| BOB   | : Bay of Bengal                                      |
| CAPE  | : Convective Available Potential Energy              |
| CCA   | : Canonical Correlation Analysis                     |
| CCs   | : Correlation Coefficients                           |
| CFCs  | : Chlorofluorocarbons                                |
| CGCM  | : Coupled Global Climate Model                       |
| CMAP  | : CPC Merged Analysis of Precipitation               |
| CMIP3 | : Coupled Model Intercomparison Project 3            |
| CTM   | : Chemical Transport Model                           |
| CV    | : Coefficient of Variation                           |
| DJF   | : December-January-February                          |
| ECMWF | : European Center for Medium-range Weather forecasts |
| EMR   | : Ensemble Multiple linear Regressions               |
| ENSO  | : El Nino Southern Oscillation                       |
| ERSST | : Extended Reconstructed Sea Surface Temperature     |
| ESM   | : Earth System Model                                 |
| GCM   | : General Circulation Model                          |
| HS    | : Hit Score  |
| HSS   | : Heidke Skill Score                                 |
| IAV   | : Interannual Variability                            |
| IMD   | : India Meteorological Department                    |
| IO    | : Indian Ocean                                       |
| IOD   | : Indian Ocean Dipole                                |
| IODM  | : Indian Ocean Dipole Mode                           |
| IPCC  | : Intergovernmental Panel on Climate Change          |
| ISMR  | : Indian Summer Monsoon Rainfall                     |
| ITCZ  | : Inter-Tropical Convergence Zone                    |
| JJAS  | : June-July-August-September                         |

|       |  |
|-------|--|
| JMA   | : Japan Meteorological Agency                      |
| LPA   | : Long Period Average                              |
| LRF   | : Long Range Forecasting                           |
| MAM   | : March-April-May                                  |
| MME   | : Multi-Model Ensemble                             |
| MRI   | : Meteorological Research Institute                |
| MSLP  | : Mean Sea Level Pressure                          |
| NAO   | : North Atlantic Oscillation                       |
| NAR   | : Non-linear Auto Regression                       |
| NARMA | : Non-linear Auto Regression Moving Average        |
| NCAR  | : National Centre for Atmospheric Research         |
| NCEP  | : National Centre for Environment Prediction       |
| NEM   | : Northeast Monsoon                                |
| NOAA  | : National Oceanic and Atmospheric Administration  |
| NPO   | : North Pacific Oscillation                        |
| OGCM  | : Ocean General Circulation Model                  |
| ON    | : October-November                                 |
| OLR   | : Outgoing Long-wave Radiation                     |
| PCA   | : Principal Component Analysis                     |
| PPR   | : Projection Pursuit Regression                    |
| RMSE  | : Root Mean Square Error                           |
| SAARC | : South Asian Association for Regional Cooperation |
| SAT   | : Surface Air temperature                          |
| SM    | : Summer Monsoon                                   |
| SMR   | : Summer Monsoon Rainfall                          |
| SOI   | : Southern Oscillation Index                       |
| SRES  | : Special Report on Emission Scenario              |
| SST   | : Sea Surface Temperature                          |
| TBO   | : Tropical Biennial Oscillation                    |
| TRMM  | : Tropical Rainfall Measuring Mission              |
| WCRP  | : World Climate Research Programme                 |
| WMO   | : World Meteorological Organization                |

# CHAPTER 1

## INTRODUCTION

### 1.1 Introduction

The most important feature in the meteorology of South Asia is the seasonal alternation of atmospheric flow patterns associated with the monsoons, due to seasonally modulated excess heating of the land masses of Asia in summer and cooling in winter, compared to the waters of the Indian Ocean and the China Seas. During the summer season (JJAS), the seasonal wind reversal at the lower levels and the associated south-to-north migration of the Inter-Tropical Convergence Zone (ITCZ) is modified by the land-ocean contrasts and orographic barriers. While the Asian summer monsoon (also known as southwest monsoon) is a consequence of the thermal differences between the land and the sea in general terms, it is primarily due to the seasonal shifting of thermally produced planetary belts of pressure and winds under continental influences.

In Bangladesh, the agricultural economy with large growing population is closely linked with the performance of its monsoon systems, namely summer monsoon (SM) or southwest monsoon, active during June to September. Bangladesh critically depends on the SM to grow Aman rice crop. Therefore, long-range forecasting (LRF) of summer monsoon rainfall (SMR) is a high priority in Bangladesh as there is no dynamical and statistical model to give the LRF for Bangladesh. An accurate forecast of seasonal SMR over the country has an increasing demand for decision makers and planners of the country in mitigating any kind of disaster like food crisis and water scarcity.

Bangladesh has four seasons namely, premonsoon (March-May), monsoon (June-September), postmonsoon (October-November) and winter (December-February). Monsoon (June-September) is also known as summer monsoon (SM) which contributes around 70.7% of its annual rainfall over Bangladesh. SM is an important source of water for Bangladesh during June-September. SM accounts for most of the annual rainfall over Bangladesh.

Fig. 1.1 shows the seasonal rainfall patterns over Bangladesh. This figure is generated by observed rain-gauge data of BMD. It clearly reveals that SM (JJAS) is major rainfall season over Bangladesh. SMR has a critical socio-economic significance, not much

focused work has so far been done to understand the variability and predictability of SMR over Bangladesh. The interannual variability of rainfall is very high, which significantly affects the agricultural sector over Bangladesh. The interannual variability of Aman (summer crop) food grains production anomalies over Bangladesh are shown in Fig. 1.2 along with those of SMR, which clearly reveals that almost all the extremes in the two time series closely correspond to each other. The correlation between the two time series is 0.13 which is not statistically significant.

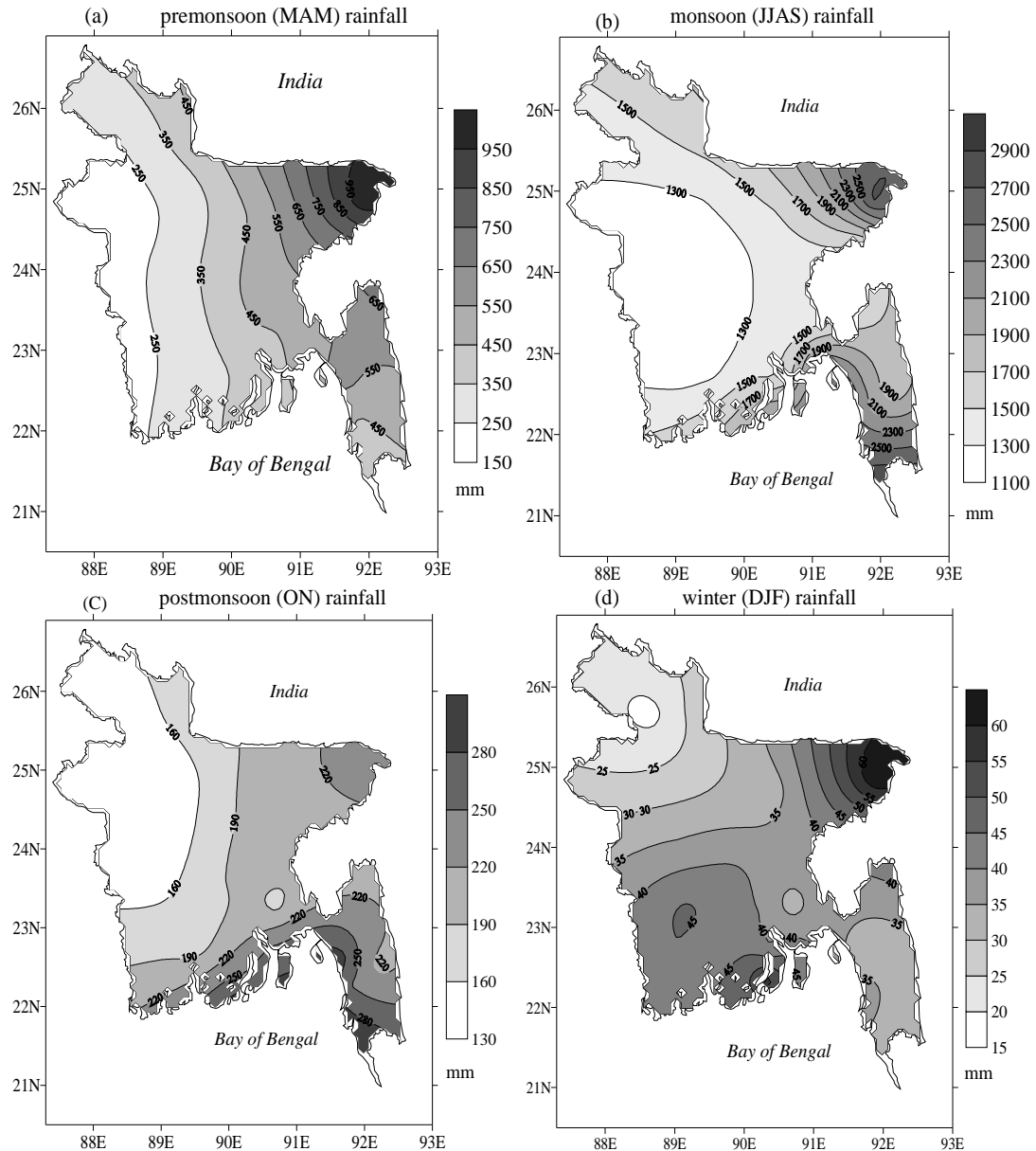


Fig. 1.1: Spatial pattern of seasonal mean precipitation (mm) during (a) premonsoon, (b) monsoon, (c) postmonsoon and (d) winter over Bangladesh for the period 1961-2008.

The seasonal evolution of surface circulation parameters, viz., mean sea level pressure, mean surface air temperature and wind for the South Asian domain are shown in Figs. 1.3-1.5, respectively, showing the distinct features associated with the SM season in comparison to the other seasons of the year.

Keeping in view the importance of SMR over Bangladesh, this research makes a detailed study of the system to understand the variability and synoptic features over the region during the SM season to understand the phenomenon and try to predict the system at least one season in advance, so that it will be beneficial for farmers, people of Bangladesh as well as for government too, in decision making and planners.

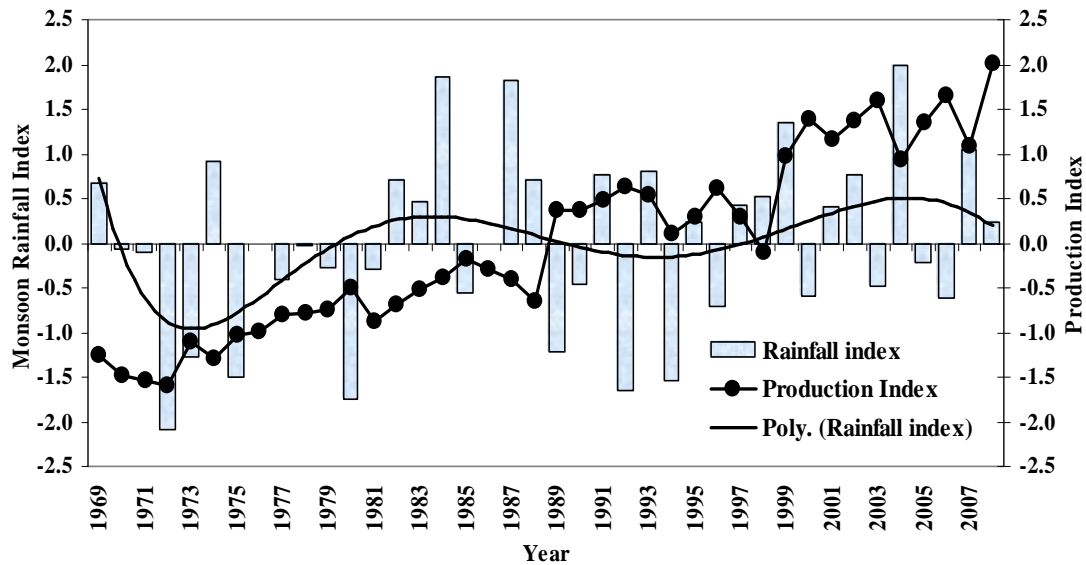


Fig. 1.2: Year to year variation of food grain production and SMR during June - September, 1969-2008. The values shown are backward differenced crop production and standardized monsoon rainfall index expressed as change from their respective values in previous years.

## 1.2 Climatological features of SM season

To provide the necessary background, the most important features of the climatology of SM season are presented in this section, based on the NCEP/NCAR reanalysis data.

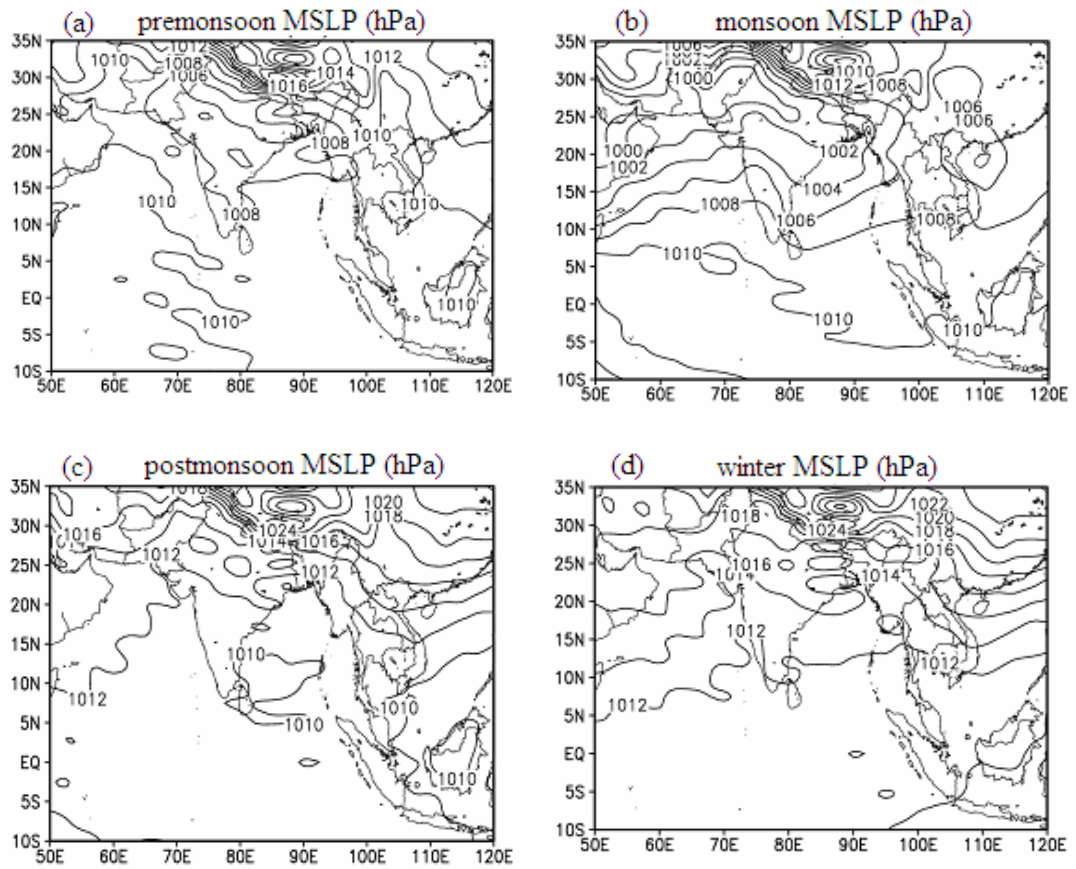


Fig. 1.3: Spatial pattern of seasonal mean sea level pressure (hPa) during (a) premonsoon, (b) monsoon, (c) postmonsoon and (d) winter over South Asia for the period 1961-2008.

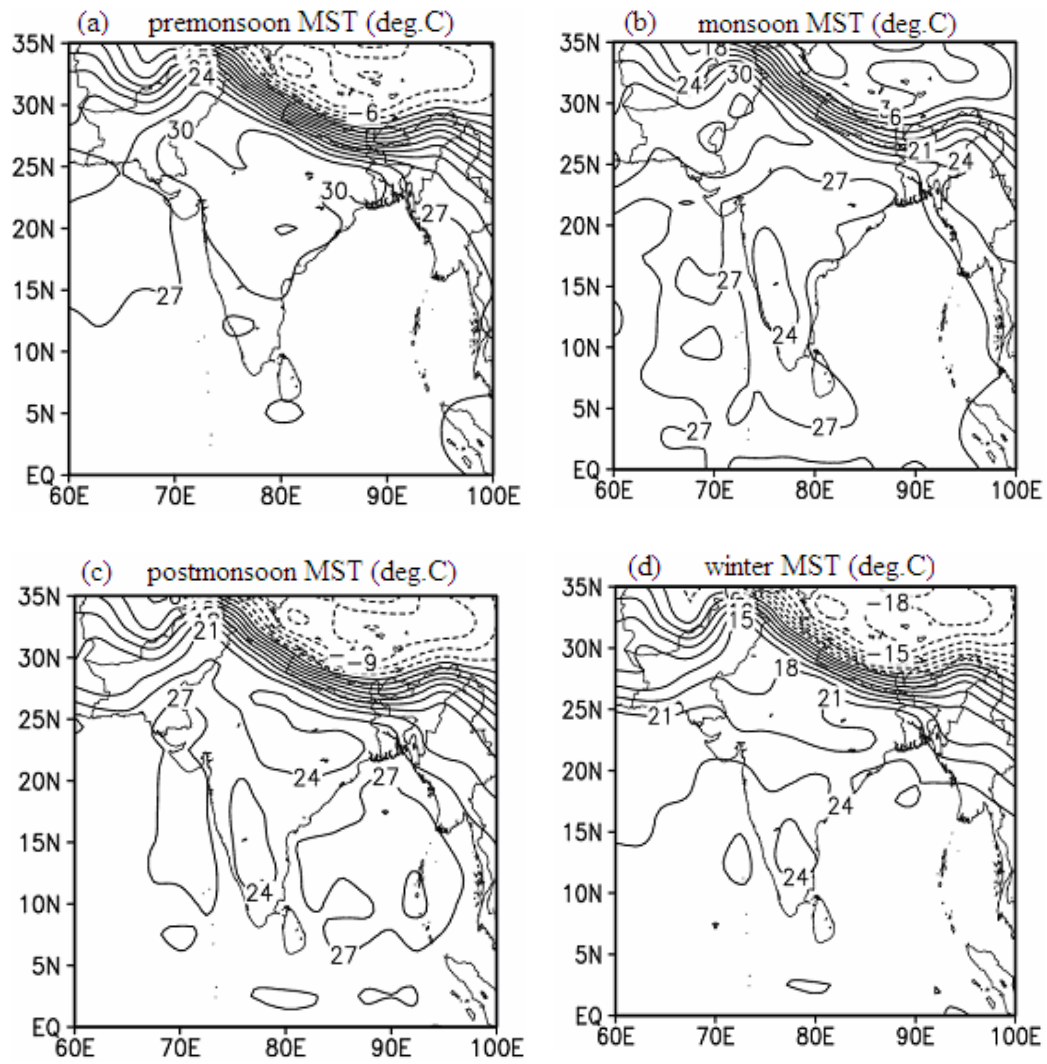


Fig. 1.4: Spatial pattern of seasonal mean surface temperature (MST) at 2m during (a) premonsoon, (b) monsoon, (c) postmonsoon and (d) winter over South Asia for the period 1961-2008.

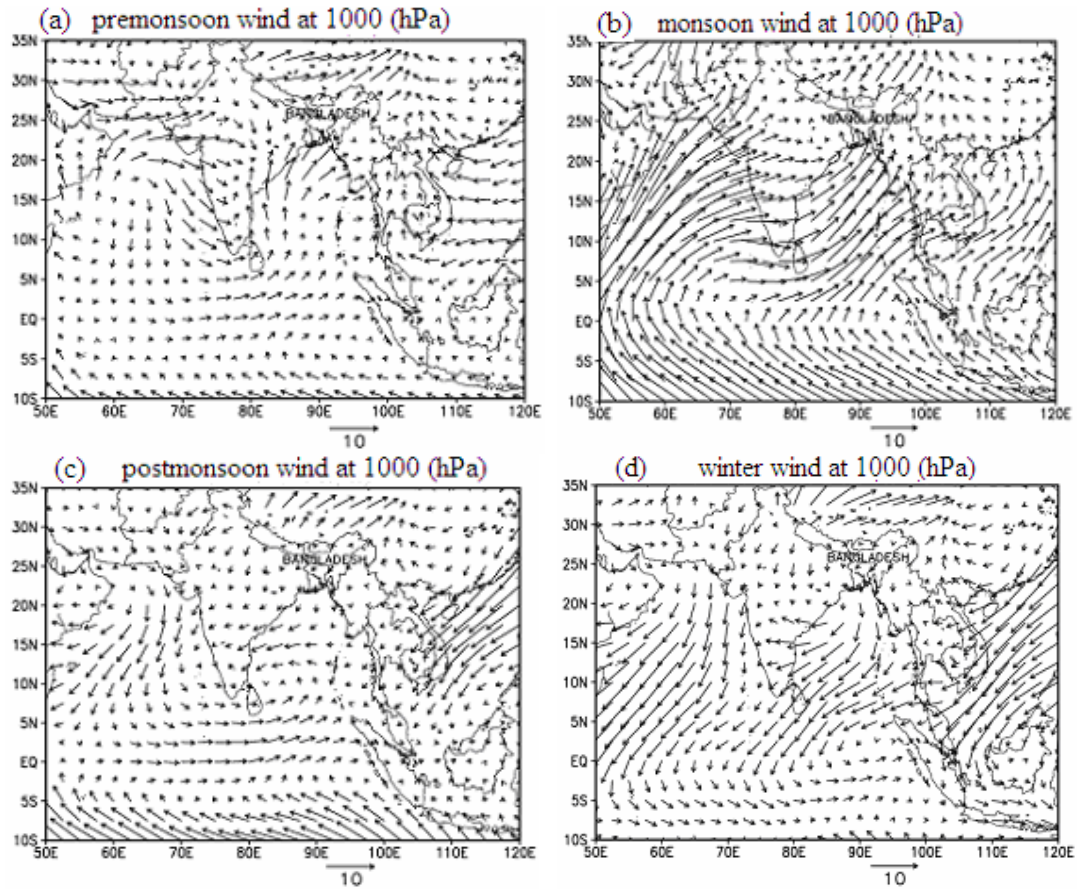


Fig. 1.5: Circulation pattern of seasonal mean wind (m/s) at 1000 hPa during (a) premonsoon, (b) monsoon, (c) postmonsoon and (d) winter for the period 1961-2008.

### 1.2.1 Surface temperature

The monthly mean climatology of mean surface air temperature during June-September is presented in Fig. 1.6. The surface air temperatures are relatively higher over the land than over the Bay of Bengal. During the SM season the temperatures are more over northwestern part of Asia, ranging from  $27^{\circ}$  to  $33^{\circ}$  C, decreasing northwards. There is not much month to month variation within the season in Bangladesh.

The monsoon having been traditionally looked upon as a thermally driven large scale circulation, attempts have always been made to examine its relationships with temperature over the land and sea surface. Liang *et al.* [1] have examined the role of land-sea distribution in the formation of the Asian SM through a series of interesting and idealized numerical experiments; their results show that the existence and geometric shape of land-sea distribution crucially affects the Asian SM. In the hypothetical

situation of there being only the subtropical Eurasian landmass and no ocean, a weak SM may develop over its southeastern corner, but there would be no tropical SM. In the opposite case of an 'aquaplanet', no monsoon would develop at all. It is the existence of tropical land that induces cross-equatorial flow and strong low level southwesterlies over the tropical regions, leading to the formation of the Asian SM over India as well as Bangladesh, the Bay of Bengal and the South China Sea.

### **1.2.2 Mean sea level pressure**

The monthly mean climatology of mean sea level pressure during June-September is shown in Fig. 1.7. During the SM season, pressures are relatively lower over land mass area particularly north of about  $25^{\circ}$  N and after that increase both northwards and southwards. In June, a low pressure area exists over the Bay of Bengal. It often extends to north by way of a trough and into the land mass area of India and Bangladesh as a depression. Deviations from the normal wind pattern occur when there is a depression or deep depression in the Bay of Bengal. By and large, the general orientation of the depression and fluctuations in its intensity govern rainfall. When the trough of depression is well defined over land and the seasonal low pressure over the Bay of Bengal is also well marked rainfall over India and Bangladesh is normally active.

The intense land heating of the northern hemisphere in summer produces a low pressure belt which extends from North Africa to India. The core of this low pressure belt lies over northwest India and adjoining Pakistan and is called the heat low. A deeper heat low is associated with a larger north-south pressure gradient over India and stronger monsoon activity. The monsoon trough is a low pressure area that in its normal position runs from the heat low across the Gangetic plains into the head Bay of Bengal. The oscillations of the monsoon trough during the monsoon season have a close bearing on the rainfall pattern over India. When the monsoon trough is situated at or to the south of its normal position, rainfall activity is strong. When it moves to the north of its normal position, rainfall activity becomes subdued and in the extreme case of it's migrating to the Himalayan foothills there is a break in the monsoon.

The monsoon trough is the only synoptic scale system that contributes to the rainfall activity over India and Bangladesh. Monitoring the movement of the monsoon trough is of great help in forecasting the monsoon activity on the short and medium range time scale.

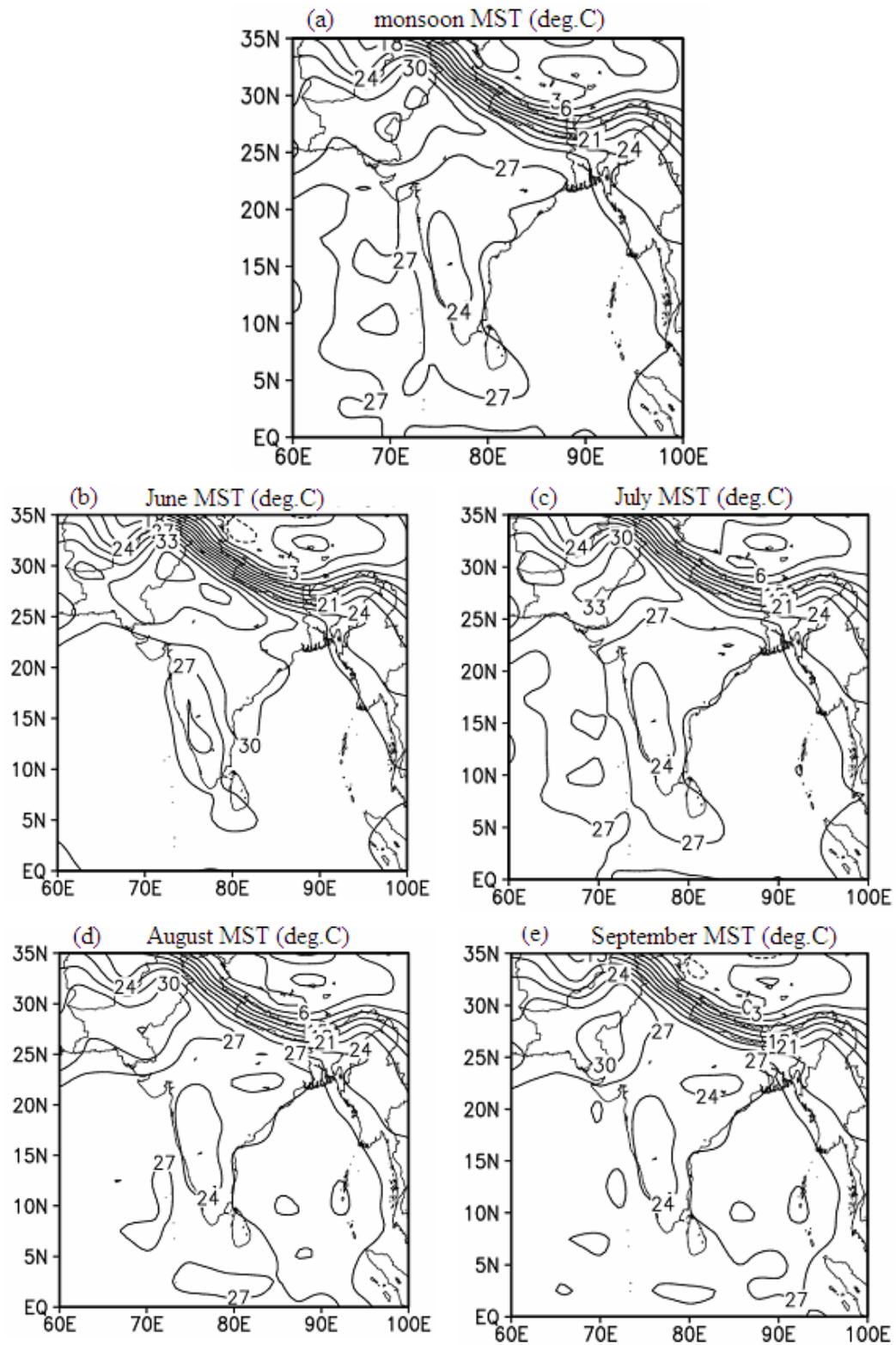


Fig. 1.6: Spatial pattern of seasonal and monthly mean surface temperature (MST) ( $^{\circ}\text{C}$ ) at 2m during (a) monsoon, (b) June, (c) July, (d) August and (d) September over South Asia for the period 1961-2008.

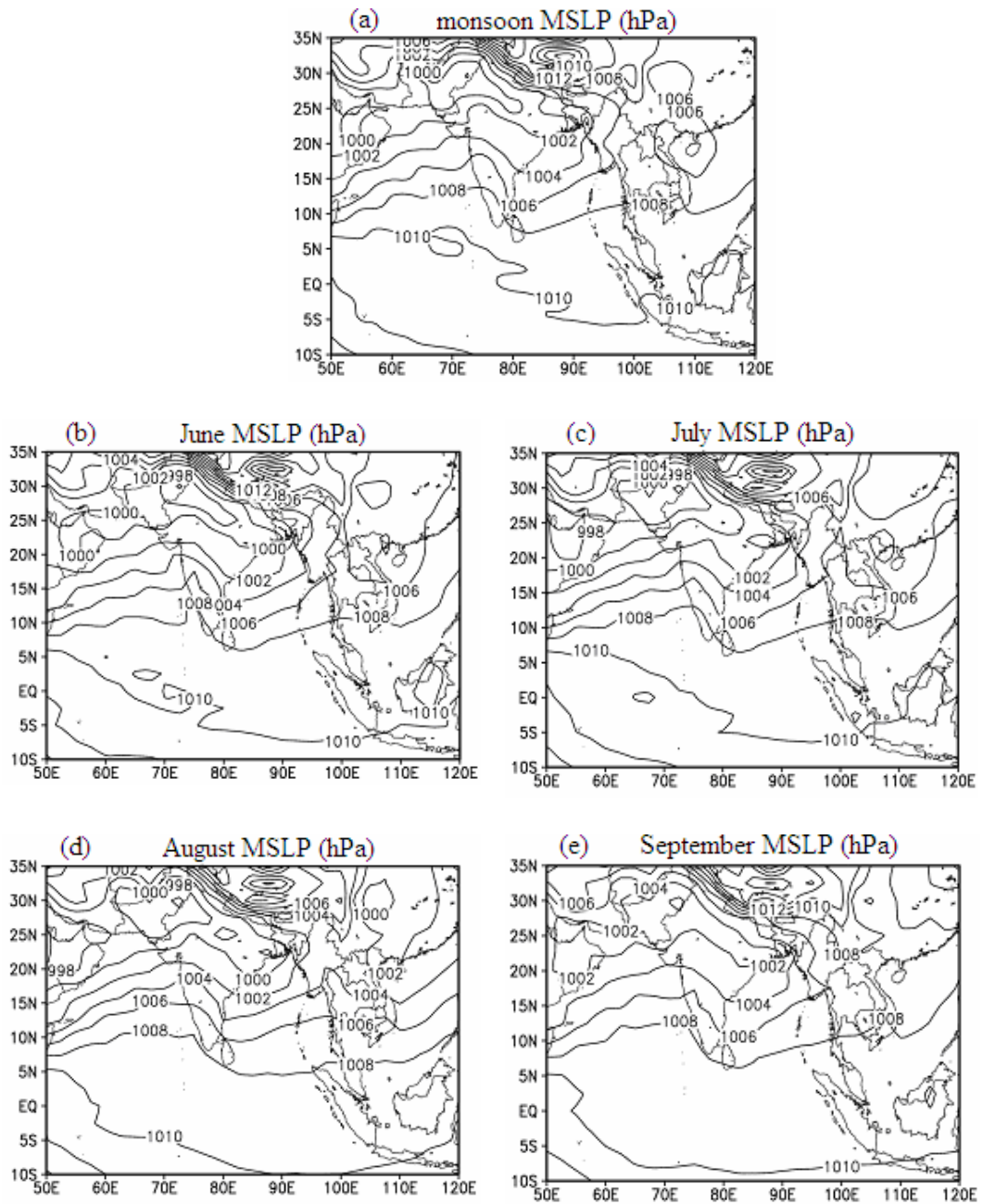


Fig. 1.7: Spatial pattern of seasonal and monthly mean sea level pressure (MSLP) during (a) monsoon, (b) June, (c) July, (d) August and (e) September over South Asia for the period 1961-2008.

### 1.2.3 Tropospheric winds

Fig. 1.8 shows the seasonal and monthly mean patterns of the surface winds during the SM season. In June, winds are from west to southwest, more westerly off the west coast of the Peninsula and practically southwesterly in the Bay of Bengal. Between  $5^{\circ}$  N and  $18^{\circ}$  N and west of  $65^{\circ}$  E, the speed is 15 kt in the Arabian Sea and Bay of Bengal. Elsewhere the range is 5-10 kt [2].

In July, southerlies occur over Bangladesh and West Bengal and southwesterlies to westerlies elsewhere. Strongest winds are in the southwest Arabian Sea. Nearer the west coast of the Peninsula, the direction is westsouthwest to west, except along the Kerala coast where westerlies are observed. Mean speeds over land are not more than 10 kt. They are between 10 kt and 15 kt along the west coast. In the Arabian Sea west of  $68^{\circ}$  E and between  $10^{\circ}$  N and  $20^{\circ}$  N, it is over 15 kt. Over most of the Bay of Bengal and the rest of the Arabian Sea, the speed is about 10 kt. Winds are somewhat weaker between the equator and  $5^{\circ}$  N (Fig. 1.8). August is similar to July. In the month of September, there is a weakening wind, particularly over the sea areas. In September, winds are west-northwesterly in the Arabian Sea to the east of  $65^{\circ}$  E. The lower tropospheric winds are cross equatorial flow and the strong southwesterlies of the monsoon are clearly evident.

At 850 hPa, the prominent features are the existence of high pressure over the Indian Ocean (Fig. 1.9), which is replaced by westerlies during the SM season. At 200 hPa, winds are easterly to northeasterly over Indian Ocean and a large part of the South Asian landmass. Strong tropical easterlies below to the south of  $25^{\circ}$  N (Fig. 1.10) in the SM period, which concentrate into a core of high winds known as the easterly jet stream with a core speed of 25-30 m/s. The easterlies may not be extending to north of  $30^{\circ}$  N along the latitude, as the few available winds at  $30^{\circ}$  N show westerlies at 200 hPa as shown in Fig. 1.10.

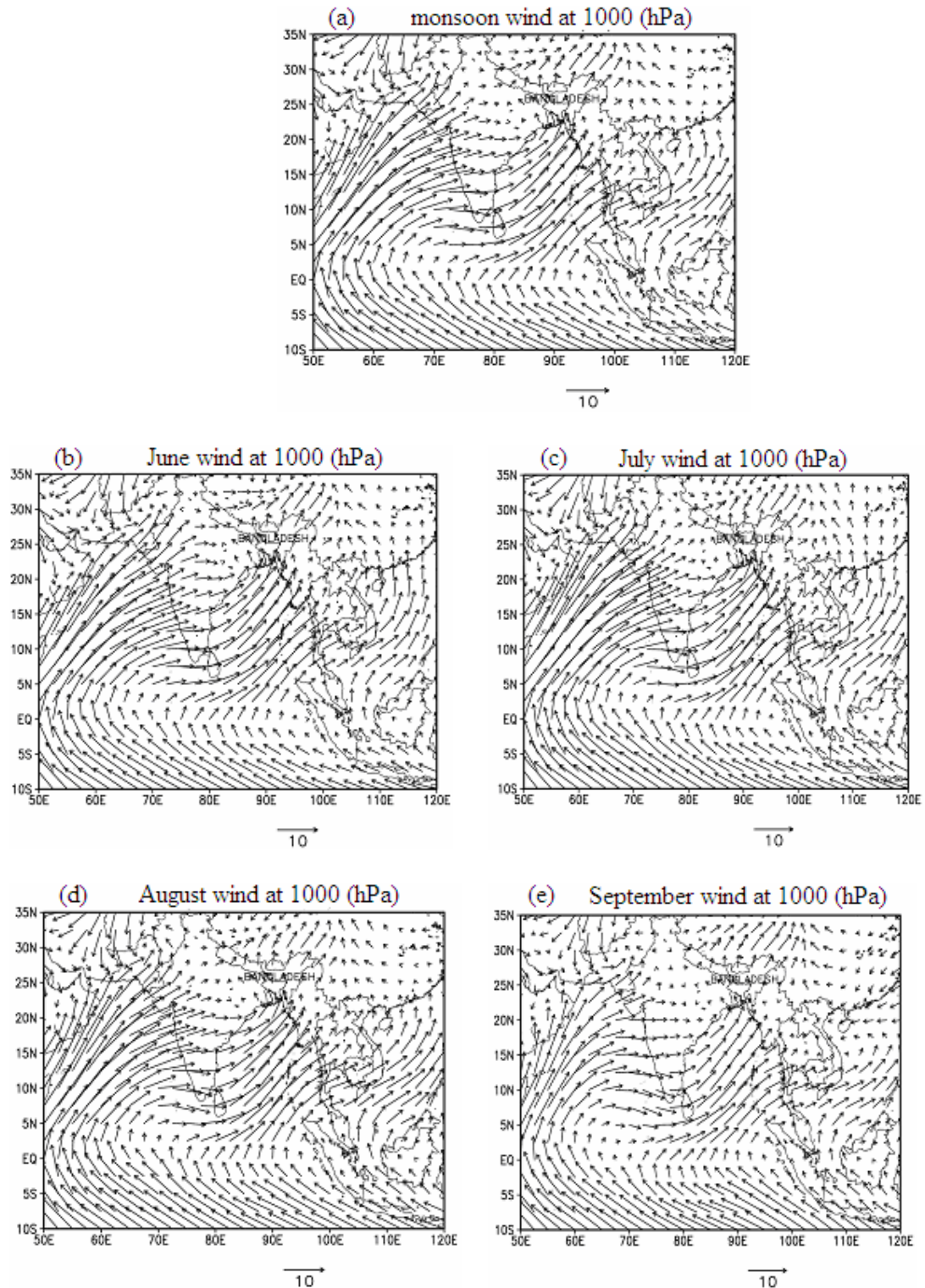


Fig. 1.8: Circulation pattern of seasonal and monthly mean wind (m/s) at 1000 hPa during (a) monsoon period, (b) June, (c) July, (d) August and (e) September over South Asia for the period 1961-2008.

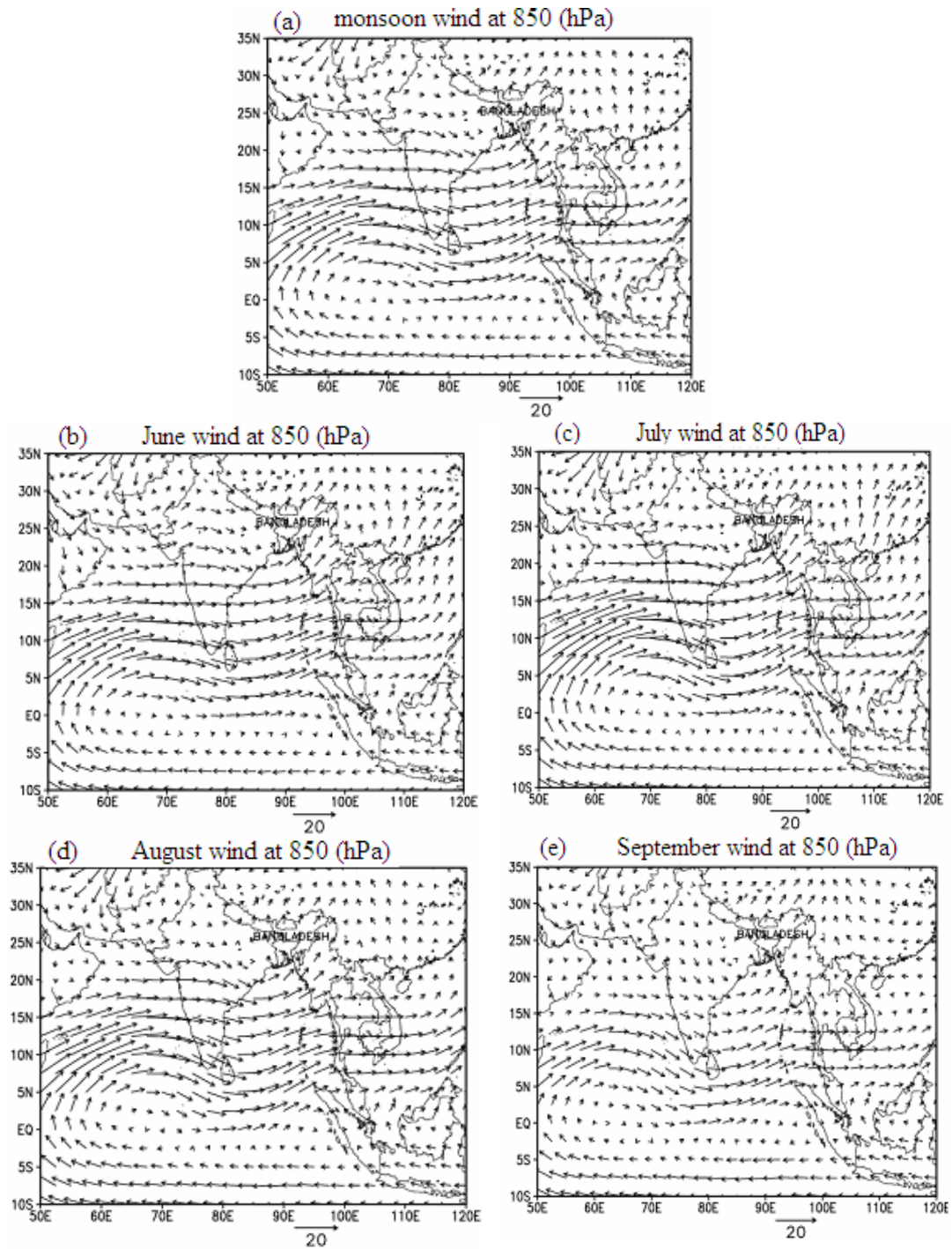


Fig. 1.9: Circulation pattern of seasonal and monthly mean wind (m/s) at 850 hPa during (a) monsoon period, (b) June, (c) July, (d) August and (e) September over Asia for the period 1961-2008.

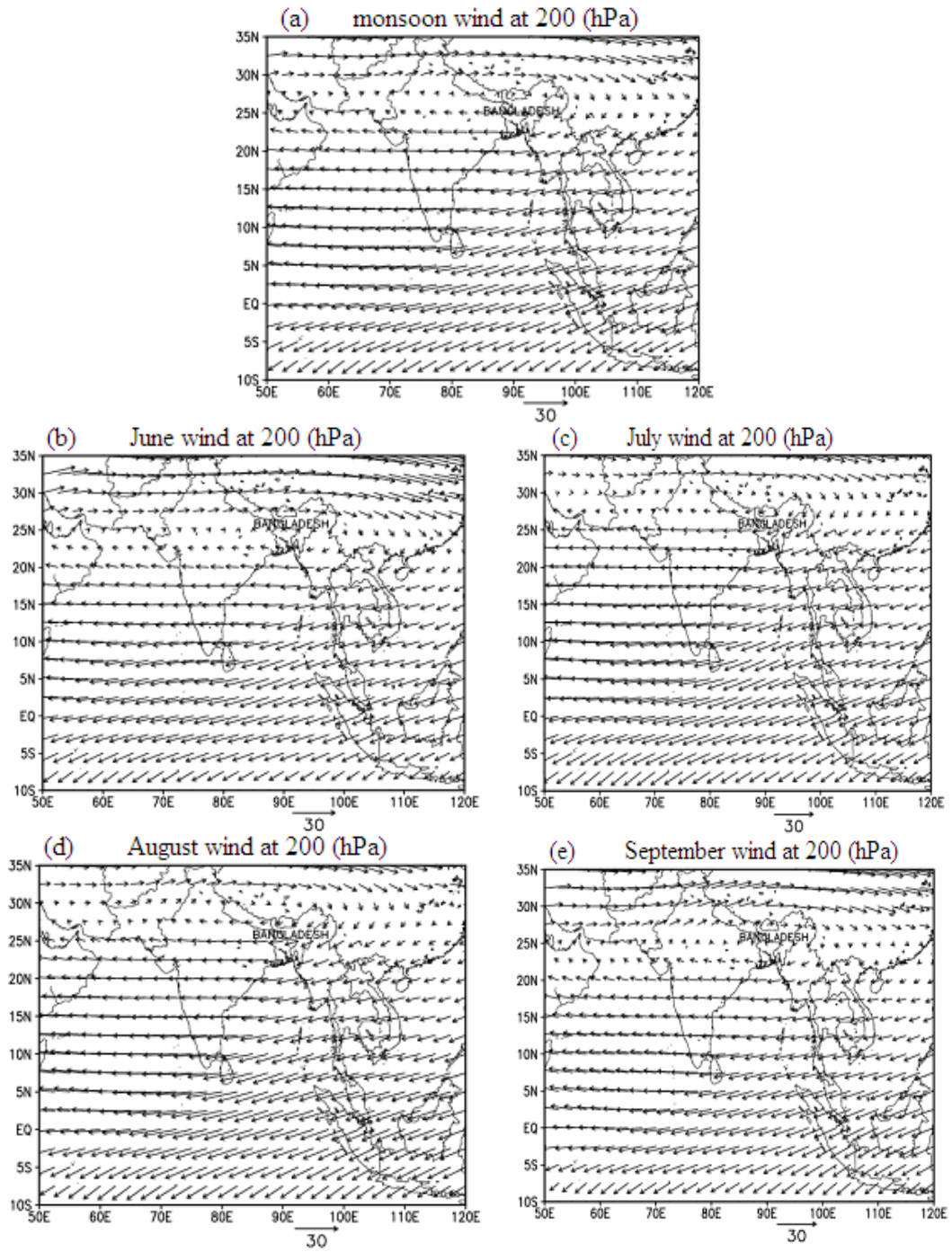


Fig. 1.10: Circulation pattern of seasonal and monthly mean wind (m/s) at 200 hPa during (a) monsoon period, (b) June, (c) July, (d) August and (e) September over Asia for the period 1961-2008.

### **1.3 Chief synoptic features during the SM season**

#### **1.3.1 Westerly waves**

During the SM season, westerly waves are common especially in the lower latitudes. They are inverted, migratory wave-like disturbances or troughs in the tropical region that move from west to east, generally creating only a shift in winds and rain. The low-level convergence and associated convective weather occur on the western side of the wave axis. Normally, it moves slower than the atmospheric current in which it is embedded and is considered a weak trough of low pressure. It is often associated with possible tropical depression development and is also known as tropical waves.

#### **1.3.2 Inter-tropical convergence zone**

The Inter-Tropical Convergence Zone (ITCZ) is a series of convergence zones, also known as equatorial trough, existing over  $5^{\circ}$  to  $15^{\circ}$  latitude on one side of equator and occasionally on both sides of the equator. ITCZ has a dominant role over the climate of tropics.

The monthly mean outgoing long wave radiation (OLR) values are shown in Fig. 1.11 illustrating the latitudinal variation of maximum cloud zone over the tropics during the course of the year. The movement of maximum cloud zone is very well captured by the OLR; values  $230 \text{ W/m}^2$  or less represent convective clouds [2]. The position of ITCZ is at far northern latitude during monsoon months around  $25^{\circ}$  N, which starts shifting southwards with the withdrawal of SM. As the season advances, it moves southwards and reaches near equator in December.

The ITCZ that circles the globe is a region of lower tropospheric wind discontinuity with horizontal velocity convergence and net upward motion. The ITCZ migrates north-south in association with the movement of the sun, and the tropical rain belt shifts along with it. These seasonal wind reversals and changes in precipitation patterns are not just confined to the traditional monsoon domains, but they also occur elsewhere in the ITCZ region.

There are large regional variations in the seasonal alignment of the ITCZ. Over the eastern Pacific and Atlantic oceans, it remains to the north of the equator throughout the year. In other regions, it moves from the north of the equator in northern summer to the south of the equator in southern summer. Over land, the ITCZ is located over the

warmest regions while over the sea; it is located over the highest Sea Surface Temperature (SST) regions. From West Africa to Southeast Asia, there is a discontinuity between the westerlies in the near-equatorial region and the easterly trade winds on either side of the ITCZ. The westerlies are largely the southeast trade winds which have changed direction after crossing the equator. Over the Atlantic and Pacific Oceans the discontinuity is between the northeast and southeast trades of the two hemispheres.

As far as the South Asian monsoon is concerned, the monsoon oscillation is stronger in the northern hemisphere than in the southern hemisphere and it is stronger over south and Southeast Asia than elsewhere in the northern hemisphere. This can be attributed to the Himalayan mountains and the elevated Tibetan plateau producing diabatic heating over a large area of the middle troposphere, the Indian Ocean to the south providing abundant moisture supply and the strong meridional gradients of temperature [3].

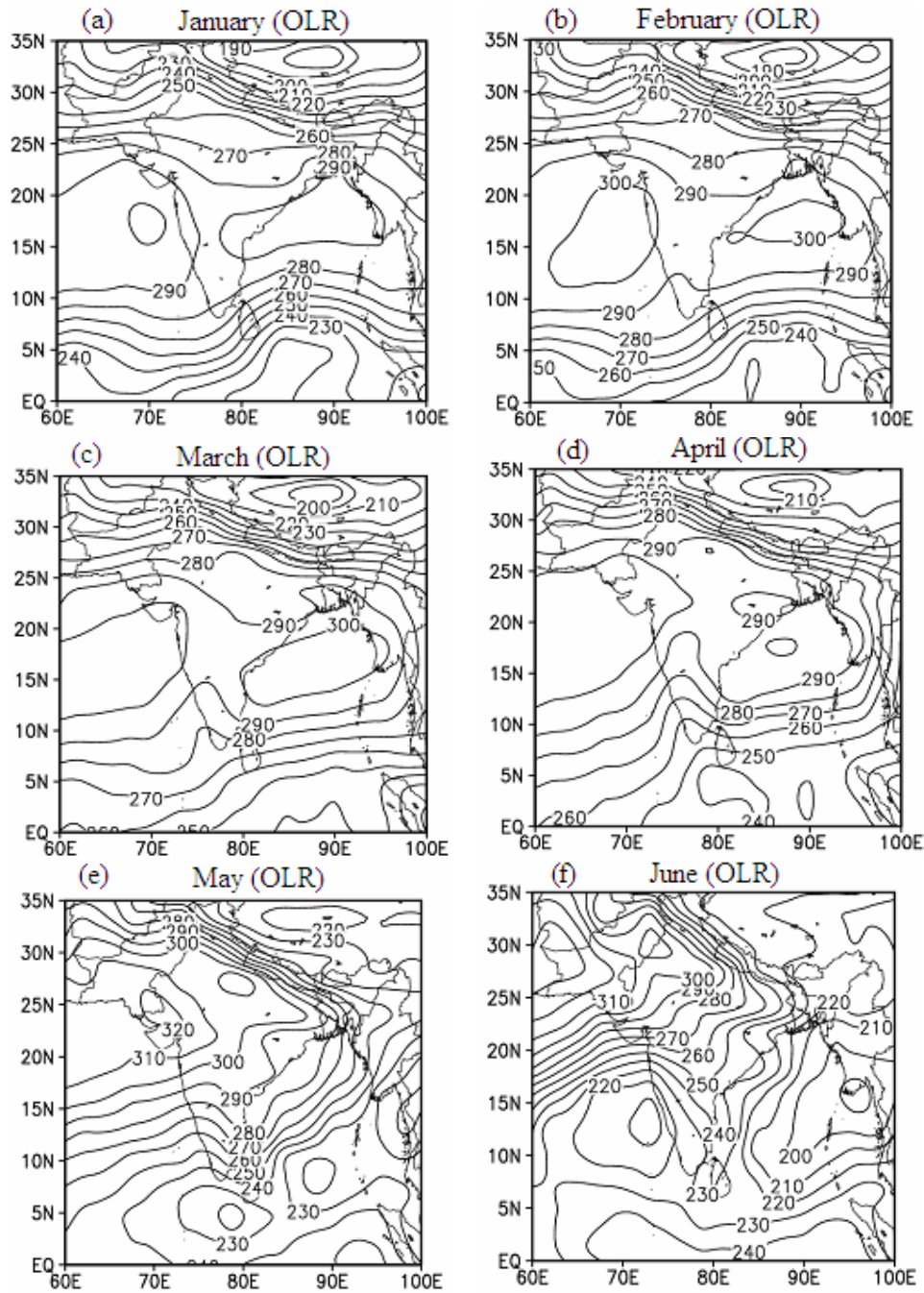


Fig. 1.11: Spatial pattern of monthly mean outgoing long wave radiation (OLR) ( $\text{w/m}^2$ ) during (a) January, (b) February, (c) March, (d) April, (e) May and (f) June over South Asia for the period 1961-2008.

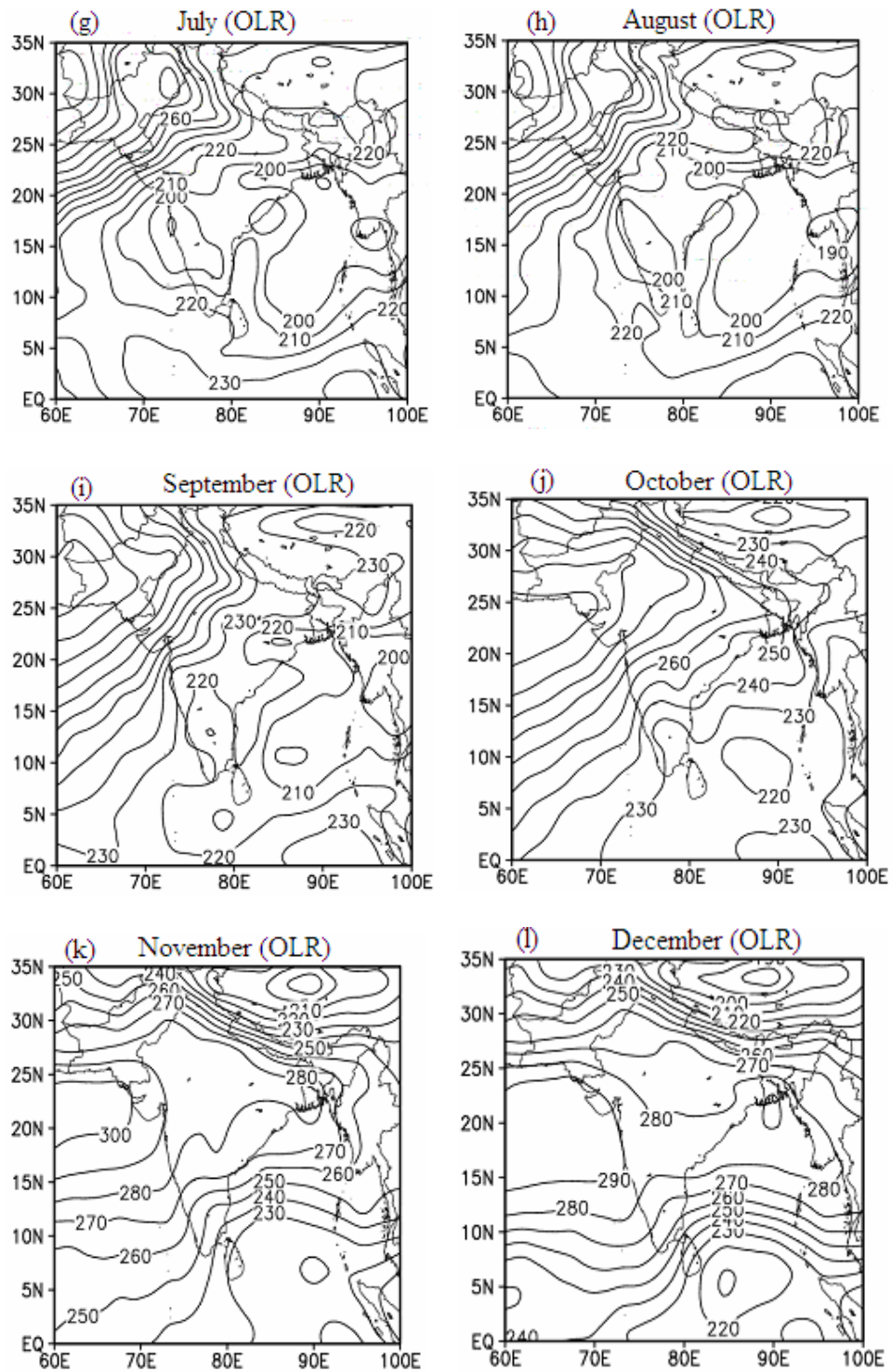


Fig. 1.12: Same as Figure 1.11, but for (g) July, (h) August, (i) September, (j) October, (k) November and (l) December.

## 1.4 Monsoon depression

Monsoon depressions generally form at the head of the Bay of Bengal in the monsoon trough which extends southeastward from Pakistan towards the Bay across North India. They occur during the months of June to September when the SM covers the entire Bay. In late August and September, however, whenever the monsoon trough shifts southwards, the area of formation of these depressions is displaced into the Central Bay. Depressions are rare in the Arabian Sea, though occasionally a Bay of Bengal depression, after traveling over India, may emerge in the Northeast Arabian Sea and even intensify.

The formation of the depression is generally preceded by a fall of pressure in the North Bay, the isallobaric low moving westward from Myanmar and further east. Winds in the lower troposphere over West Bengal and Bangladesh back with the approach of the low; the cyclonic circulation is first seen at levels of 1.5 km (850 hPa) and above and extends to the surface thereafter. These isallobaric 'lows' have been described variously as low pressure waves, easterly waves etc. About four or five low pressure waves move into the head Bay of Bengal per month during the SM season. Two or three of them intensify into monsoon depressions each month and the rest move westward as low pressure waves. Some meteorologists consider these low pressure waves as remnants of Pacific typhoons striking the coasts of Southeast Asia. The depressions intensify while moving west-northwestward over the North Bay. The pressure departure at the centre rarely exceeds 10 or 12 mb and winds over sea reach 30 to 35 knots. They do not normally attain tropical cyclone intensity due to their short sea travel and the unfavorable upper air conditions [4].

Most of the monsoon depressions have a typical life span of 3 to 5 days, but some may last even up to a week. When the seasonal trough intensifies and a closed low appears, a monsoon depression is likely to grow out of it. The development may occur either in situ or because of the arrival of an easterly wave. In a day or two, the low intensifies into a depression with winds of 22-33 knots. Depressions move at about 4° latitude or longitude per day but if they re-curve, they gather speed. In many years, the advance of the monsoon over Northeast India takes place in association with a depression.

After passing inland across the Orissa coast the depressions weaken. Though their central pressure remains almost unaltered, the area covered by the cyclonic circulation increases, thus reducing the pressure gradients considerably. They continue to move west-

northwest or northwest for nearly a thousand miles. Some of them occasionally take a westerly or even a northerly course. After traveling overland to east Rajasthan, the depressions have a tendency to re-curve, move into the Punjab and break up over the Himalayas. Otherwise they continue to move northwestward into Pakistan and fill up over the desert areas. A prematurely re-curving depression breaks up over Nepal or the Eastern Himalayas.

The most significant feature of these depressions is the heavy rainfall in the left forward sector. The heavy rain belt associated with the depression extends about 250 miles to the left of the track [5]. There is hardly any heavy rain to the right as long as the depression continues its westerly or northwesterly course. After re-curvature, however, the heavy rain belt shifts to the north and northeastern sector. Rainfall amounts of 100 to 200 mm per day are frequent in the left forward sector; heavier downpours causing local floods are also quite common. Depressions closely following each other along the same track during a month cause floods to the left of their track and drought to the right.

Monsoon depressions are intense low pressure systems that often form over the warm oceans with less vertical wind shear. During the SM season, maximum number of depression develops over the Bay of Bengal region. Their monthly frequencies for the period 1891-1990 are shown in Figs. 1.13-1.14.

It is observed that in June, depression form over North Bay of Bengal and very few are formed over central Bay of Bengal. Their tracks are normally north northwestwards, they strike the coast between  $18^{\circ}$ - $22^{\circ}$  N (Fig. 1.13a). Some of them move across the Orissa and giving widespread rainfall over this region and emerges into the Arabian Sea. Some of them move across the Gangatic West Bengal and Bangladesh coast. In July, depression activity is maximum (Fig. 1.13b), and a good number of depression move across the Orissa and Madhya Pradesh and sometimes emerge into Pakistan. In August, depression activity is mostly confined over Orissa and West Bengal (Fig. 1.14c). Only few of them cross the east coast of India. In September, depression activity is reduced and mostly confined over Orissa and West Bengal of India. Depression continues it's westerly or northwesterly and recurve it northeastern direction (Fig. 1.14d).

Generally, 4 to 6 monsoon depressions form every year but the number is highly variable. There were 7 monsoon depressions in the year 1961, 1966, 1968, 1977 and 2006, respectively during the period 1961-2008 (Fig. 1.15). There was other years when only

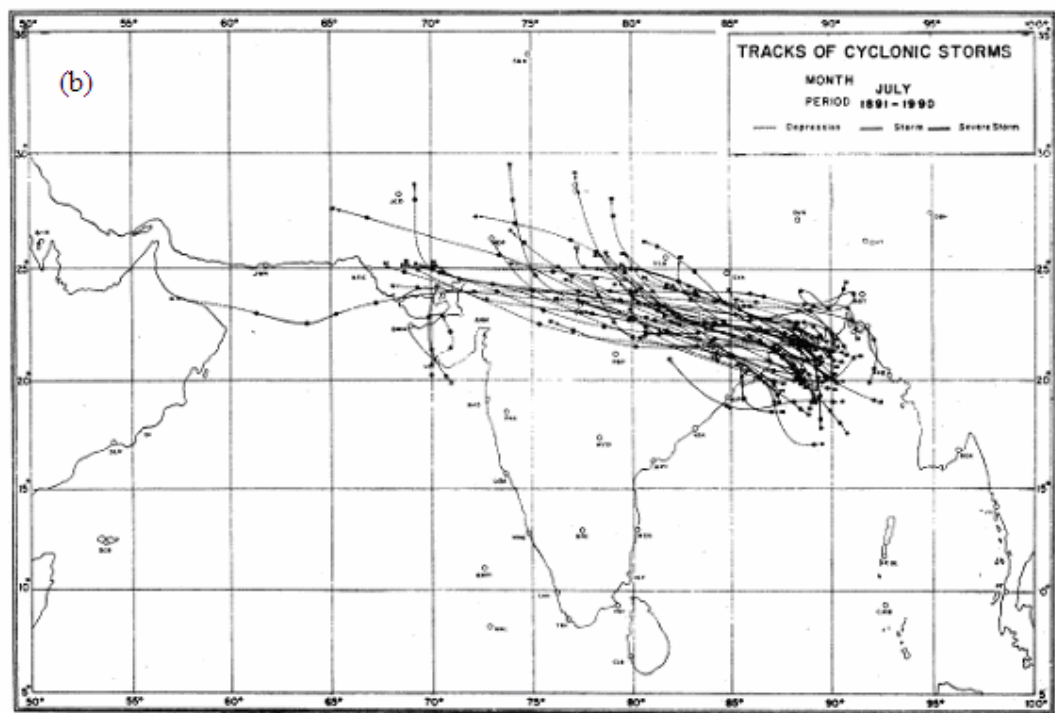
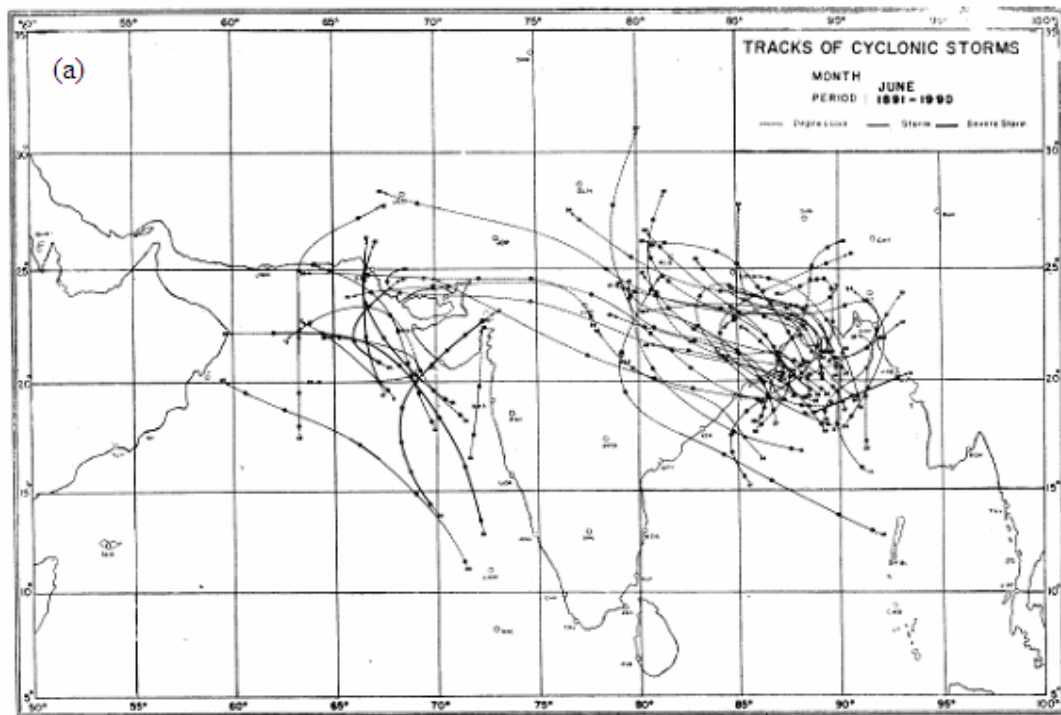


Fig. 1.13: Tracks of storms during (a) June and (b) July over Bay of Bengal (BOB) (source IMD)

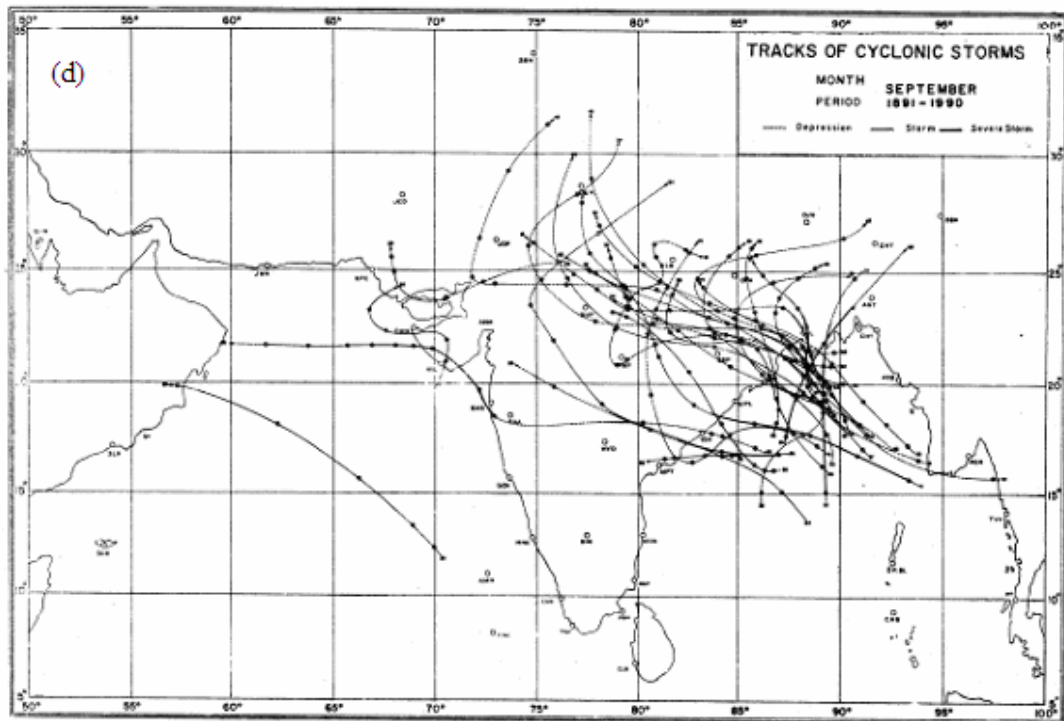
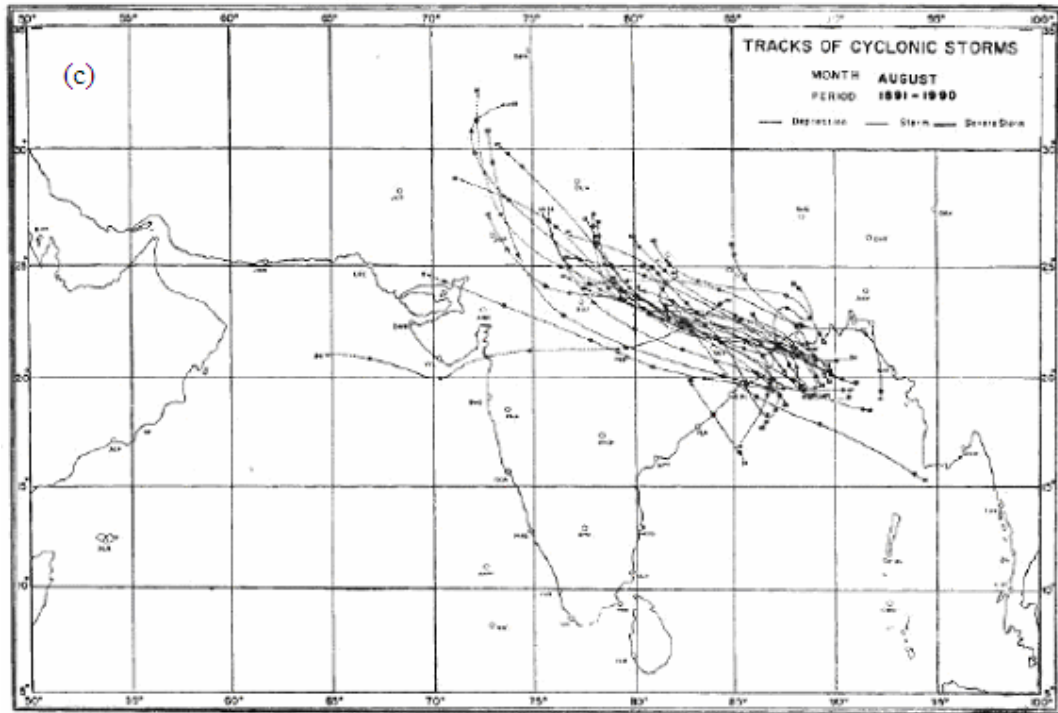


Fig. 1.14: Same as Fig. 1.13, but for (c) August and (d) September.

a single depression had formed. The number of monsoon depressions is also seen to have a decreasing long term trend in recent years (Fig. 1.15). The regression equation with values of  $R^2$  for monsoon depression over Bay of Bengal (BOB) has been obtained for the period 1961-2008. The values of  $R^2$  during the period 1961-2008 are statistically significant at 1% level.

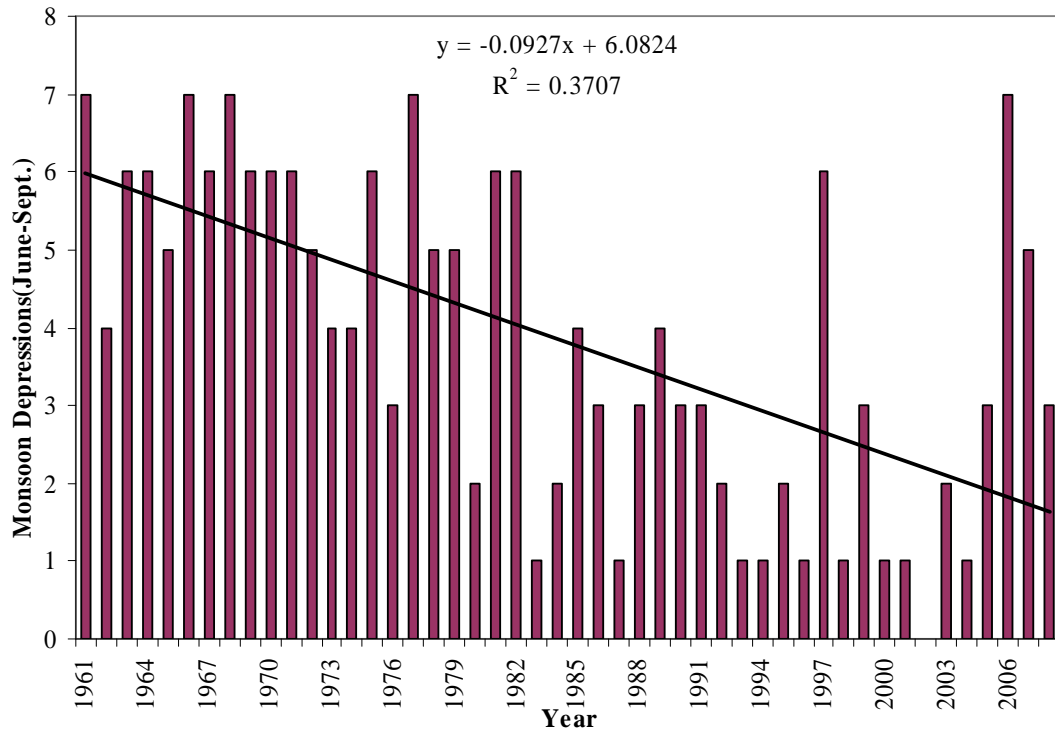


Fig. 1.15: Trends in monsoon depression frequency over Bay of Bengal (BOB).

### 1.5 Objectives with specific aims

Understanding the variability within the natural systems and coping with it are among the most fundamental factors affecting the course of human development. Societies and cultures throughout the world have developed based in large part of their ability to adapt effectively to their anticipated climates. When climatic variables such as temperature and precipitation patterns depart significantly from expected historical seasonal averages, the results, if unanticipated, could be catastrophic. In the Bangladesh context, the interannual variability of SMR occasionally leads to large-scale deficient/droughts and excess/floods over different parts of Bangladesh. In view of the critical influence of such variability on agricultural and industrial production, forecasting of the SMR, at least one season or one

month in advance, assumes profound importance for policy making and planning of mitigatory efforts.

However, not much attention is given to examine the interannual variability of SMR over Bangladesh and to predict SMR also. No global scale teleconnections were explored over Bangladesh for SMR. No previous study has examined the predictive relationship of global circulation anomalies on SMR of Bangladesh also.

In view of the critical importance of the SMR to the economy of Bangladesh and its complex variability in time and space, an attempt is made in the present thesis to examine in detail the rainfall variability over Bangladesh on administrative divisional scale. The overarching objectives of the thesis are to document the detailed characteristics of the interannual variability of SMR, identify regional/global teleconnections and reliable precursors that can be exploited for statistical seasonal prediction, and to develop a suitable prediction scheme. The aims of this work are as follows:

1. to study the details characteristics of the interannual /decadal variability of SMR
2. to identify regional/global teleconnections with the SMR and reliable precursors that can be exploited for statistical seasonal prediction, and to develop a suitable prediction scheme
3. to utilize dynamical model for LRF of SMR in Bangladesh.
4. to project of SMR is made for the year 2015-2034 and 1975-2099 using by AGCM.
5. to compare the results between AGCM SMR and regression model SMR.

## **1.6 Thesis at a glance**

**Chapter 1:** This chapter gives the brief description of the summer monsoon rainfall (SMR) and its variability. It also contains climatological features of SMR season and objectives with specific aims.

**Chapter 2:** This chapter basically focuses on the review of the previous related research works.

**Chapter 3:** This chapter contains the description of the regional/global data sets as well as Bangladesh rainfall data. The details of these data sets, methods of preparation, quality of the data are described in this chapter. The statistical methods used in the study are also discussed in this chapter.

**Chapter 4:** SMR index has been prepared to characterize the strength of the SMR. This index is used for studying the interannual variability of SMR. In this chapter, various aspects of the interannual variability and their implications for large-scale deficient/excess rainfall on administrative divisional scale as well as decadal variability of SMR are also discussed.

**Chapter 5:** In this chapter the teleconnections between SMR and global parameters have been investigated. For this purpose, the spatial patterns of correlations between SMR of Bangladesh and various regional/global meteorological parameters have been worked out to identify precursors for the SMR variability.

**Chapter 6:** This chapter deals with the identification predictors for the long range forecasting (LRF) on the basis of teleconnections for SMR variability. Diagnostic studies of historical data sets, over the years, have been used to identify the reliable predictors for SMR and these predictors constitute as important components of LRF model development. The statistical model has been developed using these predictors.

**Chapter 7:** A high resolution (20 km) climate model (dynamical model) named Meteorological Research Institute-Atmospheric General Circulation Model (MRI-AGCM) is employed in generating SMR for Bangladesh. In this chapter, SMR climatology in Bangladesh derived from 20 km AGCM is calibrated with the observed data for the period 1979-2003 and validated during 2004-2006. The projections for SMR are made during the period 2015-2034 and 2075-2099 in Bangladesh.

**Chapter 8:** This chapter comprises of an overall summary of the research work, along with the major findings and conclusions. Finally, aspects of possible future work to extend the findings from this research are proposed.

## CHAPTER 2

### LITERATURE REVIEW

In this chapter we introduce some of the overview of long range forecast of summer monsoon rainfall (SMR). SMR has not been studied extensively over Bangladesh. Prediction of SMR at least one season in advance is one of the most important problems in tropical climate.

#### 2.1 Reviews on SMR

Kripalani and Kulkarni [6] reported their study the Asian monsoon climate exhibits variability in a variety of time scales. The predictability of the seasonal mean monsoon depends on the nature of the interannual variability (IAV) of the monsoon. Extensive studies on IAV of different components of the Asian monsoon have led to better documentation and better understanding of physical mechanisms responsible for IAV of the monsoon. Various components of the Asian monsoon also exhibit significant interdecadal variability. Modulation of IAV by the interdecadal variability influences predictability of the seasonal monsoon rainfall.

Krishnamurti *et al.* [7] found their study, the correlation between several predictors and the Indian summer monsoon rainfall (ISMR) has been found to undergo interdecadal variations forcing the India Meteorological Department (IMD) to drop many of the original predictors in their recent statistical model. A better understanding of the interdecadal variability may, therefore, be very important in improving the predictability of the seasonal monsoon climate. However, the space-time structure of the monsoon interdecadal variability is less well documented than the IAV and mechanisms responsible for it are poorly understood. This problem is largely related to the lack of availability of good quality data for a sufficiently long period.

Blanford [8], who studied meteorological conditions in relation to the monsoon rainfall of India, concluded that Himalayan snow cover could influence climate and weather of the plains of India. He postulated that excessive winter and spring snowfall in the Himalayas and Hindukush delays the advance of SM and results in less rainfall during monsoon season. He also observed that droughts may be associated with high pressure in Mauritius, Australia and over a great part of Asia. He issued tentative forecasts of monsoon rainfall for the years 1883-1885 on the basis of snowfall in the Himalayas. The

success achieved by these tentative forecasts created a climate of confidence, and it was decided in 1885 that a monsoon forecast be issued routinely every year. The first regular forecast for India and Burma was prepared on June 4, 1886, on the basis of general weather condition over India and on snowfall in the Himalayas and Sulaiman range during January-May preceding the monsoon.

Eliot [9] who succeeded Blanford in 1887, included conditions over the whole of India as a predictor parameter, and in the next year he also included the conditions over the Bay of Bengal and the Arabian Sea. In 1888 and 1889, the forecast consisted of two parts (a) the preliminary memorandum issued in the third week of May and (b) the final memorandum issued about the 9<sup>th</sup> of June. From 1890, the preliminary memorandum was dropped. The forecasts became more and more ambitious and the size of the forecast grew from 3 pages in 1886 to 22 pages in 1892. India experienced another great famine in 1899 which was not predicted and the newspapers made scathing comments on the forecasts.

Walker [10] reported his study, theory of general circulation was necessary for putting seasonal prediction on a scientific basis. He argued that in the absence of such a theory statistical studies can be pursued since the results of such studies are likely to give clues to a possible physical basis. He commenced studies of statistical relationships, both concurrent and antecedent, between Indian weather and world weather. His studies on world weather confirmed two pressure oscillations (a) North Atlantic (between the Azores high and Icelandic low) and (b) North Pacific (between the North Pacific high and the Aleutian low). His search for global predictors for forecasting Indian monsoon rainfall brought out the important result as a pressure see-saw between the Indian Ocean and Argentina is a very large-scale phenomenon. For the first time Walker called this phenomenon the Southern Oscillation. He described this oscillation as a tendency for air to be removed from the Pacific areas for accumulation in and around the Indian Ocean and vice versa.

Walker [11] found that led to the development of the first objective models based on statistical correlations between monsoon rainfall and antecedent global atmosphere, land and ocean parameters. Since then, IMD's operational LRF system has undergone changes in its approach and scope from time to time. Walker also developed regression equations with the predictors: snow accumulation over the Himalayas at the end of May,

South American pressure (mean of March, April and May), Mauritius pressure of May and Zanzibar rain for April and May for forecasting monsoon rainfall over India and Burma. During 1907 and 1908, this regression equation was used only as a guide to the inferences drawn from the current forecast method in use. The issue of official forecasts based on Walker's regression equation commenced from 1909. The objective approach of Walker's forecast method helped in the deletion of detailed discussions about the behavior of the factors and their anticipated influence on monsoon rainfall and thereby considerably reduced the size of the forecast memorandum. Walker also examined the relationship between solar activity, as measured by the annual value of the mean sunspot number, and meteorological parameters at many stations. Based on his empirical studies, Walker was apparently convinced about the reality of the solar-weather relationship, but he concluded that sunspot numbers play only a minor role in influencing the seasonal weather over India.

Walker [12] developed in 1924 the following regression equations for forecasting the normalized anomaly of monsoon rainfall over Peninsular ( $\Delta RP$ ) and Northwest India ( $\Delta RNW$ ).

$$\Delta RP = 0.20P1 - 0.32P2 - 0.24P3 - 0.22P4 - 0.26P5 - 0.12P6 \quad 2.1$$

$$\Delta RNW = 0.04P1 - 0.14P4 - 0.48P5 - 0.30P7 - 0.24P8 - 0.06P9 \quad 2.2$$

where the predictor parameters are,

P1 = normalized anomaly (i.e., anomaly divided by standard deviation) for April and May South American Pressure (mean of Santiago, Buenos Aires and Cordoba).

P2 = normalized Zanzibar May rainfall anomaly.

P3 = normalized Java rainfall (October-February) anomaly.

P4 = normalized Cape Town pressure (September-November) anomaly.

P5 = normalized South Rhodesian rainfall (October-April) anomaly.

P6 = normalized Dutch Harbor temperature (December-April) anomaly.

P7 = normalized anomaly of snow accumulation over the western Himalayas by the end of May.

P8 = normalized anomaly of Dutch Harbor temperature (March-May).

P9 = normalized anomaly of equatorial pressure.

Equatorial pressure =  $\frac{1}{3}$  [ $\frac{1}{2}$  Seychelles Pressure (February + March) +  $\frac{1}{4}$  Batavia Pressure (January-April) +  $\frac{1}{3}$  Port Darwin Pressure (March-May)]

Walker has also mentioned that the multiple correlation coefficients between monsoon rainfall and the predictors used is 0.76 for Peninsular as well as northwest India monsoon rainfall. Until 1955, the predictors used in the regression equations for forecasting monsoon rainfall were from the surface or sea level. In 1956, Calcutta and Bangalore upper level winds were included as predictors in the regression equation for forecasting Peninsular monsoon rainfall and Agra-Gwalior and Calcutta upper level winds in the regression equation for forecasting northwest India monsoon rainfall.

Walker [13] himself verified his forecasting formulae. He computed a forecast of All-India rainfall for the later periods 1909-1921 and 1909-1927 by using the "1908 forecast formula" and then computed correlation coefficients between forecast and actual rainfall. The correlation coefficients for these periods are 0.55 and 0.56 suggesting fairly good stability in the later periods. He also verified the two "1924 forecast formulae" for northwest India and Peninsula for the later period 1924-1936. In all, there were 18 forecasts, 9 for northwest India and 9 for the Peninsula. According to Walker, forecasts should be issued only when there is a 4 to 1 chance of success. In 8 of these forecasts, this condition is satisfied but in 2 cases only the sign of the forecast departure is correct. On a careful scrutiny by Walker of the forecasts issued before the monsoon seasons of 1905-1932, two-third were correct. However, the verification of such general forecasts is subject to uncertainty.

Montgomery [14] who reviewed the work of Walker examined the stability of the predictors used by Walker in the preparation of forecasting formulae for monsoon rainfall by computing the correlation coefficients between monsoon rainfall and these predictors for later periods and comparing these correlation coefficients with those obtained by Walker. Among the predictors used by Walker in his 1924 formula for forecasting of monsoon rainfall for Peninsular India, Montgomery also found that South American pressure, Dutch Harbor temperature and south Rhodesian rainfall have

maintained their original correlation, and have thus exhibited stability. In this connection, it may be mentioned that the lengths of periods over which the correlation coefficients for the predictors for forecasting Peninsula monsoon rainfall have been compared are very dissimilar, the periods used by Montgomery being much smaller. Montgomery carried out verification of Walker's formulae for forecasting monsoon rainfall for the Peninsula. Using Walker's formulae, he computed the forecasts for the later periods 1920-1936 and 1924-1936 and as a measure of verification of these forecasts he computed the correlation coefficients between the forecast and actual rainfall. For the 1919 and 1924 formula the correlation coefficients were 0.21 and 0.12. These small and nonsignificant correlation coefficients showed that the earlier good relationship was not sustained for later periods.

Normand [15] reported the most remarkable of Walker's results was the discovery that the June-August Southern Oscillation Index (SOI) had a correlation coefficient of 0.8 with the same index for the following winter season (December-February) and only 0.2 with that for the preceding winter. Normand also verified the monsoon forecasts issued during the period 1931-1948, 16 each for the Peninsula and northwest India for the whole season, and 14 for the Peninsula and 15 for northwest India for August-September rainfall. Of these 61 forecasts, 10 were wrong. On pure chance, the numbers of forecasts estimated wrong on the basis of a normal distribution, and on the basis of actual distribution for 1931-1948 are 23 and 17, respectively. The number of the wrong forecasts allowable on the 4 to 1 standard was 12. Thus the regression forecasts have done much better than chance forecasts, but only slightly better on the 4 to 1 standard. However, the period 1931-1948 is not quite typical in that it has experienced relatively less droughts. It was also found that the proportion of wrong forecasts for the worst monsoon years was 66 percent, which is large. Considering all these points, Normand posed the question, "Are the relationships, though real, now so small that they are of insufficient value for the issue of useful forecasts?" Finally, Normand expressed the hope that persistent patterns of flow in the middle or upper troposphere may prove to be of prognostic value, but lacking a background of theory we will still have to depend on statistical methods. The development during the last decade, as hoped by Normand, has brought out the April ridge at 500 mb as a middle tropospheric flow parameter characterized by some persistence and well-related to the Indian monsoon rainfall.

Jagannathan and Khandekar [16] reported for the first time, examined the relationship between contour heights of different isobaric surfaces up to 400 mb at Indian radiosonde stations for the months March through May and Indian Peninsular monsoon rainfall, based on the data for 1944-1958. They showed that the height and thickness between two pressure levels for some locations are useful predictors. Utilizing these predictors, they obtained three regression equations based on all data up to 1958 and verified for one independent year 1959. The three regression equations gave forecast departures of Peninsular rainfall as 7.5, 7.9 and 6.1 inches against the actual departure of 11.2 inches.

Jagannathan [17] found his study at present, the India Meteorological Department (IMD) gives its long-range forecast in seven categories, large defect ( $\leq 50\%$  of normal), moderate defect (50% to 74% of normal), slight defect (75% to 89% of normal), normal (90% to 110% of normal), slight excess (11% to 125% of normal), moderate excess (126% to 150% of normal) and large excess ( $> 50\%$  of normal). Jagannathan also studied the stability of the different predictors used by the IMD in the regression equations for forecasting the monsoon rainfall over Peninsular and northwest India over different decades of the period 1881-1960. According to him none of the predictors showed stable correlations over all the decades of the period. It may, however, be mentioned that a decade is perhaps too small for studying the stability of a relationship. The mean standard deviation and covariance and consequently the correlation coefficients for 10-year periods are subjected to high random sampling fluctuations. In view of this, fading of the relationship or change of the relationship from direct to inverse and vice versa could be due to random sampling fluctuations. On the basis of study by Jagannathan, American pressure, Dutch Harbor temperature and Bangalore 6 km winds have shown good stability.

Ramdas [18] evolved a regression equation for forecasting the date of establishment of the summer monsoon over Travancore-Cochin (the present Kerala state), south Kanara, Ratnagiri district and Colaba district. They used April Seychelles rain; mean westerly wind component over Agra (or average of Delhi and Gwalior) from 1 to 3 km during the first half of May, April Darwin pressure, Cochin pressure minus Jaipur pressure in April, October-April south Rhodesian rainfall and April Rhodesian rainfall as predictors. The regression equations were developed on the basis of all available data up to 1950. They have not given any verification on independent years 1951-1954. However, on the basis of the general indication of the behavior of the predictors, they have inferred for these

independent years whether the onset over the west coast (which covers all the four areas) would be about the normal date, not far from the normal date, later than a particular date or earlier than a particular date, and have tried to verify such general forecasts for the west coast.

Gadgil *et al.* [19] addressed in a very recent study, the major problems of the statistical and dynamical methods for LRF of monsoon rainfall in view of the recent forecast failures in 2002 and 2004. Their analysis revealed that IMD's operational forecast skill based on statistical methods has not improved over seven decades despite continued changes in the operational models. For the LRF of the ISMR, three main approaches are used. The first is the statistical method, which uses the historical relationship between the ISMR and global atmosphere-ocean parameters. The second approach is the empirical method based on a time series analysis. This method uses only the time series of past rainfall data and do not use any predictors. The third approach is based on the dynamical method, which uses general circulation models of the atmosphere and oceans to simulate the summer monsoon circulation and associated rainfall. In spite of its inherent problems, at present, statistical models perform better than the dynamical models in the seasonal forecasting of ISMR. The dynamical models have not shown the required skill to accurately simulate the salient features of the mean monsoon and its interannual variability.

Gowariker *et al.* [20] found their study during the period of 1988-2002, IMD's operational forecasts were based on the 16-parameter power regression and parametric models. The forecasts issued during this period were qualitatively correct. However, the mean forecast error during this period was more than the mean error of the forecasts based on climatology alone. This model failed to predict the severe drought of 2002. Following the failure of forecast in 2002, a critical evaluation of the 16-parameter power regression and parametric models was made and in 2003, two new models (8 and 10 parameter models) were introduced for the operational work. Further a two-stage forecasting strategy was also adopted with the provision for a forecast update by end of June/first week of July.

## 2.2 **Review on teleconnection**

Parthasarathy and Pant [21] identified the relationships between the ISMR and the Southern Oscillation. According to them the Correlation Coefficients (CCs) between the

Indian summer monsoon series and the Southern Oscillation Index (SOI) of summer monsoon (JJA), autumn (SON) and winter (DJF) minus spring (MAM) seasons are correlated and significant at 1% level. However, they also reported that the CCs between SOI during the preceding winter and spring seasons and ISMR are not sufficiently high for long range forecasting.

Chowdhury [22] found that other than the summer monsoon (JJAS) could not identify any significant correlation between SOI (during the preceding winter and spring seasons) and rainfall in downstream Bangladesh and upstream India along the greater GBM basins. Other than JJAS, the MAM in Bangladesh did not show any correlation to SOIs. Chowdhury also reported on significant rainfall along with severe flooding during the summer in 1987 and the high correlation of rainfall along the Meghna basin in India and Bangladesh. Chowdhury has identified in his research, except for the Ganges basin where Chowdhury observed some weak-to-moderate association (significant at 5% level). Chowdhury current study also faces several difficulties in understanding this change in the monsoon-ENSO relationship.

Krishnamurti *et al.* [23] reported that during the summer monsoon of 1987, the monsoon was very weak and most of the areas receiving normally abundant rains (e.g. Gangetic plains, the west Ghats, and eastern and central part of India) had deficient rainfall amounting to  $\leq 50\%$  of its normal value. They further added that except for some parts of Bangladesh, west Bengal and Bihar of India, where normal rainfall occurred, the whole region had below normal rainfall. The monsoon withdraws from the northernmost part of India in September 1987. During September, above normal rains over the northeastern states of India resulted in some flooding in that area.

Kumer *et al.* [24] identified that most of the El Ninos are associated with drought years over India, while the La Nina events are associated with flood years. Despite this strong association, quantitative correspondence between the strength of the ENSO and the rainfall anomaly is relatively weak and therefore not sufficient for long range forecasting.

Kripalani *et al.* [25] studied the rainfall variability over Bangladesh, Nepal and India, and investigated connections between them. Their most important result is that rainfall over Bangladesh shows significant positive relationships with rainfall over northeast India (along the Meghna basin) only. The correlation of Bangladesh rainfall with other parts of India is insignificant and even positive.

Kane [26] identified that the dynamic links between ENSO and the weather and climate in the Indo-Pacific region are most effective when, in El Nino years, SO minima and SST maxima occur in the middle of the calendar year. Bangladesh climate is dry only with strong El Nino and SOI minima.

Kinter *et al.* [27] gave some interesting highlights on recent changes in the connection of the Asian monsoon to ENSO. Before 1976, ENSO was uniquely and closely related to the atmospheric circulation and precipitation in the Indian sector. After 1976, the Asian monsoon rainfall was not a good indicator of the activity of ENSO.

Kumar *et al.* [28] identified the weakening of the relationship between the Asian monsoon and ENSO. Therefore, in the context of Bangladesh climate, scientific views about the existence and strength of El Nino and teleconnections with climate anomalies in Bangladesh have been explained by Walker during the 1920s. According to his observations, lower than average atmospheric pressure prevails in the region from Australia to India when higher than average atmospheric pressure prevails in the eastern tropical Pacific Ocean. The scientific reason is that air flows from high pressure regions to low pressure ones. As a result, a huge volume of moisture comes from the Pacific Ocean to Bangladesh and India; due to the prevailing low atmospheric pressure in this area at that time, the moisture laden air rises, causing heavy rainfall in Bangladesh and India. This difference in wind flow is named the Southern Oscillation. It is also called the Walker Circulation. Research in Bangladesh relating to El Nino has just begun. However, there is evidence of historical interest in El Nino and La Nino in Bangladesh during the ancient era.

Hossain *et al.* [29] identified that during major El Nino years Bangladesh is often a victim of flooding, particularly in the case of a high positive value of the SOI.

Douglas *et al.* [30] identified the potential for long range forecasting of flows in the Ganges and concluded that a significant relationship exists between the natural variability of the Ganges annual flow and the ENSO index.

### **2.3 Review on AGCM rainfall**

Kelkar [31] reported in recent years, because of the availability of computer power that was unimaginable decade earlier, it is becoming possible to design models of increasing complexity. However, our knowledge of many of the physical atmospheric and oceanic

processes is yet far from complete, while some of the processes like cloud formation and rain, which are otherwise known well, have not yet been parameterized in models in a satisfactory manner. In the particular case of the monsoon, the anomalies in the surface boundary conditions like snow cover or SST have been used for over a century in statistical models to predict the monsoon rainfall. However, it must be accepted that the complete chain of physical and dynamical connections has not been identified even today. The present generation of Atmospheric General Circulation Models (AGCMs) has such large systematic errors in simulating both the mean and the variability of monsoon rainfall that it is difficult to isolate the result of boundary forcings over the system noise produced by the intrinsic variability due to internal dynamics.

Gates [32] was the first organized international effort to determine the systematic errors of AGCMs on seasonal and interannual time scales in the Atmospheric Model Intercomparison Project (AMIP). For purposes of comparison and validation, all models were run for an identical period of ten years 1979-1988 and with observed SST and sea ice conditions. This was followed by several diagnostic subprojects with emphasis on specific physical processes and phenomena.

Gadgil and Sajani [33] discussed the interannual variation of the Indian monsoon simulated by 30 AGCMs in this major international effort. Under the AMIP diagnostic subproject on the monsoons, an analysis of the seasonal precipitation associated with the African, Asian and the Australian-Indonesian monsoon was carried out. The period chosen for the AMIP runs 1979-1988 included two major ENSO events of 1982-1983 and 1987-1988 and covered a large range of variations of the Indian monsoon rainfall. The AMIP monsoon subproject was therefore able to throw light on how well the models existing at that time could simulate the monsoon variability on the seasonal to interannual time scale. Gadgil and Sajani showed that the seasonal migration of the major rain belt observed over the African region, was reasonably well-simulated by almost all the models. However, the seasonal variation of the rain belt of the Asia-West Pacific sector was captured well only by some models, termed as class I models, but not by others, termed as class II models. For the Indian monsoon, a further complexity arises as during July-August there is a primary rain belt over India, a secondary one over the equatorial Indian Ocean and a third one over the Himalayan foothills. Whereas in some class I models, e.g. Geophysical Fluid Dynamics Laboratory (GFDL), the rainfall over the Indian monsoon zone occurred in association with the seasonal migration of the

planetary scale rain belt, in some class II models, e.g. Centre for Ocean-Land Atmosphere (COLA), the rainfall was associated with a regional system with a smaller longitudinal extent. Very few models were able to distinguish well between good and poor monsoon seasons, but class I models showed better skill in this respect. The mean rainfall pattern for the models of class I over the Indian region was closer to the observed one than for class II. The simulation of the mean rainfall pattern by National Centre for Environmental Prediction (NCEP) appeared to be the most realistic. Some models were able to capture only the deficient rainfall years over India like 1979, 1982, 1986 and 1987 and some other models could simulate only the years of excess rainfall.

Gadgil and Joseph [34] reported their study the early results of the AMIP2 project in which 20 different models were compared for their ability to simulate the monsoon features in the contrasting years 1979, 1982, 1983, 1987 and 1988. It was observed that the NCEP model was able to get the correct sign of the departure from the mean during all the five years, the European Centre for Medium-Range Weather Forecast (ECMWF) model in four out of five years, and the COLA model in only two years. The magnitude of the deficit or excess was not realistically simulated by any of the models, with NCEP overestimating it in three out of five years and ECMWF underestimating it in four years. Another model intercomparison project had been organized under the Climate Variability and Predictability (CLIVAR) Monsoon Intercomparison Project in which 11 AGCMs had been tested. They did not show any skill in their ensemble simulations of the SMR anomalies during the 1997-1998 El Nino events.

Wang *et al.* [35] found their analysis to test the simulation skill of five state-of-the-art AGCMs in seasonal precipitation for a 20-year period 1979-1998. These models were forced by identical observed SST and sea-ice, following the design of the AMIP. Each model made 6-10 member integrations to minimize the weather noise and enhance the climate signal. A multi-model ensemble mean was made to reduce uncertainties arising from the models parameterization of sub grid scale processes. Wang however, demonstrated that climate modeling and prediction by prescribing the lower boundary conditions was inadequate when dealing with the particular phenomenon of the Asian SMR. They showed that an AGCM which can simulate realistic SST-rainfall relationship when coupled with an ocean model fails when forced by the same SSTs that are generated in its coupled run. Observed seasonal mean rainfall and SST anomalies are negatively correlated in heavy rainfall regions of the Asian summer monsoon.

Furthermore, SST anomalies trail behind the rainfall by a month, suggesting that it is the SST anomalies which are forced by the atmospheric anomalies. This means that for a good monsoon prediction, the atmospheric feedback on the SST is critical.

Sajani *et al.* [36] examined the fidelity of the AGCM of the Meteorological Research Institute (MRI), Japan, run in an ensemble mode with observed SST, in simulating ISMR and its interannual variation. While the simple ensemble mean captured the essential features of the rainfall climatology and its extreme anomalies, it still showed a systematic bias in simulating the mean seasonal variation of rainfall over the Asia-Pacific region. When this bias was removed the model was able to capture the precipitation response to fluctuations in SST boundary forcing more realistically. It has been accepted since long that atmospheric process cannot be predicted beyond a time limit of two weeks if they are considered in isolation. Any prediction on a longer time scale can be attempted only with the involvement of land and ocean processes which are far slower and evolve over several months or even years. AGCMs are basically designed for the purposes of short and medium range numerical weather prediction only. If they are run for longer periods, they would not know of the changing ocean conditions, and would have to be provided with SST and sea ice data, either as observed or predicted separately.

## CHAPTER 3

### DATA AND METHODOLOGY

In this chapter, detailed information about the data and methodologies used in the present study is provided.

#### 3.1 Data used

The following are the various types of data sets used in the diagnostics of observed summer monsoon rainfall (SMR) variability and also the analysis of its teleconnections.

##### 3.1.1 Rainfall

Bangladesh Meteorological Department (BMD) rain-gauges daily rainfall data are used in this study. The quality of any rainfall data set depends basically on the network of the rain-gauges and it is important to avoid the inhomogeneity resulting from a variable record length and the associated variable spatial distribution of stations.

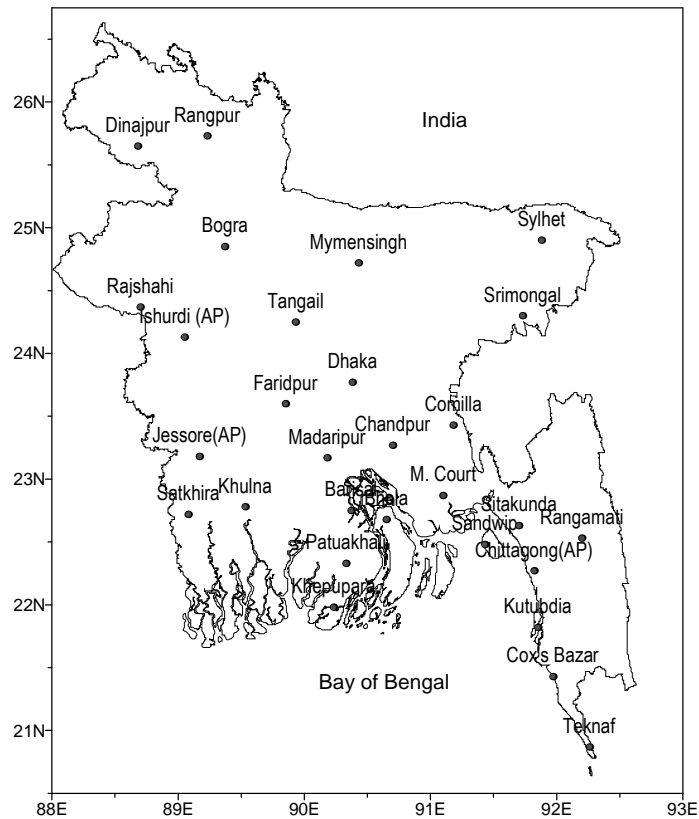


Fig. 3.1: Rain gauge network stations considered over Bangladesh.

Over about 28 stations data beginning from 1961 were scrutinized carefully for their completeness and proper geographical coverage of the country. Fig. 3.1 shows the rain-gauge network considered over Bangladesh. This network is considered to be adequate for administrative divisional and larger spatial means of rainfall over Bangladesh. Rainfall data of the 28 stations are obtained from the BMD.

The monthly Climate Prediction Centre (CPC) Merged Analysis of Precipitation (CMAP) has also been used during the period (1979-2007). The CMAP is a technique which produces pentad and monthly analyses of global precipitation in which observations from rain gauges are merged with precipitation estimates from several satellite-based algorithms (infrared and microwave). The analyses are on a  $2.5^{\circ} \times 2.5^{\circ}$  latitude/longitude grid. Spatial coverage extends from  $88.75^{\circ} \text{ N} - 88.75^{\circ} \text{ S}$  and  $1.25^{\circ} \text{ E} - 358.75^{\circ} \text{ E}$ .

### **3.1.2 NCEP/NCAR reanalysis data**

The National Centre for Environmental Prediction/National Centre for Atmospheric Research (NCEP/NCAR) reanalysis project is using a state-of-the-art analysis/forecast system to perform data assimilation using past data from 1948 to the present [37]. A subset of this data has been processed to create monthly means of a subset of the original data. There are also files containing data from variables derived from the reanalysis and some other statistics. The data assimilation and forecast model are based on the global system which was implemented operationally at NCEP in January 1995. The model is run at a horizontal resolution of T62 (209 km), and with 28 vertical levels.

The monthly mean data sets of various parameters such as Mean Sea Level Pressure (MSLP), Wind and Surface Air temperature (SAT) during the 48 years period 1961-2008 have been used in the present thesis. These data sets have a spatial coverage of  $2.5^{\circ} \times 2.5^{\circ}$  grids with  $144 \times 73$ . NCEP/NCAR data sets are available at 17 pressure levels but for the present thesis, only three levels namely 1000, 850 and 200 hPa have been considered.

### **3.1.3 Sea surface temperature**

The extended reconstructed sea surface temperature (ERSST) data set was constructed using the most recently available International Comprehensive Ocean-Atmosphere data Set of SST data [38] and improved statistical methods that allow stable reconstruction

using sparse data. This data set of SST has a spatial coverage of  $2.0^\circ \times 2.0^\circ$  global grid with  $89 \times 180$  points for the period of 1854-2011. Currently, the ERSST version 2 (ERSST.v2) is available, which is an improved extended reconstruction. In the reconstruction, the high-frequency SST anomalies are reconstructed by fitting to a set of spatial modes. Compared to the earlier reconstruction, version 1 (v1), the improved reconstruction better resolves variations in weak-variance regions.

(a) ENSO index

Monthly Niño3 and Niño3.4 (the region bound by  $150^\circ$ - $90^\circ$  W,  $5^\circ$  S- $5^\circ$  N and  $5^\circ$  N- $5^\circ$  S,  $120^\circ$ - $170^\circ$  W) SST index data for the period 1961-2008 have been taken from the NOAA site.

(b) Indian Ocean Dipole (IOD) index

Indian Ocean Dipole (IOD) index which is an index based on the SST anomaly difference between the western and eastern tropical Indian Ocean for the period 1961-2008 has been taken from HadISST data sets ([www.jamstec.go.jp](http://www.jamstec.go.jp) web site).

### **3.1.4 Outgoing long wave radiation (OLR)**

For this study, NOAA interpolated OLR data from 1961-2008 were used. The data set has a spatial coverage of  $2.5^\circ \times 2.5^\circ$  grids with  $144 \times 73$  points. Interpolated OLR data provided by the NOAA-CIRES Climate Diagnostics Center, Boulder, Colorado, USA, from their Web site. (<http://www.cdc.noaa.gov/>)

### **3.1.5 Monsoon depression data**

Monsoon depression data has been taken from "India Meteorological Department web site" India ([http://www.imd.gov.in/section/nhac/dynamic/Monsoon\\_frame.htm](http://www.imd.gov.in/section/nhac/dynamic/Monsoon_frame.htm)), for the period 1961-2008.

### **3.1.6 MRI-AGCM simulations data**

Atmospheric General Circulation model (AGCM) was run at earth simulator centre in Japan. The output of AGCM has been used to give the LRF for Bangladesh. Depending on the available AGCM data the analysis period was made for 1979-2006, 2015-234 and 2075-2099, respectively. SMR scenario/projection has also been produced by this model for near future and future for Bangladesh. The model has a horizontal spectral truncation

of TL959 corresponding to about a 20 km horizontal grid spacing and has 60 levels with a 0.1 hPa (altitude of about 65 km) top.

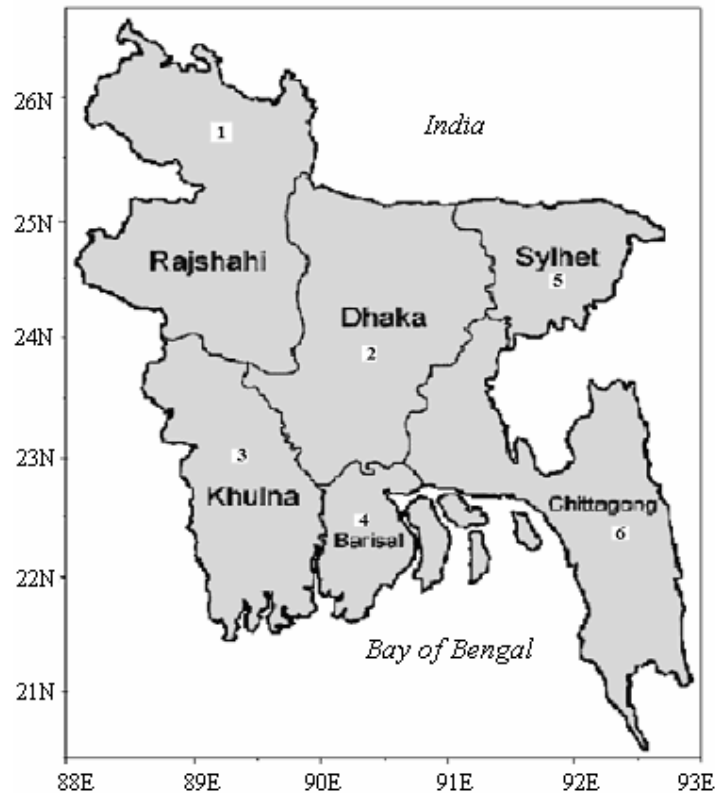


Fig. 3.2: Administrative divisions of Bangladesh.

## 3.2 Methods

### 3.2.1 Rainfall data processing methods

Bangladesh is divided into 6 administrative divisions and these administrative divisions are demarcated based on geopolitical considerations. Fig. 3.2 shows the 6 administrative divisions of Bangladesh namely Rajshahi, Dhaka, Khulna, Barisal, Sylhet and Chittagong among which the administrative divisions 5 (Sylhet) and 6 (Chittagong) some parts are the hilly regions. Rajshahi, Dhaka, Khulna, Barisal, Sylhet and Chittagong consists number of rain-gauge stations by 6, 5, 5, 4, 2 and 10 respectively. The monthly rainfall series for the 6 administrative divisions have been prepared by assigning the district areas as the weight for each rain-gauge station. The number of rain-gauges considered in calculations of administrative division's average.

The above described rainfall series of 6 administrative divisions, have been prepared by using the data from 28 stations during the period 1961-2008. The SMR over the whole country has been calculated as the area weighted average of the monsoon rainfall data of 28 rain-gauge stations (Fig. 3.1) during the above period in Bangladesh. The long period average (LPA) for the period 1961-2000 of the seasonal SMR is 1701 mm and the coefficient of variation is about 11.6%. The SMR of Bangladesh was expressed in percentage departure of LPA.

(a) Composite analysis

Composite analysis is a technique in which the patterns associated with the extremes of a meteorological phenomenon are studied. In this technique, extreme events are calculated by putting some threshold value. For example in case of SMR extremes events are identified as excess and deficient years on the basis of  $\pm 1$  standard deviations of their time series. The mean quantities of various parameters associated with excess and drought years are studied by plotting the respective spatial patterns. On the other hand, calculate the standardized values by subtracting the mean from the original values and dividing by the standard deviation.

### 3.2.2 Statistical model development process

Correlation fields between SMR of Bangladesh and monthly mean SST, SAT and SLP at each grid point in each month were computed by using Mat Lab software. Areas with maximum correlation were identified.

First to identify predictors which are correlated with SMR of Bangladesh based on teleconnections. After identifying the predictors, statistical model has been developed using these predictors for LRF of SMR over Bangladesh.

### 3.2.3 Linear correlation

Correlation denotes the numerical measure of the closeness of agreement between two or more variables. As a measure of intensity or degree of linear relationship between two variables, Karl Pearson developed a formula called *correlation coefficient*. This Pearson's coefficient of the correlation is normally denoted by R.

$$R = \frac{\sum (Y - \bar{Y})(Y' - \bar{Y}')}{\sqrt{\sum (Y - \bar{Y})^2 \sum (Y' - \bar{Y}')^2}}$$

where  $\bar{Y}$  and  $\bar{Y}'$  are the sample averages of the  $Y$  and  $Y'$ , respectively.

The significance test is carried out by using Student's t-distribution:

$$t_{\text{cal}} = r \sqrt{\frac{n-2}{1-r^2}}$$

Where  $r$  is the correlation coefficient,  $n$  is the number of data and  $(n-2)$  is the degree of freedom. If  $t_{\text{cal}} > t_{0.05}$  or  $t_{0.01}$ , the correlation coefficient is significant on the basis of a one-tailed test of Student's distribution.

The model forecasts BIAS and root mean square error (RMSE) are calculated in the following way.

$$\text{BIAS} = \frac{\sum(Y' - Y)}{n}$$

$$\text{RMSE} = \sqrt{\frac{\sum(Y' - Y)^2}{n}}$$

where  $\bar{Y}$  and  $\bar{Y}'$  are the sample averages of the  $Y$  and  $Y'$ , respectively, and  $n$  is the number of training period.

The verification statistics have been used for the category forecasts are (a) hit score (HS), (b) Heidke skill score (HSS), HS is the proportion of the correct forecasts and is computed as the ratio of forecasts in the correct category to the total number of forecasts. The HSS is the HS adjusted to account the proportion of forecasts that would have been correct by chance in the absence of skill and is computed as  $[(3/2) \times \text{HS}] - 1/2$ . For a good model, the HSS should be more than 0.33 (i.e., 1/3rd of the forecasts are categorically correct).

### 3.2.4 Sliding correlations

The secular variations of relationship between SMR and various parameters have been examined by means of sliding correlations. This technique provides an idea of consistency of the relationship between the two variables. In this technique, the correlation coefficient is calculated for each sliding period on the series. The length of the sliding period is selected as 11, 21, 31 years. Generally the length of the sliding period is selected on the basis of length of the time series. For example, if data is 50 years and length of sliding period is 21 years, the correlation coefficients are computed

for sliding period of 1951-71, 1952-72, 1953-73, etc. and the correlation coefficient value is assigned to the central year of the sliding window.

### 3.2.5 Significance between two means

Often, in the analysis of climatic fluctuations, one may be interested not much in the overall behavior of a time series as in a comparison between the mean values of the series in two different periods of records. In a case where an abrupt slippage of the mean is suspected, this approach has an obvious interpretation. However, a test that is especially powerful for detecting inconsistency of the mean in other respects as well, including trend.

If the two means of two sub-periods of the time series are denoted by  $\bar{X}_1$ ,  $\bar{X}_2$  respectively, and the corresponding number of values on which each mean is based is denoted by  $N_1$  and  $N_2$ , the test statistics to be computed is

$$t_d = \frac{\bar{X}_1 - \bar{X}_2 - (\mu_1 - \mu_2)}{\left[ \frac{N_1 S_1^2 + N_2 S_2^2}{N_1 + N_2 - 2} \left( \frac{1}{N_1} + \frac{1}{N_2} \right) \right]^{1/2}}$$

Here,  $(\mu_1 - \mu_2)$  is the expected difference between  $\bar{X}_1$  and  $\bar{X}_2$  according to the null hypothesis, which for the case of randomness is appropriately set equals to zero. The quantities  $S_1^2$  and  $S_2^2$  are respectively the sample variance of  $X_i$  in the two sub-periods.

For null hypothesis of randomness, the distribution of  $t_d$  give above follows the Student's t-distribution for  $(N_1 + N_2 - 2)$  degrees of freedom. The test should be based on a comparison of the magnitude  $|t_d|$  with the t-distribution appropriate to a two-tailed form of test, at the desired level of significance.

### 3.2.6 Regression analysis

Regression analysis goes beyond the demonstration of a casual relationship between two or more variables, by predicting or estimating specific value for one variable in terms of another. Regression methods bring out relations between variables, especially between variables whose relation is imperfect in that we do not have one y for each x.

(i) *Simple linear Regression*

If we take case of two variables X and Y, we shall have two Regression lines:

Regression of X on Y

Regression of Y on X

The former gives the most probable value of X for given values of Y and the latter gives the most probable value of Y for the given value of X. However, when there is a perfect correlation between the two variables, the regression lines between the two variables will coincide. The farther the two regression lines from each other, the lesser the degree of correlation and nearer the two regression lines to each other, the higher is the degree of correlation. If the variables are independent, r is zero and the lines of regression are perpendicular to each other.

The simple regression is of the form  $Y = a + bX$

Where, 'a' and 'b' are called *regression coefficients*. The coefficients 'a' determine the intercept of the fitted line and 'b' determines the slope of the line.

The constants 'a' and 'b' of the equation determine the position of the line completely. After getting the value of 'a' and 'b' we can draw any number of straight line fit to the data. But the problem is how to obtain a single line which best fits the given data. The criterion which is used to determine the best fit is known as method of least squares. The least square criterion demands that the sum of square of vertical deviations or distance from the points to the line is a minimum.

To demonstrate how a least square line is fitted to a set of paired data, let us suppose that the line has the equation.

$$Y = a + bX$$

Where the symbol Y' is used to differentiate between observed values of Y and the corresponding values calculated by the mean of the equation of the line. For each given value of X we thus have an observed value Y and the calculated value Y'.

Now, the least square criterion requires that we find the numerical value of the constants 'a' and 'b' appearing in the equation  $Y' = a + bX$  for which the sum of squares 'E' is given by

$$E = \sum (Y - Y')^2 = \sum (Y - a - bX)^2$$

is as small as possible.

From the principle of maxima and minima, the partial derivative of E with respect to 'a' and 'b' should vanish completely, i.e.

$$\frac{\partial E}{\partial a} = 0 = -2 \sum (Y - a - bX) \quad \text{and} \quad \frac{\partial E}{\partial b} = 0 = 2 \sum (Y - a - bX)X$$

These can be simplified as

$$\begin{aligned} \sum Y &= na + b \sum X \\ \sum XY &= a \sum X + b \sum X^2 \end{aligned}$$

These two equations, known as *normal equations* for the regression line, give a unique solution for 'a' and 'b', satisfying the least square criterion. Here, n is the number of pairs of observations,  $\sum X$  and  $\sum Y$  are, respectively the sums the sum of the given X's and Y's,  $\sum X^2$  is the sum of square of X's and  $\sum XY$  is the sum of the products obtained by multiplying each of the given X's by the corresponding observed value of Y. With the help of regression equation perfect prediction is practically impossible. What is needed, then, is a measure which would indicate how precise or conversely how inaccurate the prediction of Y is, and based on X. The measure is called *standard error of estimate*. The standard error of estimate has the same concept as standard deviation. The standard deviation measures the dispersion about the mean, while the standard error of estimate measures the dispersion about the regression line. The formula for calculating the standard error of estimate is

$$S_{y.x} = \sqrt{\frac{\sum (y - Y')^2}{n - 2}}$$

The smaller the value of standard error of estimate, the closer will be the scatter of the points towards the regression line.

The statistical significance of the regression coefficients is determined by computing their standard errors, as given below:

$$\begin{aligned} S_a &= S_{y.x} \sqrt{\frac{1}{n} + \frac{n\bar{X}^2}{(n\sum X^2) - (\sum X)^2}} \\ S_b &= S_{y.x} \sqrt{\frac{n}{(n\sum X^2) - (\sum X)^2}} \end{aligned}$$

### 3.2.7 Multiple linear regression

The relationship studied by simple linear regression have all been of the type where the changes in one variable were considered as due to, or associated with, the differences in one other variable. But in many types of problem the changes in one other variable may be due to number of other variables, all acting at the same time. Thus the variations in the yield of crop are the combined results of variations in rainfall, temperatures, sunshine, etc., at different stage during the growth season. Under laboratory conditions, all the variables except the one whose effect is being studied can be held constant, and the effect determined of variations in the one remaining varying factor upon the dependent variable.

However, for many of the problems in statistics, like those in atmospheric science, such controls cannot be used. The multiple regressions enable us to understand the nature of and quantify such complex interacting variables.

The simple linear regression model presented in earlier section can easily be generalized to include two or more independent variables as follows.

$$X_1 = a + b_2X_2 + b_3X_3 + \dots + b_{k+1}X_{k+1}$$

Here  $X_1$  represents the dependent variable and  $X_2, X_3, X_4, \dots, X_{k+1}$  represents  $k$  independent variables. This equation is called *multiple regression equation*. The coefficients  $b_2, b_3, \dots, b_{k+1}$  are called *partial regression coefficients*. The partial indicates that they show the relation of  $X_1$  and the corresponding independent variable, excluding the influence the other independent variable. Thus, in the case of two independent variables  $X_2$  and  $X_3$ , excluding the effect of  $X_3$ . In terms of notations used in partial correlation,  $b_2$  is synonymous to  $b_{123}$ . In the multiple regression equation,  $a$ , the  $X_1$  intercept, indicates the mean of the distribution of  $X_1$  when  $X_2 = X_3 = \dots = X_{k+1} = 0$ .  $b_m$  ( $m=2,3,4, \dots, k+1$ ) indicates the change in  $X_1$  when  $X_m$  increases by one unit while the other independent variables remain constant.

The calculation procedure for multiple linear regression equation, which involves estimation of the coefficients  $a, b_2, b_3, \dots, b_{k+1}$  and their tests of significance, is a direct extension of that already discussed for simple linear regression equation above.

The method of least squares stipulates that the sum of squares of deviations,

$$\Sigma(X_1 - X'_1)^2 \text{ i.e. } \Sigma(X_1 - a - b_2X_2 - b_3X_3 - \dots - b_{k+1}X_{k+1})^2$$

should be minimized, where  $X_1$  indicates an estimate of  $X_1$  from the multiple regression equation. For this purpose, the solution is obtained by equating to zero the partial derivatives of the above expression with respect to the coefficients  $a, b_2, b_3, \dots, b_{k+1}$ .

This result in a system of normal equations is as follows:

$$\begin{aligned} \Sigma X_1 &= na + b_2 \Sigma X_2 + b_3 \Sigma X_3 + \dots + b_{k+1} \Sigma X_{k+1} \\ \Sigma X_1 X_2 &= n \Sigma X_2 + b_2 \Sigma X_2^2 + b_3 \Sigma X_2 X_3 + \dots + b_{k+1} \Sigma X_2 X_{k+1} \\ \dots & \dots \dots \dots \dots \dots \\ \dots & \dots \dots \dots \dots \dots \\ \dots & \dots \dots \dots \dots \dots \\ \Sigma X_1 X_{k+1} &= a \Sigma X_{k+1} + b_2 \Sigma X_2 X_{k+1} + b_3 \Sigma X_3 X_{k+1} + \dots + b_{k+1} \Sigma X_{k+1}^2 \end{aligned}$$

These are  $k+1$  simultaneous equations with  $k+1$  unknowns, which uniquely determines the values of  $a, b_2, b_3, \dots, b_{k+1}$ .

The solution of normal equations will become quite laborious there are more than four independent variables. In such case the matrix inversion method is employed to solve them. A computer program for fitting regression equations generally uses this method.

In matrix notation, the normal equations can be expressed as,

$$\begin{bmatrix} \Sigma X_1 \\ \Sigma X_1 X_2 \\ \Sigma X_1 X_3 \\ \dots \\ \dots \\ \dots \\ \Sigma X_1 X_{k+1} \end{bmatrix} = \begin{bmatrix} \Sigma X_2 & \Sigma X_3 & \dots & \Sigma X_{k+1} \\ \Sigma X_2^2 & \Sigma X_2 X_3 & \dots & \Sigma X_2 X_{k+1} \\ \Sigma X_2 X_3 & \Sigma X_3^2 & \dots & \Sigma X_3 X_{k+1} \\ \dots & \dots & \dots & \dots \\ \dots & \dots & \dots & \dots \\ \dots & \dots & \dots & \dots \\ \Sigma X_2 X_{k+1} & \Sigma X_3 X_{k+1} & \dots & \Sigma X_{k+1}^2 \end{bmatrix} \begin{bmatrix} a \\ b_2 \\ b_3 \\ \dots \\ \dots \\ \dots \\ b_{k+1} \end{bmatrix}$$

or in symbolic form  $[C] = [A] [B]$

Now, multiply both sides by the inverse matrix of  $[A]$  i.e.  $[A]^{-1}$

$$[A]^{-1} [C] = [A]^{-1} [A] [B] = [B]$$

Thus the solution of the coefficients contained in  $[B]$  is obtained by multiplying the inverse matrix of  $[A]$  and  $[C]$ .

If, instead of actual values of the variables, their derivatives from respective means are used, the first equations gets eliminated and all the terms will become zero, so that we have k equations to estimate  $b_2, b_3, \dots, b_{k+1}$ . Then we can revert back to the equation in terms of actual values, by estimating from the relation:

$$a = \bar{X}_1 - (b_2 \bar{X}_2 + b_3 \bar{X}_3 + \dots + b_{k+1} \bar{X}_{k+1})$$

where

$\bar{X}_1, \bar{X}_2, \bar{X}_3, \dots, \bar{X}_{k+1}$  are the corresponding means.

### 3.2.8 Moving averages

A moving average dampens fluctuations in a time series by taking successive averages of groups of observations. A moving average of a time series is obtained by replacing each successive, overlapping sequence of 'i' observations in the series by the mean of that sequence. The first sequence contains observations  $X_1, X_2, X_3, \dots, X_i$ , the second sequence contains observations  $X_2, X_3, \dots, X_{i+1}$ , and so on 'i' denotes the length of the moving average. The term 'i' of the moving average should be the same as the period of the seasonal fluctuation's in the time series, or a multiple of the period. The moving average of a particular term is assigned to the mid-point of the period covered by it. However, if the term is an even number, the central point falls between two consecutive time steps. To avoid this, centering is done by taking second moving averages over two time units, on the smoothed series obtained by the first even period moving averages. This synchronizes them with the original time steps.

### 3.2.9 Coefficient of variance

Coefficient of Variation, CV = standard deviation / mean. In other words coefficient of variation is defined ratio of the standard deviation to the mean. The value of CV is calculated only for non-zero mean.

### 3.2.10 Cramer's test

The statistical significance of the moving mean as well as decadal averages was examined using the Cramer's test statistics as follows:

The t-statistics,  $t_k$  is computed as

$$t_k = \frac{\bar{R}_k - \bar{R}}{\sigma} \left[ \frac{n(N-2)}{N-n(1+k^2)} \right]^{0.5}$$

Where,  $\bar{R}_k = \bar{R}_k - \bar{R} / \sigma$

$\bar{R}$  is the mean and  $\sigma$  is the standard deviation of the series for the total number of years (N) under investigation;  $\bar{R}_k$  is the mean for each successive n-year.

### 3.2.11 Calibration process of AGCM

Observational data of BMD has been used for validation of high resolution AGCM generated SMR during the period 1979-2006. The BMD observation network density is very low. Many grids are found which contain no observation site when the whole Bangladesh is gridded at 20 km by 20 km in the model resolution. Since, it is important to find the appropriate calibration method for the application of high resolution AGCM for seasonal SMR studies in Bangladesh, analyses have been carried out on point-to-point basis. In this procedure, observational data at a particular site is considered as the representative for that location [39]. Grid value of the model data is compared with the observed data representing that grid. If more than one observation site exist within a grid, the average value of all the observational sites within that grid is considered as representative value for that grid. Daily rain-gauge rainfall data collected from BMD are processed to obtain monthly and seasonal values. The model simulated rainfall are extracted through GrADS for 28 sites of BMD (point value) and then are converted into monthly and seasonal values which are then averaged to obtain as a country average. Estimated rainfall is also obtained by using equation (3.1) for validation.

The bias correction method of the World Climate Research Programme (WCRP) is used in this study as described WCRP [40]. To find out the estimated rainfall the following equation is used:

$$RF_{\text{estimated}} = \langle X \rangle + (Y_j - \langle Y \rangle) \quad (3.1)$$

Where  $RF_{\text{estimated}}$  is the rainfall that will be projected for future,  $\langle X \rangle$  and  $\langle Y \rangle$  are the long term climatological averages derived from the observed and model variable (for the observed period 1979-2003),  $j$  identifies the initial times and  $r$  the forecast range. This estimated rainfall is useful for validation of high resolution AGCM in Bangladesh.

## CHAPTER 4

### RAINFALL VARIABILITY OF SUMMER MONSOON

#### 4.1 Introduction

The summer monsoon (SM) contributes around 70.7% of its annual rainfall over Bangladesh. Therefore, failure of monsoon in any particular year over a particular administrative division results in drought situation, ultimately affecting the economics of the country.

Study of interannual variability of SM over Bangladesh so far has been very limited. Predicting the likely physical behavior of the monsoon system and the resulting distribution of rainfall over different part/region of Bangladesh of the SM season is an extremely challenging task. Bangladesh is a small country with a multiplicity of climate patterns like northwest regions get less rainfall and northeast and southeast regions get more rainfall during SM season in Bangladesh. Farmer wants to know in advance of the arrival date of the monsoon so that they can plan and organize their activities during the SM season accordingly.

In order to simplify matters, meteorologists have taken recourse to averaging the monsoon rainfall over the country as a whole and over the entire monsoon season. For simplicity of computation and comparability of statistics, the period 1 June to 30 September has come to be regarded as the SM season, regardless of the fact that the dates of commencement and cessation of monsoon rainfall differ widely across the Bangladesh. Summer monsoon rainfall (SMR) has been found to serve as a good index of the overall monsoon behavior for the country and SM season as a whole for any year.

This chapter describes the SMR as well as its index. The index so identified will be used to study the various aspects of interannual and decadal variability of SMR as well as the administrative divisional monsoon rainfall, the dominant spatial modes in the monsoon rainfall over Bangladesh and periodicities in various rainfall series. For this purpose rainfall data during the period 1961-2008 has been used.

## 4.2 Interannual variability of SMR

The nature of the interannual variability of the SMR in Fig. 4.1 depicts the manner in which the SMR has varied between 1961 and 2008, the Fig. 4.1 showing the departure from the normal rainfall value of 1701 mm in each year during this period. Fig. 4.1 shows the interannual variability of all Bangladesh area weighted seasonal monsoon rainfall expressed as the percentage departures from LPA for the period 1961-2000. The LPA for the period 1961-2000 is 1701 mm. In Fig. 4.1 the horizontal dashed lines correspond to the  $\pm 11.6\%$  departure. The years in which the percentage departures are less than  $-11.6\%$  or more than  $+11.6\%$  are called deficient (excess) or drought (flood) monsoon years. Remaining years are called normal monsoon years. It is seen that the deficient rainfall during the period 1961-2008, the lowest and second lowest seasonal rainfall have occurred in 1972 (77.3% of the normal) and 1962 (81.8% of the normal) and excess rainfall at the same period, highest and second highest in 2004 (126.3%) and 1984 (124.6%), respectively. There were 8 excess monsoon years and 8 deficient monsoon years i.e. fifty-fifty excess and deficient years on the above period (1961-2008). Of the observed 8 deficient years, 5 years (about 67%) occurred in the first 20 years period (1961-1980) and one excess year (1974) occurred at the same period. During the long prevailing period of 1981-2008, there were only three deficient years (1989, 1992 and 1994) and 8 excess years (1974, 1984, 1987, 1993, 1999, 2002, 2004 and 2007) for the same period. During the recent 14 years (1995-2008), there were no deficient rainfall years. Two consecutive deficient years, as in 1972-1973 and 1992-1994 were rare events in the history of SMR over Bangladesh. There were two cases of one after one year of two consecutive excess years (1984 & 1987 and 2002 & 2004). The pairs of years 1973-1974 and 1993-1994 show extreme contrasting events of SMR of Bangladesh, the interannual difference in the rainfall being highest during 1973-1974 (about 13% of the normal). Also there is no case of the occurrence of three or more consecutive deficient/excess monsoon years during the period 1961-2008. It is observed that the most noticing point in the rainfall series is that the magnitude of positive highest anomaly is relatively higher than that of negative highest anomaly. This could be due to the fact that large-scale vertical motion and moisture convergence, which brings rainfall, on scale of the country as a whole, under persistent excess/flood conditions. The good rainfall regimes occur on the scale of synoptic scale disturbances, enhancing rainfall over the area of ascent. Table 4.1 shows the seasonal rainfall anomalies for excess and deficient

rainfall seasons over Bangladesh for the period 1961-2008. Again it is seen that the deficient years are characterized by persistent negative monthly rainfall anomalies during the entire monsoon season. Excess rainfall years, on the other hand, show greater variability from one to the other monsoon months.

Fig. 4.1 shows solid circle represent the El Nino years and open circle represent the La Nina years. Out of the 8 deficit/drought years during the period of 1961-2008, 3 years (about 38%) were associated with El Nino events. Similarly out of the 8 excess years, 3 years (about 38%) were associated with La Nina events. This indicates that the association between deficient monsoon rainfall and El Nino is not strong than that between excess monsoon rainfall and La Nina, i.e. fifty-fifty relation and that there are forcing other than the SSTs over east Pacific as well as Indian Ocean, which can influence the Indian monsoon as well as Bangladesh monsoon.

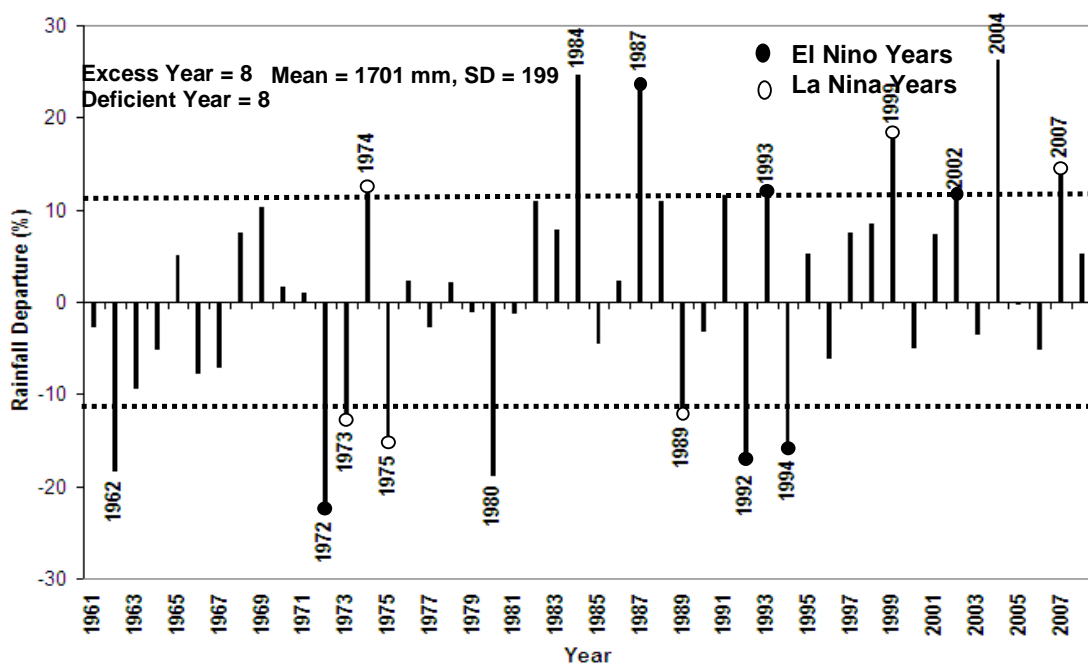


Fig. 4.1: Interannual variability of SMR of Bangladesh.

### 4.3 SMR patterns

Spatial distribution of SMR for the period 1961-2008 is represented in Fig. 4.2. Some places orography play an important role in determining the spatial distribution of rainfall over Bangladesh.

Table 4.1: Seasonal rainfall anomalies observed over Bangladesh during extreme SMR years during the period 1961-2008.

| Excess Monsoon Rainfall Years |          | Deficient Monsoon Rainfall Years |          |
|-------------------------------|----------|----------------------------------|----------|
| Years                         | JJAS (%) | Years                            | JJAS (%) |
| 1974                          | 13.2     | 1962                             | -18.2    |
| 1984                          | 24.6     | 1972                             | -22.7    |
| 1987                          | 24.3     | 1973                             | -12.8    |
| 1993                          | 12.1     | 1975                             | -15.5    |
| 1999                          | 18.6     | 1980                             | -18.7    |
| 2002                          | 11.6     | 1989                             | -12.3    |
| 2004                          | 26.2     | 1992                             | -17.6    |
| 2007                          | 15.0     | 1994                             | -16.0    |

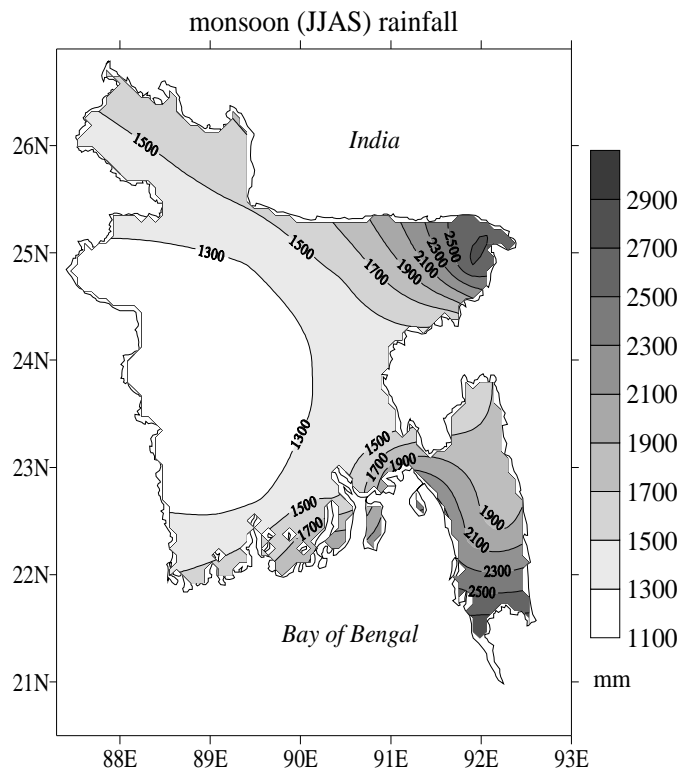


Fig. 4.2: The spatial distribution of SMR of Bangladesh during the period 1961-2008.

The lowest rainfall shows over western region of Bangladesh. The highest rainfall, more than 2900 mm, is received over the northeast region due to orographically induced precipitation. The gradient of precipitation along the west-east direction in northeast and

southeast region is very high. These patterns are primarily determined by the SM, which is called the rainy season in Bangladesh.

#### **4.3.1 Identification of homogeneous administrative divisional monsoon rainfall**

To define the SMR season over Bangladesh, June to September rainfall over various administrative divisions of this country has been worked out. It has been found that six administrative divisions namely Dhaka, Chittagong, Sylhet, Rajshahi, Khulna and Barisal, though with vastly varying contribution to the annual rainfall as well as SMR. Out of the six administrative divisions, Sylhet has the highest percentage of its annual rainfall contributed by the SMR, whereas Khulna has the lowest rainfall contribute during SMR. The annual cycles of rainfall over Bangladesh as well as its administrative divisions are presented in Fig. 4.3.

The Fig. 4.3 analysis forms the basis to define a homogeneous region for SMR index. Chittagong (Table 4.2) receives 74.6% (2211.7 mm) of its annual rainfall during the SM season, whereas in terms of absolute quantity, Sylhet receives more amount of rainfall than Chittagong. Sylhet hilly region receives most of its annual rainfall during SM season (2107.6 mm), and its annual percentage during SM season is 64.6%. However, SMR of Barisal administrative division is 1656.9 mm, Dhaka administrative division is 1358 mm, Rajshahi administrative division is 1325.8 mm, and Khulna administrative division is 1206.4 mm, where the annual contribution of SMR are 70.7, 65.4, 73.8 and 71.2% respectively as shown in Table 4.2. To further establish the homogeneity of the constituent administrative divisions, the correlation matrix among the administrative divisions rainfall for 48 years (1961-2008) has been examined. This indicates that the intercorrelations between the administrative divisions are positive and statistically significant at 5% level (Table 4.3). Homogeneous SM administrative division has thus been identified, firstly on the basis of rainfall received during the SM season and secondly with the help of relationships between the administrative divisions.

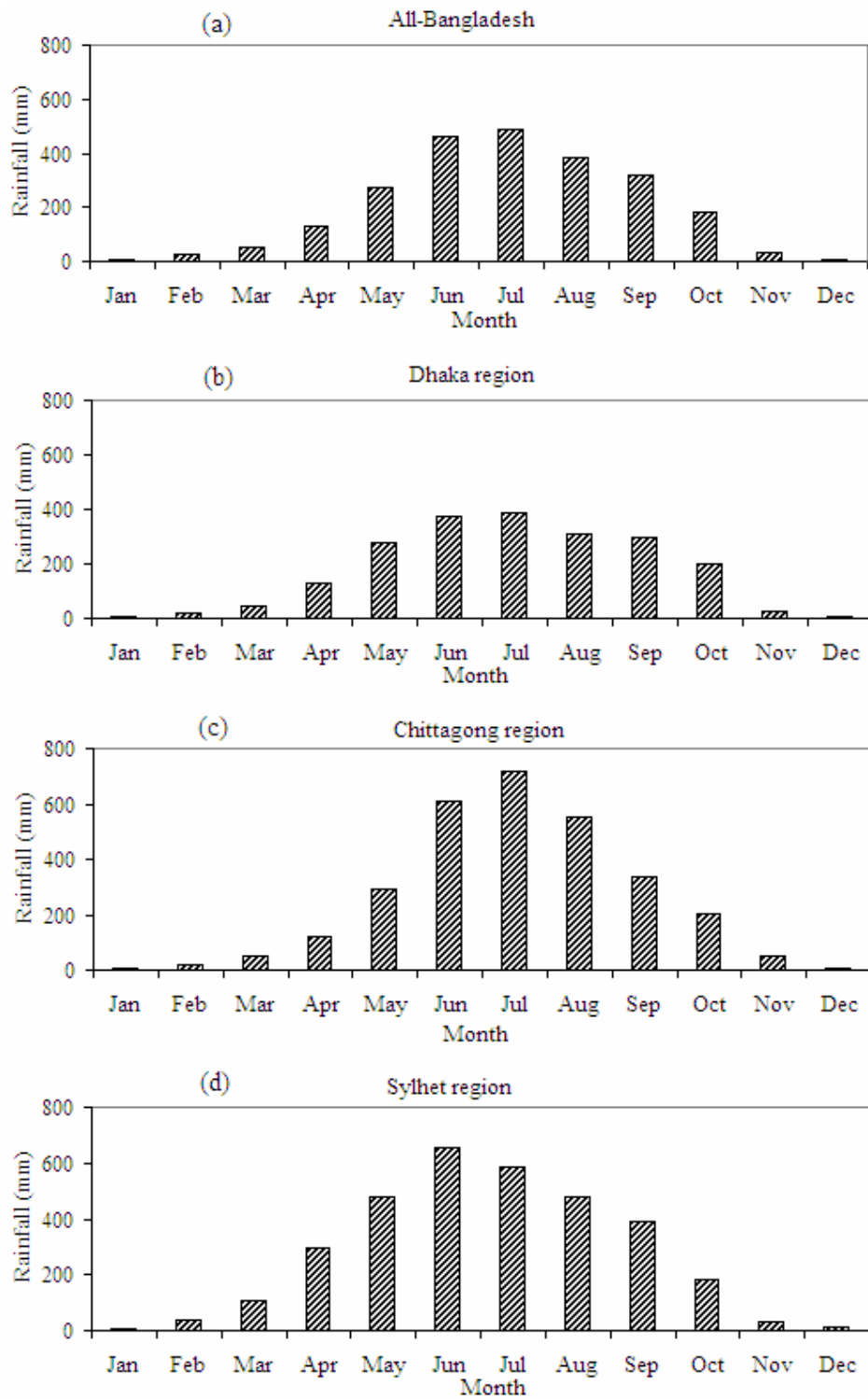


Fig. 4.3: Annual cycles of rainfall (mm) over Bangladesh including six administrative divisions namely (a) All-Bangladesh, (b) Dhaka, (c) Chittagong and (d) Sylhet.

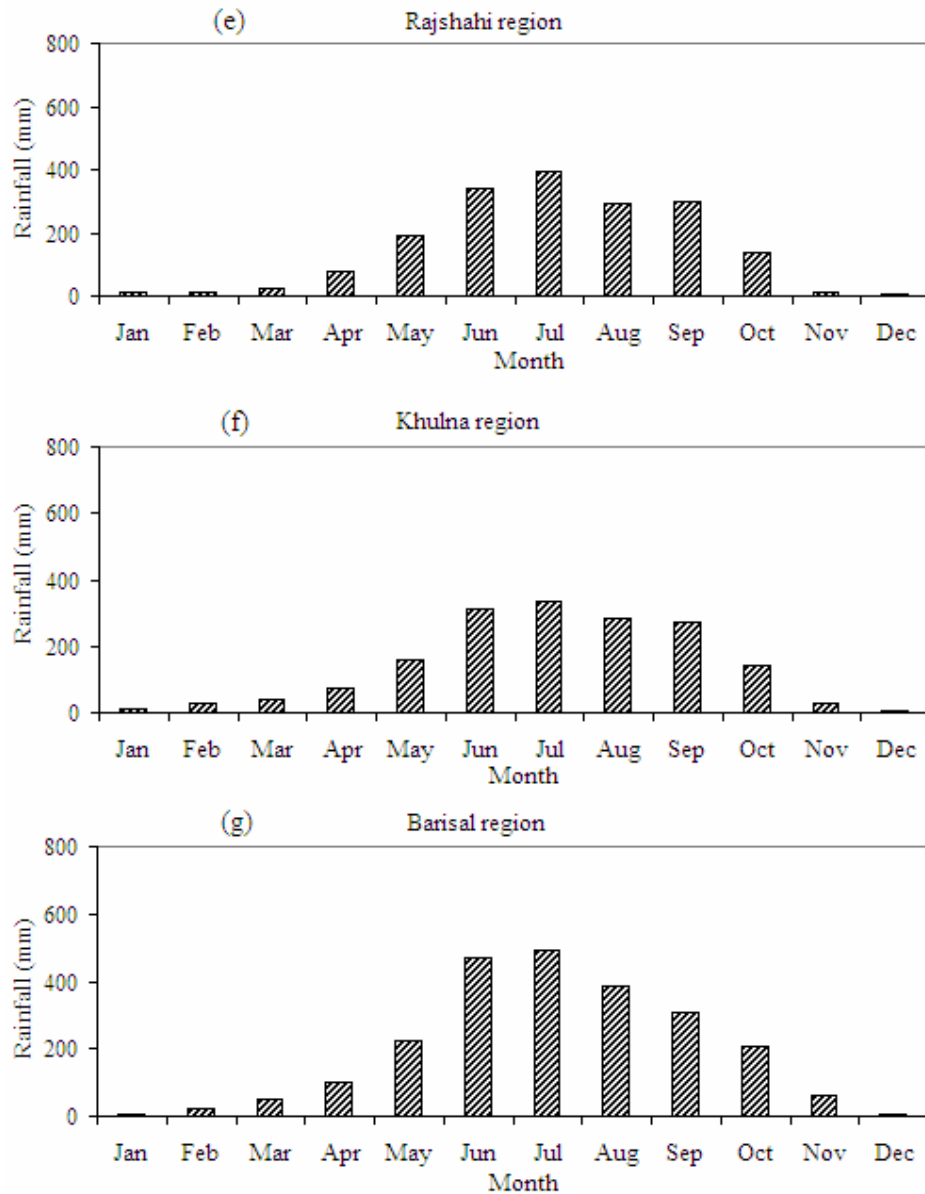


Fig. 4.4: Same as Fig. 4.3, but for (e) Rajshahi, (f) Khulna and (g) Barisal.

Area weighted average time series of SM administrative division is prepared on the basis of homogeneous region so identified. Area weighted time series of SM region is correlated with all the six administrative divisions of SM region (Table 4.3). It is very much clear from the table that area weighted time series of SM region is statistically significantly (at 5% level) correlated with rainfall over each of 6 administrative divisions.

Table 4.2: Statistical properties of SMR over Bangladesh and six administrative divisions for the period 1961- 2008.

| <b>Statistics</b>                     | <b>June<br/>(mm)</b> | <b>July<br/>(mm)</b> | <b>August<br/>(mm)</b> | <b>September<br/>(mm)</b> | <b>June-<br/>Sept.<br/>(mm)</b> | <b>Annual<br/>rainfall<br/>(mm)</b> |
|---------------------------------------|----------------------|----------------------|------------------------|---------------------------|---------------------------------|-------------------------------------|
| <b>SMR over Bangladesh</b>            |                      |                      |                        |                           |                                 |                                     |
| Rainfall (mm)                         | 461.8                | 515.6                | 420.4                  | 303.3                     | 1701.0                          | 2404.0                              |
| Standard Deviation (mm)               | 111.3                | 108.7                | 102.8                  | 75.3                      | 199                             | -                                   |
| CV (%)                                | 23.9                 | 21.1                 | 24.4                   | 24.7                      | 11.6                            | -                                   |
| Rainfall as percent of season's total | 27.1                 | 30.3                 | 24.7                   | 17.8                      | -                               | -                                   |
| Seasons total as percent of Annual    | -                    | -                    | -                      | -                         | 70.7                            | -                                   |
| <b>Dhaka</b>                          |                      |                      |                        |                           |                                 |                                     |
| Rainfall (mm)                         | 371.9                | 383.9                | 306.7                  | 295.5                     | 1358.0                          | 2077.0                              |
| Standard Deviation (mm)               | 119.2                | 114.1                | 103.4                  | 136.8                     | 238.0                           | -                                   |
| CV (%)                                | 32.1                 | 29.7                 | 33.7                   | 46.3                      | 17.5                            | -                                   |
| Rainfall as percent of season's total | 27.4                 | 28.3                 | 22.6                   | 21.8                      | -                               | -                                   |
| Seasons total as percent of Annual    | -                    | -                    | -                      | -                         | 65.4                            | -                                   |
| <b>Chittagong</b>                     |                      |                      |                        |                           |                                 |                                     |
| Rainfall (mm)                         | 610.2                | 715.8                | 551.2                  | 334.5                     | 2211.7                          | 2966.7                              |
| Standard Deviation (mm)               | 183.6                | 175.0                | 167.1                  | 122.0                     | 312.9                           | -                                   |
| CV (%)                                | 30.1                 | 24.4                 | 30.3                   | 36.5                      | 14.1                            | -                                   |
| Rainfall as percent of season's total | 27.6                 | 32.4                 | 24.9                   | 15.1                      | -                               | -                                   |
| Seasons total as percent of Annual    | -                    | -                    | -                      | -                         | 74.6                            | -                                   |
| <b>Rajshahi</b>                       |                      |                      |                        |                           |                                 |                                     |
| Rainfall (mm)                         | 340.9                | 395.5                | 293.7                  | 295.7                     | 1325.8                          | 1796.8                              |
| Standard Deviation (mm)               | 130.2                | 124.7                | 101.0                  | 110.0                     | 249.1                           | -                                   |
| CV (%)                                | 38.2                 | 31.5                 | 34.4                   | 37.2                      | 18.8                            | -                                   |
| Rainfall as percent of season's total | 25.7                 | 29.8                 | 22.2                   | 22.3                      | -                               | -                                   |
| Seasons total as percent of Annual    | -                    | -                    | -                      | -                         | 73.8                            | -                                   |

| <b>Statistics</b>                     | <b>June<br/>(mm)</b> | <b>July<br/>(mm)</b> | <b>August<br/>(mm)</b> | <b>September<br/>(mm)</b> | <b>June-<br/>Sept.<br/>(mm)</b> | <b>Annual<br/>rainfall<br/>(mm)</b> |
|---------------------------------------|----------------------|----------------------|------------------------|---------------------------|---------------------------------|-------------------------------------|
| <b>Khulna</b>                         |                      |                      |                        |                           |                                 |                                     |
| Rainfall (mm)                         | 314.2                | 336.1                | 284.5                  | 271.7                     | 1206.4                          | 1695.5                              |
| Standard Deviation (mm)               | 108.8                | 111.1                | 83.4                   | 118.0                     | 226.6                           | -                                   |
| CV (%)                                | 34.6                 | 33.1                 | 29.3                   | 43.4                      | 18.8                            | -                                   |
| Rainfall as percent of season's total | 26.0                 | 27.9                 | 23.6                   | 22.5                      | -                               | -                                   |
| Seasons total as percent of Annual    | -                    | -                    | -                      | -                         | 71.2                            | -                                   |
| <b>Barisal</b>                        |                      |                      |                        |                           |                                 |                                     |
| Rainfall (mm)                         | 470.0                | 491.5                | 388.0                  | 307.5                     | 1656.9                          | 2343.0                              |
| Standard Deviation (mm)               | 179.1                | 144.4                | 107.4                  | 123.0                     | 265.6                           |                                     |
| CV (%)                                | 38.1                 | 29.4                 | 27.7                   | 40.0                      | 16.0                            | -                                   |
| Rainfall as percent of season's total | 28.4                 | 29.7                 | 23.4                   | 18.6                      | -                               | -                                   |
| Seasons total as percent of Annual    | -                    | -                    | -                      | -                         | 70.7                            |                                     |
| <b>Sylhet</b>                         |                      |                      |                        |                           |                                 |                                     |
| Rainfall (mm)                         | 652.7                | 585.2                | 479.2                  | 390.5                     | 2107.6                          | 3261.6                              |
| Standard Deviation (mm)               | 200.3                | 197.4                | 152.9                  | 154.3                     | 398.0                           | -                                   |
| CV (%)                                | 30.7                 | 33.7                 | 31.9                   | 39.5                      | 18.9                            | -                                   |
| Rainfall as percent of season's total | 31.0                 | 27.8                 | 22.7                   | 18.5                      | -                               | -                                   |
| Seasons total as percent of Annual    | -                    | -                    | -                      | -                         | 64.6                            | -                                   |

Table 4.3: Correlations between SMR and different administrative divisions of Bangladesh. Most of the values are significant about above 5% level, for the period 1961-2008.

| Region     | SM  | Dhaka | Chittagong | Rajshahi | Khulna | Barisal | Sylhet |
|------------|-----|-------|------------|----------|--------|---------|--------|
| SM         | 1.0 |       |            |          |        |         |        |
| Dhaka      | 0.7 | 1.0   |            |          |        |         |        |
| Chittagong | 0.7 | 0.4   | 1.0        |          |        |         |        |
| Rajshahi   | 0.7 | 0.5   | 0.3        | 1.0      |        |         |        |
| Khulna     | 0.6 | 0.4   | 0.3        | 0.4      | 1.0    |         |        |
| Barisal    | 0.6 | 0.2   | 0.4        | 0.4      | 0.4    | 1.0     |        |
| Sylhet     | 0.5 | 0.2   | 0.2        | 0.2      | 0.1    | 0.0     | 1.0    |

#### 4.4 Statistical properties of SMR

The statistical properties of SMR and six administrative divisional rainfall series, like average/mean rainfall, standard deviation, coefficient of variation, range of highest and lowest rainfall recorded with years for the period 1961-2008 have been discussed. The main statistical parameters are given in Table 4.2.

##### 4.4.1 Mean seasonal rainfall and its annual contribution

The mean SMR is 1701 mm, which is 70.7% of its annual rainfall. Chittagong receives highest amount of rainfall 2211.7 mm, Khulna receives the lowest amount of rainfall 1206.4 mm, Rajshahi receives 1325.8 mm but percentage wise it is 74.6%, 71.2% and 73.8%, respectively, of its annual.

##### 4.4.2 Standard deviation and coefficient of variation

The standard deviation of SMR series is 199 mm, and coefficient of variation (CV) is 11.6%. For different administrative divisions, lower CVs are observed over higher rainfall regions; lowest and highest CVs are 14.1% and 18.9% in Chittagong and Sylhet, respectively (Table 4.2).

##### 4.4.3 Range and extreme years

The range is the simplest measure of dispersion. This is the difference between highest and lowest observed values. The details of the range and range expressed as percentage of normal, highest, and lowest rainfall observed along with the corresponding years are

given in Table 4.4. It is seen from the table that the range for SMR series is 833 mm and it is about 49% of the normal. The highest recorded rainfall is 2148.0 mm in the year 2004 and it is about 26% more than normal. The lowest observed rainfall in the year 1972 was 1315.6 mm which is 23% below normal.

The extreme variability of the SMR of different administrative divisions of Bangladesh has also been brought out in Table 4.4. It is seen that there are no administrative divisions with the range smaller than their mean. There are four administrative divisions namely Dhaka, Rajshahi, Khulna and Sylhet, for which the range is more than seventy percent of its mean.

In all, the six administrative divisions, the highest rainfall recorded during the SM season was more than 49% above normal. There are four administrative divisions in which the highest rainfall was more than 38% above normal, viz., Dhaka (149.4% above normal, 1984), Rajshahi (145.5% above normal, 1987) Khulna (138.9% above normal, 2004) and Sylhet (144.7% above normal, 1974). In all the 6 administrative divisions, the lowest year recorded rainfall was less than about 39% of its normal except in Dhaka and Chittagong, where it was about 32% less than the normal. The year of lowest seasonal rainfall was 1972 for SM as well as for two administrative divisions namely Khulna and Rajshahi, respectively. The rainfall received over Chittagong and Sylhet in 1980 below normal was 32% and 40%, respectively. It can thus be seen that over Bangladesh the incidence of lowest rainfall can be of much larger extent than the incidence of highest rainfall.

Table 4.4: SMR of Bangladesh and its administrative division's highest and lowest rainfall records and range during the period 1961-2008.

| Region     | Highest rainfall record |               |             | Lowest rainfall record |               |             | Range  |           |
|------------|-------------------------|---------------|-------------|------------------------|---------------|-------------|--------|-----------|
|            | Year                    | Rainfall (mm) | % of Normal | Year                   | Rainfall (mm) | % of Normal | mm     | % of Mean |
| SM         | 2004                    | 2148.0        | 126.3       | 1972                   | 1315.0        | 77.3        | 833.0  | 48.9      |
| Dhaka      | 1984                    | 2029.3        | 149.4       | 1994                   | 921.0         | 67.8        | 1108.3 | 81.6      |
| Chittagong | 1961                    | 2749.6        | 124.3       | 1980                   | 1510.2        | 68.3        | 1239.4 | 56.0      |
| Rajshahi   | 1987                    | 1928.8        | 145.5       | 1994                   | 819.4         | 61.8        | 1109.4 | 83.6      |
| Khulna     | 2004                    | 1676.0        | 138.9       | 1966                   | 735.7         | 61.0        | 940.5  | 77.9      |
| Barisal    | 1979                    | 2031.3        | 122.6       | 1964                   | 938.0         | 56.6        | 1093.3 | 65.9      |
| Sylhet     | 1974                    | 3050.0        | 144.7       | 1980                   | 1261.5        | 60.0        | 1788.5 | 84.8      |

## 4.5 Excess and deficient rainfall years of SM

The amount of rainfall received over Bangladesh during SM is an important factor in assessing the amount of water available to meet various demands of agriculture, irrigation and other human activities. Therefore, distribution of rainfall in time and space is very important factor to be examined critically. A common method to identify the excess and deficient rainfall years on an administrative divisional scale is, if the departure of rainfall in a year is -11.6% or less than -11.6%, it is said to be deficient/drought year and if 11.6% or greater than 11.6%, it is called to be excess/flood year. This criterion is based on only mean rainfall and does not take variability of rainfall over the administrative divisional region into consideration. In view of this, following criterion is used to identify the deficient and excess rainfall years.

Let  $X$  is the SMR for the  $i^{\text{th}}$  year,  $M$  is the long term mean, and  $CV$  is the Coefficient of Variation in percent. Then, if  $X \geq M+CV$ , the  $i^{\text{th}}$  year is called the excess rainfall year and if  $X \leq M-CV$ , the  $i^{\text{th}}$  year is called the deficient rainfall year(IMD). All the excess and deficient years defined by the above criterion are given decade wise in Table 4.5 and Table 4.6, respectively. If the number of excess/deficient year in a decade is greater than 3, it may be considered as a decade of high incidence of excess/deficient rainfall.

The rainfall time series of SMR of Bangladesh and all six administrative divisions are shown in Fig. 4.1 and Figs. 4.5. Brief description is given below for all the rainfall time series regarding excess and deficient rainfall years, frequencies of occurrence of two/three consecutive excess and deficient rainfall years, decades of high incidence of excess/deficient rainfall, and decades free from excess and deficient rainfall years.

Table 4.5: Excess rainfall year (1961-2008) of SM season

Excess year  $\geq$  mean + CV

| Region/<br>Decade | SM<br>season    | Dhaka    | Chittagong      | Rajshahi | Khulna          | Barisal             | Sylhet          |
|-------------------|-----------------|----------|-----------------|----------|-----------------|---------------------|-----------------|
| 1961-1970         | -               | 1965     | 1961, 65        | -        | 1965,<br>70     | 1969                | 1970            |
| 1971-1980         | 1974            | 1971     | -               | 1973, 76 | 1974,<br>78     | 1979                | 1974,<br>76     |
| 1981-1990         | 1984,<br>1987   | 1984, 86 | 1982, 84,<br>87 | 1984, 87 | 1984            | 1982, 83,<br>84     | 1981,<br>88, 89 |
| 1991-2000         | 1993, 99        | 1991, 93 | 1998, 99        | 1995, 99 | 1999            | 1995, 99            | 1993            |
| 2001-2008         | 2002, 04,<br>07 | 2004, 07 | 2004            | 2002     | 2004,<br>06, 07 | 2001, 02,<br>04, 07 | -               |
| <b>Total</b>      | <b>8</b>        | <b>8</b> | <b>8</b>        | <b>7</b> | <b>9</b>        | <b>11</b>           | <b>7</b>        |

Table 4.6: Deficient rainfall year (1961-2008) of SM season

Deficit year  $\leq$  mean - CV

| Region/<br>Decade | SM<br>season        | Dhaka           | Chittagong              | Rajshahi            | Khulna      | Barisal                 | Sylhet          |
|-------------------|---------------------|-----------------|-------------------------|---------------------|-------------|-------------------------|-----------------|
| 1961-1970         | 1962                | -               | -                       | 1961, 62,<br>66, 67 | 1962,<br>66 | 1962, 63,<br>64, 65, 67 | -               |
| 1971-1980         | 1972, 73,<br>75, 80 | -               | 1972, 73,<br>75, 79, 80 | 1972, 75            | 1972,<br>73 | 1972                    | 1971,<br>73, 80 |
| 1981-1990         | 1989                | 1989            | 1989                    | -                   | 1982,<br>89 | 1985                    | 1986            |
| 1991-2000         | 1992, 94            | 1992,<br>94, 96 | 1992                    | 1994                | 1998        | 1992                    | 1994,<br>99     |
| 2001-2008         | -                   | 2000,<br>01, 03 | -                       | 2006                | -           | -                       | 2008            |
| <b>Total</b>      | <b>8</b>            | <b>7</b>        | <b>7</b>                | <b>8</b>            | <b>7</b>    | <b>8</b>                | <b>7</b>        |

#### **4.5.1 Dhaka administrative divisional rainfall**

Dhaka administrative divisional rainfall time series consists of 8 excess and 7 deficient rainfall years during the period 1961-2008 (Fig. 4.5a). There are two occasions of consecutive two deficient rainfall years after one year interval viz. 1992-1994-1996 and 2000-2001-2003. Similarly, there are three occasions of consecutive two excess rainfall years after one year interval for the period 1984-1986, 1991-1993 and 2004-2007. Dhaka administrative divisional rainfall consists of two decades of high incidence of deficient rainfall viz. 1991-2000 and 2001-2008 and three decades of high incidence of excess rainfall viz. 1981-1990, 1991-2000 and 2001-2008. There are two decades 1961-1970 and 1971-1980, when there was no deficient rainfall year, whereas all the decades are marked by at least one excess rainfall year in each.

#### **4.5.2 Chittagong administrative divisional rainfall**

There are 8 excess and 7 deficient rainfall years during the period 1961-2008 (Fig. 4.5b). There is one occasion of consecutive about five deficient rainfall years in one decade during the period 1971-1980 viz. 1972-1973-1976-1979-1980. Similarly, there was one occasion of three consecutive excess rainfall years after one year interval viz. 1982-1984-1987 and there was one occasion of two consecutive excess rainfall year viz. 1998-1999. Chittagong had three decades of high incidence of deficient rainfall viz. 1971-1980, 1981-1990, 1991-2000 and also four decades of high incidence of excess rainfall viz. 1961-1970, 1981-1990, 1991-2000 and 2001-2008. There are two decades 1961-1970 and 2001-2008, when there was no deficient rainfall year and there was one decade viz. 1971-1980, when there is no excess rainfall year.

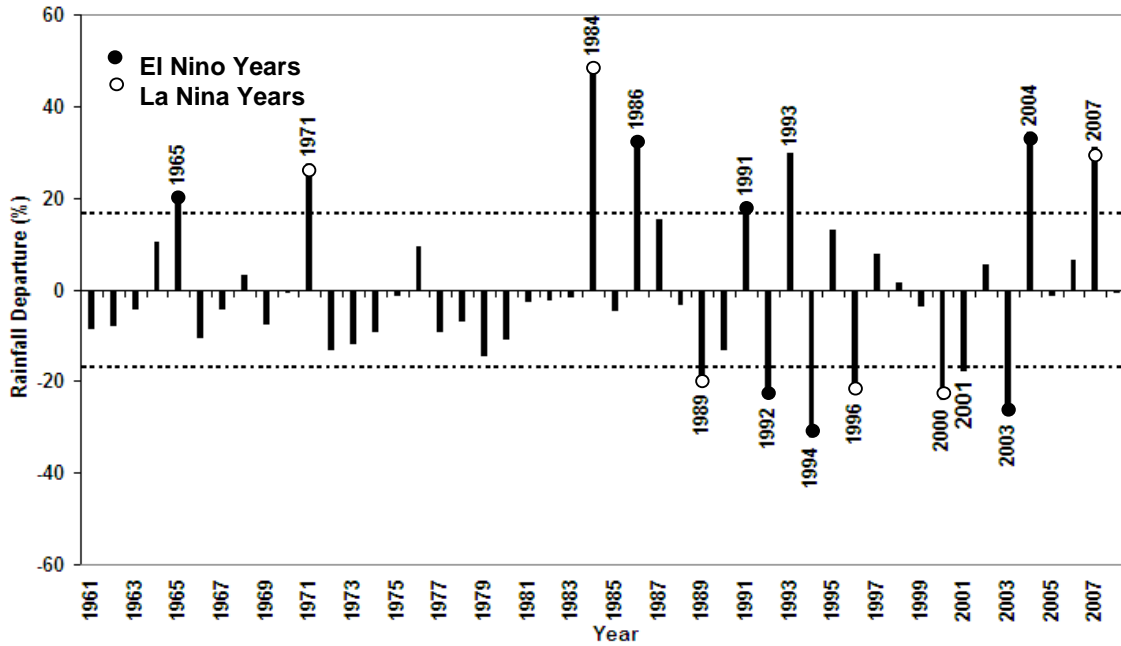


Fig. 4.5a: Dhaka administrative divisional rainfall variability during the period 1961-2008 and its association with ENSO. Horizontal dash line represents CV (%).

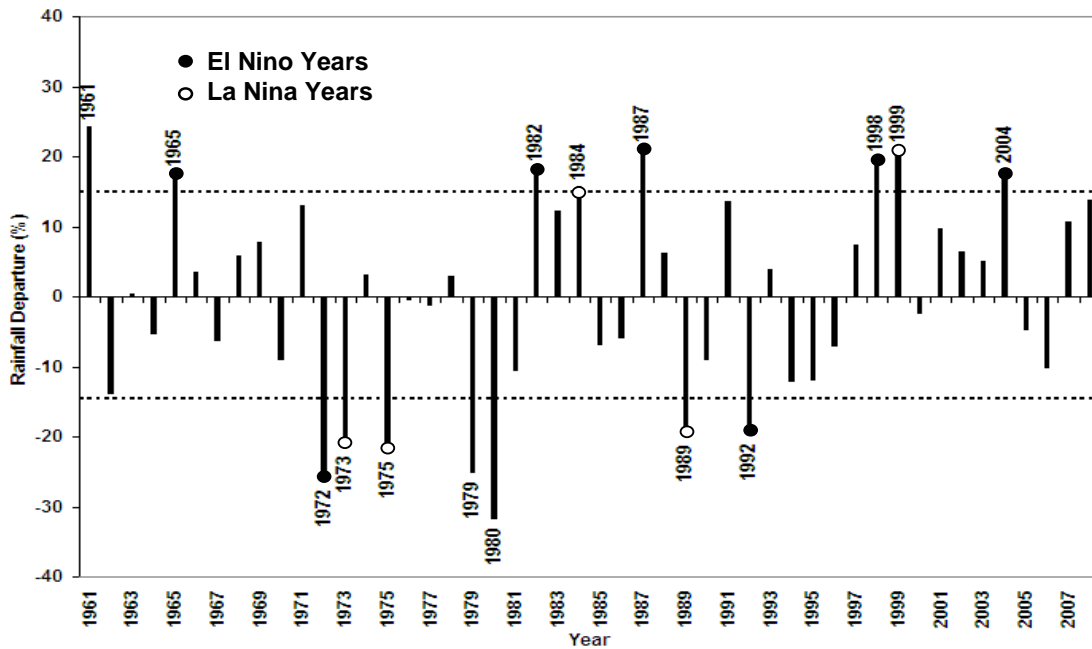


Fig. 4.5b: Same as Fig. 4.5a, but for Chittagong divisional rainfall.

### 4.5.3 Rajshahi administrative divisional rainfall

Rajshahi administrative divisional rainfall time series had 7 excess and 8 deficient rainfall years during the period 1961-2008 (Fig. 4.5c). There are two occasions of consecutive two deficient rainfall year's viz. 1961-1962, 1966-1967 and one deficient rainfall year after two years interval 1972-1975. Similarly, three occasions of three excess rainfall years after two years interval viz. 1973-1976, 1984-1987 and 1995-1999. Rajshahi had four decades of high incidence of deficient and excess rainfall year's viz. 1961-1970, 1971-1980, 1991-2000, 2001-2008 and 1971-1980, 1981-1990, 1991-2000 and 2001-2008, respectively. There was one decade no deficient rainfall year during the period 1981-1990 and no excess rainfall year during the period 1961-1970 in the whole period 1961-2008.

### 4.5.4 Khulna administrative divisional rainfall

Khulna administrative divisional rainfall had 9 excess and 7 deficient rainfall years during the period 1961-2008 (Fig. 4.5d). There were one occasion of consecutive two deficient rainfall year's viz. 1972-1973 and similarly, one occasion of consecutive two excess rainfall year's viz. 2006-2007.

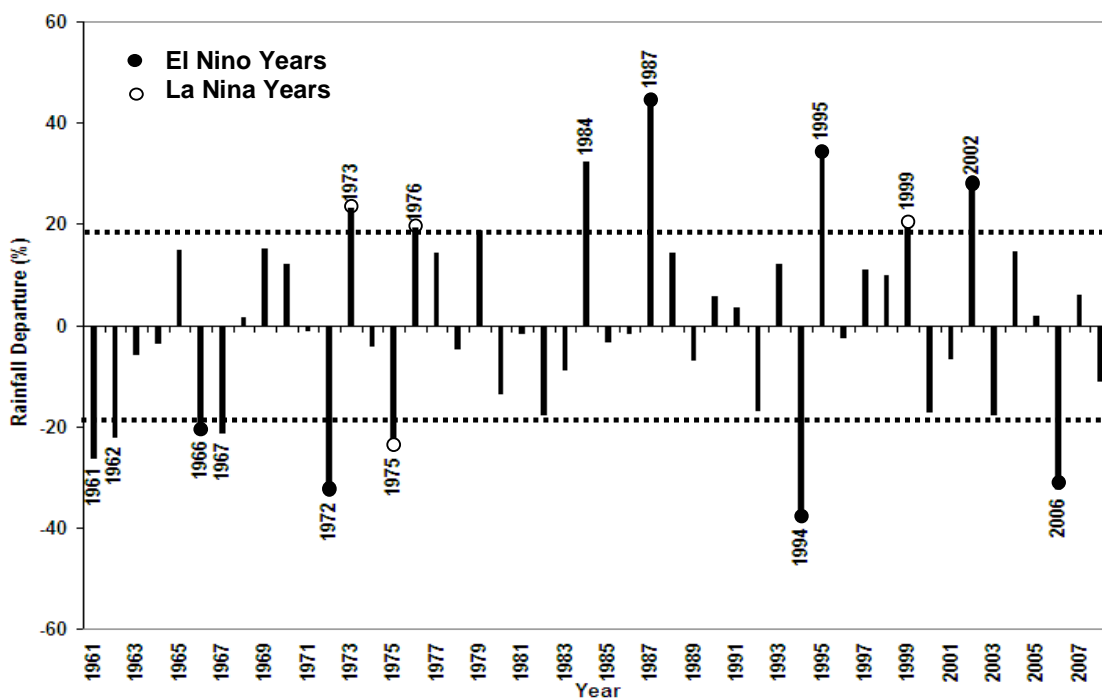


Fig. 4.5c: Same as Fig. 4.5a, but for Rajshahi divisional rainfall.

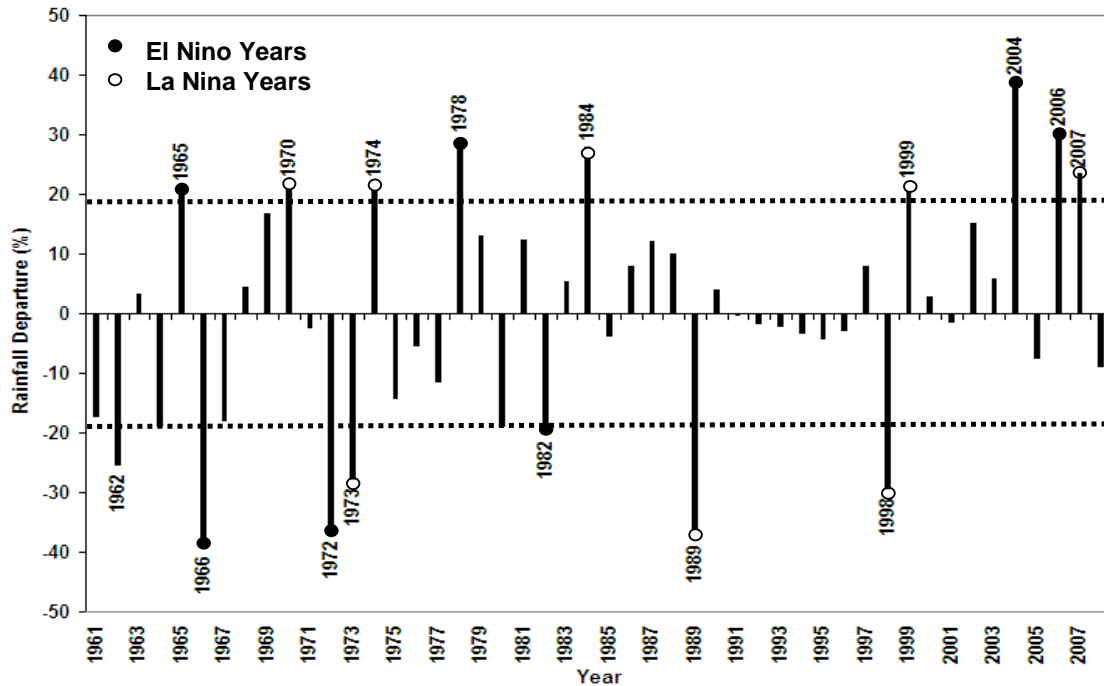


Fig. 4.5d: Same as Fig. 4.5a, but for Khulna divisional rainfall.

There were four decades of high incidence of deficient rainfall year's viz. 1961-1970, 1971-1980, 1981-1990, 1991-2000 and five decades of high incidence of excess rainfall years viz. 1961-1970, 1971-1980, 1981-1990, 1991-2000 and 2001-2008, respectively. There was one decade in 2001-2008, when there was no deficient rainfall year during the whole period 1961-2008.

#### 4.5.5 Barisal administrative divisional rainfall

Barisal administrative divisional rainfall had 11 excess and 8 deficient rainfall years during the period 1961-2008 (Fig. 4.5e). There is one occasion of consecutive five deficient rainfall years viz. 1962-1963-1964-1965-1967, similarly two occasions of consecutive two excess rainfall years viz. 1982-1983, 2001-2002. There was one decade of high incidence of deficient rainfall years viz. 2001-2008 and there were five decades of high incidence of excess rainfall years viz. 1961-1970, 1971-1980, 1981-1990, 1991-2000 and 2001-2008, respectively. There was one decade viz. 2001-2008 when no deficient rainfall year was noticed.

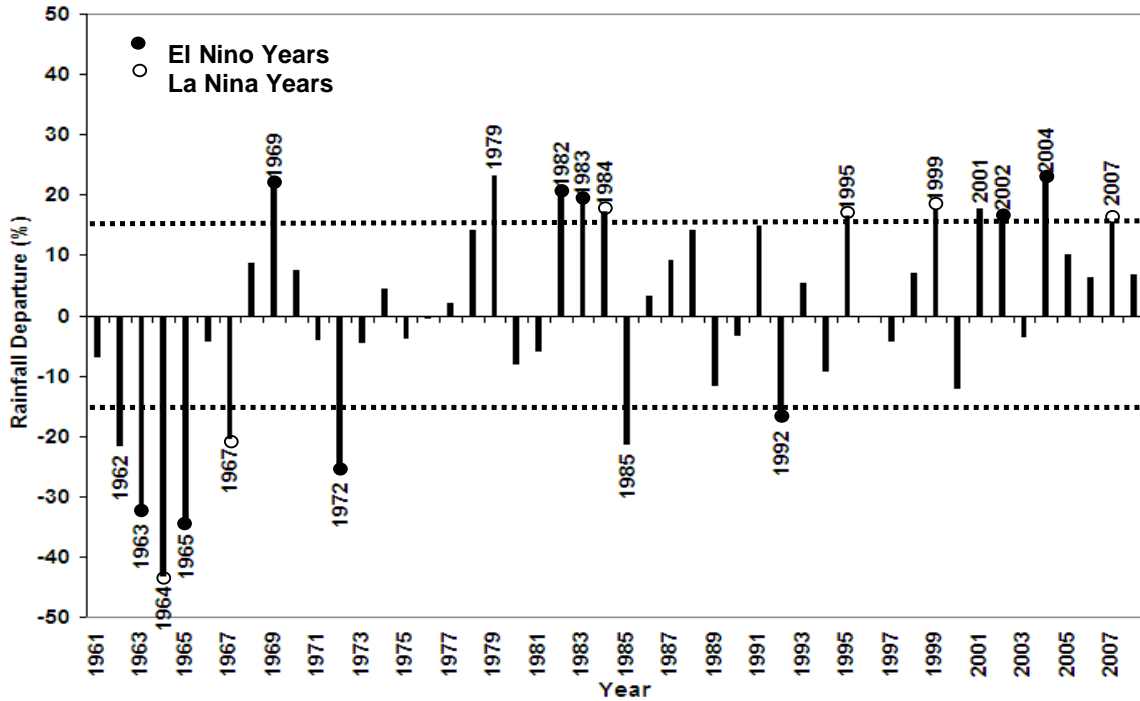


Fig. 4.5e: Same as Fig. 4.5a, but for Barisal divisional rainfall.

#### 4.5.6 Sylhet administrative divisional rainfall

Sylhet administrative divisional rainfall had 7 excess and 7 deficient rainfall years during the period 1961-2008 (Fig. 4.5f). There was one occasion of consecutive two deficient rainfall years after one year interval viz. 1971-1973, similarly one occasion of consecutive two excess rainfall years after one year interval viz. 1974-76. Sylhet had four decades of high incidence of deficient rainfall viz. 1971-1980, 1981-1990, 1991-2000 and 2001-2008 whereas there was one decade viz. 1961-1970 when there was no deficient rainfall year. similarly, four decades of high incidence of excess rainfall viz. 1961-70, 1971-80, 1981-90, 1991-2000 whereas there was one decade viz. 2001-2008 when there was no excess rainfall year.

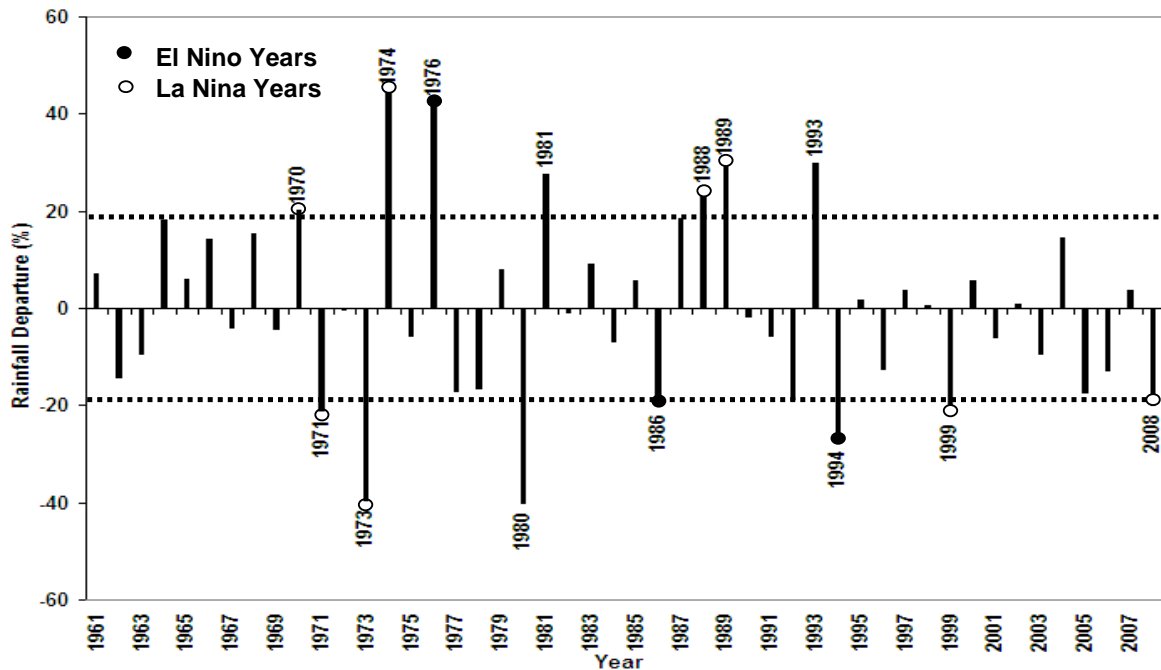


Fig. 4.5f: Same as Fig. 4.5a, but for Sylhet divisional rainfall.

## 4.6 Decadal variability of SMR

The decadal variability of SMR of Bangladesh and six administrative divisional rainfall has been studied by applying Cramer’s test for 11-year running means [41]. The computational procedure is explained in chapter-3. The statistics, which compares the 11-year means with the overall mean, has been used to isolate periods (if any) of above- and below-average rainfall and also to test the trend of the time series.

### 4.6.1 SMR over Bangladesh

The short-term decadal climate fluctuations have been studied by applying Cramer’s test for the 11-year running means [41]. The 11-year Cramer’s *t*-statistics for Bangladesh SMR are presented in Fig. 4.6. The most striking features are the epochs of above and below-normal rainfall. The epochs tend to last for about a decade. Generally, the rainfall epochal regimes closer to the equatorial belt tend to last for a decade [21]. Although the variability during the earlier decades (1971-1991) appears to be large and the recent decades (1991–2001) appear to be small, it may be due to short period of data (Fig. 4.6a). This behaviour is part of the natural variability.

The decadal variability for SMR reveals that the mode was on the negative side during the period prior to 1978; thereafter, most of the time it has been on the positive side during the period 1981-2001. After 1978 the general increasing trend of the mode may be due to global warming.

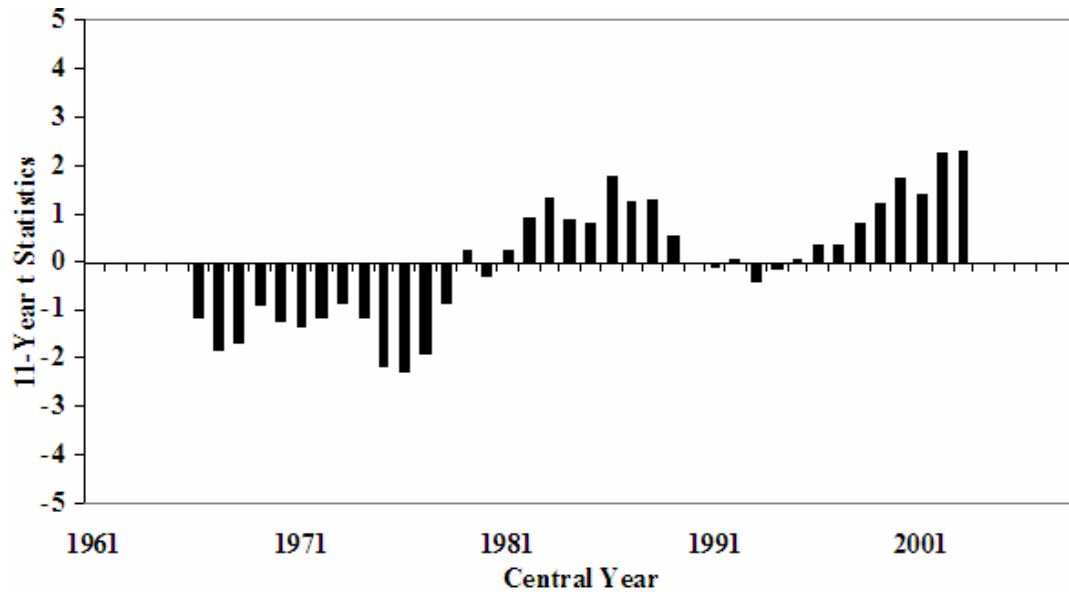


Fig. 4.6: The values of Cramer’s  $t$ -statistics for the 11-year running means of SMR of Bangladesh depicting decadal variability and the epochs of above and below-normal rainfall. Values are plotted at the centre of the 11-year period.

#### 4.6.2 Dhaka divisional rainfall

The 11-year running Cramer’s  $t$ -statistics for Dhaka is presented in Fig. 4.6a. The Dhaka divisional rainfall shows major turning points during 1970, 1979 and 1991. In recent decades, the variability and the epochs of above and below normal rainfall vary in a similar fashion (Fig. 4.6a). The most striking features are the epochs of above and below-normal rainfall. The period 1979-1990 is characterized by above-normal rainfall with very low frequency of flood. The periods 1970-1978 and 1992-2001 are characterized by below-normal rainfall with very low frequency of droughts. No trends depicting a longer-term climatic change are detected.

#### 4.6.3 Chittagong divisional rainfall

The values of Cramer’s  $t$ -statistics for the 11-year running means for SMR over Chittagong division are depicted in Fig. 4.6b. Whereas the standardized values show

random fluctuations, Cramer's  $t$ -statistics reveals interesting results. The decadal variability for SMR reveals that the mode was on the negative side during the period prior to 1994; thereafter, most of the time it has been on the positive side.

The Chittagong divisional rainfall shows major turning points during 1967 and 1995 (Fig. 4.6b). The variability is low during the epochs of below normal rainfall except in recent decades when variability is above normal during the epochs of above normal rainfall (Fig. 4.6b).

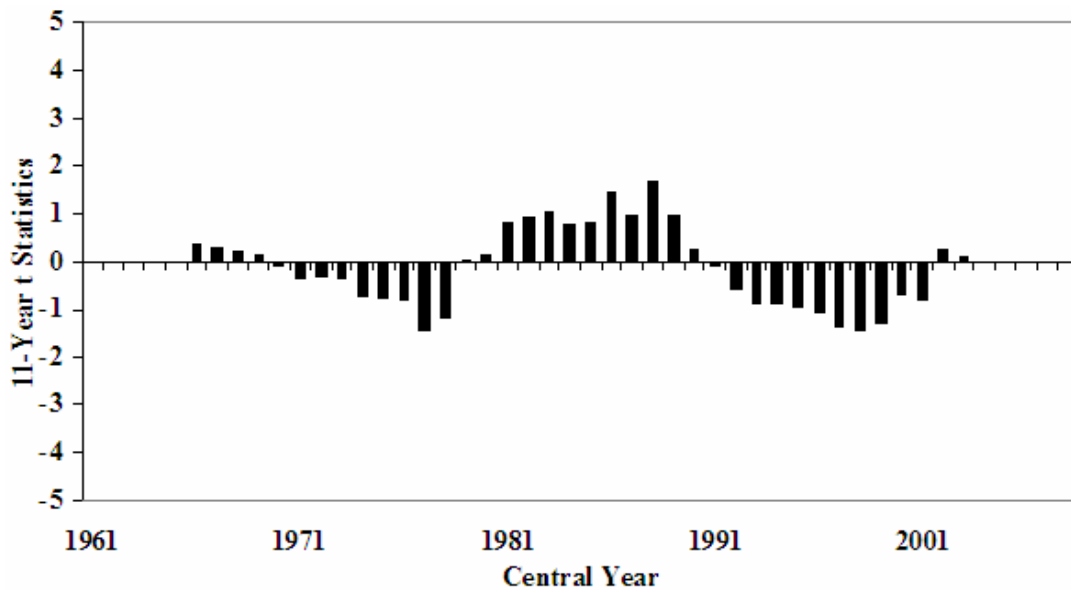


Fig. 4.6a: Same as Fig. 4.6, but for Dhaka divisional rainfall.

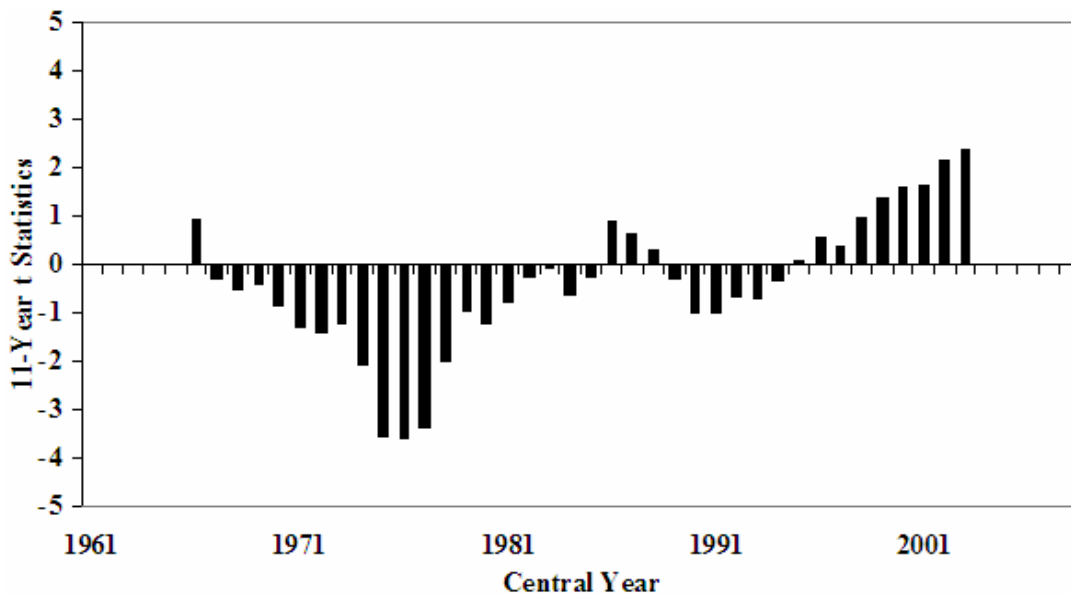


Fig. 4.6b: Same as Fig. 4.6, but for Chittagong divisional rainfall.

#### 4.6.4 Rajshahi divisional rainfall

The Rajshahi divisional rainfall shows major turning points during 1966 and 1978 (Fig. 4.6c). The values of Cramer's  $t$ -statistics for the 11-year running means for SMR are presented in Fig. 4.6c. The Cramer's  $t$ -statistics reveals interesting results. The decadal variability for SMR reveals that the mode was on the negative side during the period prior to 1971; after 1978 most of the time it has been on the positive side. Although the variability during the earlier decade (1966-1971) and the recent decades (1979-2002) appears to be large, the variability in between period appears to be small (Fig. 4.6c). Whether this behaviour is part of the natural variability or after 1978 the general increasing trend of the mode may be due to global warming.

#### 4.6.5 Khulna divisional rainfall

The 11-year running Cramer's  $t$ -statistics for Khulna divisional rainfall is presented in Fig. 4.6d. The Khulna divisional rainfall shows major turning point during 1966, 1979, 1990 and 1998. In recent decades, the variability and the epochs of above and below normal rainfall vary in a similar fashion (Fig. 4.6d).

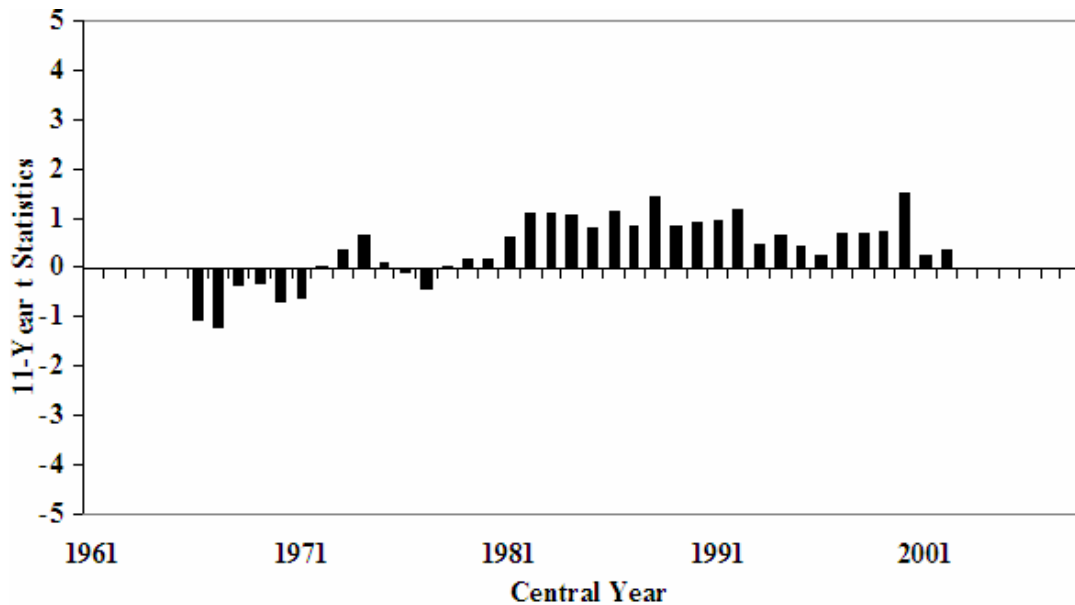


Fig. 4.6c: Same as Fig. 4.6, but for Rajshahi divisional rainfall.

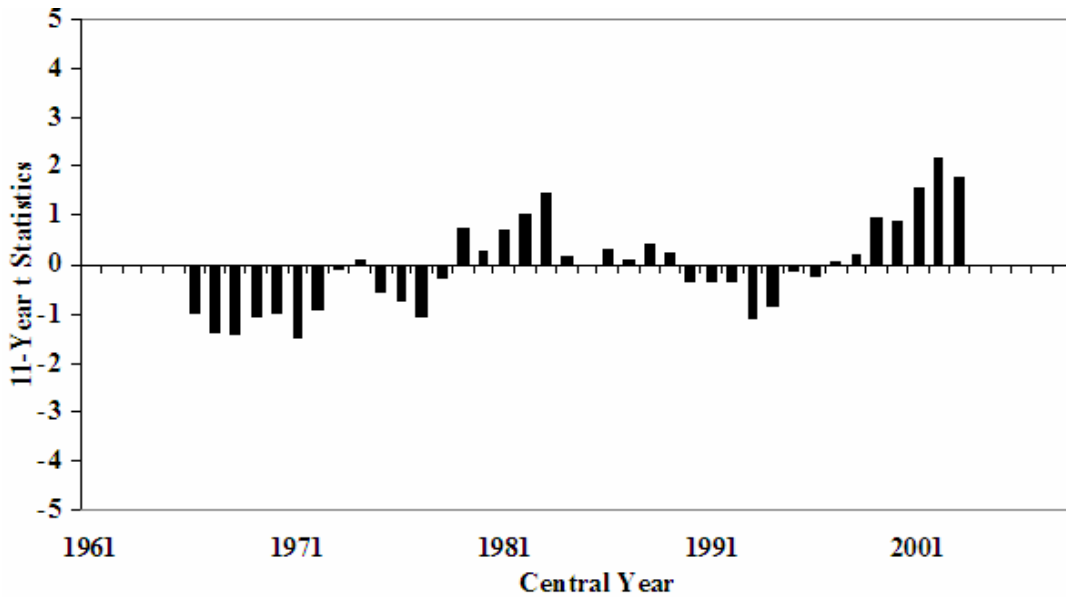


Fig. 4.6d: Same as Fig. 4.6, but for Khulna divisional rainfall.

The epochs tend to last for about a decade. The most striking features are the epochs of above and below-normal rainfall. The period 1979-1989 characterized by normal rainfall and 1997-2003 are by above-normal rainfall with very low frequency of flood. The periods 1966-1978 and 1990-1996 are characterized by below-normal rainfall with very low frequency of droughts.

#### 4.6.6 Barisal divisional rainfall

The 11-year running Cramer's  $t$ -statistics for Barisal divisional rainfall is depicted in Fig. 4.6e. The Barisal divisional rainfall shows major turning point during 1966 and 1973. The most striking features are the epochs of above and below-normal rainfall. The period 1966-1972 is characterized by deficient rainfall with very high frequency of drought. The period 1973-2003 is characterized by above-normal rainfall with very low frequency of flood. The variability is above normal to below normal throughout the period, except in earlier decade (1966-1972) with high variability with epochs of very high deficient rainfall (Fig. 4.6e).

#### 4.6.7 Sylhet divisional rainfall

The Sylhet divisional rainfall shows major turning points during 1966 and 1994 (Fig. 4.6f). The Cramer's  $t$ -statistics for the 11-year running means for SMR is depicted in Fig. 4.6f. Whereas the standardized values show random fluctuations for Sylhet divisional

rainfall, Cramer's  $t$ -statistics reveals interesting results. The decadal variability for SMR reveals that the mode was on the positive side during the period prior to 1994; thereafter, most of the time it has been on the negative side. However, the variability is low during the epochs of above normal rainfall except in recent decade when variability is below normal during the epochs of below normal rainfall. Although the variability during the earlier decades (1966-1993) appears to be large and the recent decades (1994-2004) appears to be small, whether this behaviour is part of the natural variability or may be due to global warming.

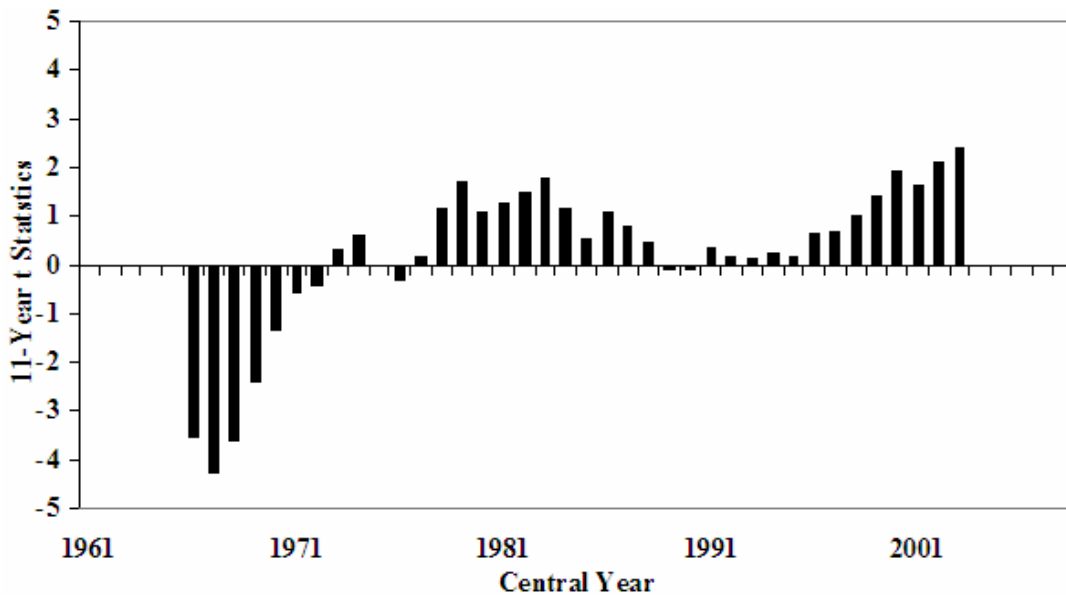


Fig. 4.6e: Same as Fig. 4.6, but for Barisal divisional rainfall.

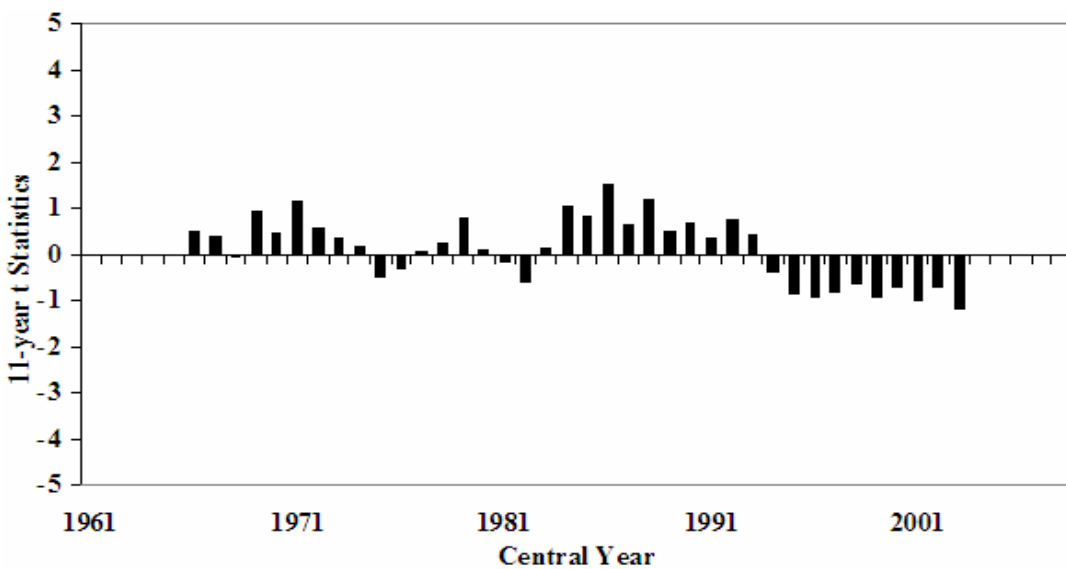


Fig. 4.6f: Same as Fig. 4.6, but for Sylhet divisional rainfall.

## CHAPTER 5

### TELECONNECTION OF SUMMER MONSOON RAINFALL

#### 5.1 Introduction

It is obvious that the South Asian monsoon as well as Indian monsoon, being such a large component of the global weather and climate system, will have positive and negative associations with other entities. Many of these associations are of a concurrent nature, having little value for monsoon prediction. The Summer Monsoon (SM) may also exert a strong influence on future events in the global atmosphere or ocean. In fact, the SM is often thought of as playing more of an active role in the climate system rather than a passive one [42]. The behaviour of the monsoon does not always resemble that of a weak slave ordered about by parameters from across the Pacific Ocean. At times the monsoon may assume the role of the master and drive the El Nino Southern Oscillation (ENSO) phenomenon instead. The monsoon and ENSO could perhaps be more appropriately described as selectively interactive systems [43]. However, the inverse problem in which the monsoon is regarded as casting its influence on future global events, though important has not evoked much interest among monsoon forecasters.

The origin of the term teleconnection as used in the context of the monsoon is not very certain. Gilbert Walker with whose work this term is often associated does not appear to have used it in the several monographs and memoirs that he wrote. The credit for coining this word perhaps goes to Bjerkenes [44].

The real monsoon teleconnections refer to those situations or developments in the land-ocean-atmosphere system which occur several months or may be even years, prior to the onset of the monsoon over Asia as well as India, and are known to exert a strong influence on the monsoon rainfall. During the time period that elapses between the detection of such signals and the arrival of the monsoon, these antecedent factors would be working together, or against each other, towards the making or unmaking of the monsoon. In a sense, the monsoon can be visualized as going through a long buildup process, during which it gets progressively manipulated by global factors that predetermine its behaviour and the amount of rain that it would produce.

SM is a major large-scale seasonal phenomenon, and is believed to be closely linked to several regional/global circulation features. It is important to unravel these linkages in terms of teleconnections of summer monsoon rainfall (SMR) anomalies with various basic parameters in the global domain. The parameters considered here are sea surface temperature, surface air temperature-2m and mean sea level pressure.

The main purpose is to investigate whether there are any spatio-temporal preferences of the anomalies in these parameters associated with SMR variability. This analysis has been done by simple correlation analysis using the NCEP/NCAR reanalysis data, for the period 1961-2008. Details of the data sets are provided in Chapter 3.

## 5.2 Global correlation patterns

### 5.2.1 Sea surface temperature of June-September (JJAS)

The sea surface temperature (SST) anomaly in the tropical Pacific is one of the most important factors of the interannual variability of the tropical monsoon circulation. The anomaly in energy exchange between the atmosphere and the ocean and its subsequent

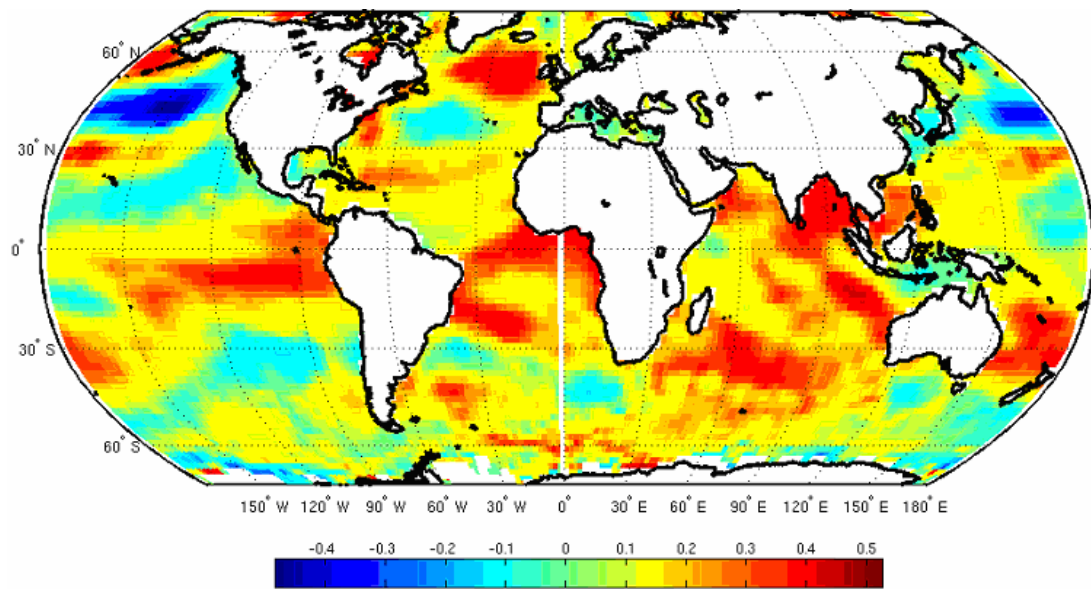


Fig. 5.1: Spatial pattern of seasonal (June – September) correlation coefficients between SST and SMR of Bangladesh.

feedback associated with the SST anomalies makes it a likely cause of climatic variability [45]. Warm equatorial Pacific SST anomalies, referred to as El Niño events, have been found to be associated with deficient SMR over India [46]. Angell [47] and

Mooley and Parthasarathy [48] found significant negative associations between Indian SMR and SST anomalies over the eastern equatorial Pacific Ocean.

The spatial patterns of correlation coefficients (CCs) between SMR and concurrent seasonal mean SST is negative (-0.5) over northeastern Pacific about 50° N based on the data period 1961-2008 are presented in Fig. 5.1, which suggest that deficient rainfall is associated with warm SSTs over northeastern Pacific region. Thus, El Niño/Southern Oscillation (ENSO) has not much dominant role in SMR variability over Bangladesh. Indian Ocean also shows positive CCs with SMR suggesting that this region has a strong impact on SMR over Bangladesh. Indian Ocean Dipole Mode (IODM) is a phenomenon that also occurs over this region. Although, severe droughts in India have been associated with El Niño events, El Niño does not always produce droughts reported by Kumar and Rajagopalan et al. [49]. For instance, in 1997 (strong El Niño year) India experienced higher than normal rainfall and, in 2002 (weak El Niño year) the Indian monsoon presented a deficit rainfall which was found by Maity and Kumar [50].

The roles of both ENSO and IODM will be examined in detail later in this chapter to bring out their impact on SMR variability and predictability.

### **5.2.2 Sea surface temperature of March-May (MAM)**

The spatial patterns of CCs between SMR of Bangladesh and pre-monsoon (MAM) seasonal mean SST is to be found positive (0.3), but not strong correlation over equatorial eastern Pacific and also found to be negative (-0.3) correlation over northeastern Pacific about 50° N based on the data period 1961-2008 are presented in Fig. 5.2, which suggest that above normal rainfall is associated with warm SSTs over equatorial eastern Pacific region. Thus, ENSO has not much dominant role in SMR variability over Bangladesh. Indian Ocean also shows positive CCs with SMR suggesting that this region has an impact on SMR over Bangladesh.

### **5.2.3 Sea surface temperature of December-February (DJF)**

The spatial patterns of CCs between SMR of Bangladesh and winter (DJF) seasonal mean SST is found to be negative (-0.3), but not strong correlation over northeastern Pacific and also found to be positive and strong correlation ( $> 0.4$ ) over southwestern Indian Ocean based on the data period 1961-2008 are presented in Fig. 5.3, which suggest that deficient rainfall is associated with warm SSTs over northeastern Pacific

region. Thus, ENSO has not much dominant role in SMR variability over Bangladesh. Indian Ocean also shows positive CCs with SMR suggesting that this region has a strong impact on SMR over Bangladesh.

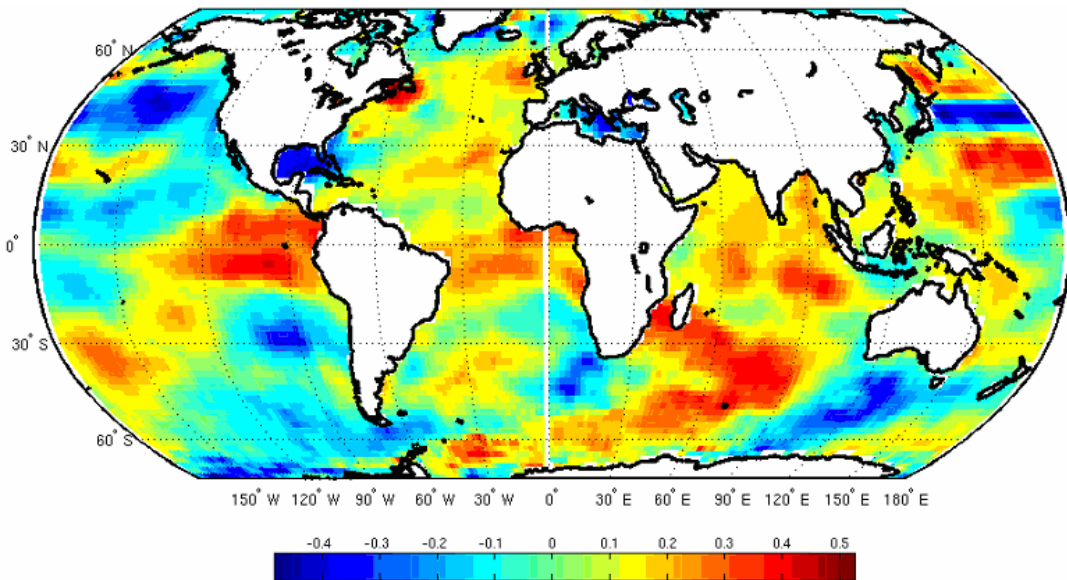


Fig. 5.2: Same as Fig. 5.1, but for pre-monsoon (MAM) season.

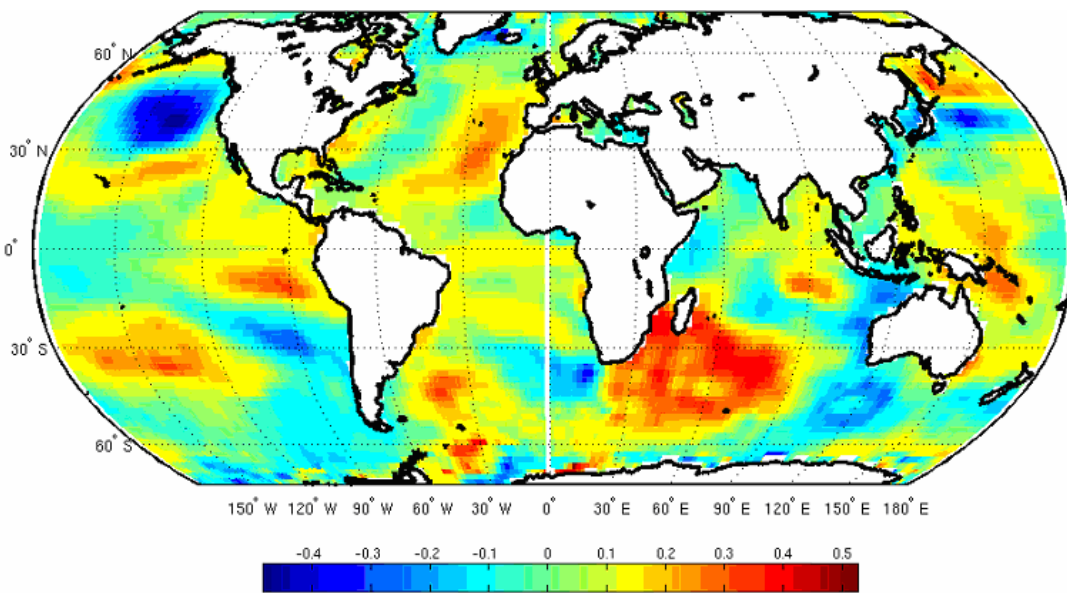


Fig. 5.3: Same as Fig. 5.1, but for winter (DJF) season.

#### 5.2.4 Monthly sea surface temperature of January through May

Correlations coefficient were determined for individual calendar months with lead times up to five months before the SM season of Bangladesh. From up to five months lead time, January through May, a significant positive relationship between SMR of Bangladesh and SST of the southwest Indian Ocean was found in the month of February. All other monthly correlations were not found to be significant. Thus, the correlation was performed between February SST over Indian Ocean and SMR of Bangladesh. Where the same SST region shows a positive correlation with Bangladesh SMR for different lead times for different months, only the one with the highest positive correlation over the largest area was included in this study. From Figs. 5.4(a-e), it can be seen that January, February, March, April and May SST of the Indian Ocean is positively correlated with SMR of Bangladesh. In this case the February SST was used because it showed the highest correlation (0.44) over southwest Indian Ocean (30°-36° S latitude and 74° -78° E longitude) over large area than the others area (Fig. 5.4b). The correlations are weak over rest of the Indian Ocean and Bay of Bengal SST with SMR over Bangladesh as shown in Figs. 5.4 (a-e).

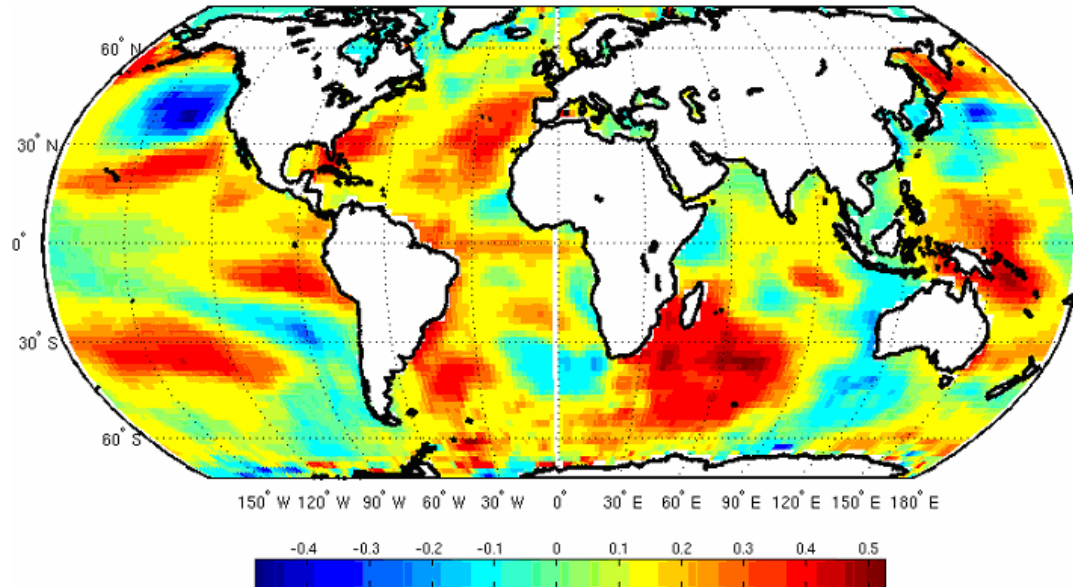


Fig. 5.4a: Spatial pattern of January correlation coefficients between SST and SMR of Bangladesh.

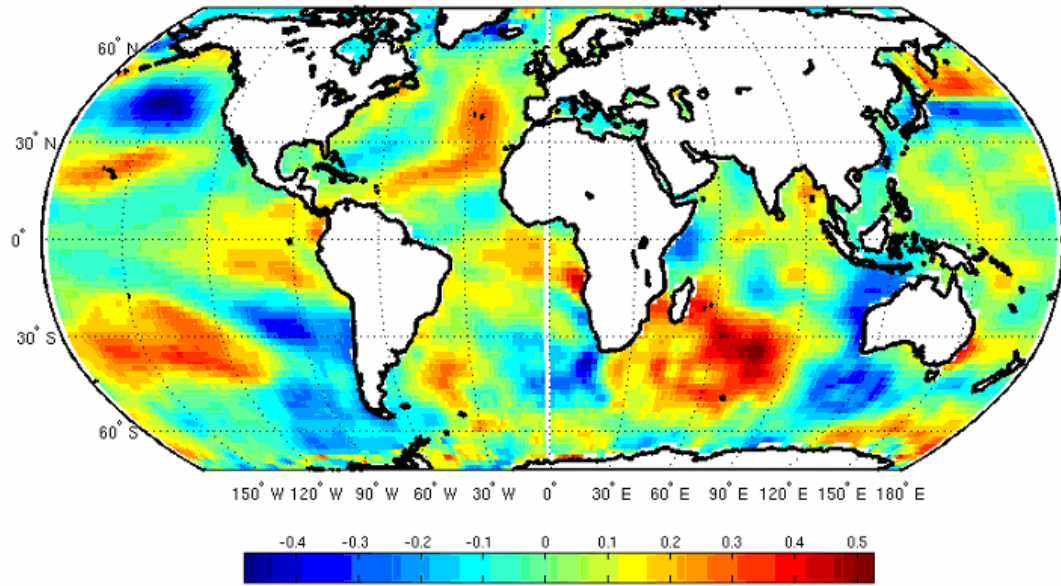


Fig. 5.4b: Same as Fig.5.4a, but for the month of February.

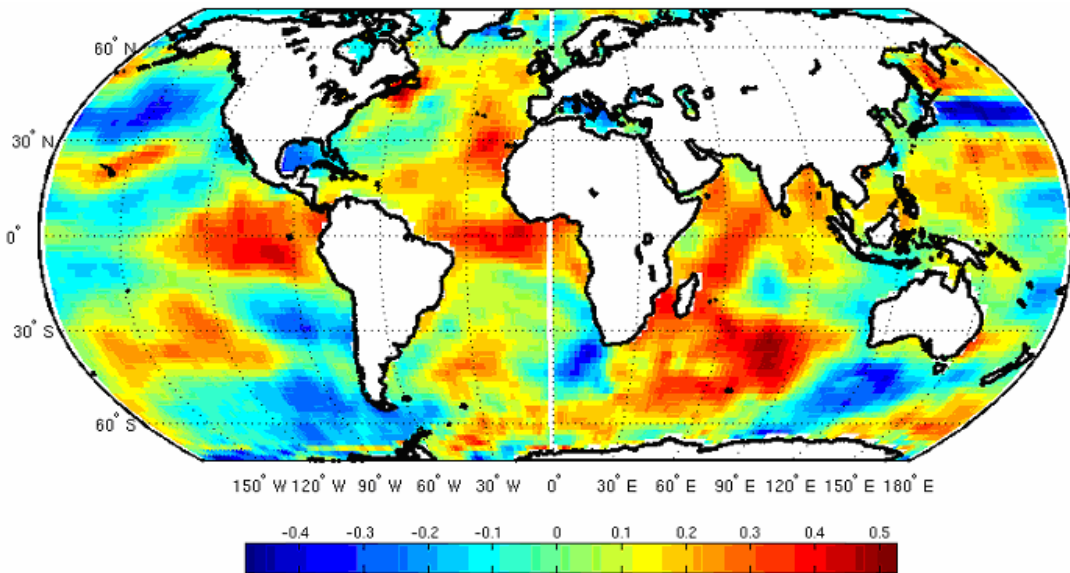


Fig. 5.4c: Same as Fig.5.4a, but for the month of March.

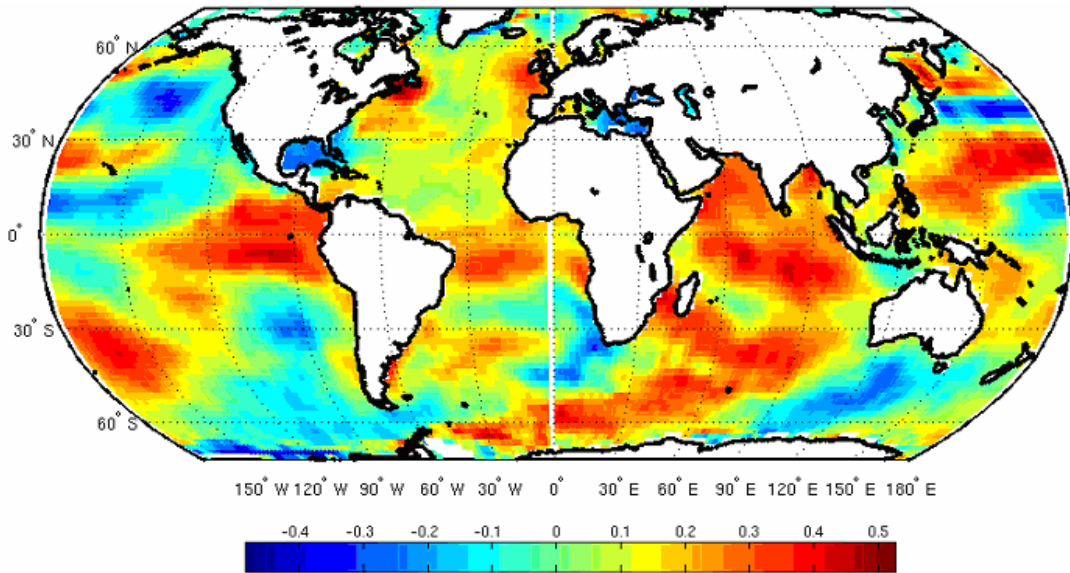


Fig. 5.4d: Same as Fig. 5.4a, but for the month of April.

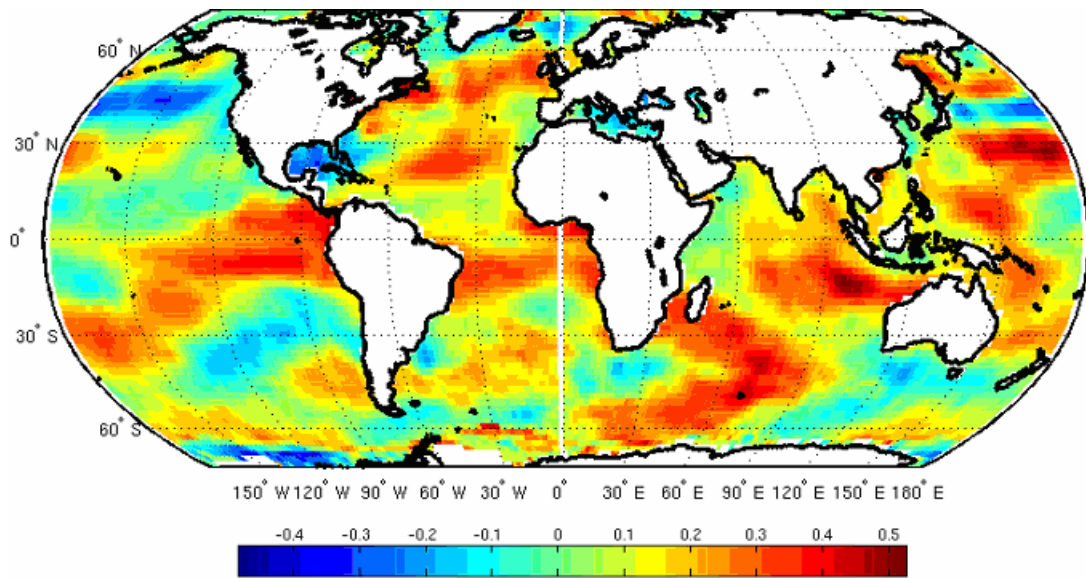


Fig. 5.4e: Same as Fig. 4.4a, but for the month of May.

### 5.2.5 Surface air temperature of June-September (JJAS)

The spatial patterns of CCs between SMR of Bangladesh and concurrent surface air temperature (at 2m level) based on the data period 1961-2008 are presented in Fig. 5.5, which reflects similar spatial patterns as SST (Fig. 5.1).

### 5.2.6 Surface air temperature of March-May (MAM)

The spatial patterns of CCs between SMR of Bangladesh and pre-monsoon SAT (at 2m level) based on the data period 1961-2008 are presented in Fig. 5.6. The CCs are found to be negative (-0.3) but not strong over Europe and also strong positive correlation found over Somalia during the above mentioned period, which suggests that above normal SMR over Bangladesh is associated with high SAT over Somalia and extended up to Oman.

### 5.2.7 Surface air temperature of December-February (DJF)

The spatial patterns of CCs between SMR of Bangladesh and winter SAT (at 2m level) based on the data period 1961-2008 are presented in Fig. 5.7. The CCs are shown negative over northern Australia and also positive correlation shown near Mauritius during the above mentioned period. This suggests that above normal SMR over Bangladesh is associated with high SAT over this region.

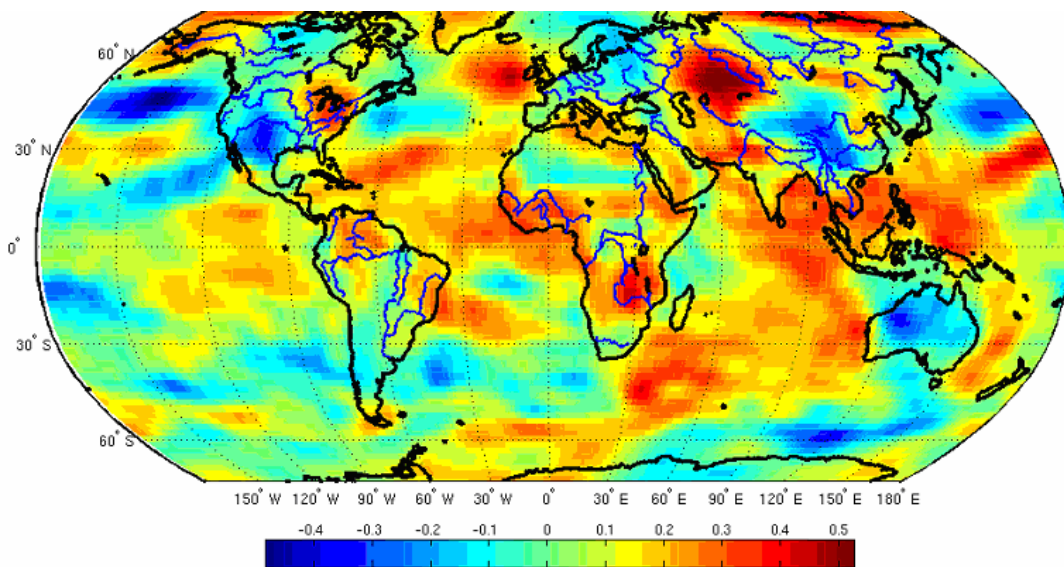


Fig. 5.5: Spatial pattern of monsoon seasonal (June – September) correlation coefficients between SAT and SMR of Bangladesh.

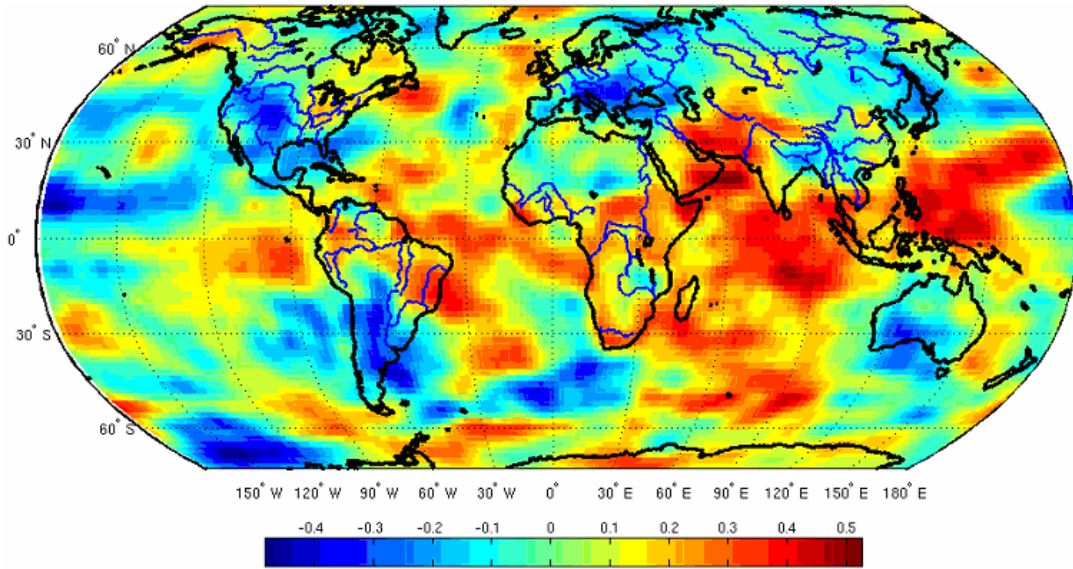


Fig. 5.6: Same as Fig. 5.5, but for pre-monsoon (MAM) season.

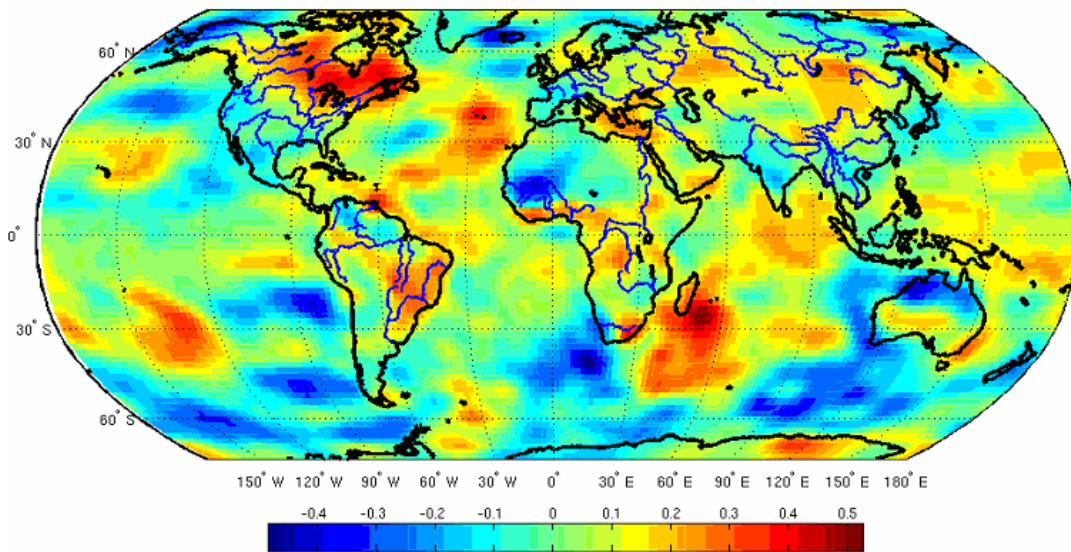


Fig. 5.7: Same as Fig. 5.5, but for winter (DJF) season.

### 5.2.8 Monthly surface air temperature of January through May

Correlation coefficients were found for individual calendar months with lead times up to five months preceding the SM season of Bangladesh. From up to five months lead time, January through May, SAT in the month of April over Somalia is highly positive and significantly correlated with the SMR of Bangladesh. The correlations are weak over rest of the part of the globe in the month of April as shown in Fig. 5.8d. Thus, the correlation was performed between April SAT over Somalia and SMR of Bangladesh. Such type of

predictor (e.g. SAT) will be helpful to develop the regression model to predict SMR of Bangladesh. From Fig. 5.8a, it can be seen that SAT in the month of January over South America is positively correlated with SMR of Bangladesh but not strong correlation like in the month of April. The intention of this research is to be found correlation between SAT and SMR of Bangladesh around the Asia but not find out anywhere in the globe and should also find out physical meaning of the parameters (predictors) with the SMR of Bangladesh. From the Fig. 5.8b, it is observed that February SAT over North America is positively correlated with SMR of Bangladesh. Similarly, from Fig. 5.8c, it is found that SAT in the month of March over Oman is positively correlated with SMR of Bangladesh but not strong correlation than others month (like in April). From Fig. 5.8e, it is seen that the correlation between SAT for the month of May and SMR of Bangladesh is not strong than the other months.

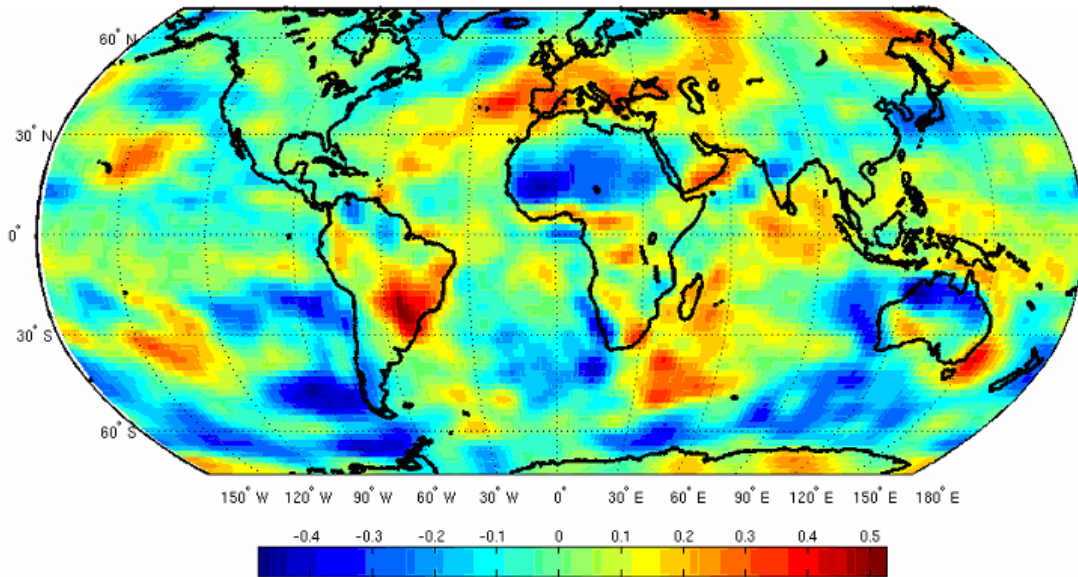


Fig. 5.8a: Spatial pattern of January correlation coefficients between SAT and SMR of Bangladesh.

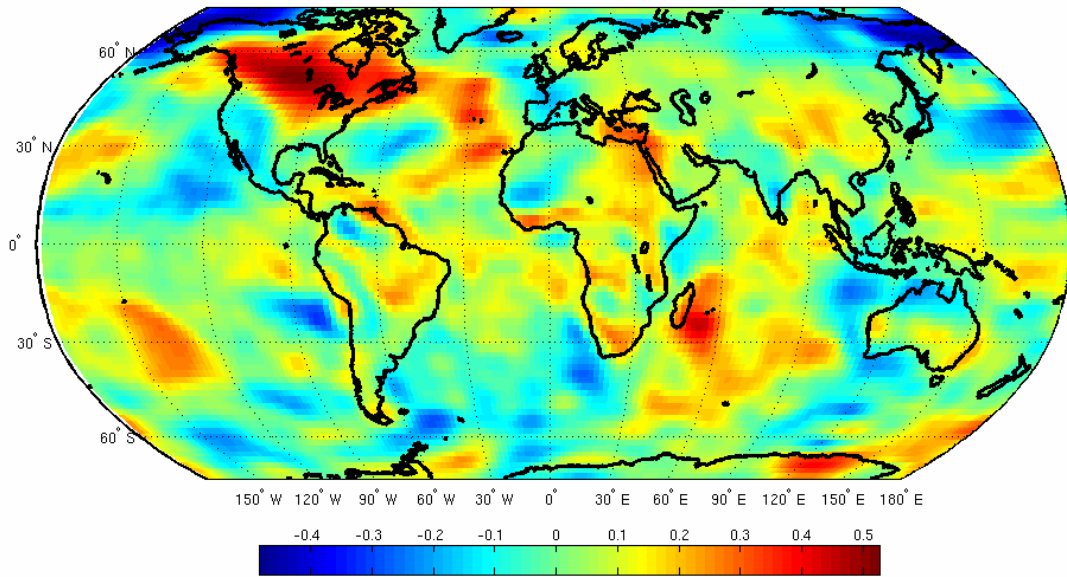


Fig. 5.8b: Same as Fig. 5.8a, but for the month of February.

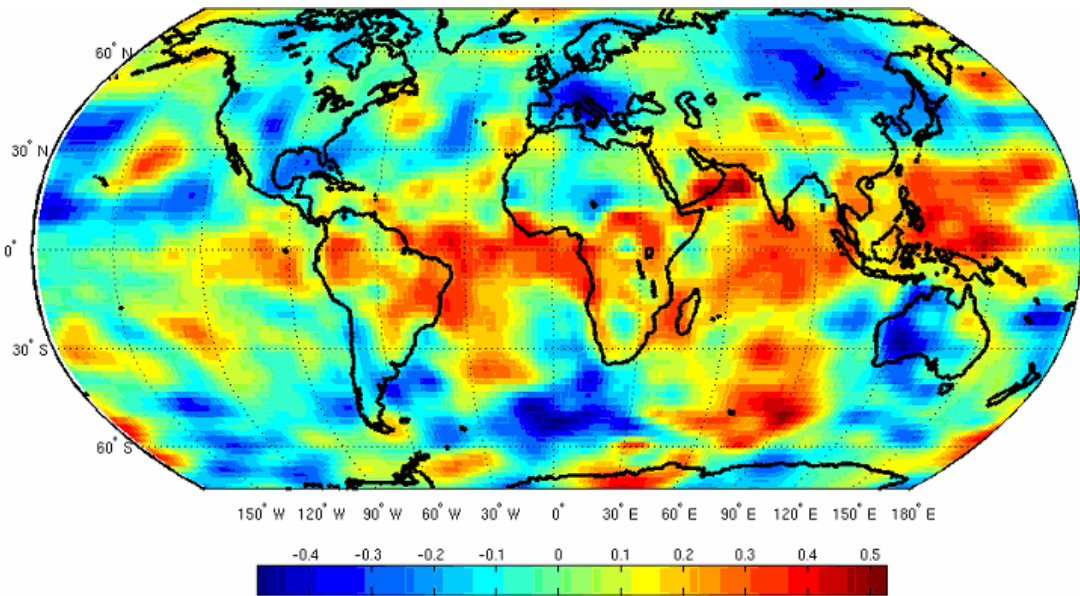


Fig. 5.8c: Same as Fig. 5.8a, but for the month of March.

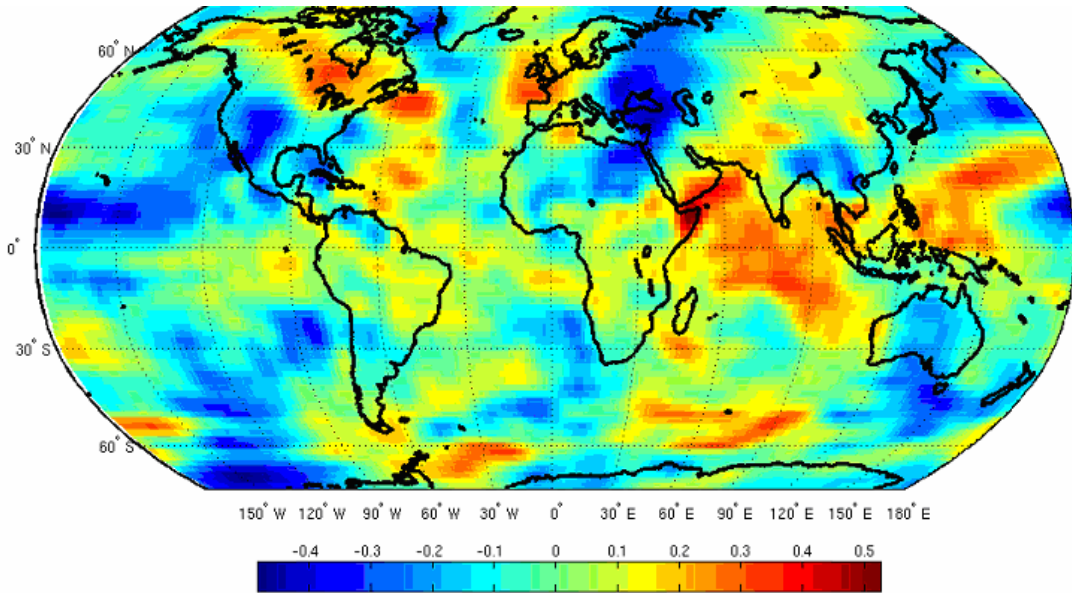


Fig. 5.8d: Same as Fig. 5.8a, but for the month of April.

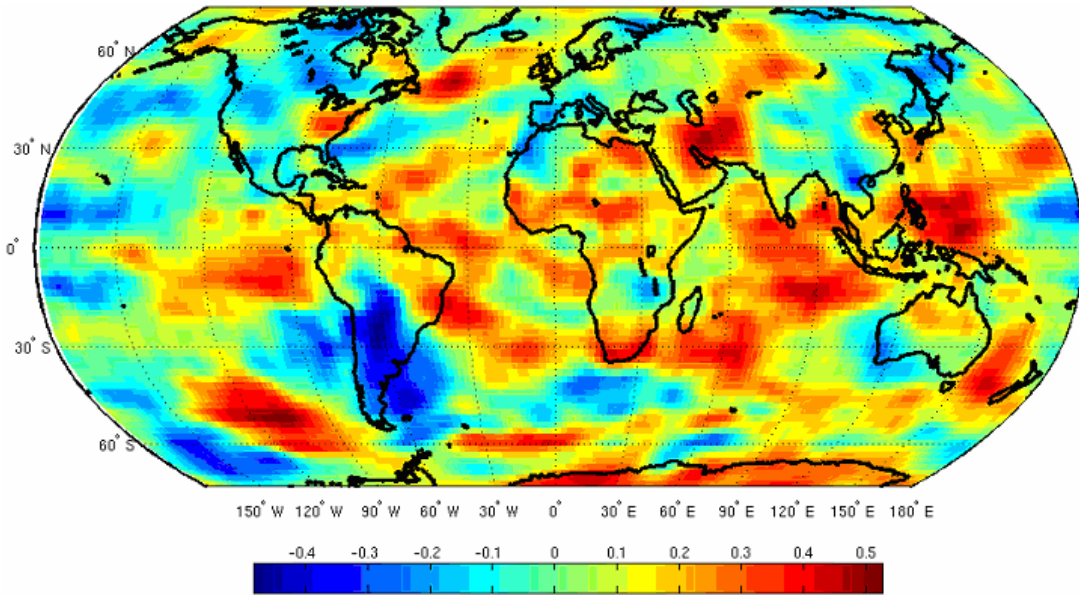


Fig. 5.8e: Same as Fig. 5.8a, but for the month of May.

### 5.2.9 Mean sea level pressure of June-September (JJAS)

The spatial patterns of CCs between SMR of Bangladesh and concurrent MSLP are shown in Fig. 5.9 based on the period 1961-2008, which suggests that normal to above normal SMR of Bangladesh is associated with high MSLP over west Pacific extended up to central Pacific. On the other hand, the CCs between SMR of Bangladesh and concurrent MSLP as shown is negative ( $< -0.3$ ) over northeastern Pacific Ocean, which

suggests that deficient rainfall is associated with high MSLP over this region, i.e. vice versa.

#### 5.2.10 Mean sea level pressure of March-May (MAM)

The spatial patterns of CCs between SMR of Bangladesh and pre-monsoon MSLP are shown in Fig. 5.10 based on the period 1961-2008, which suggests that above normal SMR is associated with high MSLP over central Pacific Ocean.

#### 5.2.11 Mean sea level pressure of December-February (DJF)

The spatial patterns of CCs between SMR of Bangladesh and winter MSLP are shown in Fig. 5.11 during the period 1961-2008, which suggests that normal to above normal SMR of Bangladesh is associated with high MSLP over Indian Ocean. The CCs are shown positive over southern Indian Ocean but not strong correlations over this region during the above period.

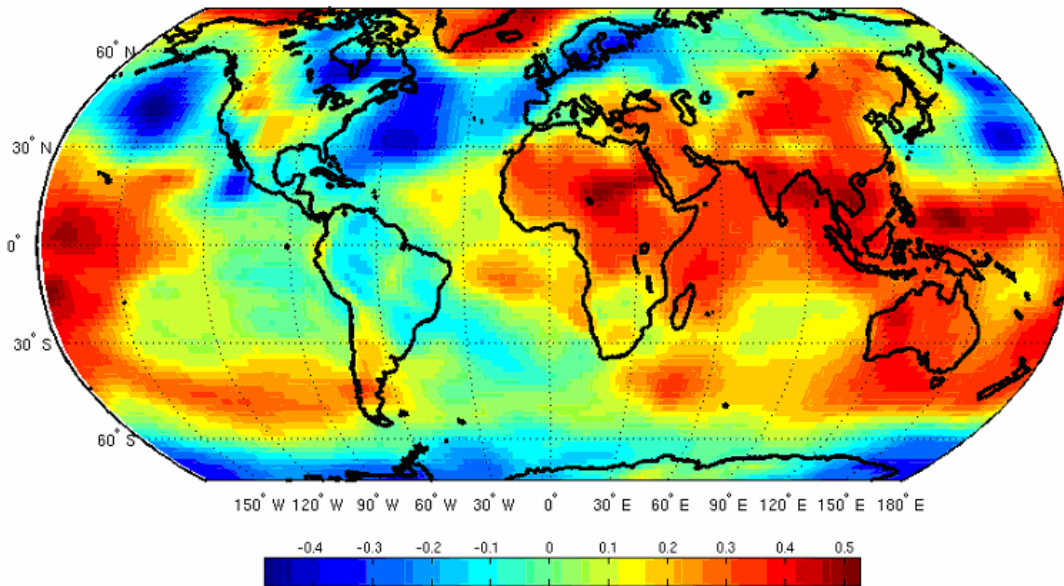


Fig. 5.9: Spatial pattern of monsoon seasonal (June – September) correlation coefficients between MSLP and SMR of Bangladesh.

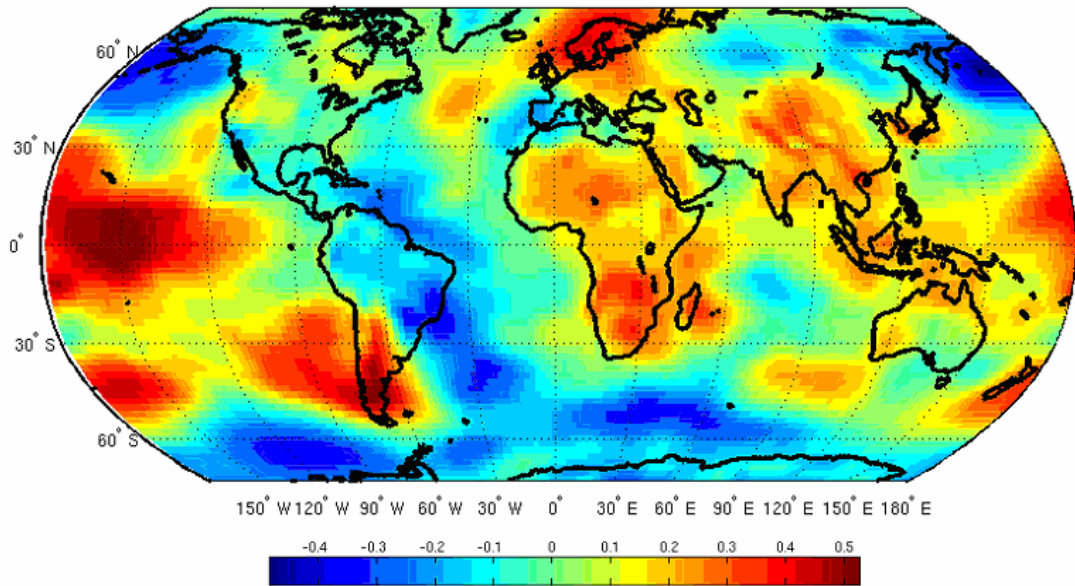


Fig. 5.10: Same as Fig. 5.9, but for pre-monsoon (MAM) season.

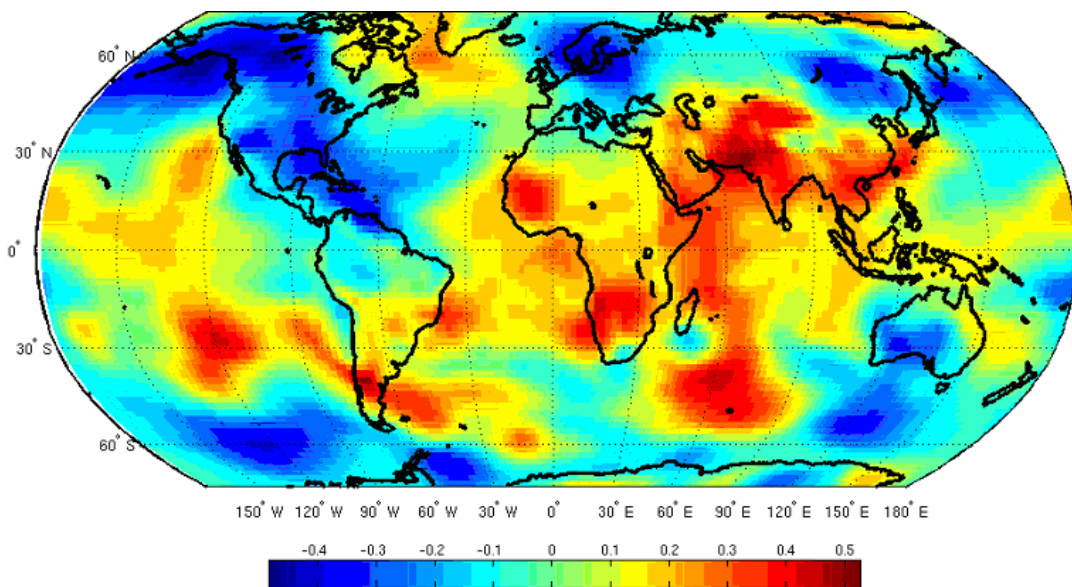


Fig. 5.11: Same as Fig. 5.9, but for winter (DJF) season.

### 5.2.12 Monthly mean sea level pressure of January through May

Correlations were determined for individual months with lead times up to five months before the SM season of Bangladesh. From up to five months lead time, January through May, a significant positive relationship between SMR of Bangladesh and SLP of the central Pacific Ocean was found in the month of April. All other months were not found strong correlations anywhere in the globe. Thus, the correlation was performed between

April SLP over central Pacific Ocean and SMR of Bangladesh (Fig. 5.12d). Where the same SLP region shows a positive correlation with SMR of Bangladesh for different lead times for different months, only the one with the highest positive correlation over the area was selected in this study. The correlations are insignificant over rest of the part of the world during this month. From Fig. 5.12(a-e), it is seen that January, February, March, April and May SLP of the central Pacific Ocean is positively highly correlated with SMR of Bangladesh. In this case the April SLP was used because it showed the highest correlation over central Pacific Ocean ( $2.5^{\circ}$  -  $7.5^{\circ}$  N latitude  $145^{\circ}$  -  $150^{\circ}$  W longitude) over large area than the others area. The correlations are weak over rest of the Ocean area as shown in Fig. 5.12(a-e).

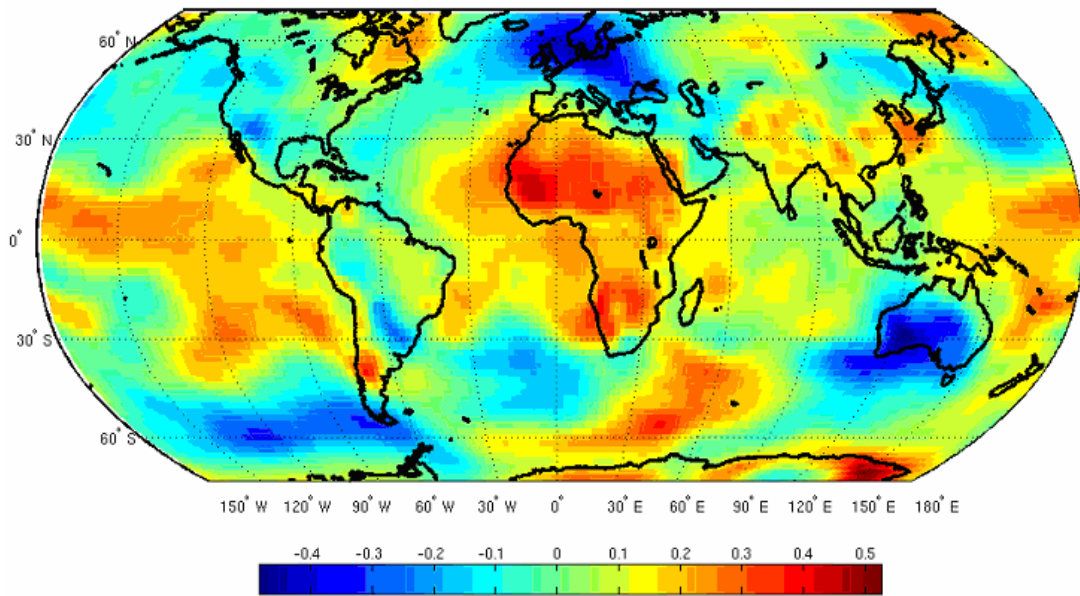


Fig. 5.12a: Spatial pattern of January correlation coefficients between MSLP and SMR of Bangladesh.

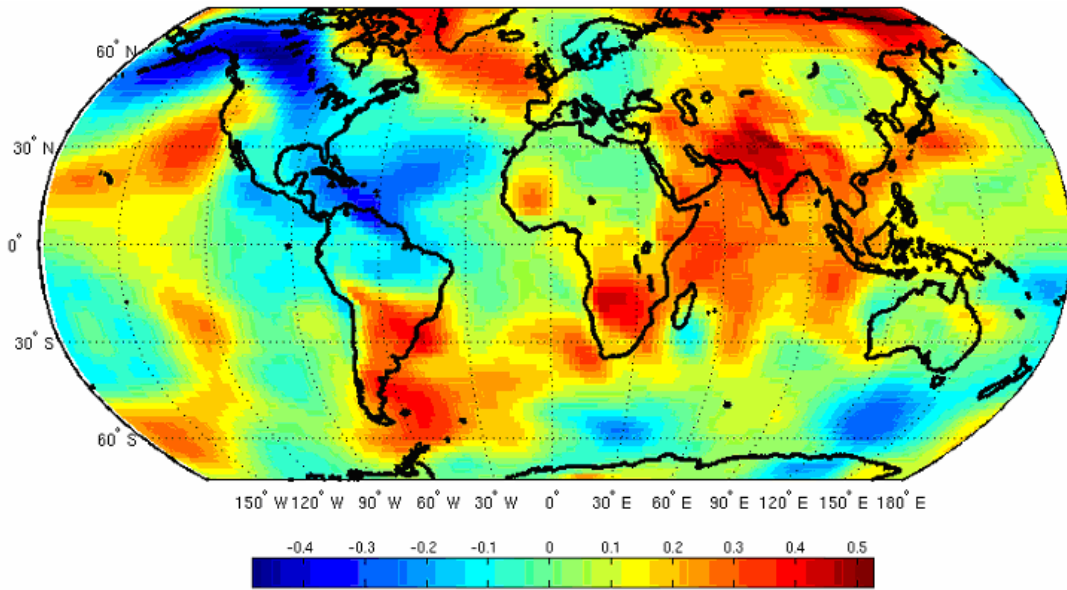


Fig. 5.12b: Same as Fig. 5.12a but for the month of February.

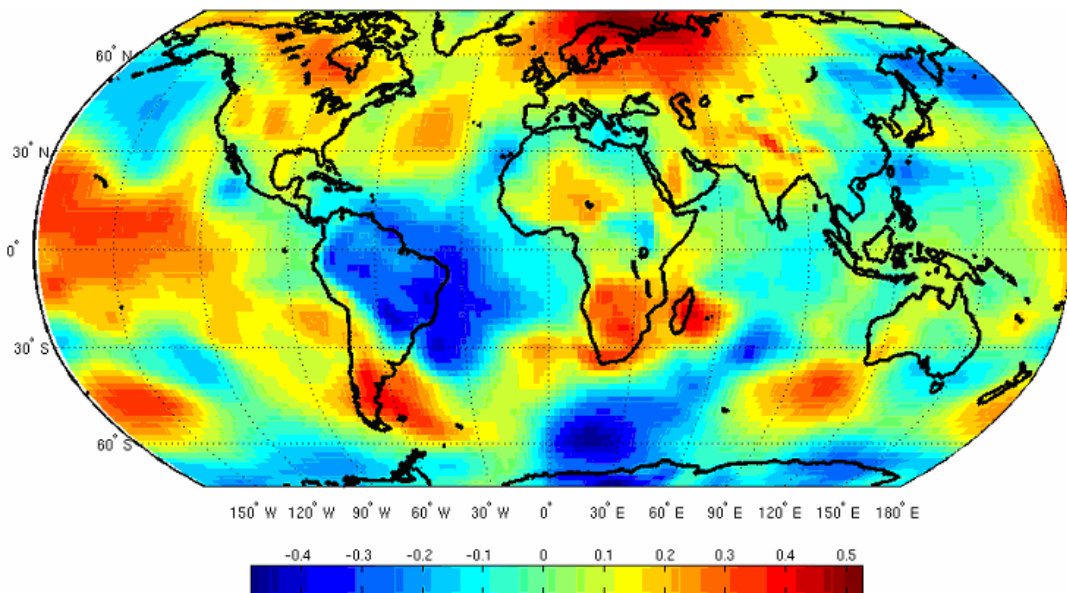


Fig. 5.12c: Same as Fig. 5.12a, but for the month of March.

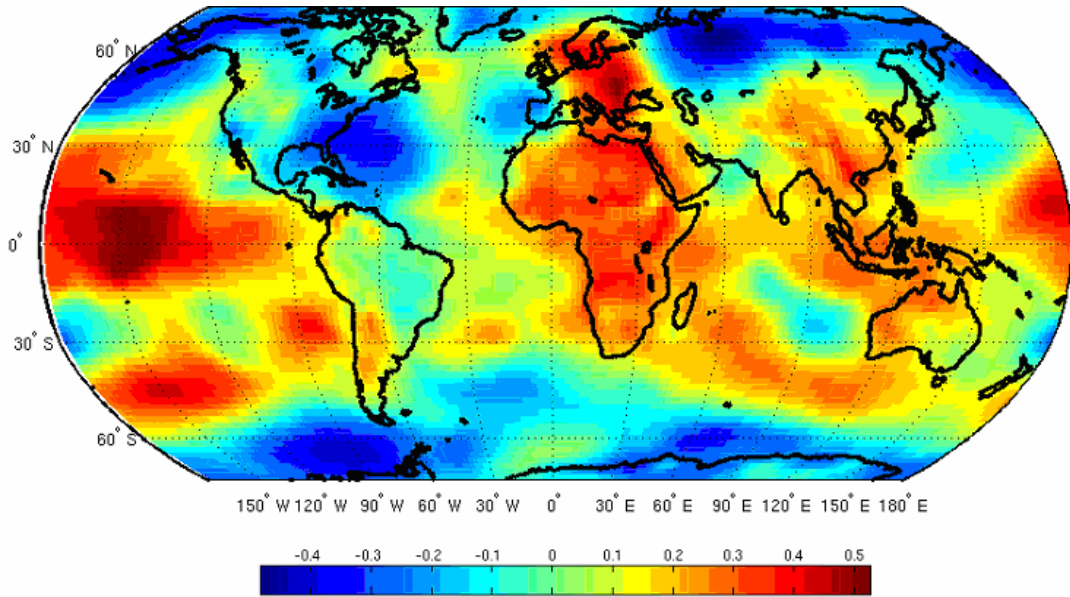


Fig. 5.12d: Same as Fig. 5.12a, but for the month of April.

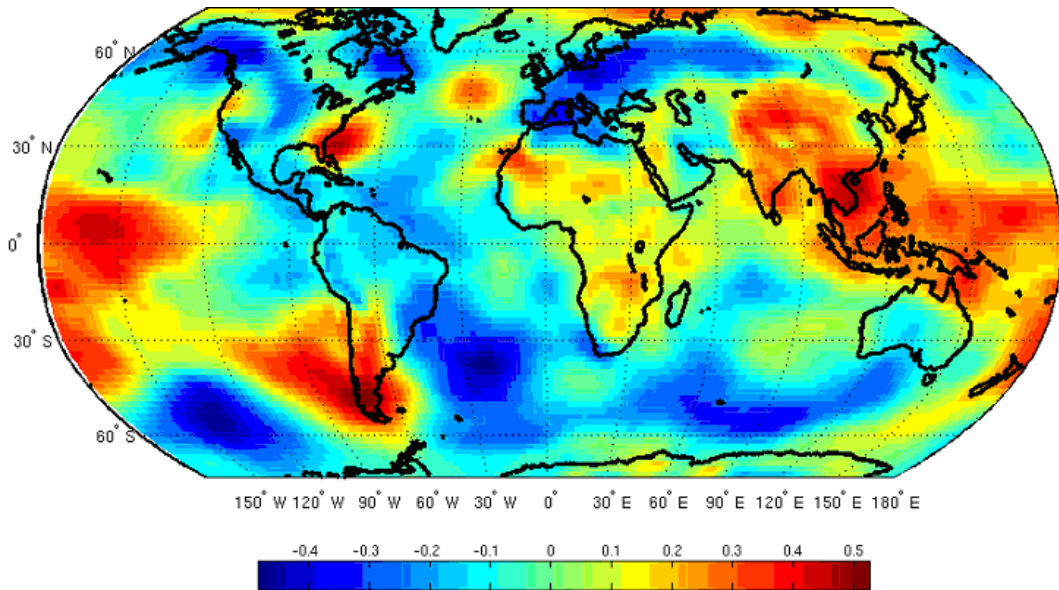


Fig. 5.12e: Same as Fig. 5.12a, but for the month of May.

### 5.3 Teleconnection between SMR and ENSO

In this section, the interannual variability of SMR over Bangladesh and its relationship with ENSO is examined. Recently, Suppiah [51] reported decadal-scale changes in the relationship of the Southern Oscillation Index (SOI) with the rainfall over Australia, India, Sri Lanka, and Tahiti, and argued that they were due to multi-decadal variations and trends during the past century. In this section, the secular variations in the

relationships between SMR and ENSO over Bangladesh, and the associated changes in circulation regimes are examined.

### 5.3.1 ENSO impact on SMR

The spatial patterns of CCs between SMR of Bangladesh and seasonal SST (concurrent JJAS and preceding two seasons, *viz.*, DJF and MAM) based on the data period 1961-2008 are presented in Figs. 5.1-5.3. The relationship first appears in pre-monsoon season and gradually strengthens and becomes extensive during the concurrent season (Figs. 5.1-5.2). However, further examination of the relationship over shorter segments of the data period reveals that the relationship is statistically insignificant (Table 5.1) during the years 1961-1984 and 1985-2008, respectively. For the earlier period 1961-1984, the CCs are nearly zero over the central and eastern Pacific in Table 5.1. For the recent period 1985-2008, the CCs are positive at and above 0.11 over the central and eastern Pacific but it is not statistically significant.

The secular variation of the ENSO-SMR relationship noted above can be clearly demonstrated by means of 21-year sliding correlations of SMR with Niño3 index for the two seasons MAM and JJAS for the period 1961-2008 (Fig. 5.13). The sliding correlations indicate conspicuous epochal variations in the relationship over the past century. During the period 1985-2008, correlations were positive and insignificant. It is interesting to note that the relationship between SMR and ENSO remained generally weak and positive during recent parts of the century. Krishna Kumar *et al.* [52] reported that the ENSO-SMR relationship over India is negative. While the correlation between ENSO and SMR is generally positive over Bangladesh but not statistically significant, it is interesting to note that its secular variation of the correlation between SMR and Niño3 SSTs (Fig. 5.13).

The secular change in the relationship between SMR of Bangladesh and Niño3 SST is further examined. There is a clear evidence for increasing trend in SSTs over tropical Pacific, particularly over Nino3 region, the relationship between SMR of Bangladesh and the SST is positive. An increasing trend in rainfall and an increasing trend in SST would not necessarily strengthen the relationship, but could shift the regression lines to an upper level. If one applies two regression lines using SSTs and SMR for two different periods (1961-1984 and 1985-2008), both lines would show positive relationship as long

Table 5.1: The correlations between SMR and ENSO during the period 1961-2008.

| <b>Region</b>         | <b>Period</b>    |                  |                  |
|-----------------------|------------------|------------------|------------------|
|                       | <b>1961-1984</b> | <b>1985-2008</b> | <b>1961-2008</b> |
| <b>Nino3 (MAM)</b>    | 0.18             | 0.14             | 0.19             |
| <b>Nino3 (JJAS)</b>   | 0.08             | 0.15             | 0.12             |
| <b>Nino3.4 (MAM)</b>  | 0.03             | 0.11             | 0.09             |
| <b>Nino3.4 (JJAS)</b> | 0.0              | 0.15             | 0.03             |

as the SSTs are also showing an increasing trend, but the question is whether these two lines are going to show any significant change in the regression coefficient or slopes? If the answer is YES, then the relationship has strengthened in recent years, if NOT the argument for a strengthening the relationship is very weak. Simply there is more rainfall for a given SST between the mid-1985 to 2008. Therefore, the slopes of the regression lines for these two periods were examined to see whether there is a change in the relationship or the relationship has strengthened. Simple linear regression lines were fitted for seasonal Nino3 SST and SMR separately during the two sub-periods 1961-1984 and 1985-2008 as shown in Figs. 5.14(a-b). A clear shift towards a stronger relationship during the recent period is indicated by this analysis. While the slope of the regression before 1984 is 20 mm/°C and also showing increasing trend whereas after 1985 the slope is 36 mm/°C which is both period not statistically significant.

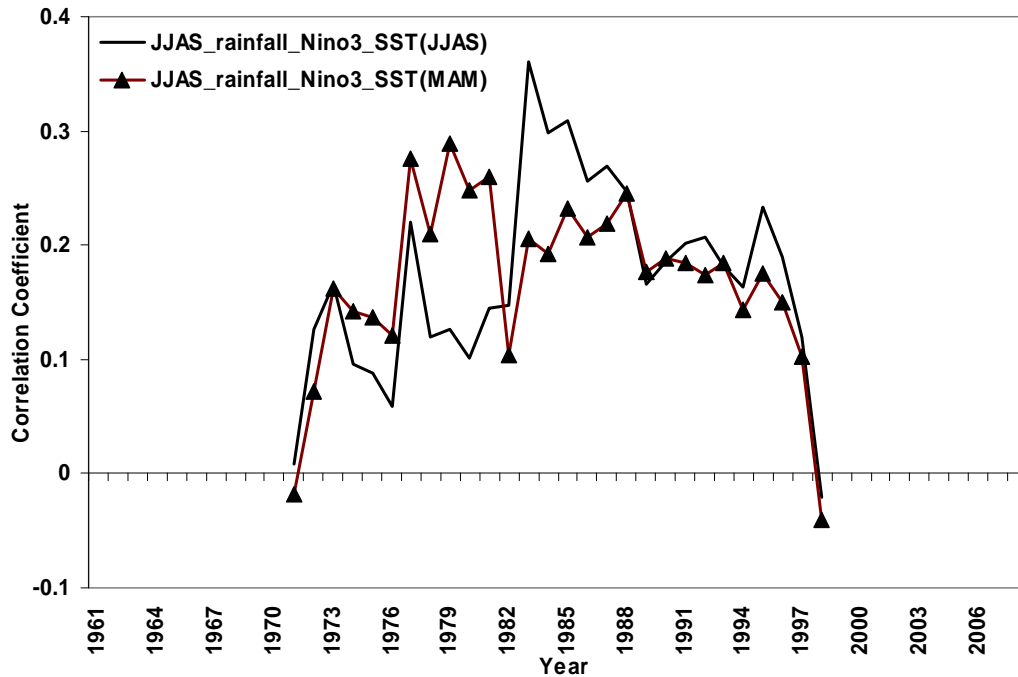


Fig. 5.13: 21-year sliding correlation of SMR with Nino3 SSTs during the pre-monsoon and monsoon seasons.

The recent surge in the relationship between SMR of Bangladesh and ENSO is further demonstrated in terms of SMR anomalies during the El Niño years for 1961-2008 (Table 5.2). While the anomalies are generally positive, it is observed that the composite average SMR anomaly during the El Niño years after 1985 is considerably large almost five times in comparison with that before 1985. The composite mean SMR anomaly during El Niño years after 1985 is about 51 mm while the same before 1985 is -12 mm. It has further been noted that the mean SMR in the two periods 1961-1984 and 1985-2008 is 1674 mm and 1771 mm, respectively. This reflects that the substantial strengthening of the relation between El Niño and SMR during the recent years is not associated with any major shifts in the SMR itself.

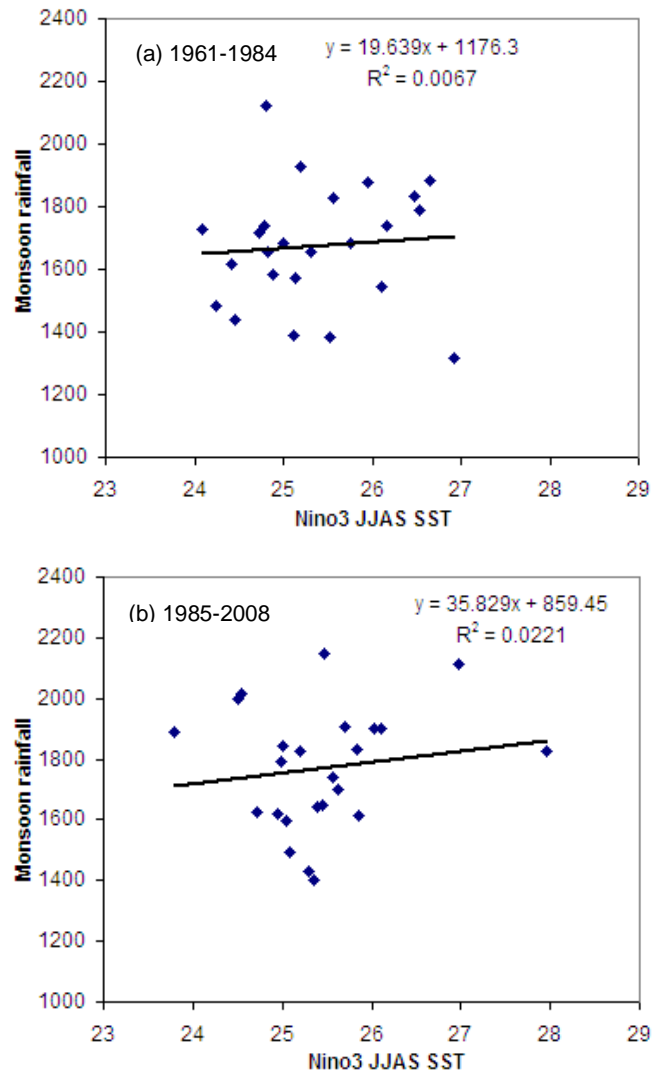


Fig. 5.14: Scatter diagram showing the relationship between Nino3 SST and SMR during the period (a) 1961-1984 and (b) 1985-2008.

Table 5.2: SMR anomalies during the El Niño years over the two halves of the period 1961-2008.

| <b>Year</b>    | <b>Anomaly (mm)</b> | <b>Year</b>    | <b>Anomaly (mm)</b> |
|----------------|---------------------|----------------|---------------------|
| 1963           | -159                | 1987           | 413                 |
| 1965           | 86                  | 1991           | 198                 |
| 1966           | -131                | 1992           | -299                |
| 1969           | 176                 | 1993           | 206                 |
| 1972           | -386                | 1994           | -273                |
| 1977           | -44                 | 1995           | 88                  |
| 1978           | 36                  | 1997           | 127                 |
| 1982           | 185                 | 2002           | 198                 |
| 1983           | 133                 | 2003           | -59                 |
| -              | -                   | 2006           | -85                 |
| <b>Average</b> | <b>-104/9 = -12</b> | <b>Average</b> | <b>514/10 = 51</b>  |

### 5.3.2 SST anomalies during the extremes of SM season

The influence of SST over Indian Ocean has been an important factor in explaining the changes in SM circulation and rainfall over South Asia. Since a considerable amount of atmospheric moisture for the region comes from the Indian Ocean, it is reasonable to assume that SST anomalies and winds over the oceanic areas would have marked influence over the weather and climate of India and Bangladesh. In the present context, it would be interesting to examine the impact of Indian Ocean SST during El-Niño years over the Bangladesh.

To examine the Indian Ocean forcing during the excess/flood and deficient/drought years of SM, composite SST anomalies patterns are worked out for the concurrent season (JJAS). For this purpose, we have identified the excess or deficient years as those having their SM seasonal rainfall anomaly magnitudes exceeding one standardized values during the data period 1961-2008. Using this criterion, we find eight excess years (viz., 1974, 1984, 1987, 1993, 1999, 2002, 2004 and 2007) and eight deficient years (viz., 1962, 1972, 1973, 1975, 1980, 1989, 1992, and 1994).

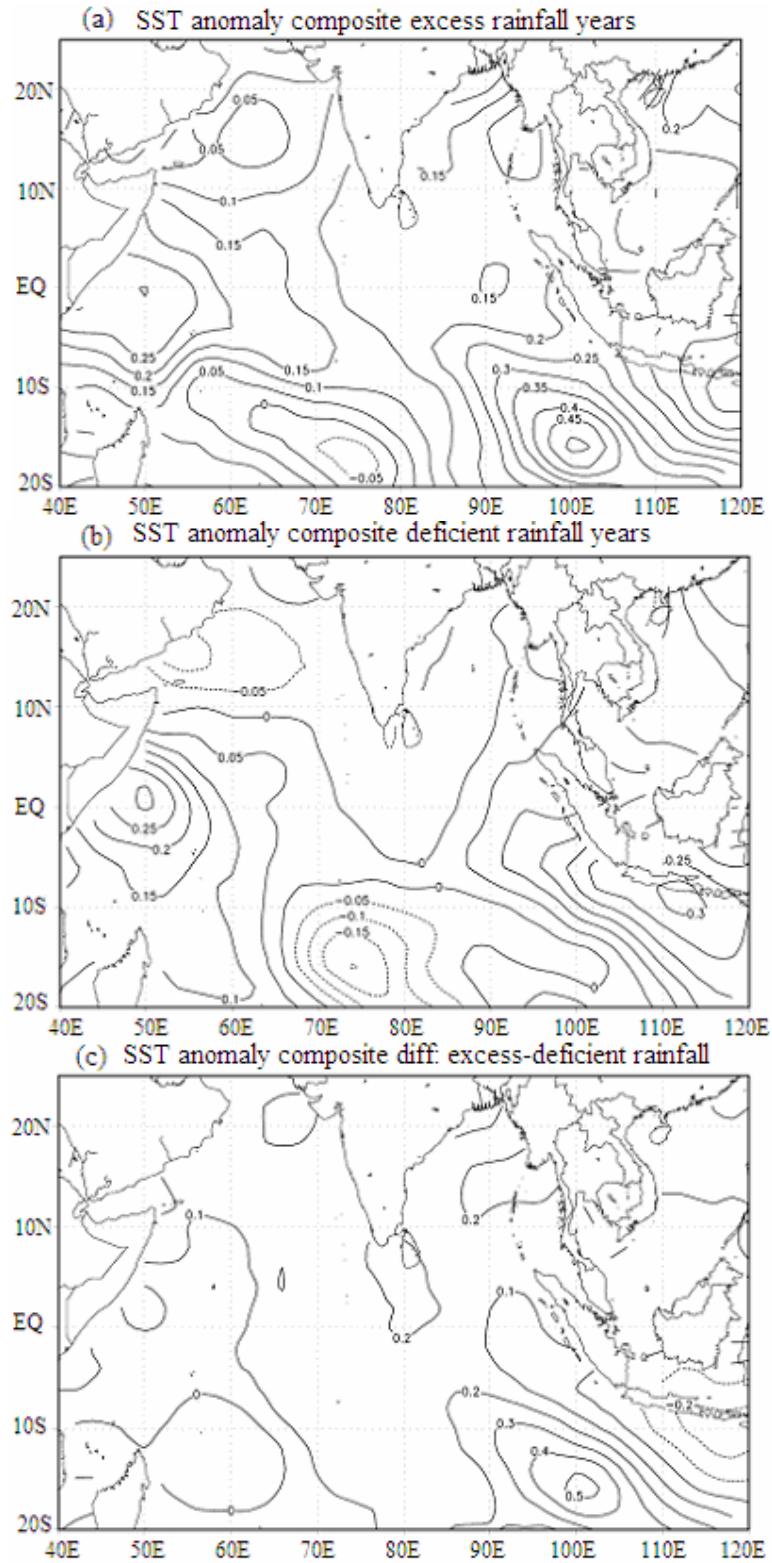


Fig. 5.15: Composite monsoon seasonal (JJAS) SST anomalies ( $^{\circ}\text{C}$ ) during (a) excess rainfall years (b) deficient rainfall years and (c) excess minus deficient years.

The excess/flood-year composite anomalies of SST over the Bay of Bengal and the Arabian Sea are positive (Fig. 5.15a), indicating conditions favorable for convection over the region supporting good SMR activity. On the other hand, during deficient/drought years (Fig. 5.15b), nearly zero and negative SST anomalies prevail around the Bay of Bengal and the Arabian Sea, a condition not for good favorable SMR activity. The excess/flood minus deficient/drought composites of the SSTs is predominantly positive all around the region, with a large area under magnitudes of  $0.4^{\circ}$  to  $0.5^{\circ}\text{C}$ . A two-tailed Student t-test indicates significant contrast between the two composites over southeast Indian Ocean (Fig. 5.15c).

### **5.3.3 SST anomalies around SM region during El-Niño years**

To examine the contrasting aspects of the SSTs over the Indian Ocean during El-Niño years for the periods 1961-1984 vis-à-vis 1985-2008, El-Niño composites of SST anomalies are worked out separately for the two periods. For this purpose, we have considered all the El Niño years that occurred during the period 1961-2008 (viz., 1963, 1965, 1966, 1969, 1972, 1977, 1978, 1982, 1983, 1987, 1991, 1992, 1993, 1994, 1995, 1997, 2002, 2003 and 2006). These 19 El Niño years have been divided into two groups representing the periods 1961-1984 and 1985-2008.

We have already seen in the previous section that warm SST anomalies over the Indian Ocean in the proximity of the South Asia region including Bangladesh are favorable for good SMR activity. The SST anomaly patterns of El Niño composites during 1985-2008 (Fig. 5.16a) are in good agreement with those for the excess years of SMR. While the SST anomalies during the El-Niño years for the period 1961-1984 are also positive over the Indian Ocean, their magnitudes are substantially lower particularly over the Bay of Bengal (Fig. 5.16b) in comparison to recent El-Niño years. The difference between the above two composites is tested by two tailed Student's t-test (Fig. 5.16c). In Fig. 5.16c, shading indicates statistical significant of the differences at and above 5% level, as determined by a two-tailed Students t-test. The composite anomalies clearly show significant differences over the Bay of Bengal. Thus, the El-Niño associated SST anomalies in the recent years have increased by nearly  $0.4^{\circ}$ - $0.5^{\circ}\text{C}$  which provided favorable conditions for enhanced convection and moisture supply to the SAARC region including Bangladesh. This appears to be one of the manifestations of the recent strengthening of the relationship between El-Niño and SMR.

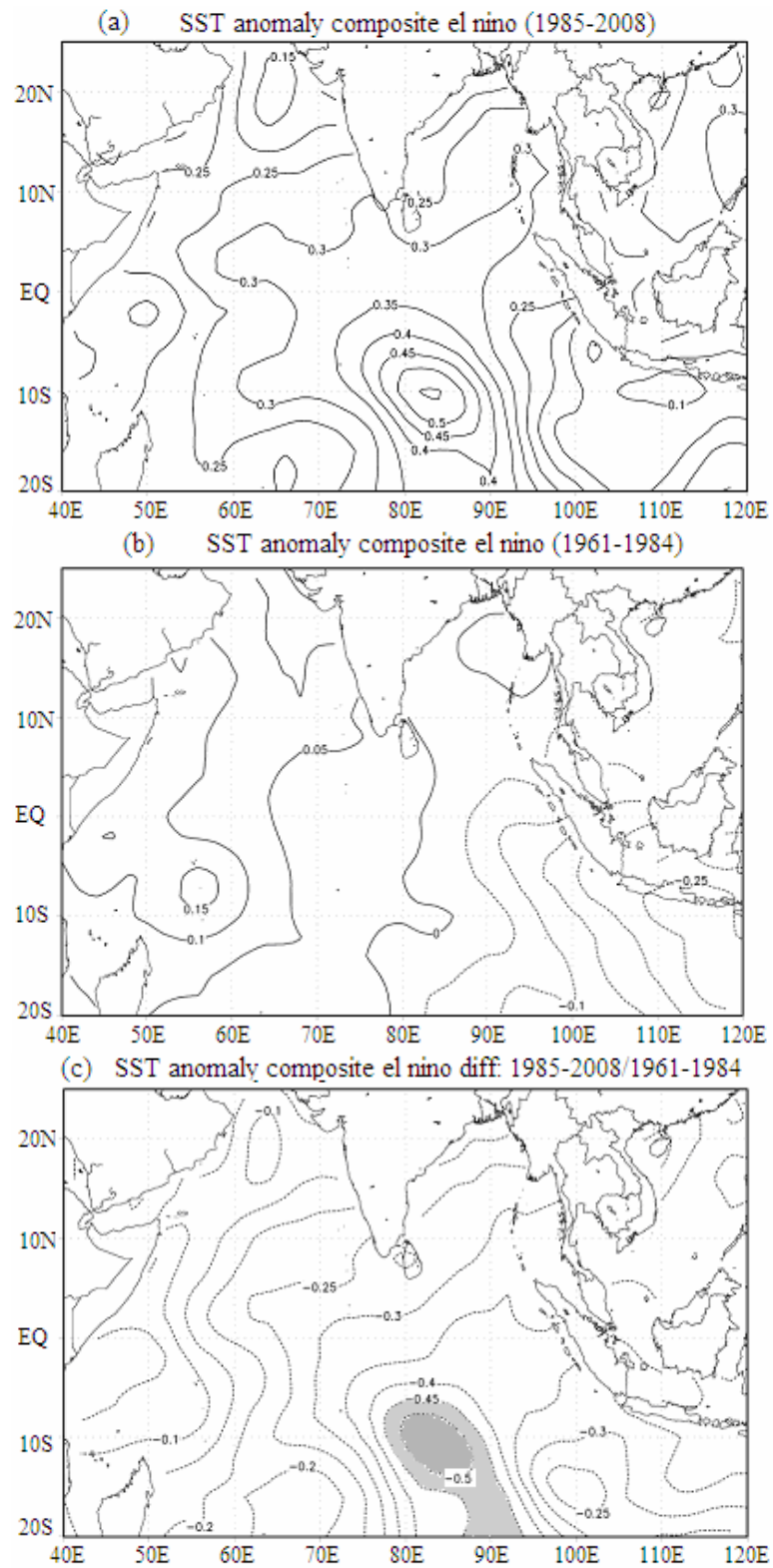


Fig. 5.16: Composite monsoon seasonal (JJAS) SST anomalies ( $^{\circ}\text{C}$ ) during El-Niño years for the two sub-periods (a)1985-2008 and (b)1961-1984, and (c) difference between the two sub-periods.

#### **5.3.4 Low-level circulation anomalies in extreme years of SM activity**

The low-level circulation during the SM season is dominated by westerly/southwesterly winds over South Asia including Bangladesh. To examine the low-level circulation anomalies during the years of extremes in SMR, composite 850 hPa wind anomalies and during the same season have been worked out for excess and deficient years. Figs. 5.17(a-b) show the composite low-level (850 hPa) wind anomalies during excess and deficient years. The wind anomalies southwesterly/ westerly over the IO and India region during the excess years, possibly due to the fact that a stronger SM is associated with the active ITCZ oriented in a northward direction along Arabian Sea after that westerly winds towards Bangladesh (Fig. 5.17a). Moisture convergence, which occurs when the distribution of winds within a given area results in a net horizontal inflow of moisture in the region, is a good indicator of the moisture availability in the region. In contrast to this feature, during the deficient years, wind anomalies are northerly/northwesterly indicating a weakening of ocean-to-land flow associated with anomalous moisture divergence in the region, particularly over southwestern Bay of Bengal and the adjoining area (Fig. 5.17b), resulting in a reduced moisture influx from the Indian Ocean as well as Bay of Bengal into the Asian region including Bangladesh.

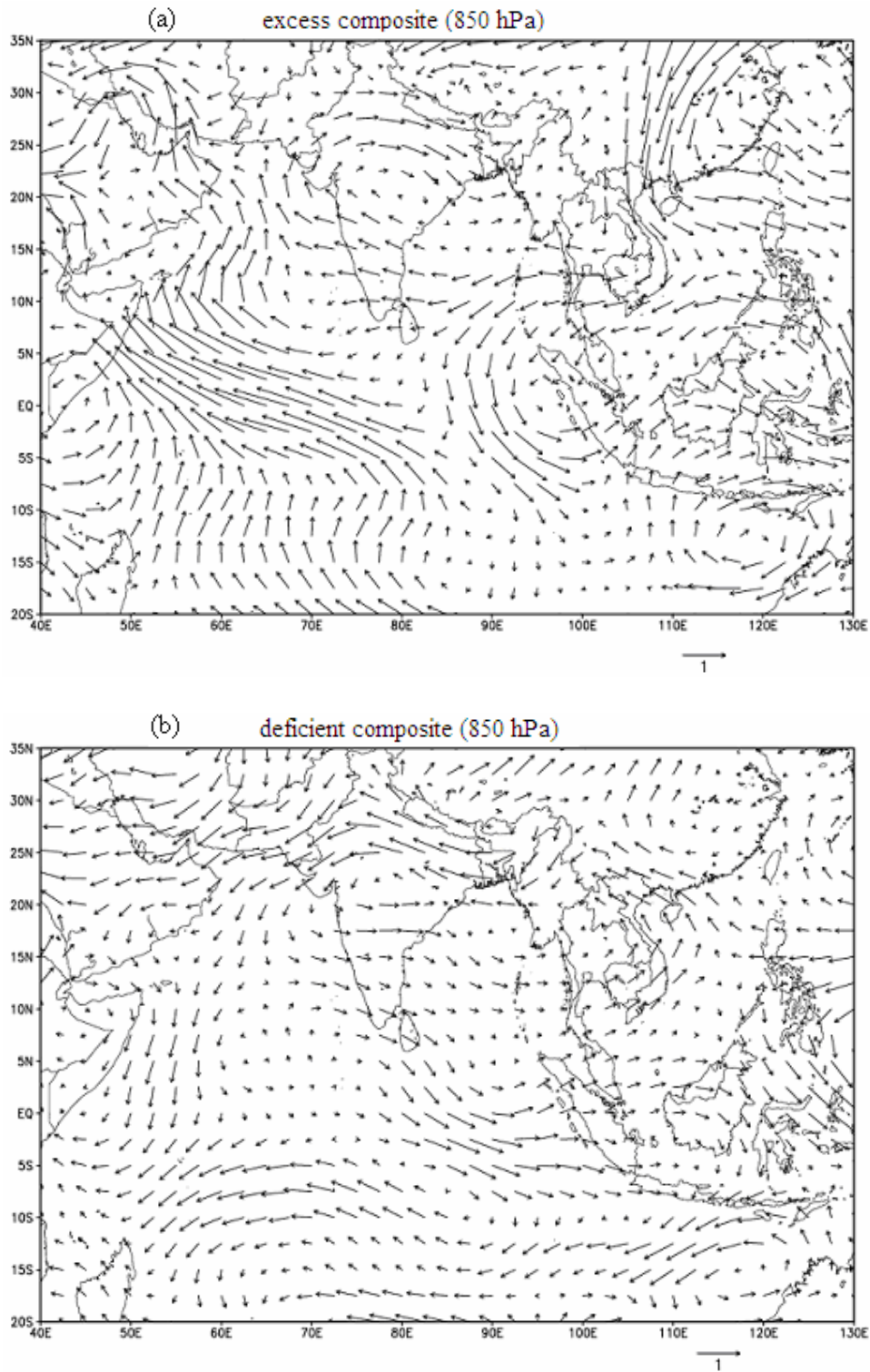


Fig. 5.17: Composite wind anomalies (m/s) at 850 hPa during the SM season for (a) excess/flood years rainfall and (b) deficient/drought rainfall years during the period 1961-2008.

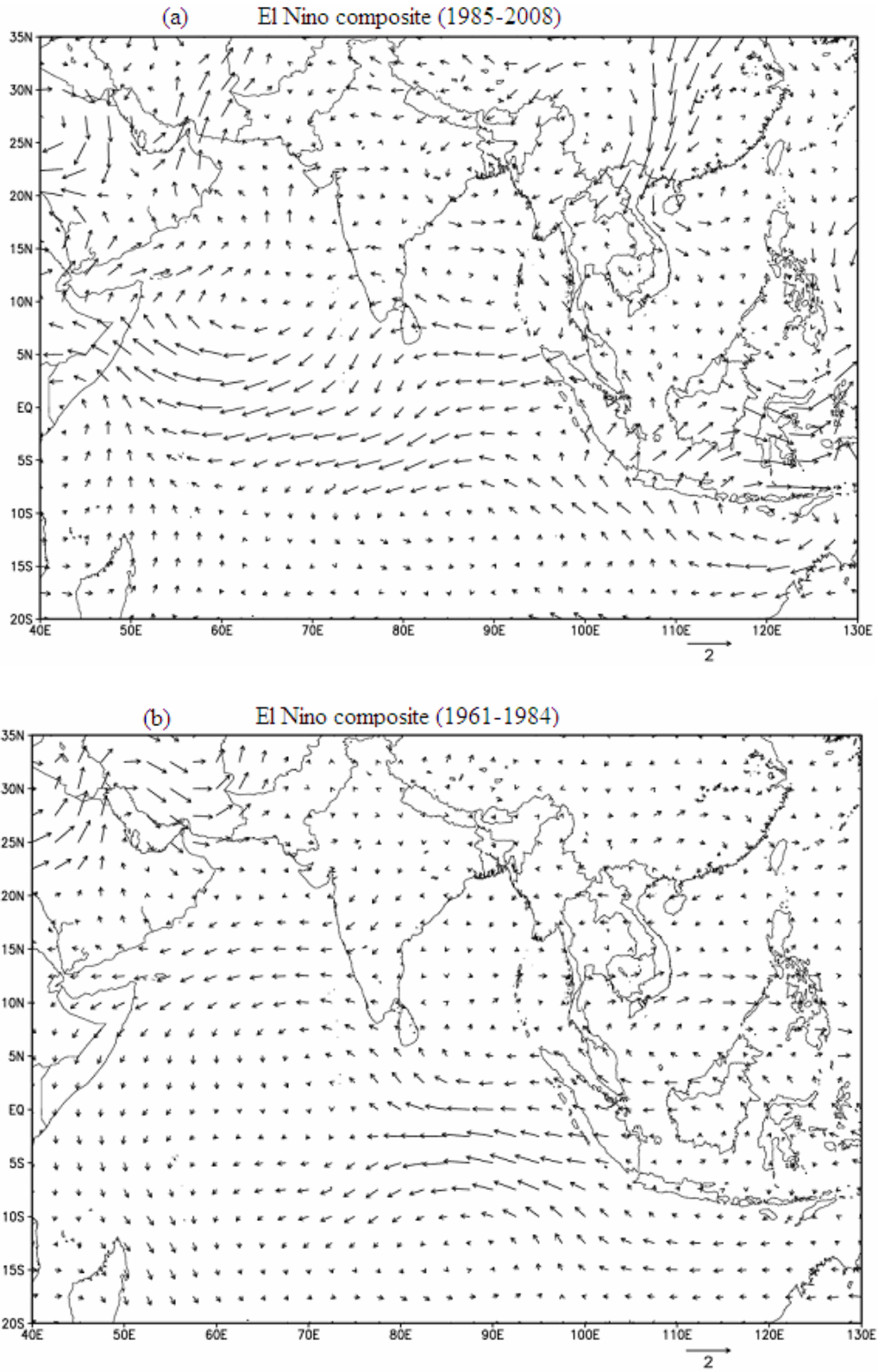


Fig. 5.18: Composite wind anomalies (m/s) at 850 hPa during the SM season for El Niño years during the two sub- periods (a) 1985-2008 and (b) 1961-1984.

### 5.3.5 Secular variations in ENSO-associated circulation anomalies

The teleconnections between SMR of Bangladesh and ENSO is best described by large-scale east-west shifts in the tropical Walker circulation. During El-Niño years, the tropical convection and the associated rising limb of the Walker circulation located in western Pacific shifts towards the central and eastern Pacific; therefore, there is anomalous subsidence over the western Pacific. It is associated with anomalous high pressure over the western Pacific and anomalous low pressure over the central and eastern Pacific. The subsidence over the western Pacific is associated with stronger easterlies at lower level over South Asia leading to higher moisture supply and good rainfall over this region.

To examine the low-level circulation features associated with the weaker and stronger phases of the relationship between ENSO and SMR of Bangladesh, composite 850 hPa wind anomalies during the same season have been worked out for the El Niño years during the periods of the respective phases. The composite circulation anomalies during the El Niño years for the period 1985-2008 are more or less similar to those associated with typical excess SMR years (Fig. 5.18a), clearly indicating that the wind anomalies over IO and Arabian Sea are easterly to southwesterly and vice versa. El Niño composites of this period also suggest anomalously higher levels of moisture convergence in the region. However, El Niño composite of SM circulation during the earlier period 1961-1984, has considerably opposite wind anomalies direction compare to the period 1985-2008 and does not seem to represent the typical excess SMR situation (Fig. 5.18b). There is no low-level moisture convergence over the region, and therefore the conditions do not seem to be favorable for good SMR activity.

Thus, the above analysis clearly indicates that the nature of ENSO impact on SMR was opposite to the earlier period (1961-1984) but recent period (1985-2008) has been increasing positive impact on SMR over Bangladesh. While it has been conjectured that the ENSO-SMR relationship over India has been weakening over the past couple of decades reported by Krishna Kumar *et al.* [52], the present study over Bangladesh indicates that the ENSO-SMR relationship has been strengthening during the recent years. Both these features are unprecedented over India and Bangladesh, and point towards a significant change in the impact of ENSO on the regional climate over South Asia.

## 5.4 SMR and Indian ocean dipole

Saji *et al.* [53] and Webster *et al.* [54] have pointed out that a unique ocean-atmosphere mode exists in the IOD with anomalous warm SSTs over the western IO and anomalous cold SSTs in the eastern IO. This mode induces unusual rainfall distribution in the surrounding areas, and is termed as the Indian Ocean Dipole Mode (IODM). This dipole mode modulates the Maha (September-October) rainfall over Sri Lanka [55-56], which lies at the middle of the dipole. The influence of the IODM on extreme SMR has been examined by correlation and composite analysis. The circulation and SST features associated with the active dipole phases and the extreme monsoon phases are determined. A comparison is made to ascertain whether a particular dipole phase has any bearing on the extreme monsoon phase.

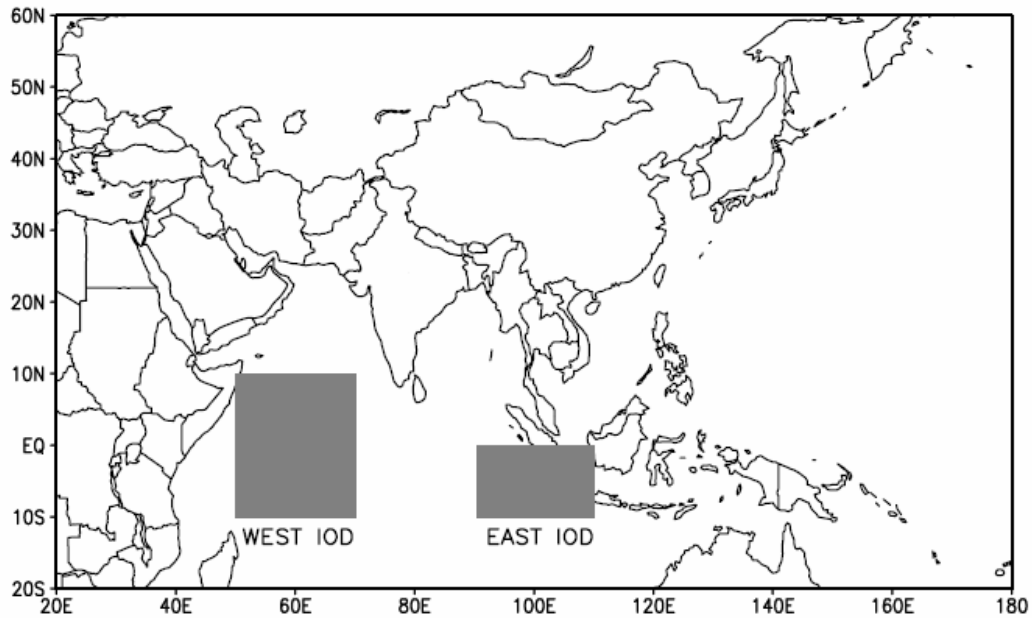


Fig. 5.19: Map showing the locations of two blocks over the western IOD and the southeastern IOD.

An index to quantify the IODM has been proposed by Saji [53]. This is the difference in SST anomaly between the tropical western IO ( $50^{\circ}$  -  $70^{\circ}$  E,  $10^{\circ}$  S -  $10^{\circ}$  N) and the tropical southeastern IO ( $90^{\circ}$  -  $110^{\circ}$  E,  $10^{\circ}$  S - Equator). The location of the two blocks is shown in Fig. 5.19. The standardized monthly time series for the IODM for the period 1961-2008 has been derived from the monthly HadISST dataset. From the monthly data,

seasonal time series for SM (JJAS) are prepared, since the mode initiates in summer, peaks in autumn and thereafter it decays. This data set is also utilized to examine the anomalous SST fields over the IO.

No time filters are applied to any of the above data sets to remove any periodic variations, nor techniques applied to remove the influence of other phenomenon (such as ENSO) since in real atmosphere IODM, ENSO and monsoons are a part of very large coupled process and not expected to behave in isolation.

#### **5.4.1 IODM and its variability**

The normal IO is warm in the east and cool in the west, associated with westerly winds blowing towards Indonesia. Indian Ocean Dipole (IOD) is a coupled ocean-atmosphere phenomenon in the IO. It is characterized by anomalous cooling of SST in the south eastern equatorial IO and anomalous warming of SST in the western equatorial IO [53]. In response to this SST changes, cooler waters in the eastern IO gives rise to easterly winds along the equator, enhancing the cooling in the eastern equatorial IO and promoting warming in the western equatorial IO [54,56]. Further in response to this, convection over the eastern (western) tropical IO is suppressed (enhanced) as the easterly wind anomaly over the central IO is intensified [57]. This state of the IO is identified as a positive IODM event, which develops rapidly in boreal summer and peaks in boreal autumn. The intensified reverse situation viz warm (cool) SST anomalies over the southeast (western) equatorial IO is termed as the negative IODM.

#### **5.4.2 Interannual and decadal variability**

The standardized IODM values and the values of Cramer's  $t$ -statistics for the 11-year running means for SM season (JJAS) are depicted in Fig. 5.20. While the standardized values show random fluctuations, the Cramer's  $t$ -statistics reveal interesting results. The decadal variability for SM season (Fig. 5.20b) reveals that during the period prior to 1977, the mode was on the negative side, thereafter most of the time it has been on the positive side during the recent decades and the general increasing trend of the mode may be due to global warming, instrumental errors or different data sources used to derive SST reconstructions. However, the fact that SMR variability is large (1966-1978, 1981-2003) when the mode is in its active phase (1966-1976, 1977-2003) and the fact that SMR and IODM variability appears to be suppressed during 1990-1996 period, suggests

that the two may be connected in some way. Further since the SMR and IODM series are generated from different sources, we speculate that the behavior cannot be attributed to instrumental or data errors.

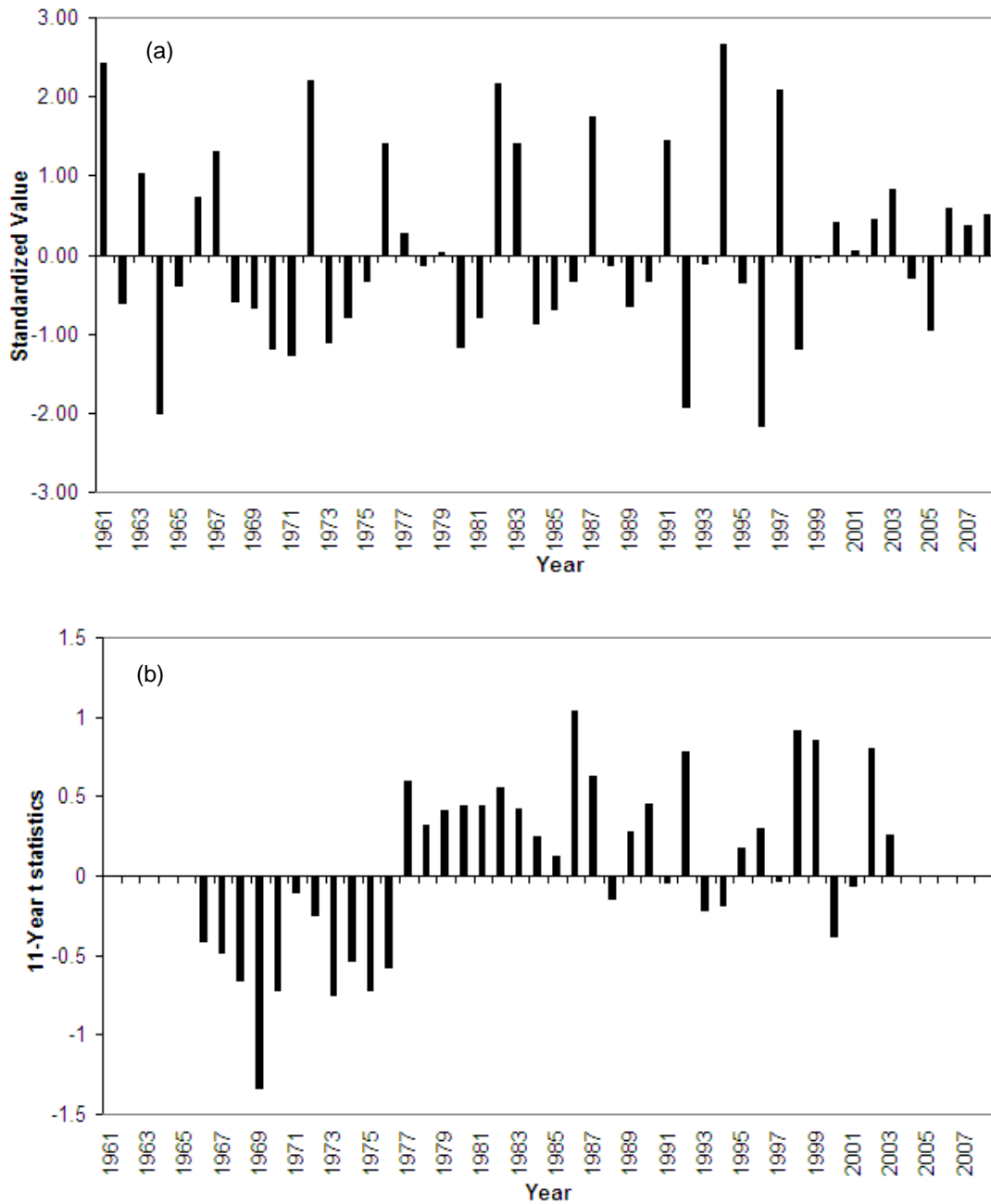


Fig. 5.20: Variability of JJAS IODM (a) year to year interannual variability and (b) the values of Cramer's  $t$ -statistics of 11 year running mean depicting decadal variability and the epochs of above and below normal rainfall. Values are plotted at the centre of 11 year period.

### **5.4.3 Relationship between SMR and IODM**

The search for the relationships usually involves the calculation of a sample cross-correlation function for the pairs of time series. The standardized IODM series for SM season (JJAS) have been subjected by statistical techniques. The correlation coefficients between SMR and JJAS IODM are 0.07. It is a weak correlation and but not statistically significant.

Another way to understand the dynamics involved in the SMR-IODM relationship is to determine the large-scale circulation features associated with the active dipole phases and the extreme monsoon phases. A comparison of these anomalous flow patterns can give us an idea whether a particular dipole mode has any impact on the extreme monsoons. Before the circulation features associated with the extremes are examined, the climatology of the wind vectors at the 850 hPa level for the SM (JJAS) is depicted in Fig. 1.9a, while the southwesterly flow is evident during the SM (Fig. 1.9a). The changes observed in this normal flow patterns due to the active dipole or extreme monsoon phases are examined in subsequent sections.

### **5.4.4 Circulation associated with active dipole phases**

To examine how the above discussed pattern changes with IODM extremes, years have been identified for the extreme positive and negative phases of the mode using objective criteria. For the data period 1961-2008, there are 11 years (1961, 1963, 1967, 1972, 1976, 1982, 1983, 1987, 1991, 1994 and 1997) where the standardized dipole index during summer are greater than +1.0. Similarly 8 years (1964, 1970, 1971, 1973, 1980, 1992, 1996 and 1998) are identified with index less than -1.0. These active dipole events are tabulated in Table 5.3. For the identified sets of positive and negative dipole indices composite anomalies for the 850 hPa vector winds are computed to examine the changes in the normal circulation flow over the IO region. The anomalies are prepared by subtracting the climatology based on the 1961-2008 period from the 11 and 8-year means. Contrasting circulation features are evident and results for the SM (JJAS) season only are also presented in Fig. 5.21.

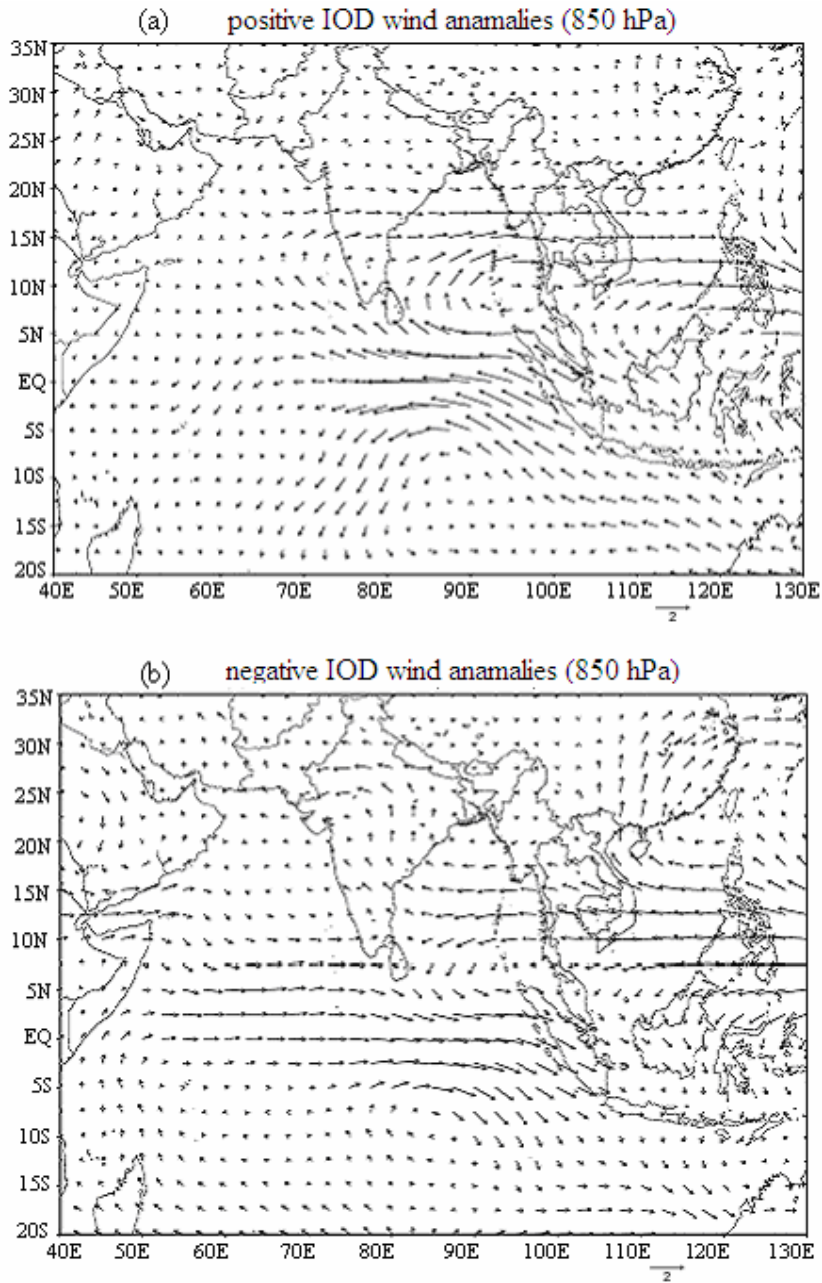


Fig. 5.21: Composite wind anomalies (m/s) at 850 hPa during the SM season for (a) Positive IOD and (b) Negative IOD during the period 1961-2008.

Fig. 5.21(a) and Fig. 5.21(b) shows the vector wind composite anomalies at 850 hPa level for the positive and negative IODM respectively. A comparison of these panels reveals remarkable opposite flow patterns for the two extremes of the dipole index over the IO region. Strong easterly / southeasterly anomalies prevail between  $10^{\circ}$  S to  $10^{\circ}$  N over the equatorial IO region for the positive phase of the dipole mode, and

westerly/easterly (over Bay of Bengal) anomalies for the negative phase of the dipole mode.

The easterly anomalies with the positive phase are larger in magnitude and heavily concentrated over the equatorial IO, suggesting that the temperature contrast between the warmer waters over the western IO and cooler over the eastern IO associated with the positive phase is much steeper than for the cooler (warmer) water over western (eastern) IO for the negative phase. This can also be inferred from Table 5.3. Whereas the average index for the 11 extreme positive events is +1.81 and 8 extreme negative is -1.50, respectively. The wind pattern associated with the positive phase, suggests a transport of moisture from the eastern IO towards the southern parts of India but not towards Bangladesh (Fig. 5.21a). Another notable feature observed during the positive phase is an anomalous anti-cyclonic circulation over the south Bay of Bengal with center around  $8.5^{\circ}$  N,  $95.5^{\circ}$  E. The easterly anomalies at the southern edge of this anticyclone will also support moisture convergence over the southern parts of India but not over Bangladesh.

However, the flow pattern associated with the negative phase of the mode suggests wind anomalies are westerly /easterly indicating conditions favorable for SM over southern parts of India.

#### **5.4.5 SST anomalies associated with active dipole events**

To examine the information on the ocean forcing, SST anomaly patterns for the positive and negative IOD phases are depicted in Fig. 5.22 based on the extremes in Table 5.3. Cold SST anomalies near the Sumatra coast and in the eastern IO and warm SST anomalies in the region of central and western IO are associated with the positive phase of the dipole (Fig. 5.22a). The contrast between the SST anomalies over the western and eastern IO is obvious.

Thus, the anomalous westward low-level winds (Fig. 5.21) in response to the anomalous zonal gradient of SST will increase the moisture transport towards over southern parts of India and enhance atmospheric convection. For the negative IOD phase, warm SST anomalies over southeast IO and cold anomalies over the western IO are seen (Fig. 5.22b). These composites also show significant difference over the western and southeast IO (Fig. 5.22c). However, the contrast between the SST anomalies over the two poles is less steep compared with the positive phase.

Table 5.3: Standardized difference in SST anomalies between the tropical western Indian Ocean and tropical southeast Indian Ocean for the SM season (JJAS) depicting IODM intensity. Table shows the 11 active positive and 8 negative events.

| <b>Active Dipole Events</b> |                |                     |                |                     |
|-----------------------------|----------------|---------------------|----------------|---------------------|
| <b>Sl. No.</b>              | <b>Year</b>    | <b>Positive IOD</b> | <b>Year</b>    | <b>Negative IOD</b> |
| 1                           | 1961           | 2.42                | 1964           | -2.00               |
| 2                           | 1963           | 1.03                | 1970           | -1.18               |
| 3                           | 1967           | 1.31                | 1971           | -1.27               |
| 4                           | 1972           | 2.21                | 1973           | -1.11               |
| 5                           | 1976           | 1.41                | 1980           | -1.17               |
| 6                           | 1982           | 2.16                | 1992           | -1.92               |
| 7                           | 1983           | 1.41                | 1996           | -2.15               |
| 8                           | 1987           | 1.75                | 1998           | -1.18               |
| 9                           | 1991           | 1.45                | -              | -                   |
| 10                          | 1994           | 2.66                | -              | -                   |
| 11                          | 1997           | 2.08                | -              | -                   |
|                             | <b>Average</b> | 1.81                | <b>Average</b> | -1.50               |

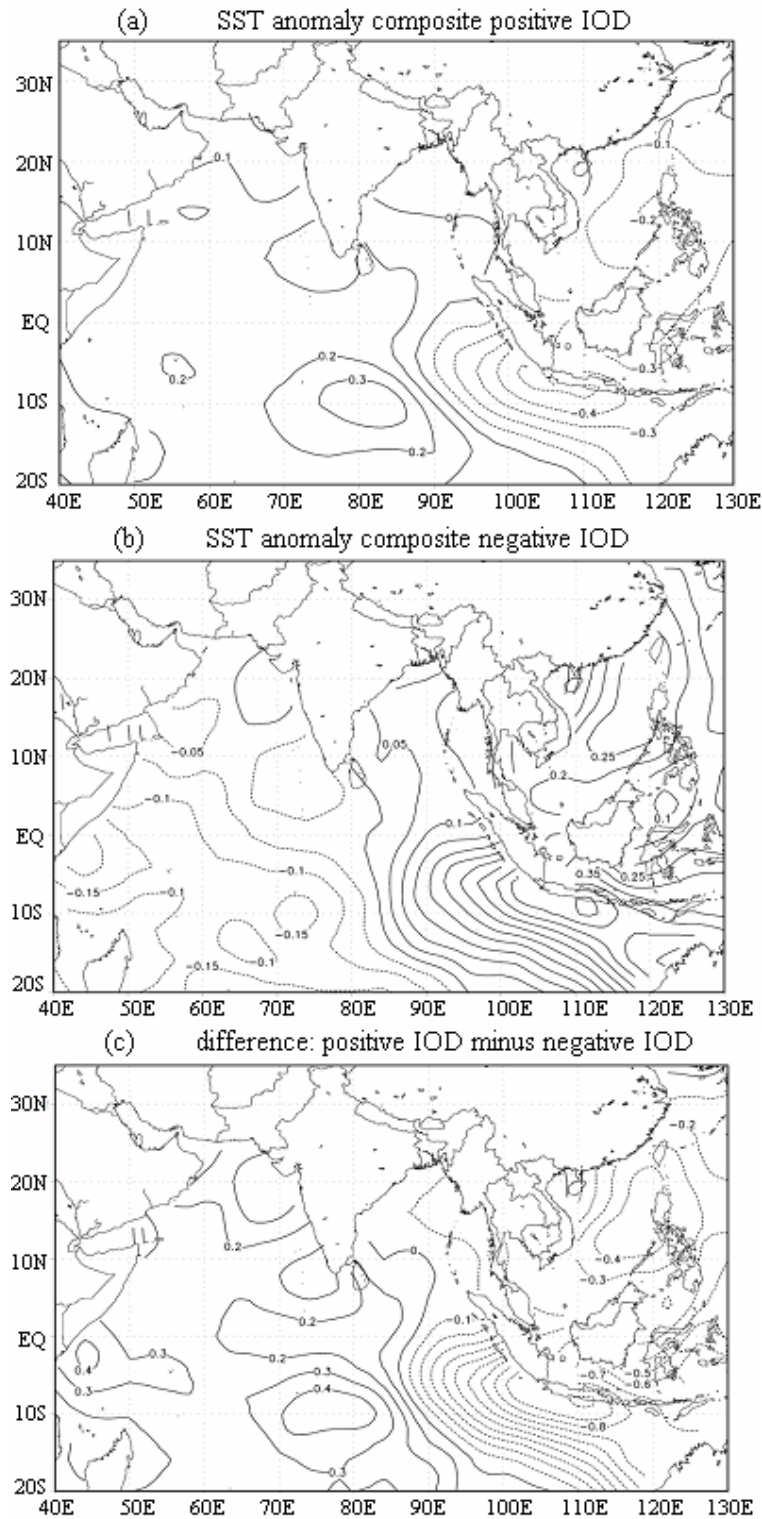


Fig. 5.22: Composite seasonal SST anomalies ( $^{\circ}\text{C}$ ) for SM during the (a) positive IOD, (b) negative IOD phases of IODM and (c) difference between the positive and negative IOD.

Fig. 5.22a and Fig. 5.22b clearly reveal that the east-west SST anomalies in the IO are coupled to the atmospheric circulation. These changes in the SST cause local air-sea interaction in the region. Thus, this anomalous coupled ocean-atmospheric phenomenon generated over the tropical IO could produce atmospheric and oceanic changes and influence the regional climate conditions.

#### **5.4.6 Circulation features associated with extreme SMR phases**

One of the important features of the SM circulation over the South Asia is the establishment of the southwesterly winds over the Indian Ocean and Bay of Bengal during the summer season. Another feature is the weak westerly winds over the North India. We have already identified monsoon extremes (years with excess/flood and deficient/drought rainfall) from the period 1961-2008. Based on these extremes composite anomalies for the 850 hPa vector winds are presented in Fig. 5.17a and 5.17b.

A comparison of Fig. 5.21a and Fig. 5.17a reveal that the flow patterns converge over southern parts of India resulting in moisture convergence over this area and enhancing monsoon activity. Thus, the positive dipole phase is favorable for excess rains over southern parts of India but not for Bangladesh. A similar comparison of the central panels of Fig. 5.21b and Fig. 5.17b shows flow patterns converging and exporting moisture towards Sumatra, away from the southern parts of India. Thus, the negative phase of the dipole phenomenon inhibits rainfall activity.

#### **5.5 SST anomalies associated with extreme SMR phases**

Again to examine the ocean forcing associated with these extreme monsoons, SST anomaly patterns for these two sets of years are shown in Fig. 5.15 for the SM season only to facilitate comparison with Fig. 5.22. Though these patterns show warm SST anomalies over western IO and eastern IO also shows positive anomaly for the excess monsoons but eastern IO shows negative for positive dipole and opposite for the deficient monsoons, the contrast between the SST anomalies over western and eastern IO is a striking as associated with the dipole phenomenon (Fig. 5.22). However a comparison of Fig. 5.15 and Fig. 5.17 also conveys ocean-atmospheric coupling.

**CHAPTER 6**  
**PREDICTOR IDENTIFICATION**  
**AND**  
**DEVELOPMENT OF REGRESSION MODEL**

**6.1 Introduction**

In view of the importance of foreshadowing seasonal rainfall for agricultural economy of the country, H. F. Blanford has initiated the system of the Long Range Forecast (LRF) way back in late 18th Century. He was the first to attempt a forecast of the monsoon based on the hypothesis that 'varying extent and thickness of Himalayan snow exercise a great and prolonged influence on climatic conditions and weather of the plains of the northwest India [8]. The system of the LRF of monsoon went through several evolutionary phases and eminent pioneers like Sir John Eliot and Sir Gilbert Walker and generation of worldwide researchers have made their contributions to this important scientific research.

Walker [13] initiated extensive studies of worldwide variations of weather element such as pressure, temperature, rainfall etc. with the main aim to develop an objective method for LRF of monsoon rainfall over India. These studies led Walker to identify three large scale pressure sea-saw patterns two in northern hemisphere viz. North Atlantic Oscillation (NAO) and North Pacific Oscillation (NPO) and one in southern hemisphere as Southern Oscillation (SO). While NAO and NPO are essentially regional phenomenon in nature, the SO has been recognized as a phenomenon with global scale influence. The SO was later linked to the oceanic phenomenon called El Niño in east equatorial Pacific characterized by warming of SST along the Peru coast. This is led to the theory of Walker circulation [44]. Walker also succeeded in removing the subjectivity in the earlier forecasting methods by involving for the first time, the concept of correlation in the field of LRF. His findings and approach are widely recognized to be scientifically valid and relevant even today.

Seasonal forecasting systems are usually categorized into two types namely dynamical and hybrid (i.e. combination of dynamical and statistical forecasting). Dynamical techniques are based on forecasts made by combined atmosphere-ocean General Circulation Models (GCMs). Efficient dynamical LRF are provided by the European

Center for Medium-range Weather forecasts (ECMWF). Statistical techniques for long range forecasting make use of the past data especially relationship between the rainfall and other weather/climate related parameters. SST is a key indication because of its relatively gradual rate of change and the highly effective ocean atmosphere coupling. Multiple techniques usually apply an assortment of mathematical and dynamical techniques, for example, by using mathematical techniques to forecast SSTs which are then used as reviews to a dynamical atmosphere-only GCM to generate long range rainfall forecasts.

The India Meteorological Department (IMD) has been issuing LRF of the summer monsoon rainfall (SMR) since 1886. It was, however the extensive and pioneering work of Gilbert Walker [10], that led to the development of the first objective models based on statistical correlations between SMR and antecedent global atmosphere, land and ocean parameters. There are many reviews on the LRF of ISMR [16]. In a very recent study, Gadgil *et al.* [19] addressed the major problems of the statistical and dynamical methods for LRF of SMR in view of the recent forecast failures in 2002 and 2004. Their analysis revealed that IMD's operational forecast skill based on statistical methods has not improved over seven decades despite continued changes in the operational models. For the LRF of the ISMR, three main approaches are used. The first is the statistical method, which used the historical relationship between the ISMR and global atmosphere-ocean parameters [58-59]. The second approach is the empirical method based on a time series analysis. This method uses only the time series of past rainfall data [60] and does not use any predictors. The third approach is based on the dynamical method, which uses general circulation models of the atmosphere and oceans to simulate the summer monsoon (SM) circulation and associated rainfall. In spite of its inherent problems, at present, statistical models perform better than the dynamical models in the seasonal forecasting of ISMR [58]. The dynamical models have not shown the required skill to accurately simulate the salient features of the mean monsoon and its interannual variability [7, 61-63]. Linear forecast of ISMR has been studied by Delsole and Shukla [59] and found that regression models based on two or three parameters could produce better results than models with using large number of predictors.

Diagnostic studies of historical datasets over the years have identified several new predictors for monsoon prediction. These parameters represent different aspects of the coupled atmospheric-ocean-land system. SM of Bangladesh, though having a relatively

limited reach in terms of rainfall, is a major large-scale seasonal phenomenon, and is believed to be closely linked to several regional/global circulation features. It is important to unravel these linkages in terms of teleconnections of SMR anomalies of Bangladesh with various basic parameters in the global domain. The parameters considered are SST, SAT-2m, MSLP.

The main purpose is to investigate whether there are any spatio-temporal preferences of the anomalies in these parameters associated with SMR variability. This analysis has been done by simple correlation analysis using the NCEP/NCAR reanalysis data, for the period 1961-2008. Details of the data sets are provided in Chapter 3.

## **6.2 Approach for predictor identification**

The CCs between the predictor field (e. g. Global SST field, SAT and MSLP) at each grid point and the predictand of SMR are computed for the month of February, April and April for SST, SAT and MSLP, respectively. The spatial maps of CCs were generated for each month and reliable predictors are identified on the basis of CCs significant at higher than 5% level. The correlation maps are generated to understand the concurrent links (in chapter 5) and not for identification of predictors. Also, such correlation maps are prepared for 6 months of the year to check the consistency of the seasonal correlation patterns but we have neither shown them here nor used for identification of the predictors excepting SST, SAT and MSLP for the month of February, April and April, respectively. After selecting the predictor through the correlation patterns, the predictor time series are prepared by means of the arithmetic average of the parameters over the rectangular spatial domain identified. The predictors that show strong and stable CC during the period of analysis are finally selected for forecasting of SMR over Bangladesh.

## **6.3 Identification of predictors for SM**

The aim in this section is to identify predictors for SMR of Bangladesh, which can then be used in statistical forecast models. The two main requirements for any useful predictors are:

- 1) a good relationship with the seasonal SMR
- 2) a reasonable lead time (i.e. months to a season)

The spatial patterns of CCs between SMR of Bangladesh and global SST, SAT and MSLP have been prepared for the data period 1961-2008. The results are discussed in the following sub-section.

### **6.3.1 Sea Surface Temperature (SST)**

The SMR is found to be correlated with SST during the month of February, and the correlation map is shown in Fig. 6.1. The strong shaded rectangular region indicates correlation that is significant at 1% level. Strong positive correlations with SST's is shown in Fig. 6.1 over southwestern Indian Ocean regions around 35° S. The correlations map indicates persistence from the pre-monsoon season (March-May) leading up to the monsoon season, thus providing the potential for a long range lead forecast.

### **6.3.2 Surface Air Temperature (SAT)**

The SMR of Bangladesh is found to be correlated with SAT over Somalia is also selected as one of the predictors (Fig. 6.2). This essentially captures the land-ocean gradient that gets set up by the land temperatures, especially during the pre-monsoon season before the start of monsoon.

### **6.3.3 Mean Sea Level Pressure (MSLP)**

The SMR of Bangladesh is found to be correlated with SLPs, the correlations are strong in the central Pacific tropical region, indicating that a higher than normal tropical pressure tends to enhance the easterlies, thereby increasing the moisture transport to Bangladesh as well as to the South Asia and consequently the rainfall. The solid rectangular boxes in Fig. 6.3 show the region of high correlation from where the predictors will be developed.

## **6.4 Predictors selection**

Based on the correlations with indices and the correlation maps with large-scale variables, predictors with high correlations with the SMR of Bangladesh have been identified (Table 6.1). The selected predictors are:

- 1) SSTs area averaged over 30.0°-36.0° S latitudes and 74.0°-78.0° E longitudes
- 2) SATs area averaged over 7.5°-12.5° N latitudes and 47.5°-50.0° E longitudes
- 3) SLPs area averaged over 2.5°-7.5° N latitudes and 145.0°-150.0° W longitudes

#### **6.4.1 Sea Surface Temperature (SST)**

Table 6.1 shows the details of the ensemble members have been used to construct the model. The correlation field between SMR of Bangladesh and SST anomaly in the southwest Indian Ocean is shown in Fig. 6.1. SST anomaly in the month of February over southwest Indian Ocean between  $30^{\circ}$ - $36^{\circ}$  S latitude and  $74^{\circ}$ - $78^{\circ}$  E longitude is positively and significantly correlated with the SMR of Bangladesh (CC=0.44 and significant at 1% level) and is indicated by the rectangular box as shown in Fig. 6.1. The correlations are weak over rest of the Indian Ocean and Bay of Bengal. The correlations are insignificant throughout the Indian Ocean and Bay of Bengal from March to May (Figure not shown). Sadhuram and Murthy [64] reported positive and highly significant correlation (CC=0.61) between ISMR and February SST anomaly in the northwest Australia region. Clark *et al.* [65] also reported insignificant correlations between ISMR and SST during pre-monsoon season (March-May) for the periods 1945-1994 and 1977-1995.

#### **6.4.2 Surface Air Temperature (SAT)**

The correlation field between SMR of Bangladesh and SAT anomaly in the month of April over Somalia is positively and highly significantly correlated with the SMR of Bangladesh (CC=0.59 and significant at 1% level). The area of SAT anomaly is indicated by the rectangular box over Somalia between  $7.5^{\circ}$ - $12.5^{\circ}$  N latitude and  $47.5^{\circ}$ - $50^{\circ}$  E longitudes as shown in Fig. 6.2. The correlations are weak over rest of the part of the globe.

#### **6.4.3 Mean Sea Level Pressure (MSLP)**

The correlation field between SMR of Bangladesh and SLP anomaly in the month of April over central Pacific Ocean is positively and highly significantly correlated with the SMR of Bangladesh (CC=0.53 and significant at 1% level). The area of surface pressure anomaly over central Pacific Ocean around equator is indicated by the rectangular box between  $2.5^{\circ}$  - $7.5^{\circ}$  N latitude  $145^{\circ}$ - $150^{\circ}$  W longitude as shown in Fig. 6.3. The correlations are insignificant over rest of the part of the world during this month. The correlations are insignificant between SMR of Bangladesh and SLP during pre-monsoon season from March to May (chapter 5).

We have considered 3 (three) predictors here. 3(three) predictors have been retained for the development of Long Range Forecast (LRF) of SMR over Bangladesh. The geographical locations of 3 (three) selected predictors are shown in Fig. 6.4.

Table 6.1: Details of predictors used for the Bangladesh SMR forecast during the period 1961-2007.

| No. | Parameters                         | Period   | Spatial domain             | CC with SMR of Bangladesh |
|-----|------------------------------------|----------|----------------------------|---------------------------|
| P1  | Southwest Indian Ocean SST anomaly | February | 30°-36° S, 74° -78° E      | 0.44                      |
| P2  | Somalia SAT anomaly                | April    | 7.5°-12.5° N, 47.5°-50° E  | 0.59                      |
| P3  | Central Pacific Ocean SLP anomaly  | April    | 2.5° -7.5° N, 145° -150° W | 0.53                      |

Significance at and above 1% level

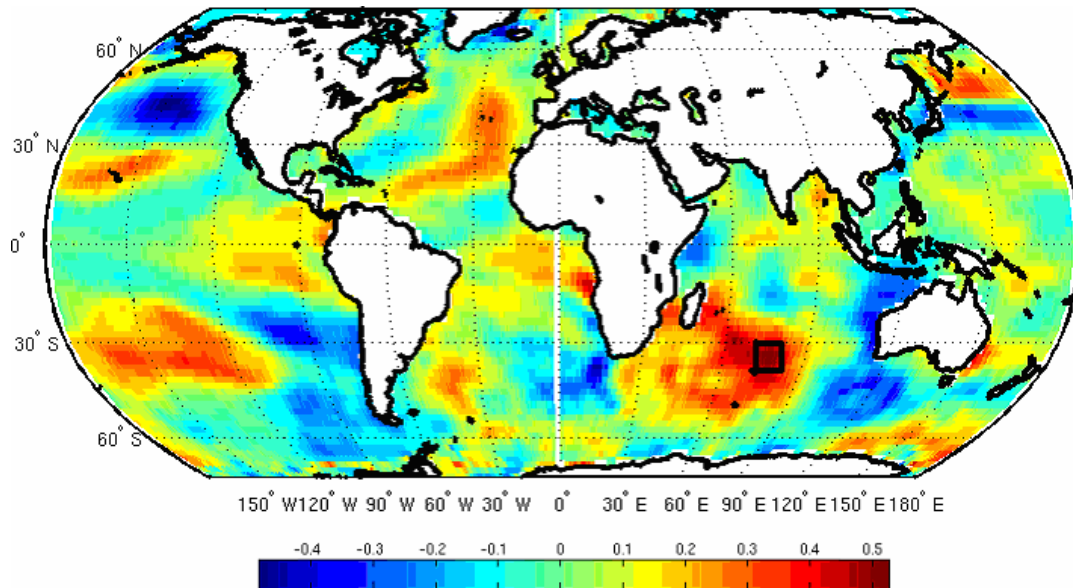


Fig. 6.1: Correlation maps between SMR of Bangladesh and SSTs in the month of February. The solid rectangular box indicates are significant at 5% level.

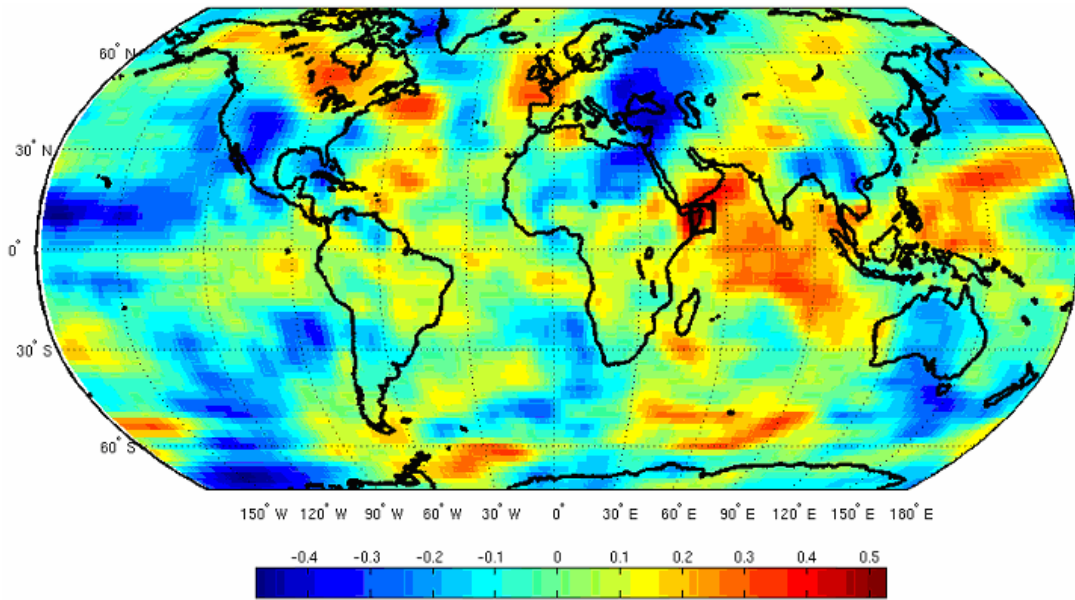


Fig. 6.2: Correlation maps between SMR of Bangladesh and SATs in the month of April. The solid rectangular box indicates are significant at 1% level.

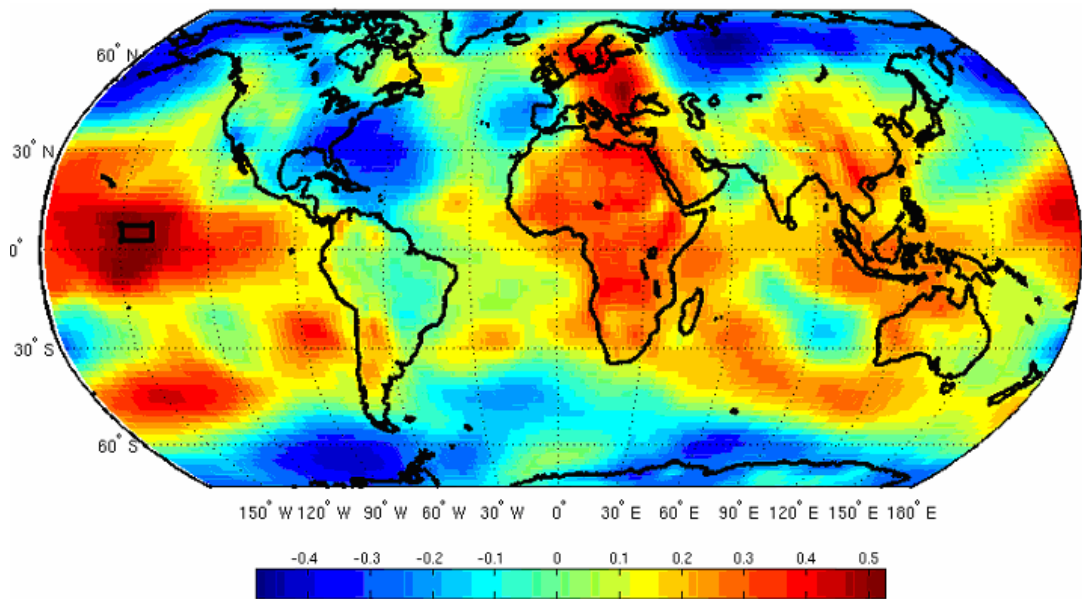


Fig. 6.3: Correlation maps between SMR of Bangladesh and SLPs in the month of April. The solid rectangular box indicates are significant at 1% level.

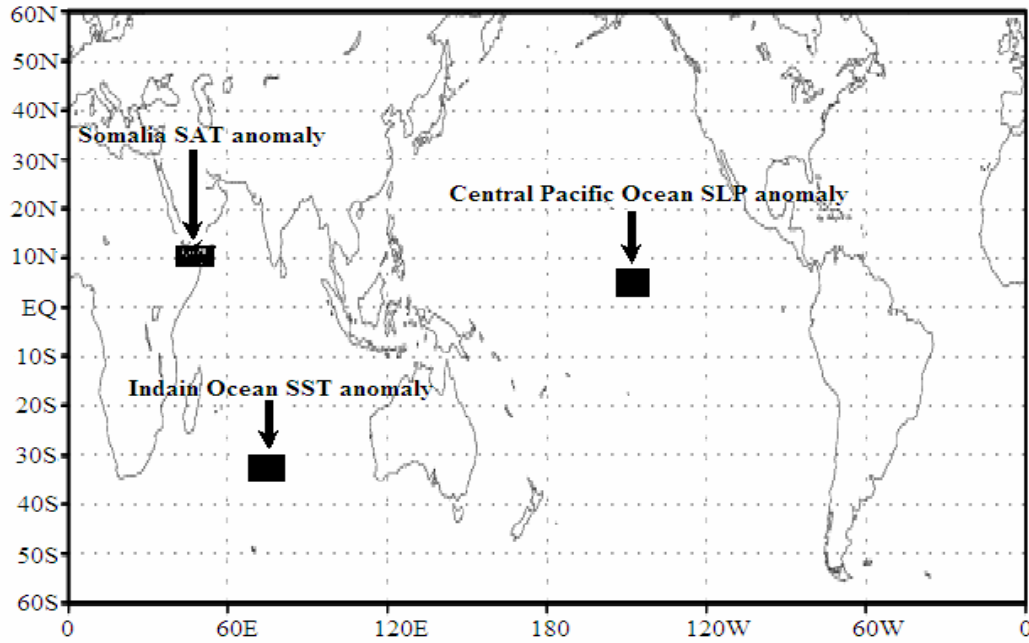


Fig. 6.4: Geographical locations of the three predictors.

## 6.5 Development of long range forecast for SMR

There are mainly two methods for long range forecast; statistical/empirical and dynamical methods.

Despite substantial efforts throughout the world, current atmospheric general circulation models cannot realistically simulate, much less predict, the structure and magnitude of the intraseasonal and interannual variability of monsoon precipitation over the Asian monsoon region, even with observed SST [66]. Coupled ocean-atmosphere models show even more deficiencies [67]. In this situation, empirical models using statistical formulation trained on observed data offer physically meaningful and practically useful alternatives to prepare seasonal forecasts.

To construct a statistical model, one first postulates an equation relating to the forecast variables, then one estimates the parameters in the model in such a way as to minimize the error of the predictions. This assumes that past statistical relations will be maintained in the future. The objective of this research is to develop a set of robust statistical models for the prediction of SMR over Bangladesh using the identified predictors. An attempt has been made to give a brief review for the SM before presenting the results of the

forecast schemes developed. The merits and limitations of the techniques are also highlighted wherever possible.

The most commonly used statistical technique for LRF of SMR is linear regression analysis [68]. The predictors for the model are either subjectively chosen as representing various important forcings on the monsoon, or entered into the scheme by following some objective criteria. Both approaches have their own limitations; the subjective selection may not optimize the variance explained, while the objective selection is highly sensitive to the data window and may result in over-fitting of the data sample [69]. As the regression model tends to acquire sample specific characteristics, the reliability is better assessed by testing on as large independent data sets as possible.

Auto-regressive integrated moving average (ARIMA) models have also been used to forecast the SMR for India as a whole as well as for south peninsula and northwest India; these were reported to have marginally better forecast skill over the multiple regression model [70]. However, autocorrelation up to 3-lags of SM, peninsular India and northwest India, do not show significant values. Gowariker *et al.* [71] developed parametric multiple power regression (MPR) models with 15 predictors for LRF of SM, which were latter modified [16] to include 16 parameters.

Rajeevan *et al.* [72] has developed two parametric multiple regression models consisting of 8 and 10 parameters each for the LRF of SM of India. India Meteorological Department (IMD) has modified their operational LRF strategy, by issuing forecast two times, once as a preliminary appraisal in April using 8 parameters and again in June using 10 parameter models as an update involving more reliable precursors like the winter-to-spring tendency in ENSO parameters. Rajeevan *et al.* [72] compared their model with the previous operational models and reported that the root mean square error of the operational forecast during the period 1996-2000 was 11% while the new 8 and 10 parameter models for the same period was 7 and 6% respectively. The model errors of 8 and 10 parameter models are 5 and 4% respectively which is of the same order as that of the 16 parameter models. They have also developed a linear discriminant analysis (LDA) model for calculating probabilities in five rainfall categories.

Raj [73] studied the behavior of antecedent meteorological parameters which provide an indication of the Northeast Monsoon (NEM). For that, he tested several parameters of SM season to identify reliable predictors for NEM. He concluded that, the monthly mean

winds, especially of the middle and upper troposphere of certain stations of India during the SM provide some indication of the ensuing NEM rainfall of the southern peninsula. He developed a single predictor equation that performed reasonably well during test period. He also pointed out that better results may be obtained by revising the regression equation using the most recent data.

Raj [74] proposed a six predictors forecasting scheme for the prediction of NEM rainfall of Tamilnadu, based on the data period 1965-1994. The model development period was 1965-1987 and 1988-1994 was the test period. The final forecast of rainfall was obtained as a weighted average of the individual forecasts based on six predictors by employing screening technique, different from the conventional ones. The system explained between 65-77% of the variance of rainfall, with a standard error of 13-18% and provided reasonably good forecast during the test period. The physical significance of the predictors has been explained based on the intensity of subtropical anticyclones over India.

Raj [75] have analyzed how the upper tropospheric features that evolve over India are related to the SM and NEM in antecedent, concurrent and succeeding time lags and that how such relations, to the extent possible could possibly lead to a better understanding of both the monsoons specially the latter and thereupon the features associated with good and poor monsoons.

Development of a statistically predictive model for LRF of SMR of Bangladesh, ensemble methods were used to develop LRF model to predict the SMR over Bangladesh.

### **6.5.1 Selection of procedures for LRF**

The empirical and statistical methods used in atmospheric science can be broadly classified into two distinct classes: linear and non-linear methods. Linear methods include (i) linear regression and correlation analysis, to determine a linear relation between the variables  $x$  and  $z$ , (ii) principal component analysis (PCA), to the correlation patterns with a set of variables  $x_1, x_2, \dots, x_n$ , (iii) canonical correlation analysis (CCA) to determine the linear relation between a set of variables  $x_1, x_2, \dots, x_n$  and another set of variables  $z_1, z_2, \dots, z_n$ . Non-linear methods include polynomial regression, logistics regression, non-linear auto regression models (NAR) and non-linear

auto regression moving average (NARMA) models etc. Linear regression, CCA, and non-linear methods have been largely used in LRF schemes.

Important issues with linear and non-linear statistical methods are the non-stationary of the data and the selection of the predictors. In most long-range climate forecast problems, there are many predictors and their physical relationship with the predictand is not well defined, then a few best among them have to be selected based on robust statistical methods.

Regarding the first point, the most widely used statistics for the model selection is Root Mean Square Error (RMSE). The significance of RMSE is tested considering the principle of parsimony [76]. This principle requires that an empirical model should employ the smallest number to predictors for an adequate representation. Therefore, even if a model with larger number of predictors has less prediction error than another with fewer predictors, it should nevertheless be rejected in favor of the model with fewer predictors, if it fails a goodness of fit test.

Different ways are proposed to detect the best relationship. One way is to select the predictor with minimum RMSE in the model development set. However, the selected predictors in this way may not produce good generalization and the prediction may be bad on the unseen data. Therefore a cross-validation procedure is recommended. In this scheme, the model development (say, N data points) is successfully divided into pairs of mutually exclusive sets, independent and dependent. A regression model is developed with each dependent set then used to predict the corresponding independent set. Repeating this procedure for all pairs, N predicted values are obtained with different regression models for each predictor variable. Values of RMSE are calculated are for each predictor, by comparing the N predicted and observed data of the entire development set. Then the best predictor is that one for which the RMSE is minimum.

In the present thesis, multiple regression model approaches have been followed to develop LRF models for SMR over Bangladesh.

### **6.5.2 Development of a multiple regression model for SMR**

In the present thesis, a stepwise multiple regression procedure based on algorithms enabling an objective way to select the predictors have been used. A set of 3 predictors have been identified for the prediction of SMR over Bangladesh (Table 6.1) provides the

pool of predictors for use in this procedure. The predictors are from the parameters SST, SAT and MSLP. These predictors are spread across the globe (Figs. 6.1-6.3), and represent various ocean-atmospheric forcings on SMR.

As discussed in Chapter 5, ENSO, and many other predictors identified and represented by various basic global parameters are showing better relationship with SMR after mid 1975's. Keeping this in view, multiple regression equations have been developed for the period 1979-2002. The model is tested using an independent verification period 2003-2012.

To check the temporal variability of the strength of the predictors to SMR of Bangladesh, moving window correlation are shown in Fig. 6.5 with SST anomalies, SAT anomalies and SLP anomalies are denoted by P1, P2 and P3, respectively. Besides, the predictors show significant correlations with the SMR of Bangladesh at two or three months lead time.

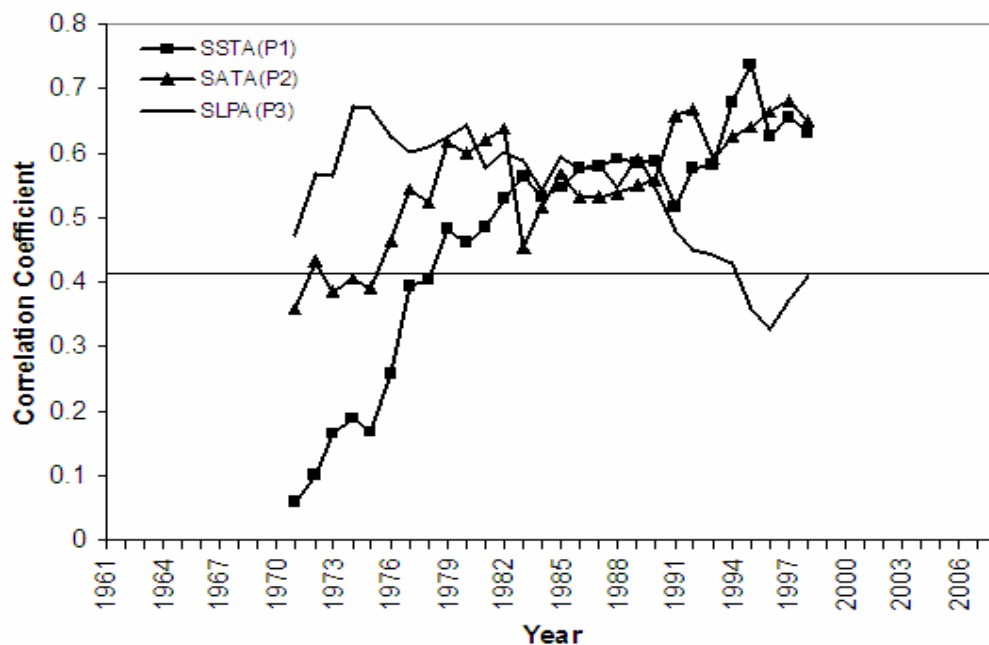


Fig. 6.5: Sliding window (21-year) correlations between the predictors (SST anomaly (P1), SAT anomaly (P2) and SLP anomaly (P3)) and SMR of Bangladesh during the period 1961-2007. Central year of the sliding window is shown in the figure. 5% significant level is indicated as solid line.

Fig. 6.5 shows the 21-year moving correlation coefficients between SMR of Bangladesh and the three predictors (P1, P2 and P3) selected for the model development during the period 1961-2007. Significant level at 5% (CC=0.43) is indicated as horizontal solid line. The relationship of most of the predictors with the SMR of Bangladesh is stable (CC values and significant at and above 5% level) during the entire period particularly during the recent years as shown in Fig. 6.5. The correlations between predictors and SMR of Bangladesh are weak during the earlier period. Clark *et al.* [65] also found weak correlations before 1970s and strong correlations during the recent decades which were attributed to the climate change in the Indian Ocean after 1976. There are significant inter-correlations between some of the predictors. Table 6.2 depicts the inter-correlation square matrix of the three predictors which have been used in the regression model. The correlation between predictors is significant which indicates that the predictors are dependent on each other. Rajeevan *et al.* [72] suggested an optimum sliding window of 23 years would minimize RMS errors. Hence, a sliding window of 24 years (1979-2002) has been chosen in this study as the training period to develop the linear regression model and the period 2003-2012 (10-year) is used for test period. The regression equation for the model is given below.

$$\text{SMR} = 91.464P1 + 114.645P2 + 106.408P3 + 1740.41 \quad (6.1)$$

where SMR of Bangladesh is compared between observed and regression model rainfall (Fig. 6.6). The year-to-year performance of observed and regression model of SMR of Bangladesh is shown in Fig. 6.6. In general, there is a good agreement between the observed and regression model (predicted values) rainfall except in the years 1980, 1984, 1992, 1994 and 1998 (i.e. 5 years) out of 24 years. This is the first time that an attempt is made to develop a regression model for SMR in Bangladesh. The model verification statistics of the regression model given in Table 6.3 shows that the RMSE of the model is 8.10% of LPA. The BIAS of the model is -0.85. The Hit Score (HS) and Heidke Skill Score (HSS) of the regression model is 55% and 0.39, respectively. The HSS is an indicator for the performance of the regression model which is within the range (0.38-0.63) of ensemble multiple linear regressions (EMR) and projection pursuit regression (PPR) models of Rajeevan *et al.* [72]. It is impressive that this simple regression model using only three parameters could capture inter annual variability of SMR of Bangladesh satisfactorily.

The CMAP data is also used for showing the model performance. During the period 1979-1984, the CMAP data shows more anomalies with opposite sign than the other years over Bangladesh because it may be due to missing data during the above period. CMAP data may be useful in verifying the broad characteristics of the rainfall patterns over the globe [77] but it can be seen from Fig. 6.6 that it is not at all close to the SMR of Bangladesh temporal analysis either qualitatively or quantitatively.

Table 6.2: Inter-correlation square matrix among the predictors that was used in the regression model during the period 1961-2007.

| Parameters name | SST  | SAT   | SLP   |
|-----------------|------|-------|-------|
| SST             | 1.00 | 0.36  | 0.30  |
| SAT             | 0.36 | 1.00  | 0.44* |
| SLP             | 0.30 | 0.44* | 1.00  |

\*significance at 1% level

Table 6.3: Forecast verification statistics of the model output computed for the period 1979-2002.

| SL No. | Verification Parameters                         |       |
|--------|---|-------|
| 1      | CC between actual and regression model rainfall | 0.75  |
| 2      | BIAS of the forecasts (% from LPA)              | -0.85 |
| 3      | RMSE of the forecasts (% from LPA)              | 8.10  |
| 4      | HS (Hit score, %)                               | 55    |
| 5      | HSS (Heidke skill score)                        | 0.39  |

It is evident that SST anomaly in Indian Ocean during pre-monsoon season is playing an important role in SMR over Bangladesh. Warm SST persists before a strong monsoon [64]. In order that SST directly influences the monsoon through evaporation and moisture supply, one would expect the positive correlations to persist through the pre-

monsoon season (March-May) leading to the onset of rainfall, which are not shown. Webster *et al.* [54] and Clark *et al.* [65] found that ISMR is strongly correlated with the Indian Ocean SST with a lead time of 3-6 months on Tropical Biennial Oscillation (TBO) time scale. Positive SST leads to the increase of surface moisture (due to enhanced evaporation) and thus a strong monsoon owing to the increased moisture in the region [78]. Hence, warm (cold) SST in the Indian Ocean increases (decreases) the local moisture flux during pre-monsoon and fall preceding SM, and lead to strong (weak) monsoon. This may be the reason for the observed correlation between SMR of Bangladesh and SST anomaly shown in the present study.

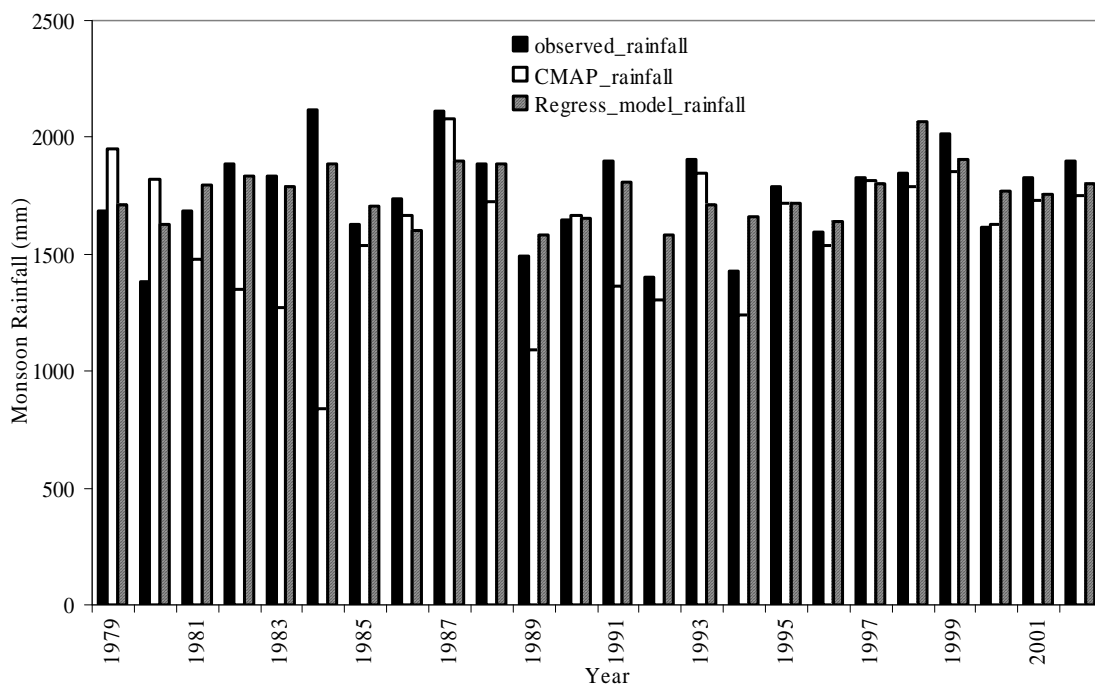


Fig. 6.6: Comparison between observed, CMAP and regression model SMR during the period 1979-2002.

In extreme cases (excess and deficient) the model was able to predict the SMR variability very well except in 1980 deficient/drought year when the model was able to capture the sign of variability that it is going to be a deficient/drought year but not the magnitude of the system. In 1987 excess/flood year when the model was able to capture the sign of variability that it is going to be an excess/flood year but not the magnitude of the system.

The model performed very well in the verification period (test period) 2003-2012 as shown in Fig. 6.7. In extreme cases, the regression model was captured well in 2004 and

2007 excess/flood years except in 2006, 2010 and 2012 deficient/drought years when the regression model captured the sign of variability; but not magnitude of the system. The forecast during the period 2003-2012 is 11% more of the mean during this period. The regression model gives the seasonal SMR forecast for 2013; it has been shown normal rainfall over Bangladesh (Fig. 6.7).

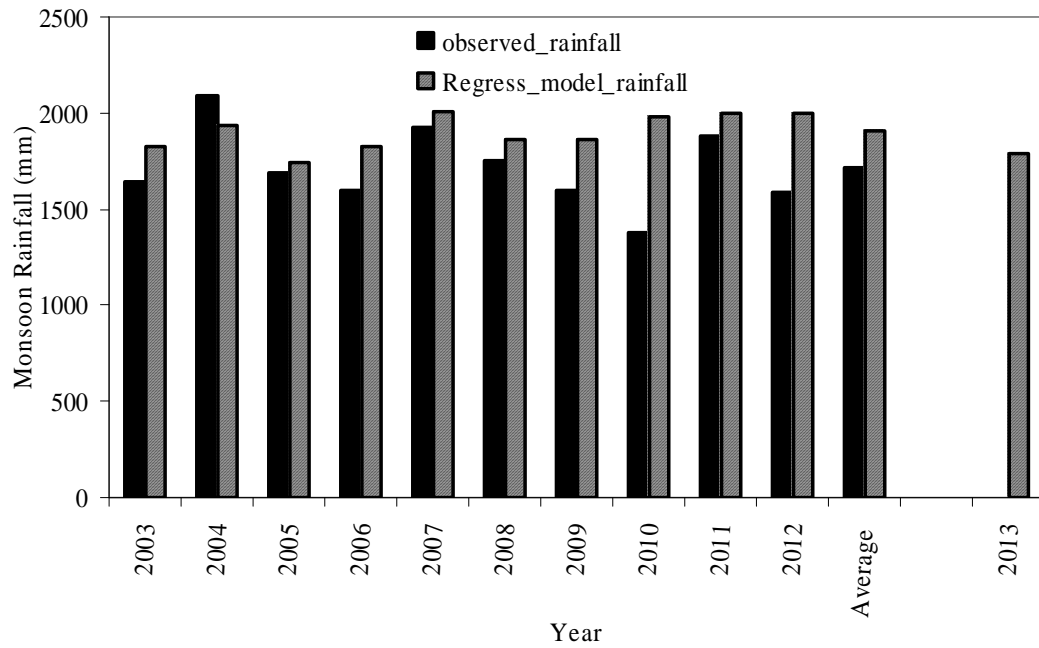


Fig. 6.7: Comparison between observed and regression model (predicted value) SMR during the verification period (test period) 2003-2012 and 2013 represents rainfall forecast for SMS over Bangladesh.

## CHAPTER 7

### DYNAMICAL PREDICTION OF SUMMER MONSOON RAINFALL

#### 7.1 Introduction

Dynamical models are useful tools to generate seasonal forecasts. They are being used at major climate prediction centers for generating operational/semi-operational global long-range forecasts. Dynamical models are based on the mathematical equations governing the physics of the atmosphere and the oceans. The advantages of dynamical models are that they are more scientific and physically based and tend to capture the events in terms of their physical causes and effects. They are also able to handle unprecedented climate events, since the basic physics would apply equally well to novel situations as to familiar situations. Statistical or empirical models can only see new situations as extrapolations of historically observed ones, and run the risk of missing any new "rules of the game" that may come about only in the new situation. On the other hand, the disadvantages of dynamical models are that they approximate some of the oceanic and/or atmospheric processes because they operate on spatial scales that are too small to be represented in the model. Moreover, dynamical models require much greater computer power than statistical models.

To evaluate the possible affect of global warming upon the meteorological phenomena of small scales in time and space is important, not only from the scientific, but also from the socio-economic viewpoints. As concentrations of greenhouse gasses increase in the atmosphere, the Intergovernmental Panel on Climate Change (IPCC) report [79] projected increase of surface air temperature, more hot days and fewer cold days and frost days over nearly all land areas. Diurnal temperature range is projected to decrease. Heavy precipitation possibly increases, due to water vapor increase in the atmosphere. While possible changes of extreme events induced by the global warming was described in the IPCC report, the description remained qualitative, partly due to the limited resolution of the existing climate models. Even the directions of the projected changes were almost uncertain for some kinds of the extreme events. By the recent advances in the computational environment, however, we have become able to run a climate model, with resolution high enough to investigate global characteristics of small-scale phenomena, and extreme events in detail.

Climate models are the most important tools available today for enhancing our scientific understanding of the great complexity of the climate system and for projection of future climate change. The Meteorological Research Institute (MRI) of Japan has been developing climate models for several decades. The first atmospheric general circulation model (AGCM), referred to as MRI-GCM-I [80], was coupled to a global ocean general circulation model (OGCM) [81] to create MRI's first generation atmosphere–ocean coupled global climate model (MRI CGCM1). Tokioka [82] used MRI-CGCM1 to conduct a global warming experiment in which they examined transient responses to a cumulative increase in the atmospheric carbon dioxide (CO<sub>2</sub>) concentration of 1% per year. The results of this experiment contributed to the 2<sup>nd</sup> Assessment Report of the IPCC [83]. A global spectral AGCM developed from the operational weather prediction model of the Japan Meteorological Agency (JMA) with a horizontal resolution of ~280 km was used to replace the earlier AGCM grid (4° × 5° horizontal resolution) in MRI-CGCM1. The resulting model became MRI's second generation CGCM, MRI-CGCM2 [84]. Several climate change projection experiments [85] based on scenarios forced by greenhouse gases and sulfate aerosol concentrations were conducted with MRI-CGCM2. An improved version of the MRI-CGCM2.3 was used in the 3<sup>rd</sup> phase of the Coupled Model Intercomparison Project (CMIP3) of the World Climate Research Programme, which compared 23 models from institutions around the world. In this intercomparison, MRI-CGCM2.3 was found to exhibit excellent climate reproducibility, which led to its being a significant contributor to the 4<sup>th</sup> Assessment Report of the IPCC (IPCC-AR4; [86]). Climate change projection results from each generation of MRIs-CGCM have been downscaled with providing boundary conditions to regional climate models [87], which, when utilized for detailed projections of climate change, have performed well in simulating the climate around Japan.

The projections of future climate change in IPCC-AR4 were based on numerous experiments with more than 20 CGCMs that yielded results with quantitative confidence levels. As a result, IPCC-AR4 contained a stronger conclusion than the previous assessment reports. That stronger statement was possible because many of the participating models were able to account for the observed climate change in the twentieth century, which suggests that these models can predict future climate change with higher confidence than before. The range of the uncertainties in the projections, however, remained as large as in the 3<sup>rd</sup> Assessment Report [79], and the main source of

the uncertainty in climate sensitivity was caused by cloud feedback. Bony and Dufresne [88] suggested that the different responses of low clouds over subtropical oceans to global warming among the simulations were the most important factor causing the sensitivity spread among the models. The uncertainty related to aerosols radiative forcing was also a large uncertainty factor. In particular, there are many questions about the modeling of the indirect effects of aerosols, which must take into account sophisticated cloud microphysics (involving a large computational cost). In addition, climate models are now expected to represent important interactions between climate and atmospheric chemistry, for instance, ozone changes associated with climate change and anthropogenic trace gases such as chlorofluorocarbons (CFCs), and volcanic impacts on climate.

Also important is the accurate quantitative estimation of feedback processes between the carbon cycle and climate change. IPCC-AR4 estimated this feedback by using earth system models of intermediate complexity, which are simplified, low resolution models. A more realistic earth system model (ESM) based on a CGCM that incorporates the full complexity of physical processes, with sufficiently high resolution, and sophisticated carbon cycle process simulation is required to achieve a more accurate quantitative estimation of this feedback.

A major theme of the next IPCC Assessment Report, IPCC-AR5 (which will have CMIP5 as its scientific basis, and is expected to appear in 2013), in addition to the long term projections (~2100 and later) as presented in past IPCC reports, is near term prediction, targeting climate change 20 to 30 years in the future and including the prediction of decadal variability as an initial value problem. More regionally precise information on climate change in the near future is required for near term projection, and climate models must be able to accurately reproduce the decadal to multi decadal variability observed in the latter half of the twentieth century, as well as the present day mean climate.

Earth System Models (ESMs) for IPCC-AR5 have been developed at several climate modeling centers. An ESM has also been developed at MRI under the special research program “Comprehensive Projection of Climate Change around Japan due to Global Warming.” In conjunction with the ESM development, a global AGCM has been developed at MRI in collaboration with JMA and the Advanced Earth Science and Technology Organization. This AGCM has performed well in reproducing the over all

atmospheric [89]. A very high resolution (20 km mesh) version of the AGCM has produced many excellent present and future climate simulation results with regard to, for example, typhoons [90], the Baiu [91], regional climate, and extreme events. This report describes the ESM that MRI has developed, called MRI-ESM1, which incorporates these successful results, in preparation for the CMIP5 experiments that will contribute to IPCC-AR5.

## **7.2 Monsoon rainfall Scenario over Bangladesh**

Summer monsoon rainfall (SMR) was simulated by a global 20 km mesh AGCM, focusing on the changes in the SMR of Bangladesh. Calibration and validation of AGCM was performed over Bangladesh for generating SMR scenarios. The model produced SMR was calibrated with a ground-based observational data in Bangladesh during the period 1979-2003. The TRMM 3B43 V6 data is also used for understanding the model performance. The AGCM output obtained through validation process and made it confident to be used for near future and future SMR projection in Bangladesh.

In the present-day (1979-2003) climate simulations, the high resolution AGCM produces the SMR better as a spatial distribution over SAARC region in comparison with TRMM but magnitude may be different. SMR projection for Bangladesh is experimentally obtained for near future and future during the period 2015-2034 and 2075-2099, respectively. This work reveals that SMR simulated by a high resolution AGCM is not directly applicable in application purpose. However, acceptable performance is obtained in estimating SMR over Bangladesh after calibration and validation. This study predicts that near future SMR on an average may decrease about -0.5% during the period 2015-2034 and future SMR may increase about 0.4% during the period 2075-2099.

Bangladesh is a small country having an area about 147570 sq. km situated in the northeastern part of south Asia within  $88.02^{\circ}$  - $92.68^{\circ}$  E and  $20.57^{\circ}$  - $26.63^{\circ}$  N. The land of Bangladesh is very flat: elevation is about 1-37 m above sea level except small portions in the southeast (elevation about 200 m) which is border with Myanmar and in the northeast (elevation about 100 m) which is border with Shillong hill of India.

Bangladesh being an agricultural country, rice is the main food and the success or failure of the crops and water scarcity in any year are always viewed with the greatest concern. A major portion of annual rainfall over Bangladesh is received during summer monsoon

(SM) season (June-September). SM is also known as southwest monsoon in Bangladesh as well as in south Asia. SMR contributes around 65-70% of its annual rainfall over Bangladesh [92]. Seasonal prediction of SM or southwest monsoon rainfall over Bangladesh has considerable application for decision making in agriculture and water resource sectors. In addition, the SM season in Bangladesh is characterized by the occurrence of severe floods due to heavy rainfall causing extensive damage to crops, road, livestock and properties associated with loss of valuable lives. Any change or variation in climate and climatic scenarios affecting the SMR over Bangladesh as well as South Asia are considered to be direct threat for economy of Bangladesh. Thus, long range prediction of SMR becomes very important for the interest of the Bangladeshi farmers and policy makers of the country.

SMR forecast is a high priority in India and Bangladesh. Because an accurate forecast of monsoon performance averaged over the country as a whole is also very useful for better macro level planning of finance, power and water resources. There are many reviews on the Indian southwest monsoon rainfall (ISMR) [15, 58-59]. A little work is done on climate change scenarios for Bangladesh using regional climate model [93]. Kusunoki [91] indicated the realistic reproduction of Baiu (Japan) rain band needs an atmospheric model with higher horizontal resolution. They investigated the future change in the Baiu rain band with a 20-km mesh global atmospheric model, using the time-slice method [94] which prescribed SST simulated by an AOGCM. It is widely recognized that global warming projections include wide range of uncertainty arising from many factors such as differences in future emission scenario, model performance, internal natural variability of climate system. Therefore, evaluation and quantification of uncertainty in global warming projection is strongly required to obtain more robust and reliable information on future climate changes [86]. Despite continuous model development, AGCMs still have systematic biases in simulating the East Asian summer monsoon rainfall such as an underestimate of precipitation amount over the western Pacific [63] and inappropriate temporal characteristics between precipitation and underlying SST [63]. Recently, a very high resolution AGCM with the horizontal grid size of about 20 km has been developed by the Meteorological Research Institute (MRI) /Japan Meteorological Agency (JMA) use in climate change studies [89] and has been used for climate change projection under increases in atmospheric concentrations of greenhouse gases and aerosols [90-91] The grid size of this model is several times smaller than that previously used in climate model

simulations. The global 20 km model is a unique one in terms of the horizontal resolution as well as its application to long term integration for global change studies. Due to the very high horizontal resolution, the model has more realistic representation of land-sea distribution and topography with elevated orography than other GCMs have ever had, so it is expected to have an ability to simulate rainfall and temperature over this region more adequately. Kitoh and Kusunoki [95] have shown a good result of a global 20-km mesh AGCM to simulate the East Asian summer monsoon climate in comparison with its lower resolution (180 km). This opportunity is employed for the first time in generating SMR scenario by using high resolution AGCM for Bangladesh.

In this thesis, SMR climatology in Bangladesh derived from 20 km AGCM was calibrated with the observed data for the period 1979-2003. Then, projections for SMR are made during the period 2015-2034 and 2075-2099 in Bangladesh on the basis of available model data. It is mentioned here that the period 1979-2003 is assumed for training period for calibration and the period 2003-2006 is used for validation purposes.

## **7.3 Model description and experimental design**

### **7.3.1 Model description**

The AGCM used in this study is called MRI-AGCM which is jointly developed by the JMA and the MRI. The model is based on an operational numerical weather prediction (NWP) model used at JMA. Some modifications were added in radiation and land surface processes as a climate model at MRI [89]. The time integration was accelerated by introducing a semi Lagrangian three dimensional advection scheme [96]. The model has a horizontal spectral truncation of TL959 corresponding to about a 20 km horizontal grid spacing and has 60 levels with a 0.1 hPa (altitude of about 65 km) top. TL959 means that the model has a spectral triangular truncation of spherical function at wave number 959 with a linear grid for wave to grid transformation. The model has 1920 grids in longitude and 960 grids in latitude. A mere increase in the horizontal resolution was found to give rise to large model biases in precipitation and temperature, much less organization of convection, and suppression of tropical cyclone generation.

Table 7.1: The specifications of the MRI-AGCM (high resolution, 20-km) model.

| <b>Items</b>          | <b>Content</b>  |
|-----------------------|---|
| Basic Equation        | Hydrostatic, primitive  |
| Horizontal structure  | Spherical harmonics (latitude) and Fourier harmonics (longitude)                        |
| Horizontal resolution | 20 km, TL959  |
| Vertical level        | 60, top at 0.1 hPa  |
| Time integration      | Semi-Lagrangian scheme  |
| Shortwave radiation   | H <sub>2</sub> O, O <sub>3</sub> , CO <sub>2</sub> , O <sub>2</sub> , aerosol           |
| Longwave radiation    | H <sub>2</sub> O, O <sub>3</sub> , CO <sub>2</sub> , CH <sub>4</sub> , N <sub>2</sub> O |
| Cumulus convection    | Prognostic of Arakawa-Schubert, Randal and Pan  |
| Boundary layer        | Mellor and Yamada, level 2 closure  |
| Gravity wave drag     | Orographic origin   |
| Cloud                 | Cumulus, Large-scale condensation   |
| Precipitation process | Prognose cloud water content  |
| Land surface          | Simple Biosphere (SiB) model  |

Therefore, MRI scientists carefully tuned the model to improve the model's present day climatology by changing the parameters in the evaporation process, cloud water content diagnosis, vertical transport of horizontal momentum in cumulus, and gravity wave drag [89]. Especially, over estimation of global average precipitation of the 20-km model was suppressed by decreasing the amount of detrainment of cloud water at the top of the cumulus, as well as decreasing transformation speed from cloud water to precipitation in the cloud scheme [89]. The version of the 20-km model used in this study is slightly different from MRI-AGCM3.0 used in the previous studies, Kusunoki *et al.* [91] and Simmons and Burridge [97] in that sea ice model and vegetation setting in land surface process is improved. For the cumulus parameterization, the Arakawa-Schubert scheme with prognostic closure is used [98]. The summary of the specifications of the 20-km model is given in Table 7.1.

### 7.3.2 Experimental Design

High resolution (20-km) AGCM experiments are conducted using the time-slice method [83,94], which is a two-tier global warming projection using an AOGCM and an AGCM with horizontal resolution higher than that of the atmospheric part of the AOGCM. Fig. 7.1 shows the schematic diagram of time-slice method.

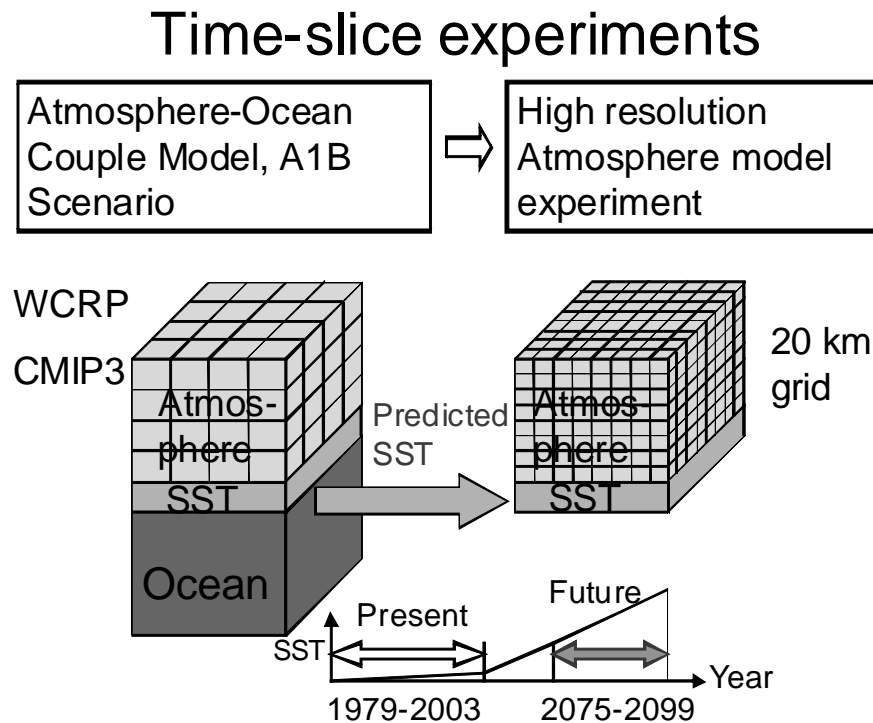


Fig. 7.1: Schematic diagram of time-slice method.

For present-day climate simulation, the 20-km model was integrated for 25 years from 1979 to 2003 (25 years) with the observed historical SST and sea ice data of HadISST. This simulation is equivalent to an Atmospheric Model Intercomparison Project (AMIP) type experiment for an atmospheric model, which is widely adopted in numerous modeling studies. For the near future climate simulation from 2015 to 2039 (25 years), changes in the Multi-Model Ensemble (MME) of SSTs projected by AOGCMs of Coupled Model Intercomparison Project 3 (CMIP3) are superposed to the detrended observed historical SST. It is mentioned here that the near future climate simulation data is used from 2015-2034 (20 years) due to lack of data. For the future climate simulations, the 20-km model was integrated for 25 years from 2075-2099 with future SSTs. The boundary SST data were prepared by superposing (a) future change in the MME of SST

projected by CMIP3 multi-model data set, (b) the linear trend in MME of SST projected by CMIP3 multi-model data set and (c) the detrended observed SST anomalies for the period 1979-2003. Future change in MME of SST was evaluated by the difference between the 20<sup>th</sup> Century experiment of IPCC Fourth Assessment Report (AR4; [86]) and future simulation under the Special Report on Emission Scenario (SRES) A1B emission scenario [79]. Future sea ice distribution is obtained in a similar fashion. Details of the method are described in Mizuta [89].

These settings are applied to each grid point and to each month. Fig. 7.2 shows the schematic diagram of SST setting for the end of 21st century simulation. The reason why we do not use the raw time series of MME SST for future climate is that averaging cancels out different phase of each CGCM SST, which smoothes year-to-year variability of SST and excludes ENSO. The time steps are 30 minutes in the resolutions.

External forcing including SST is summarized in Table 7.2.

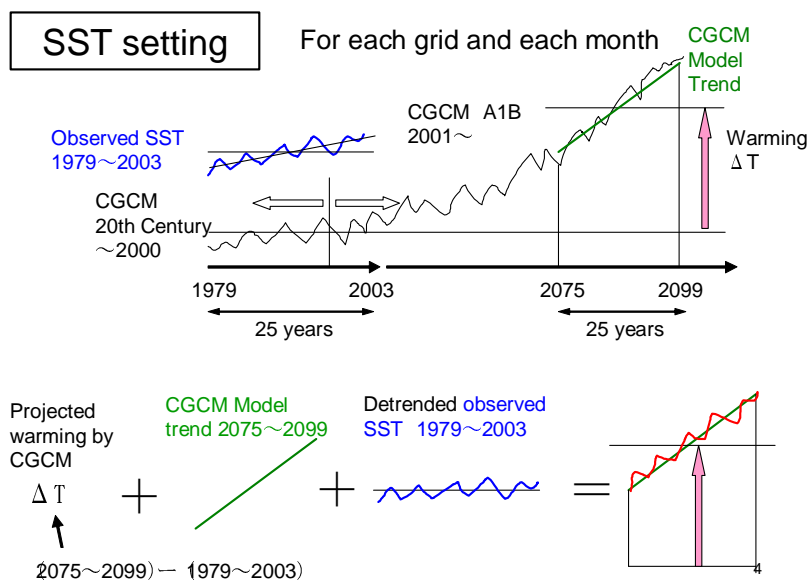


Fig. 7.2: Schematic diagram of SST setting for the end of 21st century simulation.

Table 7.2: External forcings

| Items                   | Present day                              | Near Future                                 | End of 21 <sup>st</sup> century             |
|-------------------------|--|---|---|
| Target year             | 1979-2003                                | 2015-2039                                   | 2075-2099                                   |
| Period (year)           | 25                                       | 25  | 25  |
| Sea surface temperature | Observation<br>HadISST                   | Observation + Change<br>(WCRP CMIP3<br>MME) | Observation + Change<br>(WCRP CMIP3<br>MME) |
| Sea ice compactness     | Observation<br>HadISST                   | Observation + Change<br>(WCRP CMIP3<br>MME) | Observation + Change<br>(WCRP CMIP3<br>MME) |
| Sea ice thickness       | Observation                              | Observation + Change<br>(WCRP CMIP3<br>MME) | Observation + Change<br>(WCRP CMIP3<br>MME) |
| Greenhouse gases        | Observation                              | A1B scénario                                | A1B scénario                                |
| Aérosol                 | Aérosol CTM<br>climatology 1991-<br>2000 | Aérosol CTM<br>climatology 1991-<br>2000    | Aerosol CTM<br>climatology 1991-<br>2000    |
| Ozone                   | Ozone CTM<br>climatology                 | CTM A1B scénario<br>projection              | CTM A1B scenario<br>projection              |
| Solar activity          | Constant                                 | Constant                                    | Constant                                    |
| Volcanic eruption       | None                                     | None  | None  |

## 7.4 Results and Discussion

### 7.4.1 Simulation of SMR over SAARC region

SMR is very much important for the SAARC region as it is used for agriculture and water management purposes in Bangladesh, India, Nepal and Bhutan etc. SMR (mm/d) derived from high resolution AGCM over the SAARC region are compared with TRMM V6 3B43 rainfall as shown in Figs. 7.3(a-b). High resolution AGCM simulated SMR averaged from June to September (JJAS) for the period 1979-2003 and TRMM 3B43 V6 (0.25 x 0.25 deg.) Averaged SMR for the period 1998-2010 are presented in Figs. 7.3(a-b). SMR simulated by AGCM is found to be much more consistent with TRMM observed rainfall. It is observed that most part of the Afghanistan is below 1 mm/d rainfall and western part of Pakistan showed zero rainfall and northwestern part of Pakistan showed 1-2 mm/d rainfall for SM season which are well captured by the AGCM. It is also indicated that heavy rainfall in the Western Ghat and less rainfall in the Eastern Ghat of India, southern part of Nepal and northeastern part of Bangladesh are well simulated by the AGCM. But amount is underestimated in some places over the region and overestimated around the Bay of Bengal. Model's high resolution enables us to simulate orographic rainfall as a maximum to the west of the Western Ghats in southern India and a southern periphery of the Himalaya range [99].

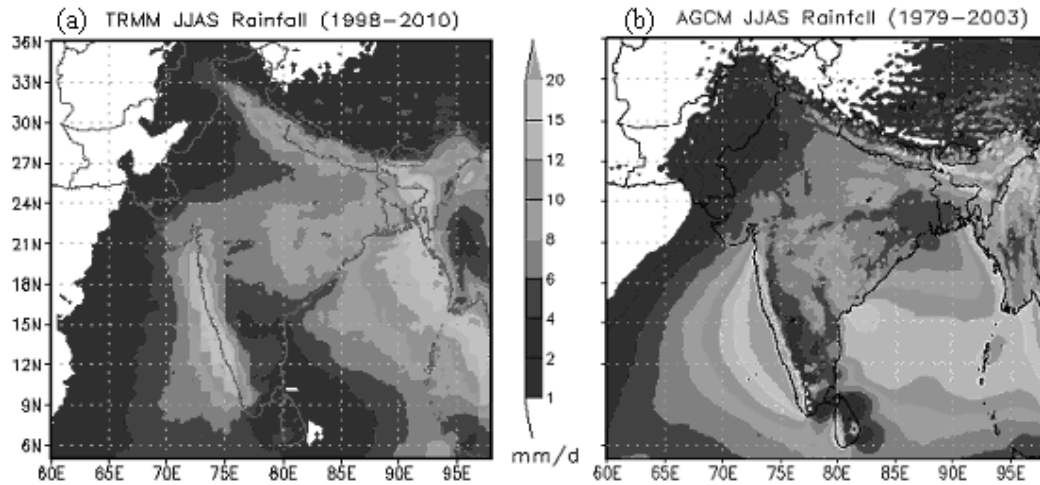


Fig. 7.3: SMR (mm/d) obtained from (a) TRMM V6 during the period 1998-2010 and (b) high resolution AGCM during the period 1979-2003.

#### 7.4.2 Interannual variation of SMR over Bangladesh

The 20-km high resolution AGCM simulation in SMR has been studied to evaluate the model skills in representing temporal variation during the period 1979-2003. It is seen that the SMR of AGCM has underestimated for all years for the same period. The high resolution AGCM SMR has also shown constant bias during the period 1979-2003 (Fig. 7.4).

The average SMR (JJAS) during the period 1979-2003 simulated by high resolution AGCM is 1033 mm with a standard deviation of 125 mm as shown in Table 7.3, whereas SMR of Bangladesh based on 28 rain-gauge stations averaged during the period 1979-2003 is 1756 mm with a standard deviation of 207 mm. The model simulated SMR is underestimated with the SMR of Bangladesh; its variability is almost half with the observed values. During the month of June, July, August and September the AGCM simulated rainfall is 365, 246, 212 and 210 mm with a standard deviation 101, 35, 28 and 36 mm, respectively. Similarly, observed SMR is 484, 525, 427 and 321 mm with a standard deviation of 137, 113, 112 and 64 mm for June, July, August and September, respectively (Table 7.3).

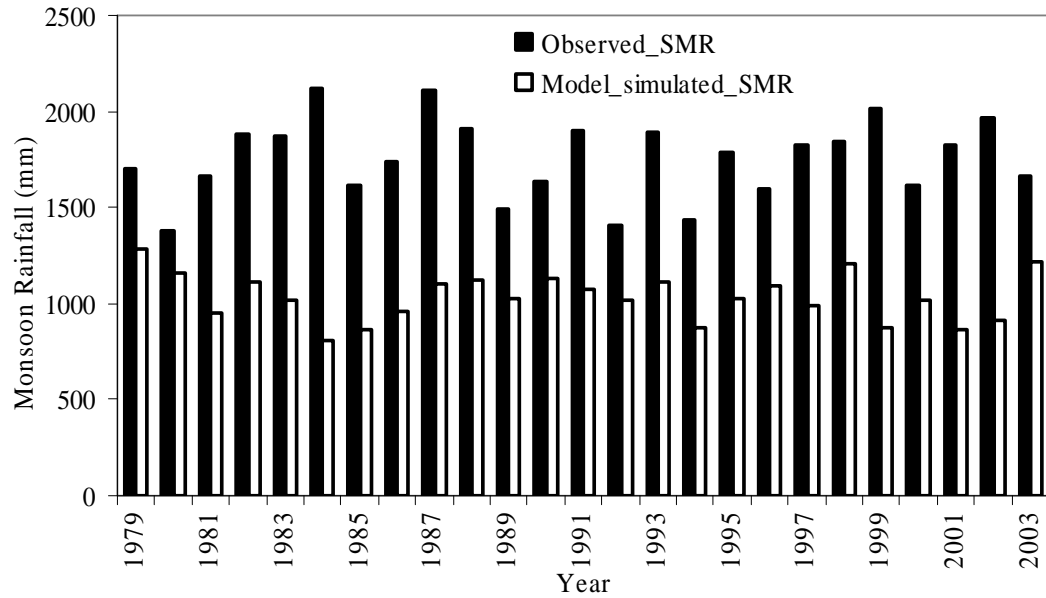


Fig. 7.4: Comparison between observed and model simulated (un-calibrated) SMR (mm) during the period 1979-2003.

Table 7.3: Statistical characteristics of observed and model simulated (un-calibrated) SMR (mm) over Bangladesh during the period 1979-2003.

| <b>Model un-calibrated SMR (mm)</b> |              |             |               |                  |                   |
|-------------------------------------|--------------|-------------|---------------|------------------|-------------------|
|                                     | <b>June</b>  | <b>July</b> | <b>August</b> | <b>September</b> | <b>SMR (JJAS)</b> |
| <b>Observed</b>                     | <b>484</b>   | <b>525</b>  | <b>427</b>    | <b>321</b>       | <b>1756</b>       |
| <b>Model</b>                        | <b>365</b>   | <b>248</b>  | <b>212</b>    | <b>210</b>       | <b>1033</b>       |
| <b>Model Bias</b>                   | <b>120</b>   | <b>279</b>  | <b>214</b>    | <b>110</b>       | <b>723</b>        |
| <b>Correlations</b>                 | <b>-0.25</b> | <b>0.19</b> | <b>-0.07</b>  | <b>-0.17</b>     | <b>-0.14</b>      |
| <b>RMSE</b>                         | <b>221</b>   | <b>299</b>  | <b>243</b>    | <b>135</b>       | <b>765</b>        |
| <b>Standard deviations</b>          |              |             |               |                  |                   |
| <b>Observed</b>                     | <b>137</b>   | <b>113</b>  | <b>112</b>    | <b>64</b>        | <b>207</b>        |
| <b>Model</b>                        | <b>101</b>   | <b>35</b>   | <b>28</b>     | <b>36</b>        | <b>125</b>        |

A summary of correlation and RMSE between observed and model simulated average SMR in Bangladesh are shown in Table 7.3. During the month of June, July, August and September, correlation between observed and model simulated SMR is found to be poor, which is not statistically significant with RMSE of 221, 300, 243 and 135 mm for June, July, August and September, respectively.

### 7.4.3 Calibration of SMR over Bangladesh

For calibration, equation (3.1) is used at each station for different months and at different observational places in Bangladesh. After calibration it is found that the high resolution AGCM SMR is reasonably consistent with observed SMR during the period 1979-2003 as shown in Fig 7.5. In general, there is a good agreement between the model calibrations and observed SMR except in the years 1979, 1980, 1984, 1989, 1992, 1996, 1999, 2002 and 2003 in which the model shows little bit underestimation by -18.1, -36.8, -17.6, -24.2, -14.3 and -17.1% for 1979, 1980, 1989, 1992, 1996, 2003 and overestimation shows by 27.7, 20.4 and 16.7% for 1984, 1999 and 2002, respectively.

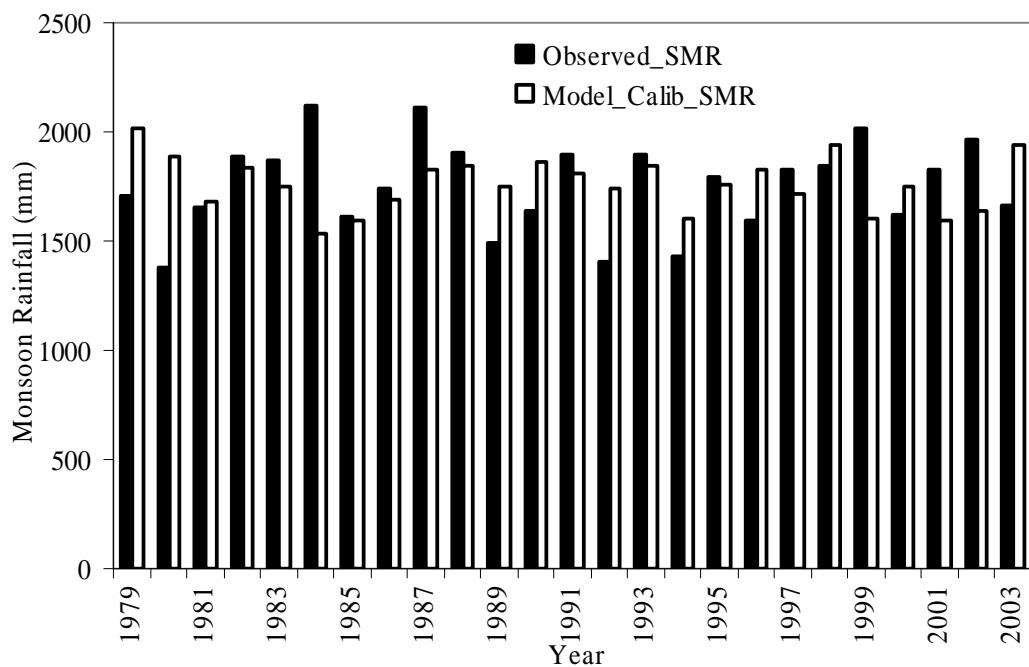


Fig. 7.5: Comparison between observed and model calibrated SMR (mm) during the period 1979-2003.

The high resolution AGCM calibrated average SMR (JJAS) during the period 1979-2003 is 1762 mm with a standard deviation of 125 mm is shown in Table 7.4, whereas SMR of Bangladesh based on 28 rain-gauge stations averaged during the period 1979-2003 is 1756 mm with a standard deviation of 207 mm. After calibration, the model SMR is compared with SMR of Bangladesh, and is found to be very close to observed value. During the month of June, July, August and September the AGCM calibrated SMR is 487, 525, 428 and 323 mm with a standard deviation 101, 35, 28 and 36 mm, respectively. Similarly, observed SMR is 484, 525, 427 and 321 mm with a standard deviation of 137, 113, 112 and 64 mm for June, July, August and September, respectively (Table 7.4).

Table 7.4: Statistical characteristics of observed and model calibrated SMR (mm) over Bangladesh during the period 1979-2003.

| <b>Model calibrated SMR (mm)</b> |             |             |               |                  |                   |
|----------------------------------|-------------|-------------|---------------|------------------|-------------------|
|                                  | <b>June</b> | <b>July</b> | <b>August</b> | <b>September</b> | <b>SMR (JJAS)</b> |
| <b>Observed</b>                  | 484         | 525         | 427           | 321              | 1756              |
| <b>Model</b>                     | 487         | 525         | 428           | 323              | 1762              |
| <b>Model Bias</b>                | -3          | 0           | -1            | -2               | -6                |
| <b>Correlations</b>              | -0.25       | 0.19        | -0.07         | -0.17            | -0.14             |
| <b>RMSE</b>                      | 186.0       | 109.0       | 115.0         | 77.4             | 251.2             |
| <b>Standard deviations</b>       |             |             |               |                  |                   |
| <b>Observed</b>                  | 137         | 113         | 112           | 64               | 207               |
| <b>Model</b>                     | 101         | 35          | 28            | 36               | 125               |

A summary of correlation and RMSE between observed and model calibrated average SMR in Bangladesh are also shown in Table 7.4. During the month of June, July, August and September, correlation between observed and model calibrated SMR is also found to be poor, which is not statistically significant with RMSE of 186.0, 109.0, 115.0 and 77.4 mm for June, July, August and September, respectively (Table 7.4).

#### 7.4.4 Validation of SMR over Bangladesh

The high resolution AGCM simulated area averaged SMR over Bangladesh is compared with the observed (rain-gauge) rainfall during the period 1979-2003 as shown in Figs. 7.6(a-b). Spatial distribution of model simulated SMR and the observed rainfall over Bangladesh are found to be almost similar except in the southeastern part of Bangladesh. Less rainfall is also observed over western part of Bangladesh. High resolution AGCM does not capture rainfall well over the southeastern part but northeastern and western part of Bangladesh rainfall is well captured by the high resolution model (AGCM). It is clear that heavy rainfall belt over northeastern part of Bangladesh is located in hilly region on the slope of Shillong hill of Meghalaya in India

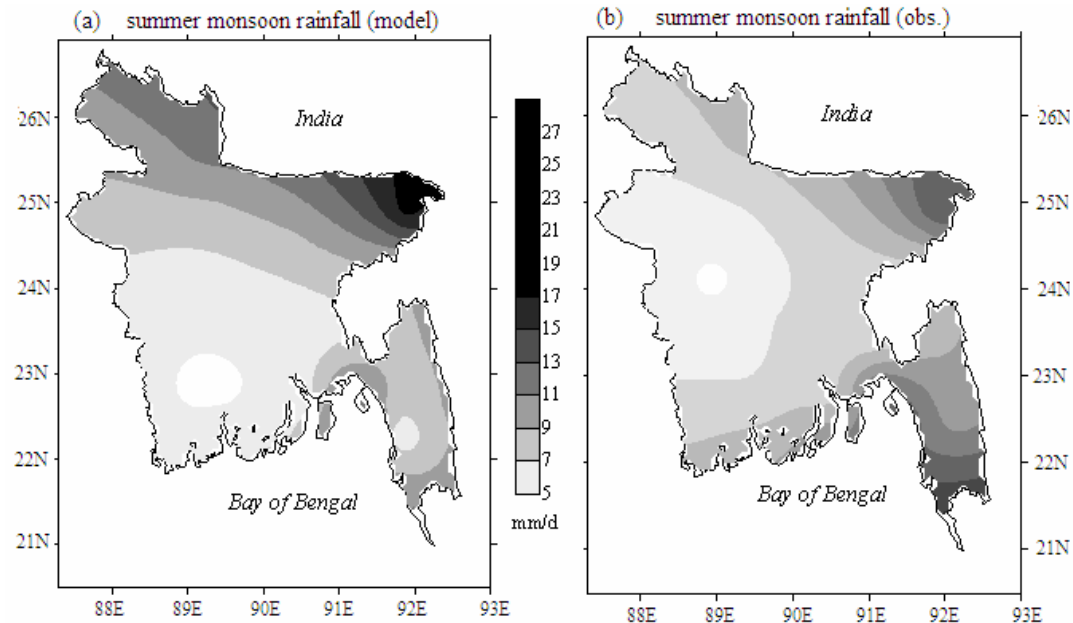


Fig. 7.6: Spatial distribution of SMR (mm/d) for (a) model and (b) observed over Bangladesh during the period 1979-2003.

and western part is located in large landmass area over Bangladesh and India. It indicates that high resolution AGCM can simulate the seasonal rainfall with a better spatial distribution. High resolution model validation is performed against observed (rain-gauge) rainfall with the help of equation 3.1. Hence, calibration value improved a lot and made it to be very close to observed value. Without calibration, model generated SMR scenarios do not match directly with the observed rainfall. The average model calibrated

rainfall coincided with observed SMR. It is indicated that calibrated SMR is quite well captured by AGCM (Fig. 7.7).

High resolution AGCM model calibrated SMR are compared with observed SMR during the period 2004-2006 as shown in Fig 7.7.

Model underestimated SMR by 17.6 and 6.8% in 2004 and 2005, whereas model overestimated 6.6% in 2006, respectively. On an average model calibrated SMR underestimated about 6.9% during the period 2004-2006. It is found that the model calibrated SMR is very close to observed rainfall. It is assumed that the high resolution AGCM performance is quite reasonable because about -6.9% biases may be considerable in long range forecasting by using a high resolution climate model. It is also indicated that this type of information may be helpful for farmers and planners of the country to mitigate water related disaster like land slide, flood and water scarcity etc.

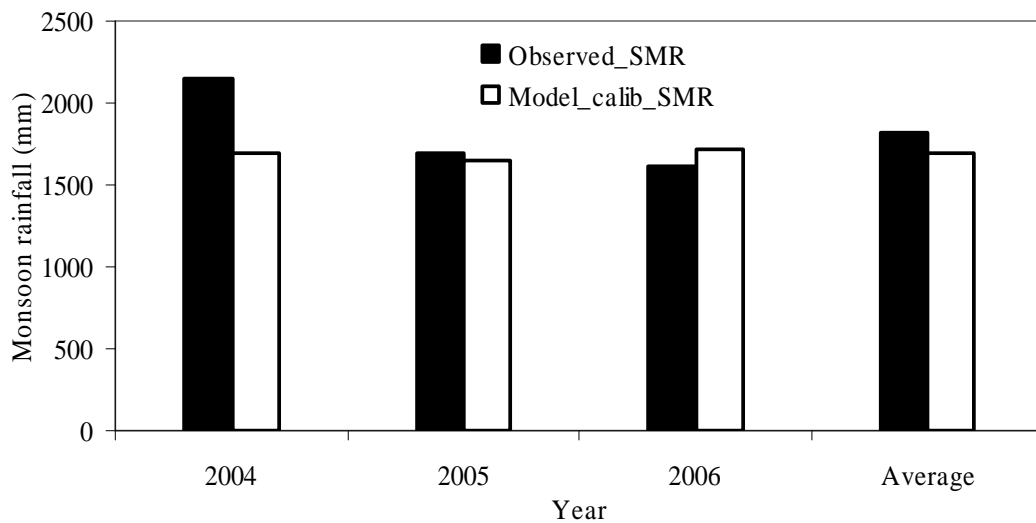


Fig. 7.7: Comparison between observed and model calibrated SMR during the period 2004-2006 and averaged SMR at the same period.

## 7.5 Projection of SMR over Bangladesh

### 7.5.1 Projections of SMR for the near future (2015-2034)

The change of model calibrated SMR during the year 2015-2034 is shown in Fig. 7.8. The seasonal rainfall is classified as normal when the actual rainfall is within Long Period Average (LPA)  $\pm$  CV. In Fig. 7.8, the horizontal solid line represents coefficient

variation (CV). The years in which the percentage departures are less than -15% (more than +15%) are called deficient (excess) or drought (flood) monsoon years. Remaining years are called normal monsoon years. It is seen that during the period 2015-2034, the lowest and second lowest seasonal monsoon rainfall may be occurred in 2030 (-27.6%) and 2016 (-23.5%) and highest and second highest in 2029 (24.7%) and 2024 (18.1%) respectively. It may be 2 excess monsoon years and 4 deficient monsoon years during the above years (2015-2034).

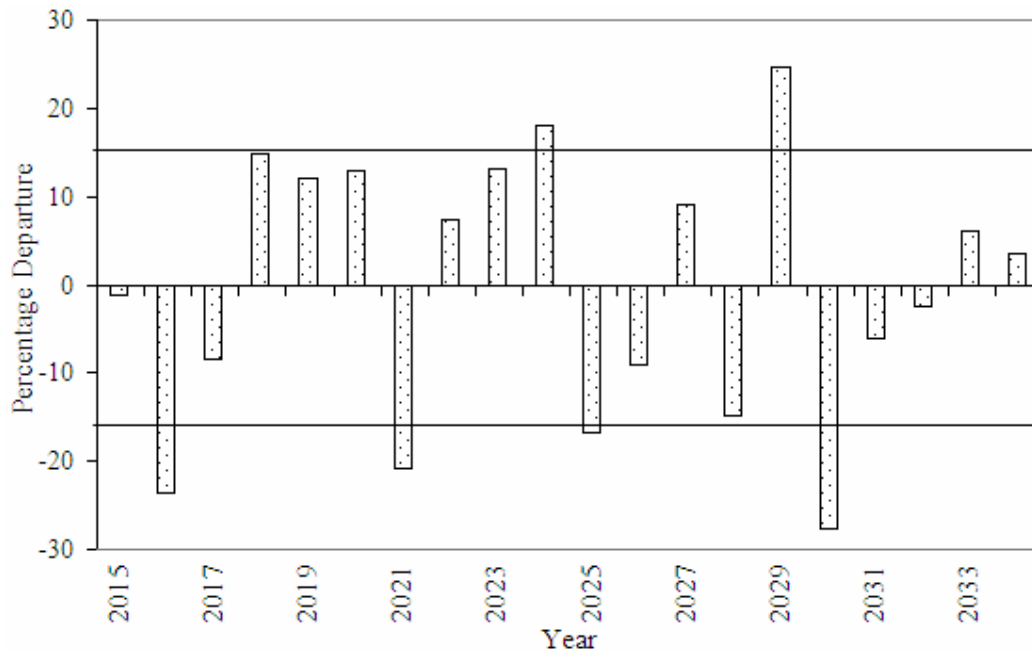


Fig. 7.8: Percentage departure of SMR (near future) over Bangladesh during the period 2015-2034.

On an average, SMR may decrease by -0.5% over Bangladesh for near future during the period 2015-2034. However, the idea may be helpful about for long range forecast is the goal of this study which is needed to the planners and stakeholders of the country.

Fig. 7.9 shows the spatial distribution of differences between model calibrated near future and observed SMR during the period 2015-2034 and base period (1979-2003), respectively. From the figure, it is seen that the change of highest SMR is observed in the northeastern part and next to highest is seen to the northwestern part whereas less SMR is found in the southwestern part of Bangladesh.

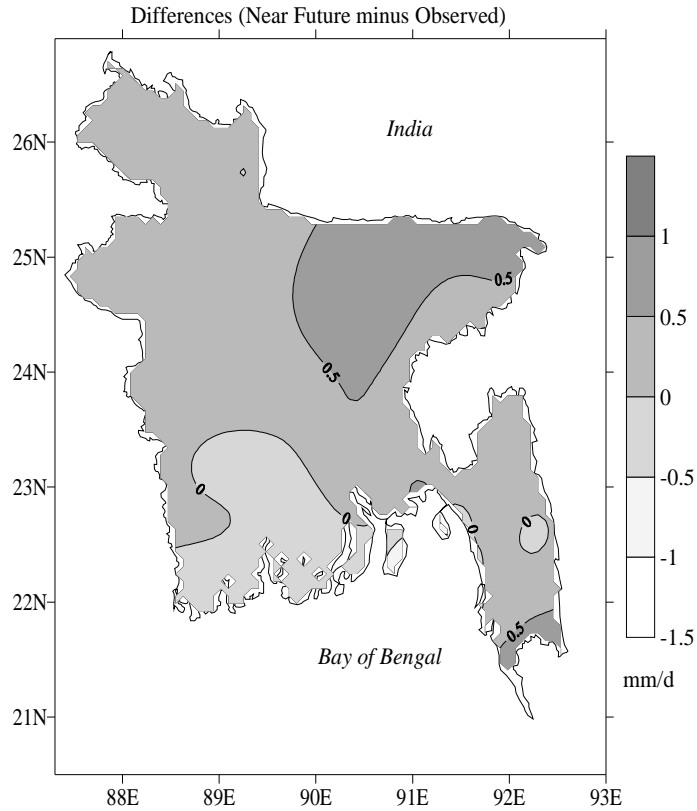


Fig. 7.9: The spatial distribution of SMR anomaly (mm/d) over Bangladesh averaged during the period 2015-2034 and base period (1979-2003).

### 7.5.2 SMR projections for the future (2075-2099)

The change of SMR for the future is found as shown in Fig. 7.10. The seasonal rainfall is classified as normal when the actual rainfall is within  $LPA \pm CV$ . In Fig. 7.10, the horizontal dashed line represents coefficient variation (CV). The years in which the percentage departures are less than -18% (more than +18%) are called deficient (excess) or drought (flood) monsoon years. Remaining years are called normal monsoon years. It is observed that during the period 2075-2099, the lowest and second lowest seasonal monsoon rainfall may be occurred in 2076 (-29.1%) and 2085 (-27.3%) and highest and second highest in 2079 (29.9%) and 2084 (24.6%) respectively. It may be found that 5 excess monsoon years and 5 deficient monsoon years in the series (2075-2099). On an average SMR may increase 0.4% over Bangladesh for future during the same period.

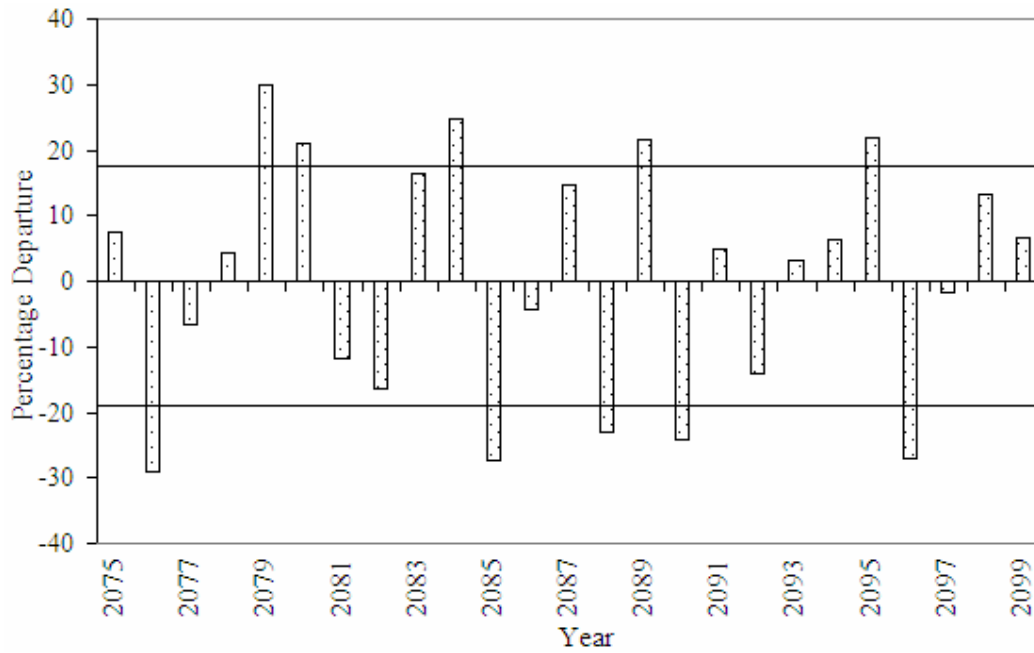


Fig. 7.10: Percentage departure of SMR (future) over Bangladesh during the period 2075-2099.

Fig. 7.11 shows the differences between spatial distributions of model calibrated future and observed SMR during the period 2075-2099 and base period 1979-2003, respectively. The average SMR throughout the country is all most similar except southeastern part of Bangladesh. Southeastern part rainfall may increase little bit of Bangladesh during the period 2075-2099.

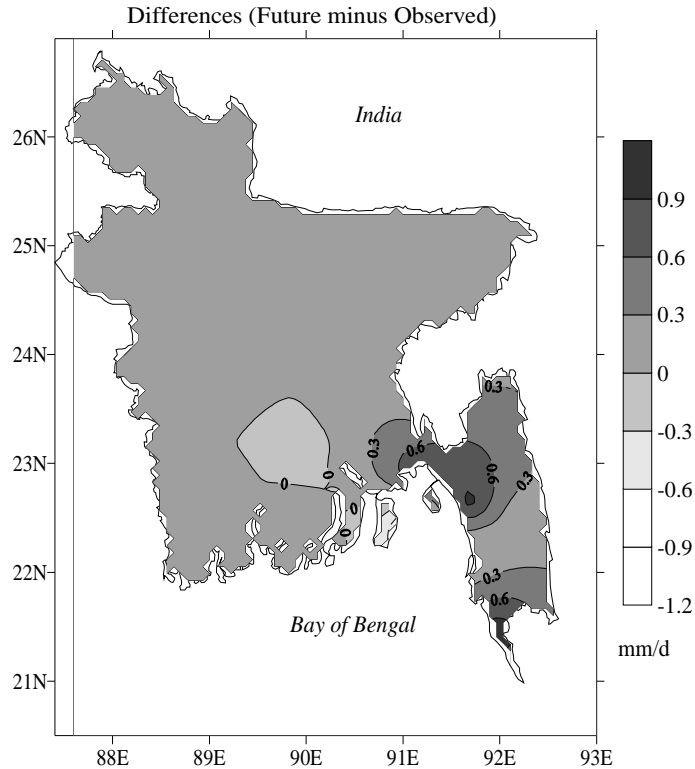


Fig. 7.11: The spatial distribution of SMR anomaly (mm/d) over Bangladesh averaged during the period 2075-2099 and base period (1979-2003).

## 7.6 Comparison of seasonal SMR among observed rainfall, AGCM rainfall and regression model rainfall

Seasonal SMR of 28 stations of Bangladesh during the period 1961-2006 has been analyzed and presented in Fig 7.12a. The year-to-year performance of observed rainfall, AGCM rainfall and regression model rainfall is shown in Fig. 7.12a. The AGCM simulated SMR is underestimated for the whole periods 1979-2006 (Fig. 7.12a). But regression model rainfall is shown good agreement with the observed rainfall during the period 1979-2006. The AGCM output is not directly useful for application purposes, without calibration, the model outputs are very risky for long term forecasting (seasonal forecast). However, after calibration, model output is shown good performance with the observed rainfall over Bangladesh (Fig. 7.12b). In general, there is a good agreement between the observed and AGCM calibrated SMR except in the years 1979, 1980, 1984, 1987, 1989, 1990, 1992, 1996, 1999, 2001, 2002, 2003 and 2004 (i.e. 13 years) out of 28 years.

Similarly, for regression model, there is a good performance between the observed and regression model SMR except in the years 1980, 1984, 1987, 1992, 1993, 1994, 1998, 2004 and 2006 (i.e. 9 years) out of 28 years.

Observed seasonal mean SMR has been compared with the AGCM calibrated mean SMR and regression model mean SMR (Fig. 7.12b) during the period 1979-2006. From Fig. 7.13, it is seen that both AGCM (1.15% underestimated) and regression model (0.31% overestimated) SMR is close to observed rainfall for the period 1979-2006. Compared with AGCM rainfall and regression model rainfall, the regression model rainfall is very close to observed rainfall (Fig. 7.13).

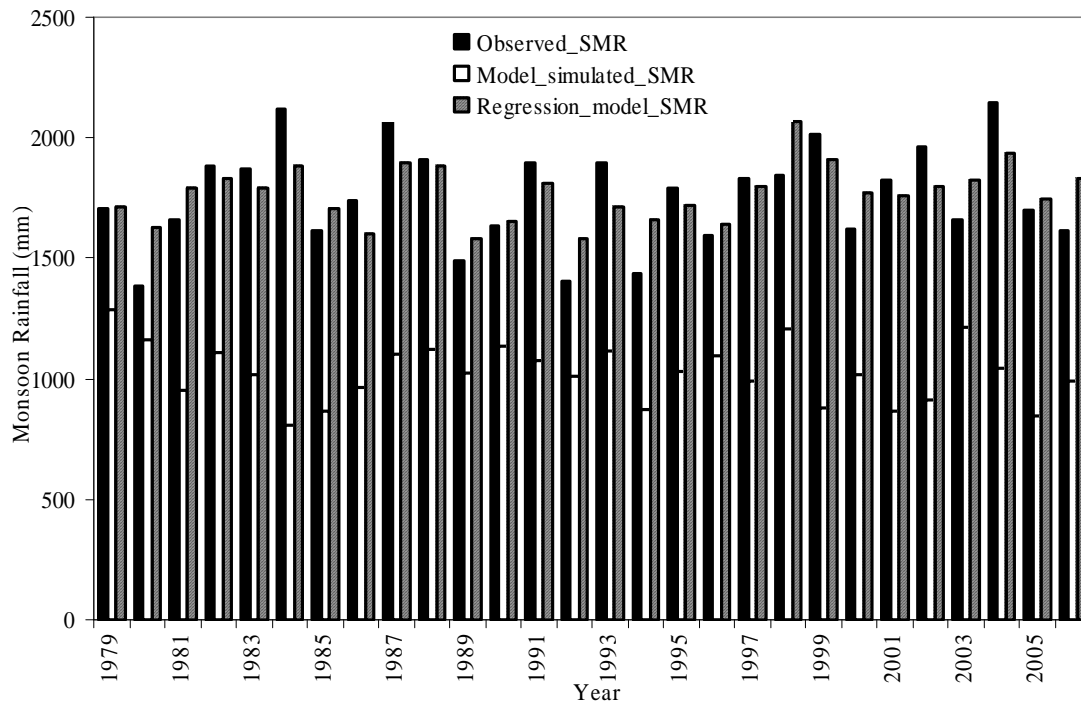


Fig. 7.12a: Comparison between observed rainfall, model simulated (uncalibrated) rainfall and regression model SMR during the period 1979-2006.

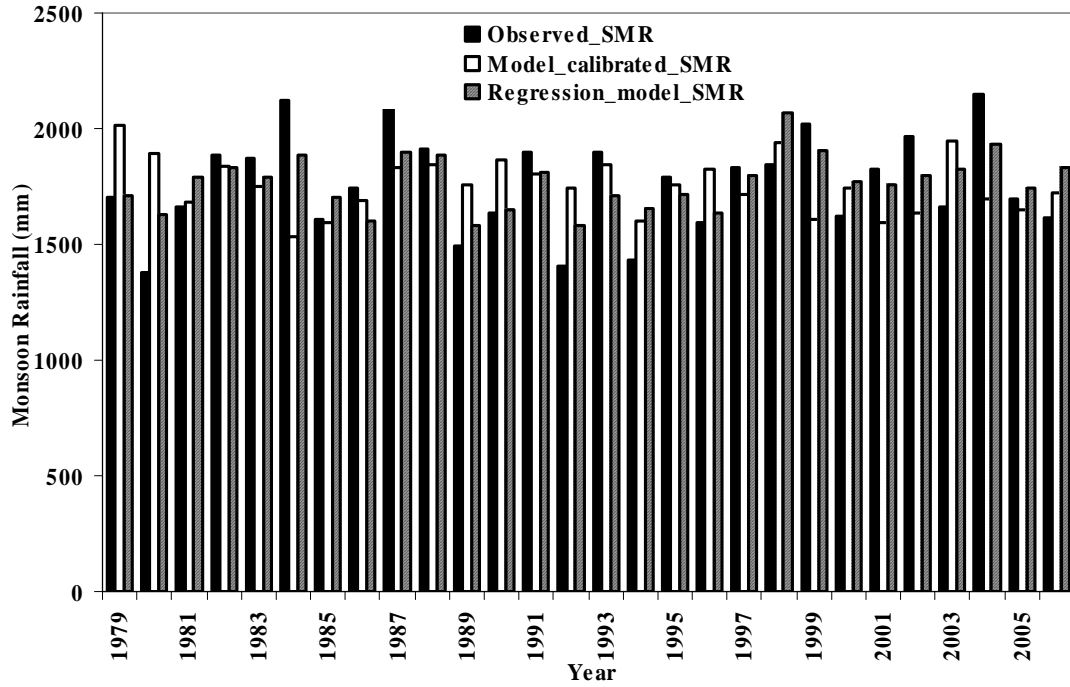


Fig. 7.12b: Comparison between observed rainfall, model calibrated rainfall and regression model SMR for the period 1979-2006.

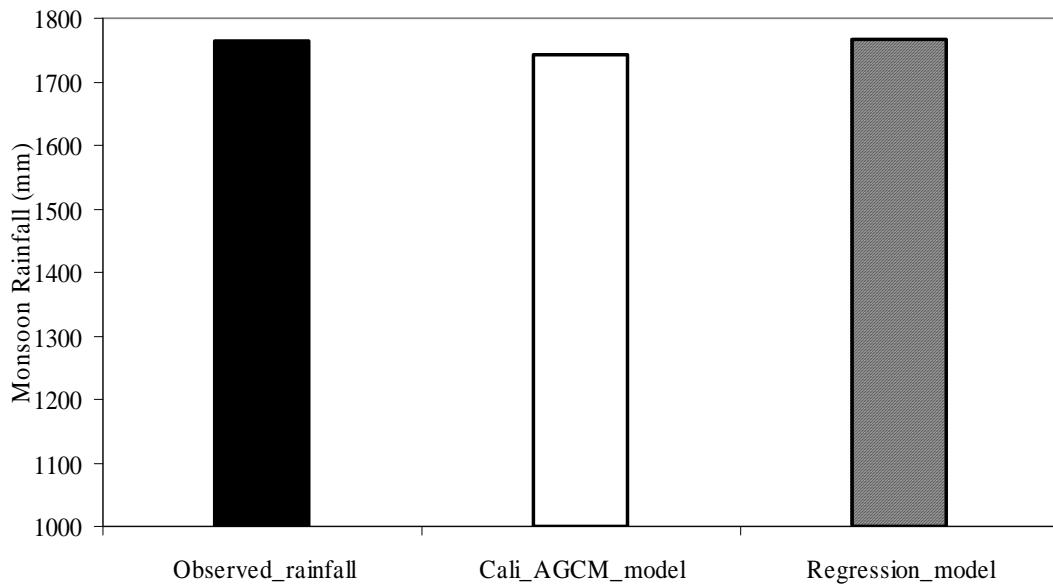


Fig. 7.13: Comparison between mean observed rainfall, mean AGCM calibrated rainfall with regression model mean SMR during the period 1979-2006.

## CHAPTER 8

### SUMMARY AND FUTURE WORKS

#### 8.1 Summary

In this thesis, a detailed study has been made on the summer monsoon (SM) interannual and decadal rainfall variability, using long historical data for the 48-year period (1961-2008). SM is active over Bangladesh during the period June-September. SM accounts for about 70.7% of the annual rainfall of the country as a whole.

Based on the observed available rainfall data, a homogeneous time series of summer monsoon rainfall (SMR) over Bangladesh has been used. While the interannual variability of SMR shows random fluctuations, the decadal variability shows alternate epochs of above and below normal rainfall. The epochs tend to last for a decade or two. However, no long-term trends have been detected. The long-term average of SMR is 1701 mm, with a standard deviation of 199 mm and its coefficient variation is 11.6%.

The SMR series consists of 8 excess and 8 deficient rainfall years during the period 1961-2008. In the decade 1961-1970 and 2001-2008 there were no excess and deficient rainfall year, respectively during the above period and was noticed while all the other decades consists excess as well as deficient rainfall years.

Teleconnections between SMR and global parameters have been investigated, and it has been found that above normal SMR is associated with warm SSTs in the month of February over southwest Indian Ocean and it is significantly correlated with SMR of Bangladesh ( $CC=0.44$  and significant at 1% level). The correlations are weak over rest of the Indian Ocean and Bay of Bengal. The correlations are insignificant throughout the Indian Ocean and Bay of Bengal for the others month. The equatorial Pacific region is also showing weak positive CCs with SMR of Bangladesh. Similarly, it is observed that above-normal SMR is associated with warm SATs in the month of April over Somalia and is significantly correlated with the SMR of Bangladesh ( $CC=0.59$  and significant at 1% level). The correlations are weak over rest of the part of the globe. Above-normal SMR is associated with high MSLP in the month of April over central Pacific Ocean is significantly correlated with the SMR of Bangladesh ( $CC=0.53$  and significant at 1% level). The correlations are insignificant over rest of the part of the world during this

month. The correlations are insignificant between SMR and MSLP during pre-monsoon season from March to May.

The relationship between SMR and ENSO has been further examined using a long time series of rainfall data. It has been shown that the relationship between the SMR and ENSO exhibited large secular variations. However, further examination of the relationship over shorter segments of the data period reveals that the relationship is statistically insignificant during the years 1961-1984 and 1985-2008, respectively. For the earlier period 1961-1984, the CCs are nearly zero over the central and eastern Pacific. For the recent period 1985-2008, the CCs are positive at and above 0.11 over the central and eastern Pacific but it is not statistically significant. The positive relationship between SMR and ENSO has strengthened a little bit after the year 1985s. Krishna Kumar *et al.* [52] reported that the ENSO-SMR relationship over India is negative. While the correlation between ENSO and SMR is generally positive over Bangladesh but not statistically significant, it is interesting to note that its secular variation of the correlation between SMR and Niño3 SSTs. During the recent El Niño years, above normal SMR is experienced due to stronger easterly wind anomalies and anomalous low-level moisture convergence with associated changes in the circulation regime throughout the troposphere, across the Arabian Sea through India to Bangladesh.

The influence of the Indian Ocean dipole mode on the SMR variability was also examined. The SMR variability appears to be enhanced during the recent decades when the dipole is active and suppressed during the decades when dipole is inactive. The lower troposphere anomalous flow pattern for the positive phase of the dipole and the anomalous flow related with the excess monsoons are somewhat similar, showing winds converging towards India. The convection arising from the convergence leads to enhanced monsoon activity over India but not strong over Bangladesh. This is also supported by the positive correlation between SMR and IODM during the whole period. For the earlier period 1961-1984, the correlation between SMR and IODM is negative. For the recent period 1985-2008, the correlation between SMR and IODM is positive (CC= 0.22) but not statistically significant. The anomalous wind flow pattern associated with the negative IODM phase and deficient monsoons are not almost similar, revealing winds diverging from the northeast India and converging and transporting moisture towards Sumatra (Indonesia). The anomalous SST patterns associated with the positive IOD/excess rainfall and negative IOD/deficient rainfall are consistent and these along

with the circulation features clearly depict the coupled ocean-atmosphere dynamics over the Indian Ocean. Thus, the enhancement of SMR by the positive dipole phase is due to the anomalously warm SSTs in the western Indian Ocean, cool SSTs in the eastern Indian Ocean and the associated large-scale convergence extending towards South India. While the suppression of the SMR by the negative phase is due to the anomalously cold SSTs in the western Indian Ocean and warm SSTs in the eastern Indian Ocean and the associated divergent circulation and transport of moisture towards Sumatra, away from India.

The SM teleconnection patterns with various global parameters revealed significant signals from various geographical regions. 3 (three) such parameters are identified which have shown potential as a predictor for SMR over Bangladesh. To check the stability of this predictor, 21 year running CC between SMR and these 3 predictors are carried out. It was observed that 3 such signals have potential as stable predictor for long range forecasting of SMR for Bangladesh. The evolution cycles of the predictors are analyzed and it has been noticed that most of them are robust in nature as a predictor for SMR.

An attempt has been made to develop a useful long range prediction scheme for SMR for Bangladesh using 3 identified predictors. The statistical model has been developed using three predictors namely Sea Surface Temperature (SST) anomalies, Surface Air Temperature (SAT) anomalies and Sea Level Pressure (SLP) anomalies are denoted by P1, P2 and P3, respectively and its represents various forcing on SMR. The model showed reasonably good result during the training period 1979-2002 and performed well during the independent verification period 2003-2012 (10-year). The CMAP data was also used for showing the model performance. The model verification statistics of the regression model: the Root Mean Square Error (RMSE) is 8.10% of LPA and the BIAS of the model is -0.85. The Hit Score (HS) and Heidke Skill Score (HSS) of the regression model are 55% and 0.39, respectively. The correlation between the regression model (predicted) rainfall and observed rainfall for the 24 years during the period 1979-2002 is 0.75. Rajeevan *et al.* [72] reported that the correlation between predicted and observed rainfall for 24 years it was 0.77-0.84 for their model.

A high resolution (20 km) climate model named MRI-AGCM is employed in generating SMR for Bangladesh. High resolution AGCM generated SMR scenario is calibrated with observed (rain-gauge) data during the period 1979-2003. The bias correction method of

the World Climate Research Programme (WCRP) is utilized for validation of AGCM generated SMR during the period 2004-2006. Better performance of AGCM through validation encourages utilizing it in SMR forecast for Bangladesh. The TRMM 3B43 V6 data is also used for understanding the model performance. The change of near future SMR was forecasted for Bangladesh by -27.6 to 24.7% for the period 2015-2034. Similarly, the change of future SMR was forecasted for Bangladesh by -29.4 to 29.4% during the period 2075-2099. On an average near future and future SMR may change by -0.5 and 0.4% during the period 2015-2034 and 2075-2099, respectively. This study find that high resolution AGCM simulated SMR is not directly useful for application purposes. Without calibration with ground base data, the model outputs are very risky in using for long term SMR forecasting. However, these results may be utilized stakeholders, policy and decision makers for multipurpose uses including water related disasters and agricultural planning for the country.

Seasonal SMR of 28 stations of Bangladesh during the period 1961-2008 has been analyzed. The year-to-year performance of observed rainfall, AGCM rainfall and regression model rainfall has been observed. The AGCM simulated SMR is underestimated for the years 1979-2006. But regression model rainfall is shown good agreement with the observed rainfall during the same period. In general, there is a good agreement between the observed and AGCM calibrated SMR except in the years 1979, 1980, 1984, 1987, 1994, 1990, 1992, 1996, 1999, 2001, 2002, 2003 and 2004 out of 28 years signifies the good performance of the AGCM over Bangladesh.

Similarly, for regression model, there is a good performance between the observed and regression model SMR except in the years 1980, 1984, 1987, 1992, 1993, 1994, 1998, 2004 and 2006 out of 28 years signifies the better performance of the regression model over Bangladesh.

Observed seasonal mean SMR has been compared with the AGCM calibrated mean SMR and regression model mean SMR during the period 1979-2006, it is seen that both AGCM and regression model SMR is close to observed rainfall for the period 1979-2006. Compared with AGCM rainfall and regression model rainfall, the regression model rainfall has been very close to observed rainfall.

The major contributions of this thesis can be outlined as follows:

- Preparation of a homogeneous long-term time series of SMR index.

- Detailed diagnostics of the teleconnections of SMR with ENSO, IOD, SST, SAT and SLP.
- Identification of 3 stable predictors based on global analysis for long-range forecasting of SMR of Bangladesh.
- Development of multiple regression models for seasonal forecasting of SMR of Bangladesh.
- Development of SMR scenarios for Bangladesh based on high resolution AGCM.

## **8.2 Future works**

The multi-model ensemble (MME) or high resolution Atmospheric General Circulation Model (AGCM) meteorological parameters (like SST, SAT, SLP etc) will be used to develop the regression model. An attempt will be made to give the seasonal rainfall forecast on administrative divisional/district scale (up-zilla scale) over Bangladesh. Strong teleconnections will also find out between SMR of Bangladesh and global meteorological parameters by using MME data. To identify and understand the major patterns of climate variability is on seasonal, decadal and longer time scales using MME data over Bangladesh. The dynamical model may be used to evaluate and enhance the different climate change scenarios.

## References

- [1] Liang, X., Lin Y., and Wu. G., "The role of land-sea distribution in the formation of the Asian summer monsoon," *Geophys. Res. Lett.*, vol. 32, L03708 doi: 10.1029/2004GL021587, 2005.
- [2] Rao, Y. P., "*Meteorological Monograph Synoptic Meteorology*," No. 1, 1976.
- [3] Asnani, G. C., "Physics and dynamics of monsoon," "*Tropical Meteorology*, vol. 1, Chap. 4, pp. 3-11, 2005c.
- [4] Ramage, C. S., "Hurricane development," *J. Meteor.*, vol. 16, pp. 227-237, 1959.
- [5] Pisharoty, P. R., and Asnani, G. C., "Rainfall around monsoon depressions over India," *Ind. J. Met. Geophys.*, vol. 8, pp. 15-20, 1957.
- [6] Kripalani, R. H., and Kulkarni, A., "Rainfall variability over south-east Asia – connections with Indian monsoon and ENSO extremes: New perspectives," *Int. J. Climatol.*, Vol. 17, pp. 1155–1168, 1997b.
- [7] Krishnamurti, T. N., Kishtawal, C. M., LaRow, T. E., Bachiochi, D. R., Zhang, Z., Williford, C. E., Gadgil, S., Surendran, S., "Multimodel ensemble forecasts for weather and seasonal climate," *J. Clim.*, Vol. 13, pp. 4196–4216, 2000.
- [8] Blanford H. F., "On the correction of Himalayan snowfall with dry winds and seasons of drought in India," *Proc. Roy. Soc. London*, vol. 37, pp 3, 1884.
- [9] Eliot, S. J., "Correlation in seasonal variation of climate" *Indian Meteor Mem. Dept.* vol. 3, pp 117-124, 1899.
- [10] Walker G. T., "Correlations in seasonal variation of weather II", *Mem. India Meteor. Dept.* vol. 21, pp 22-45, 1910.
- [11] Walker G. T., "Corrections in seasonal variation of weather VII," "The local distribution of monsoon rainfall". *Mem. India Meteor. Dept.* vol. 23, pp 23-29, 1922.
- [12] Walker G. T., "Corrections in seasonal variation of weather X," "The local distribution of monsoon rainfall". *Mem. India Meteor. Dept.* vol. 24, pp 335-345, 1924.

- [13] Walker G. T., "Seasonal weather and its prediction. British Association for Advancement of Science", *reprinted, Annual Report Smithsonian Institute*, Report 103, pp 25-44, 1933.
- [14] Montgomery R. B., "Verification of three of Walker's seasonal forecasting formula for India monsoon rain," *Mon. Wea. Rev. Supplement*, vol. 39 pp 23-24, 1940b.
- [15] Normand, C., "Monsoon seasonal forecasting," *Q. J. R. Meteorol. Soc.*, vol. 79, pp. 463–473, 1953.
- [16] Jagannathan P and Khandekar M. L., "Predisposition of upper air structure in March to May over India to the subsequent monsoon rainfall of Peninsula", *Indian J. Met. Geophys.* Vol.13 pp 305-316, 1962.
- [17] Jagannathan, P., "Seasonal forecasting in India: a review," FMU: 1-80, *India Meteorol. Dept.*, Pune, India, 1960.
- [18] Ramdas L. A., "Prediction of the date of establishment of southwest monsoon along the west coast of India," *India. J. of Meteor. and Geop.* vol 5 pp 305-314, 1954.
- [19] Gadgil, S., Rajeevan, M., Nanjundiah, R., "Monsoon prediction—why yet another failure?," *Curr. Sci.*, vol. 88, pp.1389–1400, 2005.
- [20] Gowariker, V., Thapliyal, V., Kulshrestha, S. M., Mandal, G. S., Sen, Roy, N., Sikka, D. R., "A power regression model for long range forecast of southwest monsoon rainfall over India," *Mausam*, vol. 42, pp. 125–130, 1991.
- [21] Parthasarathi, B., and Pant G. B., "Seasonal relationships between Indian Summer Monsoon Rainfall and the Southern Oscillation," *J. Climate*, vol. 5, pp 369-378, 1985.
- [22] Chowdhury, M. R., "The El Nino Southern Oscillation(ENSO) and Seasonal flooding -Bangladesh", *Theor. Appl. Climatol.* Vol., 76, pp 105-124, 2003.
- [23] Krishnamurti, T. N., Bedi, H. S., Subramaniam, M., "The Summer Monsoon of 1987," *J. Climate*, vol. 2 pp 321-340, 1989.
- [24] Kumer K. K., Soman M. K., Kumar P. K., "Seasonal forecasting of Indian Summer Monsoon Rainfall," *A review, Weather*, vol. 50(12) pp 449-467, 1995.

- [25] Kripalani R. H., Inamdar, S., Sontakke N. A., "Rainfall Variability over Bangladesh and Nepal: Comparison and corrections with features over India," *Int. J. Climatol.*, vol. 16 pp, 689-703, 1996.
- [26] Kane R. P., "Extremes of the ENSO phenomenon and Indian summer monsoon rainfall," *Int. J. Climatol.*, vol. 18, pp 775-791, 1998.
- [27] Kinter, J. I., Miyakoda, Y., Yang, S., "Recent change in the connection from Asian monsoon to ENSO," *J. Climate.*, vol. 15, pp 1203-1215, 2002.
- [28] Kumar, K. K., Rajagoalan, B., Cane M. A., "On the weakening relationship between the Indian monsoon and ENSO," *Science*, vol. 284 pp 2156-2159, 1999.
- [29] Hossain E., Alam, S. S., Imam K. H., Hoque, M. M., "Bangladesh Country Case study: Impacts and response to the 1997-1998 El Nino event", *United Nations University Press.*, pp 44-50, 2001.
- [30] Douglas, W. W., Wasimi, S. A., Islam, S., "The El Nino Southern Oscillation and long range forecasting of flows in the Ganges", *Int. J. Climatol.*, vol. 21, pp 77-78, 2001.
- [31] Kelkar R. R., "Monsoon Prediction book", *BS publications*, pp 152, 2009.
- [32] Gates W. L., "AMIP The Atmospheric Model Intercomparison Project", *Bull. Amer. Meteorol. Soci.* Vol. 73, 1992.
- [33] Gadgil, S., and Sajani, S., "Monsoon Precipitation in the AMIP runs", *Clim. Dyn.*, vol. 14, pp 659-689, 1998.
- [34] Gadgil, S., and Joseph, P. V., "On breaks of the Indian Monsoon", *J. Earth Plantery Sci.*, vol. 112, pp 529-558, 2003.
- [35] Wang, B., Ding, Q., Fu, X., Kang, I., Kyung, Jin., K., Shukla, J., and Doblas-Reyes, F., "Fundamental Challenge in Simulation and prediction of Summer Monsoon Rainfall", *Geophy. Res. Lett.*, vol. 32, doi: 10.1029/2005GL022734, 2005.
- [36] Sajani, S., Nakazawa, T., Kitoh, A., and Rajendran, K., "Ensemble Simulation of Indian summer Monsoon Rainfall by AGCM", *J. Meteorol. Soci. Japan*, vol. 85 pp 213-231, 2007.

- [37] Higgins, W., Janowiak, J., Mo, K. C., Ropelewski, C., Wang, J., Leetmaa, A., Reynolds, R., Jenne, R., Joseph, D., "The NCEP/NCAR 40-year reanalysis project," *Bull. of American Meteorol. Soc.*, vol. 77, pp. 437-471, 1996.
- [38] Smith, T. M., and R, W. Reynolds., "Improved Extended Reconstruction of SST (1854–1997)," *J. Climate.*, vol. 17, pp. 2466-2477, 2004.
- [39] Islam M. N. and Uyeda, H., "Use of TRMM in determining the climatic characteristics of rainfall over Bangladesh," *Remote Sens. Environ. Elsevier Inc.*, vol. 108(3), pp. 264-76, 2007.
- [40] WCRP, "Data and bias correction for decadal climate predictions," World Climate Research Programme report, *International CLIVAR Project Office, CLIVAR Publication Series No. 150*, 2011.
- [41] WMO, "Climate Change," Tech. Note, No. 79, 1966.
- [42] R. P. Kane., "Interannual variability of global radiation at Wageningen," *Int. J. of Climatol.*, vol.17, pp.1487–1493, 1997.
- [43] Webster, P. J., V. Magana, T. N. Palmer, J. Shukla, R. A. Tomas, M. Yanai, and T. Yasunari, "Monsoons: Processes, predictability and the prospects for prediction," *J. Geophys. Res.*, vol. 103, pp. 14451–14 510, 1998.
- [44] Bjerknes, J., "Atmospheric teleconnections from the equatorial Pacific," *Mon. Wea. Rev.*, vol. 97, pp. 163-172, 1969.
- [45] J. Chattopadhyay, and R Bhatla., "Possible influence of QBO on teleconnections relating Indian summer monsoon rainfall and sea surface temperature anomalies across equatorial Pacific," *Int. J. of Climatol.*, vol. 22(1), pp. 121-127, 2002.
- [46] Sikka, D, R., "Some aspects of the large scale fluctuations of summer monsoon rainfall over India in relation to fluctuations in planetary and regional scale circulation parameters," *Proc. Indian Acad. Sci., (Earth & Planet. Sci.)* vol. 89 pp. 179–195, 1980.
- [47] Angell, J. K., "Comparison of variations in atmospheric quantities with sea surface temperature variations in the equatorial eastern Pacific," *Mon. Wea. Rev.*, vol. 109(2), pp. 230-243, 1981.

- [48] Mooley, D. A., & Parthasarathy, B., "Indian summer monsoon and El Nino," *Pure and Applied Geophys.*, vol. 121, pp. 339-352, 1983.
- [49] Rajagopalan, B., Kumar, K. K., et al., "Unraveling the Mystery of Indian Monsoon Failure During El Niño," *Science*, vol. 314, pp. 115-119, 2006.
- [50] Maity, R., and D. N. Kumar, "Bayesian dynamic modelling for monthly Indian summer monsoon rainfall using El Niño–Southern Oscillation (ENSO) and Equatorial Indian Ocean Oscillation (EQUINOO)," *J. Geophys. Res.*, vol. 111, D07104, 2006.
- [51] Suppiah, R., "Trends in the Southern oscillation phenomenon and Australian rainfall and changes in their relationship", *Int. J. Climatol.*, vol. 24, pp 269-290, 2004.
- [52] Krishna, Kumar., K., Rajagopalan, B., Cane, M. A., "On the weakening relationship between the Indian monsoon and ENSO," *Science*, vol. 84, pp. 2156–2159, 1999.
- [53] Saji, N. H., B. N. Goswami., P. N. Vinayachandran., and T. Yamagata., "A dipole mode in the tropical Indian Ocean", *Nature*, vol. 401, pp. 360– 363, 1999.
- [54] Webster, P. J., A. M. Moore, J. P. Loschnigg and R. R. Leben, "Coupled oceanic-atmospheric dynamics in the Indian Ocean during 1997-98," *Nature*, vol. 401, pp. 356-360, 1999.
- [55] Zubair, L., S. C. Rao., and T. Yamagata., "Modulation of Sri Lanka rainfall by the Indian Ocean Dipole," *Geophys. Res. Lett.*, vol. 30, 1063, doi:10.1029/2002GL015639, 2003.
- [56] Saji, N. H., and T. Yamagata., "Structure of SST and surface wind variability during Indian Ocean dipole mode years: COADS observations," *J. Climate.*, vol. 16, pp. 2735–2751, 2003b.
- [57] Iizuka, S., T. Matsuura., and T. Yamagata., "The Indian Ocean SST dipole simulated in a coupled general circulation model," *Geophys. Res. Lett.*, vol. 27, pp 3369–3372, 2000.
- [58] Rajeevan, M., Pai, D. S., Anil, Kumar, R., "New statistical models for long range forecasting of southwest monsoon rainfall over India", NCC Research Report No 1/2005, *India Meteorol. Dept., Pune, India*, 2005.

- [59] Delsole, T., Shukla, J., "Linear prediction of the Indian monsoon rainfall. Centre for Ocean–Land–Atmosphere Studies (COLA)," *Tech. report, CTR* pp.114-58, 2002.
- [60] Iyengar, R. N., Raghukanth, S.T.G., "Intrinsic mode functions and a strategy for forecasting Indian monsoon rainfall," *Meteorol. Atmos. Phys.*, vol. 90, pp. 17–36, 2004.
- [61] Latif, M., Stockdale, T., Wolff, J., Burgers, G., Maier-Reimer, E., Junge, M. M., Arpe, K., Bengtsson, L., "Climatology and variability in the ECHAM coupled GCM," *Tellus*, vol. 46A, pp. 351–366, 1994.
- [62] Gadgil, S., Sajani, S., "Monsoon precipitation in the AMIP runs," *Clim. Dyn.* vol.14, pp. 659–689, 1998.
- [63] Kang I, S., et al., "Intercomparison of the climatological variations of Asian summer monsoon precipitation simulated by 10 GCMS," *Clim. Dyn.* vol.19, pp. 383–395, 2002.
- [64] Sadharam, Y., Murthy, T., and V, Ramana., "Simple Multiple Regression Model for long range forecasting of Indian Summer Monsoon Rainfall," *Meteorol. Atmos. Phys.*, DOI: [10.1007/s00703-007-0277](https://doi.org/10.1007/s00703-007-0277), 2007.
- [65] Clark, C. O., Cole, J. E., and Webster, P. J., "Indian Ocean SST and Indian Summer rainfall: predictive relationships and their decadal Variability," *J. Climate*, vol. 13, pp. 2503–2519, 2000.
- [66] Sperber, K. R., and T. N. Palmer., "Interannual tropical rainfall variability in general circulation model simulations associated with the Atmospheric Model Intercomparison Project," *J. Clim.*, vol. 9, pp. 2727-2750, 1996.
- [67] Delecluse, P., M. Davey., Y. Kitamura., S. G. H. Philander., M. Suarez., and L. Bengtsson., "Coupled general circulation modeling of the tropical Pacific," *J. Geophys. Res.*, vol. 103, pp. 14 357-14 373, 1998.
- [68] Hastenrath, S., "Climate Dynamics of the Tropics. Kluwer Academic Publishers," *Dordrecht, The Netherlands*, pp 488, 1991.
- [69] Parathasarathy, B., Diaz, H. F., and Eischeild, J. K., "Prediction of all India summer monsoon rainfall with regional and large scale parameters," *J. Geophys. Res.*, vol. 93, D5, pp. 5341-5350, 1988.

- [70] Thapliyal, V., "Stochastic dynamic model for long range forecasting of summer monsoon rainfall in peninsular India," *Mausam*, vol. 33, pp. 399–404, 1982.
- [71] Gowariker, V., Thapliyal, V., Sarker, R. P., Mandal, G. S., Sikka, D. R., "Parametric and power regression models: new approach to long range forecasting of monsoon rainfall in India," *Mausam*, vol. 40, pp. 115–122, 1989.
- [72] Rajeevan, M., Pai, D. S., Dikshit, S. K., and Kelkar, R. R., "New operational long range forecast models for Southwest monsoon rainfall over India and their verification for 2003," *Curr. Sci.*, vol. 86, pp. 422-431, 2004.
- [73] Raj, Y. E. A., "Statistical relation between winter monsoon rainfall and the preceding summer monsoon," *Mausam*, vol. 41, pp. 51-56, 1989.
- [74] Raj, Y. E. A., "A scheme for advance prediction of northeast monsoon rainfall of Tamilnadu, *Mausam*," vol. 49, pp. 247-254, 1998.
- [75] Raj, Y. E. A., "Seasonal variation of 200 hPA upper tropospheric features over India in relation to performance of Indian southwest and northeast monsoons," *Mausam*, vol. 55, pp. 269-280, 2004.
- [76] Box, G. E. P., G. M. Jenkins., and G. C. Reinsel., "Time Series Analysis," *3rd ed. Prentice Hall*, pp. 598, 1994.
- [77] Narkhedkar, S. G., Sinha, S. K. and Mukhopadhyay, P., "Rainfall analysis using conventional and non-conventional rainfall information on monthly scale," *Atmosfera* vol. 23(2), pp. 141-164, 2010.
- [78] Chang, C. P., Harr, P., and Ju, J., "Possible roles of Atlantic circulations on the weakening Indian monsoon rainfall-ENSO relationship," *J. Climate* vol. 14, pp 2376–2380, 2001.
- [79] IPCC, "Climate Change 2001, "The scientific Basis. Contribution of Working Group I to the Third Assessment Report of the Intergovernmental Panel on Climate Change" [Houghton, J.T.Y. Ding. D.J.Griggs. M. Noguer, P.J. vander Linden. X.. Dai, K. Maskell, and C. A. Johnson (eds.)]. *Cambridge University Press, Cambridge, United Kingdom and New York, USA*, 2001.
- [80] Tokioka, T., K. Yamazaki., I. Yagai., and A. Kitoh., "A Description of the MRI Atmospheric General Circulation Model (The MRI GCM-I)," *Tech. Report of the Meteorol. Res. In.*, vol. 13, pp. 249, 1984.

- [81] Nagai, T., T. Tokioka., M. Endoh., Y. Kitamura., "El Nino Southern Oscillation simulated in an MRI atmosphere-ocean coupled general circulation model," *J. Climate*, vol. 5, pp. 1202-1233, 1992.
- [82] Tokioka, T., A. Noda., A. Kitoh., Y. Nikaidou., S. Nakagawa., T. Motoi., S. Yukimoto., and K. Takata., "A transient CO2 experiment with the MRI CGCM," *J. Meteor. Soc. Japan*, vol. 73, pp. 817-826, 1995.
- [83] IPCC, "Climate Change 1995, "The Science of Climate Change, Contribution of Working Group I to the Second Assessment Report of the Intergovernmental Panel on Climate Change", (Eds. Houghton, J.T., L.G. Meira Filho, B.A. Callander, N. Harris, A. Kattenberg, and K. Maskell), *Cambridge University Press, Cambridge, United Kingdom and New York, USA*, pp. 572, 1996.
- [84] Yukimoto, S., A. Noda., A. Kitoh., M. Sugi., Y. Kitamura., M. Hosaka., K. Shibata., S. Maeda., and T. Uchiyama., "A new Meteorological Research Institute Coupled GCM (MRI CGCM2) —Model climate and its variability—*Pap.*" *Meteor. Geophys.*, vol. 51, pp. 47-88, doi:10.2467 / mripapers.51.47, 2001.
- [85] Noda, A., S. Yukimoto., S. Maeda., T. Uchiyama., K. Shibata., and S. Yamaki., "A New Meteorological Research Institute Coupled GCM (MRI CGCM2)—Transient Response to Greenhouse Gas and Aerosol Scenarios". *CGER'S SUPERCOMPUTER MONOGRAPH REPORT Vol.7*, National Institute for Environmental Studies, 2001.
- [86] IPCC, Climate Change 2007, "The Physical Science Basis. Contribution of Working Group I to the Fourth Assessment Report of the Intergovernmental Panel on Climate Change," (Eds. Solomon, S., D. Qin, M. Manning, Z. Chen, M. Marquis, K. B. Averyt, M. Tignor and H. L. Miller), *Cambridge University Press, Cambridge, United Kingdom and New York, USA*, pp. 996, 2007.
- [87] Takayabu, I., H. Kato., K. Nishizawa., Y. N. Takayabu., Y. Sato., H. Sasaki., K. Kurihara., and A. Kitoh., "Future Projections in Precipitation over Asia Simulated by Two RCMs Nested into MRI CGCM2.2," *J. Meteor. Soc. Japan*, vol. 85, pp. 511-519, 2007.
- [88] Bony, S., and J. L. Dufresne., "Marine boundary layer clouds at the heart of tropical cloud feedback uncertainties in climate models," *Geophys. Res. Lett.*, vol. 32, L20806, doi: 10.1029/2005GL023851, 2005.

- [89] Mizuta, R., K. Oouchi., H. Yoshimura., A. Noda., K. Katayama., S. Yukimoto., M. Hosaka., S. Kusunoki., H. Kawai. and M. Nakagawa., "20-km –mesh global climate simulations using JMA GSM model -mean climate states," *J .Meteor. Soc. Japan*, vol. 84, pp. 165-185, 2006.
- [90] Oouchi, K., J. Yoshimura., H. Yoshimura., R. Mizuta., S. Kusunoki. and A. Noda., "Tropical cyclone Climatology in a global warming climate assimulated in a 20 km-mesh global atmospheric model: Frequency and wind intensity analyses," *J. Meteor. Soc. Japan*, vol. 84, pp. 259-276, 2006.
- [91] Kusunoki, S., J. Yoshimura., H. Yoshimura., A. Noda., K. Oouchi. and R. Mizuta., "Change of Baiu rain band in global warming projection by an atmospheric general circulation model with a 20-km grid size," *J Meteor. Soc. Japan*, vol. 84, pp. 581-611, 2006.
- [92] Rahman, M. Mizanur., "A Validation of Regional climate Model simulation with Observational Data over Bangladesh, M. Phil. thesis", *Department of Physics, Bangladesh University of Engineering & Technology (BUET)*, 2006
- [93] Islam. M. N., "Rainfall and temperature scenario for Bangladesh," *The Open Atmospheric Science Journal, Bentham Open*, vol. 3, pp. 93-103, 2009.
- [94] Bengtsson, L., M. Botzet., and M. Esch., "Will greenhouse gas –induced warming over the next 50 years lead to higher frequency and greater intensity of hurricanes? ," *Tellus*, vol. 48A, pp. 57-73, 1996
- [95] Akio, Kitoh., and Shoji, Kusunoki., "East Asian summer monsoon simulation by a 20-km mesh AGCM," *Climate Dynamics* vol. 31, pp. 389-401, DOI 10.1007/s00382-007-0285-2, 2008.
- [96] Freidenreich, S. M. and V. Ramaswamy., "A new multiple band solar Radiative parameterization for General circulation models," *J. Geophys. Res.*, vol. 104, pp. 31389–31409, 1999.
- [97] Simmons, A. J., and D. M. Burridge., "An energy and angular-momentum conserving vertical finite difference scheme and hybrid vertical coordinates," *Mon. Wea. Rev.*, vol. 109, pp.758-766, 1981.
- [98] Yoshimura, H. and T. Matsumura., "A two time level vertically conservative semi Lagrangian Semi implicit double Fourier series AGCM. CAS/JSCWGNE"

*Research Activities in Atmospheric and Ocean Modeling*, vol. 35, pp. 3.25-3.26, 2005.

- [99] Yatagai. A., Xie. P., Kitoh. A., "Utilization of a new gauge-based daily precipitation dataset over monsoon Asia for validation of the daily precipitation climatology simulated by the MRI/JMA 20-km mesh AGCM," *SOLA*, vol. 1, pp.193-196, 2005.

## List of Publications

1. Md. Mizanur Rahman, M. Rafiuddin, Md. Mahbub Alam, 2013: Seasonal forecasting of Bangladesh Summer Monsoon Rainfall using simple multiple Regression Model, *Journal of Earth System Science*, **122(2)**:551-558, DOI: 10.1007/s12040-013-0287-x.
2. Md. Mizanur Rahman, M. Rafiuddin, Md. Mahbub Alam , Shoji Kusunoki, Akio Kitoh and F. Giorgi, 2013: Summer monsoon rainfall scenario over Bangladesh using a high-resolution AGCM, *Natural Hazards*, DOI: 10.1007/s11069-013-0734-7.
3. Md. Mizanur Rahman, M. Rafiuddin, Md. Mahbub Alam, 2013: Teleconnections between Bangladesh Summer Monsoon Rainfall and Sea Surface Temperature in the Indian Ocean, *International Journal of Ocean and Climate Systems*, Manuscript number IJOCS-57 13 (under review).